THE LOCAL-DENSITY-FUNCTIONAL THEORY: APPLICATION TO ATOMS AND MOLECULES

by

Yufei Guo

A thesis submitted to the Faculty of Graduate Studies and Research in partial fulfillment of the requirements for the degree of Doctor of Philosophy

Department of Chemistry
McGill University
Montreal, Quebec
CANADA

May 1990

To my family

ABSTRACT

The generalized local-spin-density functional (G-LSD) theory is proposed which avoids (a) the physical restriction used in the generalized exchange local-spin-density functional (GX-LSD) theory; (b) the homogeneous electron-density approximation in the Hartree-Fock-Slater (HFS) theory and in the Gáspár-Kohn-Sham (GKS) theory; and (c) the time-consuming step to search the optimal exchange parameter for each atom or ion in the $X\alpha$ and Ξa theories. Theoretically, the G-LSD theory is more rigorous than the GX-LSD, HFS, GKS, and Ξa theories. Numerically, the statistical total energies for atoms are better in the G-LSD theory than in the GKS theory.

Ionization potentials and electron affinities of atoms, the stability of singly and doubly charged negative ions, and the electronegativities, and hardnesses of the fractional charged atoms with $Z < 37$ are calculated by the SIC-GX-LSD theory with the GWB Fermi-hole parameters and electron-correlation correction.

The self-interaction correction (SIC) is introduced into the multiple-Scattering $X\alpha$ (MS-$X\alpha$) method and used to calculate some molecules and molecular anions. The results show that the ionization potentials from the negative of the one-electron eigenvalues are as good as those obtained in the transition state calculation and in very good agreement with experiment.

RESUMÉ

Une théorie alternative de fonctionelle de densité a été proposée. Cette théorie évite (a) la restriction physique utilisée dans la théorie de la fonctionelle de densité locale de spin d' échange généralisée (GX-LSD); (b) l' approximation de la densité d'électrons homogène dans les traitements de Hartree-Fock-Slater (HFS) et de Gaspar-Kohn-Sham (GKS); et (c) la recherche du paramètre optimal dans la méthode Xα ou Ξa, qui consomme beaucoup de temps-machine. La méthode G-LSD est plus rigoureuse que GX-LSD, HFS, GKS et la théorie Ξa et les résultats numériques de l' énergie totale statistique des atomes avec G-LSD sont meilleurs que dans le cas de GKS.

Les potentiels d' ionisation (PI) et les affinités électroniques (AE), la stabilité des ions négatifs de charges -1 et -2 a été étudiée et les électonégativités et duretés des atomes de charge fractionnaire ($Z < 37$) ont été calculés avec la SIC-GX-LSD en tenant compte de la corrélation électronique avec les paramètres de GWB.

La correction d'auto-intéraction (SIC) a été introduite en premier dans la méthode Xα de diffusion multiple (MS-Xα) et a été utilisée pour calculer quelques molécules et anions moléculaires. Les résultats montrent que les PI obtenus comme l' inverse additif des valeurs propres de l' énergie d' un électron sont aussi bons que ceux qu' on obtient avec le calcul de l' état de transition.

ACKNOWLEDGMENTS

I would like to thank all those whom I have interacted with during the time I spent on this research project; Dr. S. Manoli, Dr. A.A.Koukoulas, Mr. M.C.Wrinn, Dr. M.Berksoy, Ms. N.Gallego, and Mr. S.Suba for their useful discussions and helpful criticisms.

I wish to express my deepest gratitude to my supervisor, Dr. and Prof. M. A. Whitehead, who has encouraged and helped me constantly during this project. I wish to thank him not only for his scientific and professional advice but also for his very valuable human concerns and understanding.

For financial support I would like to thank Department of Chemistry of McGill University for granting me a "Chemistry Research Scholarship", McGill University for the award of a "Dalbir Bindra Fellowship", National Research Council of Canada for support of the research, and the McGill Computer Centre for unfunded research funds.

CONTENTS

LIST OF TABLES

LIST OF FIGURES

CHAPTER I

THE GENERALIZED LOCAL-SPIN-DENSITY FUNCTIONAL THEORY

I-1. Introduction

For an N-electron closed-shell atom, the normalized wave function is a Slater determinant[1,2]

$$\Psi(\mathbf{X}) = \frac{1}{N!} \det \begin{vmatrix} \psi_1(\mathbf{x}_1) & \psi_1(\mathbf{x}_2) & \dots & \psi_1(\mathbf{x}_N) \\ \psi_2(\mathbf{x}_1) & \psi_2(\mathbf{x}_2) & \dots & \psi_2(\mathbf{x}_N) \\ \vdots & \vdots & & \vdots \\ \psi_N(\mathbf{x}_1) & \psi_N(\mathbf{x}_2) & \dots & \psi_N(\mathbf{x}_N) \end{vmatrix} \qquad (1-1)$$

in which $\{\psi_i(\mathbf{x}_j)\}$ is a set of spin-orbitals and $\mathbf{x}_j$ stands for spatial and spin coordinates, $\mathbf{r}_j$ and σ_j, and the Hamiltonian is

$$\hat{H} = \sum_i \left(-\nabla_i^2 - \frac{2Z}{r_i} \right) + \sum_{i>j} \frac{2}{r_{ij}} \qquad (1-2)$$

in Rydberg atomic units. The expectation value of the Hamiltonian gives a total energy

$$E = \sum_i < i|f|i > + \frac{1}{2} \sum_{i,j} < ij|g|ij > - \frac{1}{2} \sum_{i,j} < ij|g|ji > \qquad (1-3)$$

where the first term is the sum of the kinetic energy and the Coulomb interaction between the electrons and nucleus; the second and third terms are the Coulomb and exchange energies for the atom. In equation (1 3), the one-electron and two-electron integrals are

$$< i|f|i > = \int \psi_i^*(\mathbf{x}_1) \hat{f}_1 \psi_i(\mathbf{x}_1) d\mathbf{x}_1 \qquad (1-4)$$

and

$$< ij|g|kt > = \int \psi_i^*(\mathbf{x}_1) \psi_j^*(\mathbf{x}_2) \hat{g}_{12} \psi_k(\mathbf{x}_1) \psi_t(\mathbf{x}_2) d\mathbf{x}_1 d\mathbf{x}_2 \qquad (1-5)$$

respectively, with

$$\hat{f}_1 = -\nabla_1^2 - \frac{2Z}{r_1} \qquad (1-6)$$

and

$$\hat{g}_{12} = \frac{2}{r_{12}} \qquad (1-7)$$

By means of the variational principle, the one-electron Schrödinger equation is written[3]

$$\left[-\nabla_1^2 - \frac{2Z}{r_1} + V_c(\mathbf{r}_1) + V_{X_i}(\mathbf{r}_1)\right] u_i(\mathbf{r}_1) = \epsilon_i u_i(\mathbf{r}_1) \qquad (1-8)$$

in which $u_i(\mathbf{r}_1)$ is the spatial part of the spin-orbital $\psi_i(\mathbf{x}_1)$, namely,

$$\psi_i(\mathbf{x}_1) = u_i(\mathbf{r}_1)\chi_i(\sigma_1) \qquad (1-9)$$

the Coulomb potential is

$$V_c(\mathbf{r}_1) = \sum_j \int u_j^*(\mathbf{r}_2)\hat{g}_{12}u_j(\mathbf{r}_2)d\mathbf{r}_2 \qquad (1-10)$$

and the Hartree-Fock exchange potential

$$\begin{aligned} V_{X_i}(\mathbf{r}_1) &= V_{X_i}^{HF}(\mathbf{r}_1) \\ &= -\frac{\sum_j \delta(\chi_i,\chi_j)\int u_i^*(\mathbf{r}_1)u_j^*(\mathbf{r}_2)\hat{g}_{12}u_j(\mathbf{r}_1)u_i(\mathbf{r}_2)d\mathbf{r}_2}{u_i^*(\mathbf{r}_1)u_i(\mathbf{r}_1)} \end{aligned} \qquad (1-11)$$

The off-diagonal Lagrange multipliers in the right-hand side of equation (1-8) were neglected. In fact, the wave functions satisfying equation (1-8) without the off-diagonal Lagrange multipliers can be obtained from the wave functions $\{\psi_i(\mathbf{x}_j)\}$ by an unitary transformation. The wave function $u_i(\mathbf{r}_1)$ is solved from equation (1-8) with equations (1-10) and (1-11) in the Hartree-Fock (HF) theory by the self-consistent-field (SCF) procedure.

The HF theory is the foundation of theoretical atomic, molecular, and solid state physics. Unfortunately, its most interesting feature, the HF exchange energy, is rather unwieldy computationally, especially for molecular and solid state calculations[4]. Consequently, a long history of simple approximations to the HF exchange energy has developed, beginning with the early work of Dirac[5] and Slater[6], and progressing to current efforts in the local-density functional (LDF) theory.

In 1951, Slater[6] derived an approximation to simplify the HF exchange potential expression, the Hartree-Fock-Slater (HFS) theory. The Slater statistical exchange approximation is

$$V_X^{HFS}(\mathbf{r}_1) = -6\left[\frac{3}{8\pi}\rho(\mathbf{r}_1)\right]^{1/3} \qquad (1-12)$$

where $\rho(\mathbf{r}_1)$ is the total electron density of a system. Equation (1-12) is based on the homogeneous electron gas. Slater's statistical exchange potential in the one-electron Schrödinger equation is only dependent on the local electron density.

Gáspár[7], Kohn and Sham[8] (GKS) developed an approximation to the HF exchange potential expression. The exchange potential in the GKS theory differs from that due to Slater, equation (1-12), by a factor of 2/3, that is,

$$V_X^{GKS}(\mathbf{r}_1) = -4\left[\frac{3}{8\pi}\rho(\mathbf{r}_1)\right]^{1/3} \qquad (1-13)$$

which is exact for systems of slowly varying high electron density.

The HFS theory describes the homogeneous free-electron system with slowly varying low electron density, and the GKS theory is exact for an inhomogeneous interacting electron system with slowly varying high electron-density. For intermediate conditions, Slater[9] proposed that the exchange potential in equation (1-12) could be scaled by an adjustable factor, α,

$$V_X^{X\alpha}(\mathbf{r}_1) = -6\alpha\left[\frac{3}{8\pi}\rho(\mathbf{r}_1)\right]^{1/3} \qquad (1-14)$$

creating the Xα theory. The scaling factor α varies between 1 and 2/3 and is determined by matching the approximate exchange energy to the HF exchange energy[10,11], or by requiring the total energy and kinetic energy to satisfy the virial theorem[12].

In 1968, Slater[13] introduced the spin-polarization concept in the Xα theory. Obviously, in the HF exchange energy expression, there is no exchange effect of the electrons with different spins. Therefore, the spin-polarized Xα (SP-Xα) theory should be more accurate than the Xα theory.

Herman et al.[14,15] derived an Xαβ theory based on the Slater statistical exchange approximation to introduce the inhomogeneity of a real system. In the Xαβ theory, the exchange potential is

$$V_X^{X\alpha\beta}(\mathbf{r}_1) = \left[\frac{2}{3} + \beta G(\rho)\right] V_X^{HFS}(\mathbf{r}_1) \qquad (1-15)$$

where $V_X^{HFS}(\mathbf{r}_1)$ is given in equation (1-12); $G(\rho)$ is

$$G(\rho) = \frac{1}{[\rho(\mathbf{r}_1)]^{2/3}}\left[\frac{4}{3}\left(\frac{\nabla_1\rho(\mathbf{r}_1)}{\rho(\mathbf{r}_1)}\right)^2 - 2\frac{\nabla_1^2\rho(\mathbf{r}_1)}{\rho(\mathbf{r}_1)}\right] \qquad (1-16)$$

and β is an additional scaling factor determined by the minimum-energy principle or the virial theorem. Boring[16] calculated some atoms and found the value of β to be very small (less than 0.01) slightly changing for different atoms.

The self-interaction terms in the Coulomb-interaction energy integral and the exchange energy integral of equation (1-3) in the HF theory cancel exactly, but not in the LDF theory, which employs the local-density approximation. In 1977, Gopinathan[17] proposed the Ξa theory to correct the self-interaction problem in the Xα theory with a correct asymptotic form for the potential, as r approaches infinity. The scaling exchange parameter, a, in the Ξa theory was determined by matching the statistical total energy in the Ξa theory to the HF total energy[18] or by the virial

theorem or theoretically[19]. The Ξa theory remarkably improves the one-electron eigenvalues for atoms[20] compared to the Xα theory, and compares well with HF. Unfortunately, the Ξa theory was based on the classical approximation,

$$1/N_s \approx \rho_i(\mathbf{r}_1)/\rho_s(\mathbf{r}_1) \qquad (1-17)$$

proposed by Kutzelnigg, et al.[21] and valid at large interelectronic distances. In equation (1-17), $\rho_i(\mathbf{r}$ and $\rho_s(\mathbf{r})$ are the charge densities of the i^{th} electron and the electrons with spin s; N_s is the total number of spin s electrons.

To avoid the homogeneous free-electron-gas approximation of the Slater model[6], at least in part, the time-consuming step of searching for the optimal exchange parameters for each atom in the Xα theory[9], and the classical approximation in the Ξa theory[17], Manoli and Whitehead[22,23] introduced the boundary conditions of the Fermi-correlation factor from the HF limit into the LDF theory and presented the generalized exchange local-spin-density functional (GX-LSD) theory, in which the exchange potential in the one-electron Schrödinger equation is orbital-dependent and the exchange parameters are fixed once either the Fermi-hole shape is chosen or the free-electron limit is used. Unfortunately, the GX-LSD theory was based on physical restrictions related to the Fermi-correlation factor.

An alternative LDF theory, the generalized local-spin-density functional (G-LSD) theory was proposed by the author and Whitehead[24] and is introduced in this chapter. The G-LSD theory is based on the boundary conditions and the sum rule of the Fermi-correlation factor obtained from the limit of HF theory and possesses the same features as the GX-LSD theory, that is, an orbital dependent potential and identical exchange parameters for all atoms in the periodic table once the Fermi-hole shape has been chosen but without any physical restriction on the Fermi-correlation factor.

In section I-2, the boundary conditions and the sum rule of the Fermi-hole

correlation factor will be introduced from both the traditional density-matrix[25] theory and the HF limit. Section I-3 introduces and emphasizes the significance of the G-LSD theory, which avoids the homogeneous free-electron-gas approximation of the conventional LDF theory, the time-consuming step in searching the optimal exchange parameters for each atom in the Xα theory, the classical approximation in the Ξa theory, and the physical restrictions in the GX-LSD theory. Comparison of the G-LSD theory with the GX-LSD theory[22], the Xα theory[9], the Ξa theory[17], and the exchange-only LSD (XO-LSD) theory[7,8] (i.e., the GKS theory), will be given in section I-4. The self-interaction problem and the self-interaction correction (SIC) will be introduced and discussed in section I-5. The one-electron Schrödinger equation is obtained by the variational principle and given in section I-6 for the G-LSD theory. Finally, the Coulomb-correlation, the correlation of electrons with different spins, and the relativistic correction, which is very important for calculating molecules with heavy atoms, will introduced in sections I-7 and I-8.

I-2. The Fermi Hole

The definition of one- and two-electron density matrices[25,26]

$$\rho(\mathbf{r}_1) = N \int |\psi(\mathbf{x}_1, \mathbf{x}_2, ..., \mathbf{x}_N)|^2 d\mathbf{r}_2 d\mathbf{r}_3 ... d\mathbf{r}_N d\sigma_1 d\sigma_2 ... d\sigma_N \qquad (1-18)$$

and

$$\rho(\mathbf{r}_1, \mathbf{r}_2) = N(N-1) \int |\psi(\mathbf{x}_1, \mathbf{x}_2, ..., \mathbf{x}_N)|^2 d\mathbf{r}_3 ... d\mathbf{r}_N d\sigma_1 d\sigma_2 ... d\sigma_N \quad (1-19)$$

allows $\rho(\mathbf{r}_1)$ to be interpreted as the probability of finding an electron at point $\mathbf{r}_1$, and $\rho(\mathbf{r}_1, \mathbf{r}_2)$ as the probability of finding any of the N electrons at the point $\mathbf{r}_1$ and simultaneously another electron at the point $\mathbf{r}_2$. In equations (1-18) and (1-19), $\psi(\mathbf{x}_1, \mathbf{x}_2, ..., \mathbf{x}_N)$ is the wave function of the system with spatial coordinates $\mathbf{r}_1, \mathbf{r}_2, ..., \mathbf{r}_N$ and spin coordinates $\sigma_1, \sigma_2, ..., \sigma_N$; N is the total number of electrons. When the electrons in the system are divided into two groups, one contains the electrons with spin s ($\uparrow$) and another with spin s' ($\downarrow$), the one- and two-electron density matrices can be written in a spin-polarized form

$$\rho(\mathbf{r}_1) = \rho_s(\mathbf{r}_1) + \rho_{s'}(\mathbf{r}_1) \qquad (1-20)$$

and

$$\rho(\mathbf{r}_1, \mathbf{r}_2) = \rho_{ss}(\mathbf{r}_1, \mathbf{r}_2) + \rho_{s's'}(\mathbf{r}_1, \mathbf{r}_2) + \rho_{ss'}(\mathbf{r}_1, \mathbf{r}_2) + \rho_{s's}(\mathbf{r}_1, \mathbf{r}_2) \quad (1-21)$$

It is obvious that $\rho_s(\mathbf{r}_1)$ is the probability of finding an electron with spin s at $\mathbf{r}_1$, $\rho_{ss}(\mathbf{r}_1, \mathbf{r}_2)$ the probability of finding an electron with spin s at $\mathbf{r}_1$ and simultaneously another with spin s at $\mathbf{r}_2$, etc.

When electronic motion is correlated, the pair-electron distribution $\rho_{ss}(\mathbf{r}_1, \mathbf{r}_2)$ is

$$\rho_{ss}(\mathbf{r}_1, \mathbf{r}_2) = \rho_s(\mathbf{r}_1)\rho_s(\mathbf{r}_2) + \rho_s(\mathbf{r}_1)\rho_s(\mathbf{r}_2) f_{ss}(\mathbf{r}_1, \mathbf{r}_2) \qquad (1-22)$$

and

$$\rho_{ss'}(\mathbf{r}_1,\mathbf{r}_2) = \rho_s(\mathbf{r}_1)\rho_{s'}(\mathbf{r}_2) + \rho_s(\mathbf{r}_1)\rho_{s'}(\mathbf{r}_2)f_{ss'}(\mathbf{r}_1,\mathbf{r}_2) \qquad (1-23)$$

with similar expressions for $\rho_{s's'}(\mathbf{r}_1,\mathbf{r}_2)$ and $\rho_{s's}(\mathbf{r}_1,\mathbf{r}_2)$.

It can be shown that[27]

$$\int \rho_s(\mathbf{r}_1)d\mathbf{r}_1 = N_s,$$

$$\int \rho_{s'}(\mathbf{r}_1)d\mathbf{r}_1 = N_{s'} \qquad (1-24)$$

$$\int \rho_{ss}(\mathbf{r}_1,\mathbf{r}_2)d\mathbf{r}_1\,d\mathbf{r}_2 = N_s(N_s-1) \qquad (1-25)$$

$$\int \rho_{s's'}(\mathbf{r}_1,\mathbf{r}_2)d\mathbf{r}_1\,d\mathbf{r}_2 = N_{s'}(N_{s'}-1) \qquad (1-26)$$

$$\int \rho_{ss}(\mathbf{r}_1,\mathbf{r}_2)d\mathbf{r}_2 = (N_s-1)\rho_s(\mathbf{r}_1) \qquad (1-27)$$

and

$$\int \rho_{ss'}(\mathbf{r}_1,\mathbf{r}_2)d\mathbf{r}_1\,d\mathbf{r}_2 = \int \rho_{s's}(\mathbf{r}_1,\mathbf{r}_2)d\mathbf{r}_1\,d\mathbf{r}_2$$

$$= N_sN_{s'} \qquad (1-28)$$

where

$$N = N_s + N_{s'} \qquad (1-29)$$

and N_s and $N_{s'}$ are the numbers of electrons with spin s and s', respectively.

The total interelectronic interaction energy, by means of the pair-electron distribution $\rho(\mathbf{r}_1,\mathbf{r}_2)$, can be expressed as

$$\frac{1}{2}\int \rho(\mathbf{r}_1,\mathbf{r}_2)\frac{2}{|\mathbf{r}_1-\mathbf{r}_2|}d\mathbf{r}_1 d\mathbf{r}_2 = \frac{1}{2}\int \rho(\mathbf{r}_1)\rho(\mathbf{r}_2)\frac{2}{|\mathbf{r}_1-\mathbf{r}_2|}d\mathbf{r}_1 d\mathbf{r}_2$$
$$+\frac{1}{2}\int \rho_s(\mathbf{r}_1)\rho_s(\mathbf{r}_2)f_{ss}(\mathbf{r}_1,\mathbf{r}_2)\frac{2}{|\mathbf{r}_1-\mathbf{r}_2|}d\mathbf{r}_1 d\mathbf{r}_2$$
$$+\frac{1}{2}\int \rho_{s'}(\mathbf{r}_1)\rho_{s'}(\mathbf{r}_2)f_{s's'}(\mathbf{r}_1,\mathbf{r}_2)\frac{2}{|\mathbf{r}_1-\mathbf{r}_2|}d\mathbf{r}_1 d\mathbf{r}_2$$
$$+\frac{1}{2}\int \rho_s(\mathbf{r}_1)\rho_{s'}(\mathbf{r}_2)f_{ss'}(\mathbf{r}_1,\mathbf{r}_2)\frac{2}{|\mathbf{r}_1-\mathbf{r}_2|}d\mathbf{r}_1 d\mathbf{r}_2$$
$$+\frac{1}{2}\int \rho_{s'}(\mathbf{r}_1)\rho_s(\mathbf{r}_2)f_{s's}(\mathbf{r}_1,\mathbf{r}_2)\frac{2}{|\mathbf{r}_1-\mathbf{r}_2|}d\mathbf{r}_1 d\mathbf{r}_2 \qquad (1-30)$$

in Rydberg atomic units.

The first term in the right-hand side of equation (1-30) is the total Coulomb-interaction energy including the self-interaction of the electrons; the second and third terms are the exchange energy, which is the main topic of this chapter; and the last two terms are the electron Coulomb-correlation energy. Before evaluating the Fermi- and Coulomb-correlation energies, the Fermi-correlation factors, $f_{ss}(\mathbf{r}_1,\mathbf{r}_2)$ and $f_{s's'}(\mathbf{r}_1,\mathbf{r}_2)$, and the Coulomb-correlation factors, $f_{ss'}(\mathbf{r}_1,\mathbf{r}_2)$ and $f_{s's}(\mathbf{r}_1,\mathbf{r}_2)$ have to be determined. Traditionally, the Fermi-correlation factors satisfy the following conditions:

(i) by the Pauli exclusion principle and equation (1-22), the probability of finding two electrons at the same position at the same time is zero,

$$f_{ss}(\mathbf{r}_1,\mathbf{r}_2) = -1 \qquad (1-31)$$

when $|\mathbf{r}_1-\mathbf{r}_2|$ equals zero;

(ii) the electrons move independently at large interelectronic distances and equation (1-22) appears to become

$$\rho_{ss}^{ind}(\mathbf{r}_1,\mathbf{r}_2) = \rho_s(\mathbf{r}_1)\rho_s(\mathbf{r}_2) \qquad (1-32)$$

when $|\mathbf{r}_1 - \mathbf{r}_2|$ approaches infinity. However, this expression is wrong because it does not preserve normalization[27]. Kutzelnigg et al.[21] have shown that the correct form of the independent pair-electron distribution function is

$$\rho_{ss}^{ind}(\mathbf{r}_1, \mathbf{r}_2) = \rho_s(\mathbf{r}_1)\rho_s(\mathbf{r}_2) - \frac{1}{N_s}\rho_s(\mathbf{r}_1)\rho_s(\mathbf{r}_2) \qquad (1-33)$$

Therefore,

$$f_{ss}(\mathbf{r}_1, \mathbf{r}_2) = -\frac{1}{N_s} \qquad (1-34)$$

as $|\mathbf{r}_1 - \mathbf{r}_2|$ approaches infinity;

and (iii) the conditional probability of finding an electron with spin s at $\mathbf{r}_2$, when one is known to be at $\mathbf{r}_1$ with spin s, is, from equation (1-22)

$$\frac{\rho_{ss}(\mathbf{r}_1, \mathbf{r}_2)}{\rho_s(\mathbf{r}_1)} = \rho_s(\mathbf{r}_2) + \rho_s(\mathbf{r}_2) f_{ss}(\mathbf{r}_1, \mathbf{r}_2) \qquad (1-35)$$

$\rho_s(\mathbf{r}_2) f_{ss}(\mathbf{r}_1, \mathbf{r}_2)$, therefore, represents the modification of the charge distribution $\rho_s(\mathbf{r}_2)$ caused by the presence of an electron with spin s at $\mathbf{r}_1$. However, the probability of finding an electron with spin s at $\mathbf{r}_2$ without the presence of any electron with spin s at $\mathbf{r}_1$ is $\rho_s(\mathbf{r}_2)$. Consequently, the difference of the probability generated by the presence of an electron with spin s at $\mathbf{r}_1$ is

$$\begin{aligned} \int \rho_s(\mathbf{r}_2) f_{ss}(\mathbf{r}_1, \mathbf{r}_2) d\mathbf{r}_2 &= \frac{1}{\rho_s(\mathbf{r}_1)} \int \rho_{ss}(\mathbf{r}_1, \mathbf{r}_2) d\mathbf{r}_2 - \int \rho_s(\mathbf{r}_2) d\mathbf{r}_2 \\ &= -1 \end{aligned} \qquad (1-36)$$

Equations (1-24) and (1-27) were used to give the last equality in equation (1-36). This is the sum rule of the Fermi-correlation factor; the total amount of the exchange charge removed by the presence of an electron with spin s at $\mathbf{r}_1$ is -1, a Fermi hole.

The Xα theory and the LSD theory with the exchange-only (the XO-LSD theory) can be generated from the Fermi-correlation factor[22,23], which was written

directly to satisfy the boundary conditions, equations (1-31) and (1-34), and the sum rule, equation (1-36).

Alternative boundary conditions can be obtained by modifying the exchange energy expression in the HF theory[22], where the exchange energy is[3]

$$E_X^{HF} = -\frac{1}{2}\int \sum_{i,j} u_i^*(\mathbf{r}_1)u_j^*(\mathbf{r}_2)u_j(\mathbf{r}_1)u_i(\mathbf{r}_2)$$
$$\delta(\chi_i,\chi_j)\frac{2}{|\mathbf{r}_1-\mathbf{r}_2|}d\mathbf{r}_1\,d\mathbf{r}_2 \qquad (1-37)$$

$u_i(\mathbf{r})$ and $u_j(\mathbf{r})$ are the one-electron spatial wave functions for the states i and j, and χ_i and χ_j are the corresponding spin wave functions; the sum is over all electrons in the system. δ is the Kronecker delta function, which means the Fermi-correlation only occurs for electrons with the same spin. Introducing a Fermi-correlation factor into the HF exchange energy expression (1-37) gives

$$E_X^{HF} = \frac{1}{2}\int \rho_s(\mathbf{r}_1)\rho_s(\mathbf{r}_2)f_{ss}^{HF}(\mathbf{r}_1,\mathbf{r}_2)\frac{2}{|\mathbf{r}_1-\mathbf{r}_2|}d\mathbf{r}_1\,d\mathbf{r}_2$$
$$+\frac{1}{2}\int \rho_{s'}(\mathbf{r}_1)\rho_{s'}(\mathbf{r}_2)f_{s's'}^{HF}(\mathbf{r}_1,\mathbf{r}_2)\frac{2}{|\mathbf{r}_1-\mathbf{r}_2|}d\mathbf{r}_1\,d\mathbf{r}_2 \qquad (1-38)$$

Therefore the Fermi-correlation factor f_{ss}^{HF} in the HF theory may be written as

$$f_{ss}^{HF}(\mathbf{r}_1,\mathbf{r}_2) = -\frac{\sum_{i,j} u_i^*(\mathbf{r}_1)u_j^*(\mathbf{r}_2)u_j(\mathbf{r}_1)u_i(\mathbf{r}_2)}{\rho_s(\mathbf{r}_1)\rho_s(\mathbf{r}_2)} \qquad (1-39)$$

and similarly for $f_{s's'}^{HF}(\mathbf{r}_1,\mathbf{r}_2)$. Equation (1-39) shows that the HF Fermi-correlation factor is the sum of electron-pair Fermi-correlation interactions, each electron-pair was of a Fermi-correlation factor.

As $\mathbf{r}_1$ approaches $\mathbf{r}_2$, equation (1-39) becomes

$$f_{ss}^{HF}(\mathbf{r}_1,\mathbf{r}_1) = -\frac{\sum_i \rho_i(\mathbf{r}_1)}{\rho_s(\mathbf{r}_1)} = -1 \qquad (1-40)$$

in which the sum is over the electrons with spin s. And as $|\mathbf{r}_1-\mathbf{r}_2|$ approaches infinity, the overlapping of the wave functions, $u_i^*(\mathbf{r}_1)$ with $u_j(\mathbf{r}_1)$ and $u_j^*(\mathbf{r}_2)$ with

$u_i(\mathbf{r}_2)$, goes to zero, except for the terms with i=j. Hence, the HF Fermi-correlation factor reduces to

$$f_{ss}^{HF,ind}(\mathbf{r}_1,\mathbf{r}_2) = -\frac{\sum_i \rho_i(\mathbf{r}_1)\rho_i(\mathbf{r}_2)}{\rho_s(\mathbf{r}_1)\rho_s(\mathbf{r}_2)} \qquad (1-41)$$

Comparing the boundary conditions of the Fermi-correlation factor, equations (1-40) and (1-41), in the HF theory with those in equations (1-31) and (1-34) in the density-matrix theory[25], shows that equations (1-31) and (1-40) are exactly the same, but that equation (1-34) differs from equation (1-41). However, the boundary condition of equation (1-34) is obtained from equation (1-33), in which the second term is somewhat arbitrarily introduced in order to satisfy the normalization of equation (1-25). Equation (1-41) is from the HF limit of the Fermi-correlation without any approximation. Furthermore, if the factor $\frac{1}{N_s}$ in the second term of equation (1-33) is replaced by the right-hand side of equation (1-41), that is

$$\rho_{ss}^{ind}(\mathbf{r}_1,\mathbf{r}_2) = \rho_s(\mathbf{r}_1)\rho_s(\mathbf{r}_2) - \sum_i \rho_i(\mathbf{r}_1)\rho_i(\mathbf{r}_2) \qquad (1-42)$$

it is easily seen[27] that integrating both sides of equation (1-42) over $d\mathbf{r}_1$ and $d\mathbf{r}_2$ leads to an identical equality, $N_s^2 - N_s = N_s^2 - N_s$. Equation (1-42) therefore satisfies the normalization condition. Consequently, equation (1-41) is considered to be a boundary condition of Fermi-correlation factor as $|\mathbf{r}_1 - \mathbf{r}_2|$ approaches infinity. Comparing equation (1-38) with the Fermi-correlation energy term in equation (1-30) shows that both the Fermi-correlation factors play the same role in the exchange energy expression.

I-3. The Generalized Local-Spin-Density Functional Theory

The GX-LSD theory[22,23] assumed that the Fermi-correlation factor in equa-

tion (1-22) was a sum over the one-electron Fermi-correlation factors

$$\rho_{ss}(\mathbf{r}_1,\mathbf{r}_2) = \rho_s(\mathbf{r}_1)\rho_s(\mathbf{r}_2) + \rho_s(\mathbf{r}_1)\rho_s(\mathbf{r}_2)\sum_i^s f_{ss}^i(\mathbf{r}_1,\mathbf{r}_2) \qquad (1-43)$$

where the summation is over the electrons with spin s. The boundary conditions of the Fermi-hole correlation factor, from equations (1-40) and (1-41), become

$$\sum_i f_{ss}^i(\mathbf{r}_1,\mathbf{r}_1) = -\frac{\sum_i \rho_i(\mathbf{r}_1)}{\rho_s(\mathbf{r}_1)} \qquad (1-44)$$

and

$$\sum_i f_{ss}^{i,ind}(\mathbf{r}_1,\mathbf{r}_2) = -\frac{\sum_i \rho_i(\mathbf{r}_1)\rho_i(\mathbf{r}_2)}{\rho_s(\mathbf{r}_1)\rho_s(\mathbf{r}_2)} \qquad (1-45)$$

and the sum rule equation (1-36) was rewritten as

$$\int \sum_i \left[\rho_s(\mathbf{r}_2) f_{ss}^i(\mathbf{r}_1,\mathbf{r}_2) + \frac{\rho_i(\mathbf{r}_2)\rho_i(\mathbf{r}_1)}{\rho_s(\mathbf{r}_1)}\right] d\mathbf{r}_2 = 0 \qquad (1-46)$$

Then, the GX-LSD theory put each component on both sides of equations (1-44)-(1-46) equal

$$f_{ss}^i(\mathbf{r}_1,\mathbf{r}_1) = -\frac{\rho_i(\mathbf{r}_1)}{\rho_s(\mathbf{r}_1)} \qquad (1-47)$$

when $\mathbf{r}_1$ approaches $\mathbf{r}_2$,

$$f_{ss}^{i,ind}(\mathbf{r}_1,\mathbf{r}_2) = -\frac{\rho_i(\mathbf{r}_1)\rho_i(\mathbf{r}_2)}{\rho_s(\mathbf{r}_1)\rho_s(\mathbf{r}_2)} \qquad (1-48)$$

when $|\mathbf{r}_1 - \mathbf{r}_2|$ approaches infinity, and

$$\int \rho_s(\mathbf{r}_2) f_{ss}^i(\mathbf{r}_1,\mathbf{r}_2) d\mathbf{r}_2 = -\frac{\rho_i(\mathbf{r}_1)}{\rho_s(\mathbf{r}_1)} \qquad (1-49)$$

This may not be true. Equations (1-47)-(1-49) cannot be obtained from equations (1-44)-(1-46). If equations (1-47)-(1-49) are satisfied by ρ and f, then, so are equations (1-44)-(1-46). This is a physical restriction and consequently the GX-LSD

theory is based on more precise boundary conditions and sum rules for the Fermi-correlation factor than the Fermi-correlation factor $f^{1}_{ss}(\mathbf{r}_1,\mathbf{r}_2)$ itself imposes.

The Fermi-correlation factor, $f_{ss}(\mathbf{r}_1,\mathbf{r}_2)$, of the electrons with spin s in equation (1-22) gives the average correlation effect of the electron densities, $\rho_s(\mathbf{r}_1)$ and $\rho_s(\mathbf{r}_2)$, at positions $\mathbf{r}_1$ and $\mathbf{r}_2$, which are the sum of the electron densities of all states at $\mathbf{r}_1$ and $\mathbf{r}_2$, respectively. The contribution from each state is different, since the electron density is not homogeneous. Manoli and Whitehead[22,23] noted this and expanded equation (1-22) into equation (1-43). The summation $\sum_i f^{1}_{ss}(\mathbf{r}_1,\mathbf{r}_2)$ still describes the average effect of the correlation.

In this work the imhomogeneity of the electron density distribution will be reflected, in part, by requiring equation (1-22) to be

$$\rho_{ss}(\mathbf{r}_1,\mathbf{r}_2)=\rho_s(\mathbf{r}_1)\rho_s(\mathbf{r}_2)+\rho_s(\mathbf{r}_1)\sum_{i}^{s}\rho_i(\mathbf{r}_2)f^{1}_{ss}(\mathbf{r}_1,\mathbf{r}_2) \qquad (1-50)$$

where the sum is over the electrons with spin s. Comparing equation (1-50) with equation (1-22), it can be seen that the interelectronic interaction energy caused by the electrons with spin s is

$$\begin{aligned}\frac{1}{2}\int\rho_{ss}(\mathbf{r}_1,\mathbf{r}_2)\frac{2}{|\mathbf{r}_1-\mathbf{r}_2|}d\mathbf{r}_1\,d\mathbf{r}_2 &\\ =\frac{1}{2}\int\rho_s(\mathbf{r}_1)\rho_s(\mathbf{r}_2)\frac{2}{|\mathbf{r}_1-\mathbf{r}_2|}d\mathbf{r}_1\,d\mathbf{r}_2 &\\ +\frac{1}{2}\int\rho_s(\mathbf{r}_1)\sum_{i}\rho_i(\mathbf{r}_2)f^{1}_{ss}(\mathbf{r}_1,\mathbf{r}_2)\frac{2}{|\mathbf{r}_1-\mathbf{r}_2|}d\mathbf{r}_1\,d\mathbf{r}_2 & \quad (1-51)\end{aligned}$$

If the second term of equation (1-51) is compared to the first term of equation (1-38), the HF expression, it can be seen that $\sum_i \rho_i(\mathbf{r}_2)f^{1}_{ss}(\mathbf{r}_1,\mathbf{r}_2)$ in equation (1-51) plays the same role as $\rho_s(\mathbf{r}_2)f_{ss}(\mathbf{r}_1,\mathbf{r}_2)$ in equation (1-38). Therefore, the boundary conditions of the Fermi-correlation factor in equation (1-51) may be expressed as

$$\sum_{i}\rho_i(\mathbf{r}_2)f^{1}_{ss}(\mathbf{r}_1,\mathbf{r}_2)=-\sum_{i}\rho_i(\mathbf{r}_1) \qquad (1-52)$$

when $|\mathbf{r}_1 - \mathbf{r}_2|$ approaches zero, and

$$\sum_i \rho_i(\mathbf{r}_2) f_{ss}^{i,ind}(\mathbf{r}_1, \mathbf{r}_2) = -\frac{\sum_i \rho_i(\mathbf{r}_1)\rho_i(\mathbf{r}_2)}{\rho_s(\mathbf{r}_1)} \qquad (1-53)$$

when $|\mathbf{r}_1 - \mathbf{r}_2|$ approaches infinity; the sum rule becomes

$$\int \sum_i \rho_i(\mathbf{r}_2) f_{ss}^{i}(\mathbf{r}_1, \mathbf{r}_2) d\mathbf{r}_2 = -1 \qquad (1-54)$$

Following the procedure to derive the LDF theory and writing the Fermi-correlation factor to reflect the HF boundary conditions given by equations (1-52) and (1-53) gives

$$\sum_i \rho_i(\mathbf{r}_2) f_{ss}^{i}(\mathbf{r}_1, \mathbf{r}_2) = \left[\frac{\sum_i \rho_i(\mathbf{r}_1)\rho_i(\mathbf{r}_2)}{\rho_s(\mathbf{r}_1)} - \sum_i \rho_i(\mathbf{r}_1)\right] h(\mathbf{r}_1, \mathbf{r}_2) - \frac{\sum_i \rho_i(\mathbf{r}_1)\rho_i(\mathbf{r}_2)}{\rho_s(\mathbf{r}_1)} \qquad (1-55)$$

where the Fermi-hole function $h(\mathbf{r}_1, \mathbf{r}_2)$ approaches 1 as $|\mathbf{r}_1 - \mathbf{r}_2|$ approaches zero and approaches zero as $|\mathbf{r}_1 - \mathbf{r}_2|$ approaches infinity. Substitution of the Fermi-correlation factor (1 55) into the sum rule (1-54) gives

$$\int \left[\frac{\sum_i \rho_i(\mathbf{r}_1)\rho_i(\mathbf{r}_2)}{\rho_s(\mathbf{r}_1)} - \sum_i \rho_i(\mathbf{r}_1)\right] h(\mathbf{r}_1, \mathbf{r}_2) d\mathbf{r}_2 - \int \frac{\sum_i \rho_i(\mathbf{r}_1)\rho_i(\mathbf{r}_2)}{\rho_s(\mathbf{r}_1)} d\mathbf{r}_2 = -1 \qquad (1-56)$$

The equations developed so far are exact.

Now, however, the local-density approximation is used to simplify equation (1-56). The conventional local-density approximation is

$$\rho_s(\mathbf{r}_2) \approx \rho_s(\mathbf{r}_1) \qquad (1-57)$$

which means the total density in the Fermi-hole is very slowly varying. If the charge density of electron i at point $\mathbf{r}_1$ also changes slowly, then,

$$\rho_i(\mathbf{r}_2) \approx \rho_i(\mathbf{r}_1) \qquad (1-58)$$

Equations (1-57) and (1-58) are a direct consequence of the local-density approximation. The Fermi-hole function is assumed spherically symmetric and localized within a radius r_F. The sum rule equation (1-56) gives the radius of the Fermi-hole r_F

$$r_F = \rho_s^{1/3}(\mathbf{r}_1)\left\{4\pi A_2 \sum_i \rho_i(\mathbf{r}_1)\left[\rho_s(\mathbf{r}_1) + B_2\rho_i(\mathbf{r}_1)\right]\right\}^{-1/3} \qquad (1-59)$$

where

$$A_2 = \int_{u_f} h(u)u^2\,du; u = r_2/r_F \qquad (1-60)$$

is an integral of a Fermi-hole function, and

$$B_2 = (\frac{1}{3} - A_2)/A_2 \qquad (1-61)$$

From equation (1-51), the exchange energy of the electrons with spin s can be written as

$$\frac{1}{2}\int \sum_i \rho_i(\mathbf{r}_1)U_{si}^G(\mathbf{r}_1)d\mathbf{r}_1 = \frac{1}{2}\int \rho_s(\mathbf{r}_1)\sum_i \rho_i(\mathbf{r}_2) \cdot f_{ss}^i(\mathbf{r}_1,\mathbf{r}_2)\frac{2}{|\mathbf{r}_1-\mathbf{r}_2|}d\mathbf{r}_1\,d\mathbf{r}_2 \qquad (1-62)$$

$U_{si}^G(\mathbf{r}_1)$ is the single-particle exchange energy density in the present work. Substituting equation (1-55) into (1-62) gives

$$\sum_i \rho_i(\mathbf{r}_1)U_{si}^G(\mathbf{r}_1) = \rho_s(\mathbf{r}_1)\int\left\{\left[\frac{\sum_i \rho_i(\mathbf{r}_1)\rho_i(\mathbf{r}_2)}{\rho_s(\mathbf{r}_1)} - \sum_i \rho_i(\mathbf{r}_1)\right] \cdot h(\mathbf{r}_1,\mathbf{r}_2) - \frac{\sum_i \rho_i(\mathbf{r}_1)\rho_i(\mathbf{r}_2)}{\rho_s(\mathbf{r}_1)}\right\}\frac{2}{|\mathbf{r}_1-\mathbf{r}_2|}d\mathbf{r}_2 \qquad (1-63)$$

If the local-density approximation, equations (1-57) and (1-58), is used again, and the Fermi-hole function is assumed spherically symmetric, equation (1-63) becomes

$$\sum_i \rho_i(\mathbf{r}_1)U_{si}^G(\mathbf{r}_1) = 8\pi r_F^2 A_1\left\{\sum_i \rho_i(\mathbf{r}_1)[\rho_i(\mathbf{r}_1) - \rho_s(\mathbf{r}_1)] - \frac{1}{2A_1}\sum_j \rho_j(\mathbf{r}_1)\rho_j(\mathbf{r}_1)\right\} \qquad (1-64)$$

where r_F is the radius of he Fermi-hole, and A_1 is a parameter depending on the shape of the Fermi-hole and defined as

$$A_1 = \int_{u_F} h(u)udu; u = r_2/r_F \qquad (1-65)$$

and

$$B_1 = (\frac{1}{2} - A_1)/A_1 \qquad (1-66)$$

When equation (1-59) is used, equation (1-64) gives

$$\sum_i \rho_i(\mathbf{r}_1)U_{si}^G(\mathbf{r}_1) = -4\left(\frac{\pi}{2}\right)^{1/3} A_1 A_2^{-2/3}\left\{\sum_i \rho_i(\mathbf{r}_1)[\rho_s(\mathbf{r}_1) + B_1\rho_i(\mathbf{r}_1)]\right\}$$
$$\rho_s^{2/3}(\mathbf{r}_1)\left\{\sum_j \rho_j(\mathbf{r}_1)[\rho_s(\mathbf{r}_1) + B_2\rho_j(\mathbf{r}_1)]\right\}^{-2/3} \qquad (1-67)$$

Letting

$$9c\alpha^{lim} = 4\left(\frac{\pi}{2}\right)^{1/3} A_1 A_2^{-2/3} \qquad (1-68)$$

equation (1-67) gives

$$U_{si}^G(\mathbf{r}_1) = -9c\alpha^{lim}\left[\rho_s(\mathbf{r}_1) + B_1\rho_i(\mathbf{r}_1)\right]$$
$$\rho_s^{2/3}(\mathbf{r}_1)\left\{\sum_j \rho_j(\mathbf{r}_1)[\rho_s(\mathbf{r}_1) + B_2\rho_j(\mathbf{r}_1)]\right\}^{-2/3} \qquad (1-69)$$

This is an orbital-dependent, single-particle exchange energy density in the generalized (G) local-spin-density functional (G-LSD) theory; it is distinguished the generalized exchange (GX) local-spin-density functional (GX-LSD) theory, since there are no physical restrictions used to derive equations (1-69) in the G-LSD theory, whereas the physical restrictions are imposed in the GX-LSD theory by assuming equations (1-47)-(1-49) to be correct.

TABLE I-1

The exchange parameters in equation (1-69) obtained using the Homogeneous (H), GWB, Wigner, and the Free-Electron Limit (FEL) Fermi holes

	H[9]	GWB[27]	$Wigner$[26,28]	FEL[22]
A_1	0.500000	0.166667	0.142256	0.119647
A_2	0.333333	0.083333	0.069849	0.057785
B_1	0.0	2.0	2.514776	3.178952
B_2	0.0	3.0	3.772147	4.768428
α^{lim}	0.866173	0.727539	0.698526	0.666667

In equation (1-69), c=$(\frac{3}{4\pi})^{1/3}$ and $\alpha^{lim} = \frac{4}{9}(\frac{2\pi^2}{3})^{1/3} A_1 A_2^{-2/3}$, which is only dependent on the Fermi-hole shape. If the Fermi-hole function $h(u)$ is known, it can be easily used to calculate the parameters for all atoms.

Slater[9] assumed the charge density to be uniform, i.e., homogeneous (H), hence

$$h^H(\mathbf{r}_2) = 1; 0 \leq r_2 \leq r_F \qquad (1-70)$$

Gopinathan, Whitehead, and Bogdanovic[27] (GWB) assumed the Fermi-hole a linear function of r, that is,

$$h^{GWB}(\mathbf{r}_2) = 1 - r_2/r_F; 0 \leq r_2 \leq r_F \qquad (1-71)$$

Gázquez and Keller[26] modified Wigner's approximation[28] (W) to the pair-correlation function of free electrons with spin s, in a seemingly more realistic form

$$h^W(\mathbf{r}_2) = \left[1 + \frac{br_2}{r_F} + b(\frac{r_2}{r_F})^2\right] exp(-br_2/r_F) \qquad (1-72)$$

determining b by requiring the free-electron-gas limit, when the number of the electrons goes to infinity.

Manoli and Whitehead[22] noted that α_s goes to 2/3, when the number of electrons in the system goes to infinity, and obtained the parameters, A_1, A_2, B_1, and B_2 independent of the Fermi-hole shape to give the free-electron-limit (FEL) Fermi-hole parameters.

Table I-1 lists the values of A_1, A_2, B_1, and B_2, and α^{lim} defined as in equations (1-60), (1-61), (1-65), (1-66), and (1-68) and calculated by using the Fermi-hole functions (1-70)-(1-72) and Manoli and Whitehead's FEL Fermi-hole[22].

I-4. The GX-LSD, Ξa, XO-LSD, and Xα Theories

The G-LSD is the master theory of a whole series of theories. Thus, the single-particle exchange energy density expressions in the GX-LSD, Ξa, XO-LSD, and Xα theories can be easily obtained from the G-LSD single-particle exchange energy density formula by using additional approximations.

The GX-LSD theory is based on the physically restricted boundary conditions, equations (1-47)-(1-49), instead of the general boundary conditions of the Fermi-correlation factor, equations (1-44)-(1-46), used in the G-LSD theory. The boundary conditions of the Fermi-correlation factor used in both the G-LSD and GX-LSD theories are generated from the HF limit of the exchange energy expression. Hence, the GX-LSD theory is a restricted G-LSD theory.

Mathematically, the G-LSD theory generates the GX-LSD theory with an additional approximation: if the $\rho_j(\mathbf{r}_1)$ in the term [.....] of the last factor of equation (1-69) is approximated by $\rho_i(\mathbf{r}_1)$, equation (1-69) becomes

$$U_{si}^{GX}(\mathbf{r}_1) = -9c\alpha^{lim}\left[\rho_s(\mathbf{r}_1) + B_1\rho_i(\mathbf{r}_1)\right]\left[\rho_s(\mathbf{r}_1) + B_2\rho_i(\mathbf{r}_1)\right]^{-2/3} \quad (1-73)$$

This is the single-particle exchange energy density in the GX-LSD theory. It can be seen that the only difference from the G-LSD theory is in the last factor.

The Ξa theory is based on the classical approximation, equation (1-17), in deriving the single-particle exchange energy density expression, which can be generated from equation (1-73). Letting $B_1 = -1$, $B_2 = 0$, and $\alpha^{lim} = a_s$, equation (1-73) reduces to

$$U_{si}^{\Xi a}(\mathbf{r}_1) = -9ca_s\left[\rho_s(\mathbf{r}_1) - \rho_i(\mathbf{r}_1)\right]\left[\rho_s(\mathbf{r}_1)\right]^{-2/3} \qquad (1-74)$$

where a_s is an adjustable parameter. This is the expression of a single-particle exchange energy density in the Ξa theory[17].

The boundary conditions of the Fermi-correlation factor used in the G-LSD and Xα theories are however different. The Xα theory can be derived from the G-LSD theory by assuming the free-electron gas homogeneous and using the homogeneous Fermi-hole parameters listed in the column 2 of Table I-1, $B_1 = 0$ and $B_2 = 0$. The single-particle exchange energy density, equation (1-69), reduces to

$$U_{si}^{H}(\mathbf{r}_1) = -9c\alpha^{lim}\rho_s^{1/3}(\mathbf{r}_1) \qquad (1-75)$$

The exchange parameter, α^{lim}, is treated as an adjustable parameter, varying between 2/3 and 1 in the Xα theory[9].

The single-particle exchange energy density expression in the XO-LSD theory can be produced from equation (1-73) for a system with very high and slowly varying electron density. Expanding the last factor on the right-hand side of equation (1-73) as a Taylor series, equation (1-73) reduces to

$$U_{si}^{GX}(\mathbf{r}_1) = -9c\alpha^{lim}\left[\rho_s(\mathbf{r}_1)\right]^{1/3}\left[1 + \frac{B_1\rho_i(\mathbf{r}_1)}{\rho_s(\mathbf{r}_1)}\right]$$
$$\left[1 + \frac{-\frac{2}{3}}{1!}\frac{B_2\rho_i(\mathbf{r}_1)}{\rho_s(\mathbf{r}_1)} + \frac{(-\frac{2}{3})(-\frac{2}{3}-1)}{2!}\frac{B_2^2\rho_i^2(\mathbf{r}_1)}{\rho_s^2(\mathbf{r}_1)} + \ldots\right] \qquad (1-76)$$

Using the fact that $\frac{\rho_i(\mathbf{r}_1)}{\rho_s(\mathbf{r}_1)}$ goes to zero, when $\rho_s(\mathbf{r}_1)$ approaches infinity, and neglecting the higher order terms, equation (1-76) becomes

$$U_{si}(\mathbf{r}_1) = -9c\alpha^{lim}\left[1 + (B_1 - \frac{2}{3}B_2)\frac{\rho_i(\mathbf{r}_1)}{\rho_s(\mathbf{r}_1)}\right]\rho_s^{1/3}(\mathbf{r}_1) \qquad (1-77)$$

Using the FEL parameters in the column 5 of Table I-1, equation (1-77) reduces to

$$U_{si}^{XO-LSD}(\mathbf{r}_1) = -6c\rho_s^{1/3}(\mathbf{r}_1) \qquad (1-78)$$

the single-particle exchange energy density expression in the XO-LSD theory[8].

Consequently, the GX-LSD, Ξa, XO-LSD, and Xα are derived from the G-LSD theory using further approximations.

I-5. The Self-Interaction Correction in the G-LSD Theory

The self-interaction energy in the exchange energy expression, equation (1-37), is cancelled exactly by the identical term in the Coulomb-interaction energy expression; there is no self-interaction problem in HF theory. However in the LDF theory the self-interaction energy term in the Coulomb-energy integral cannot be cancelled by that in the exchange-energy integral, because of the local-density approximation. The self-interaction problem in the LDF theory can be avoided[29-32] by introducing self-interaction correction terms into the Coulomb-energy integral and exchange-energy integral, separately.

The non-zero boundary condition of the Fermi-correlation factor in the G-LSD theory, equation (1-41), as $|\mathbf{r}_1 - \mathbf{r}_2|$ goes to infinity, occurs because of self-interaction. The last term on the right-hand side of equation (1-55) is clearly the self-interaction. Consequently, the self-interaction Fermi-correlation factor may be written as

$$\sum_i \rho_i(\mathbf{r}_2) f_{ss}^{i,SI}(\mathbf{r}_1, \mathbf{r}_2) = \frac{\sum_i \rho_i(\mathbf{r}_1)\rho_i(\mathbf{r}_2)}{\rho_s(\mathbf{r}_1)} \qquad (1-79)$$

in contrast to equation (1-55). The self-exchange energy is, then,

$$\frac{1}{2}\int \sum_i \rho_i(\mathbf{r}_1) U_{si}^{SI}(\mathbf{r}_1) d\mathbf{r}_1$$

$$= \frac{1}{2}\int \rho_s(\mathbf{r}_1)\sum_i \rho_i(\mathbf{r}_2) f_{ss}^{i,SI}(\mathbf{r}_1,\mathbf{r}_2)\frac{2}{|\mathbf{r}_1-\mathbf{r}_2|}d\mathbf{r}_1 d\mathbf{r}_2 \quad (1-80)$$

for electrons with spin s. Substituting equation (1-79) into (1-80), the single-particle self-exchange energy density is

$$U_{si}^{SI}(\mathbf{r}_1) = \int \rho_i(\mathbf{r}_2)\frac{2}{|\mathbf{r}_1-\mathbf{r}_2|}d\mathbf{r}_2 \quad (1-81)$$

where the integral is carried out over the self-interaction Fermi-hole. Applying the local-density approximation, the local and single-particle self-exchange energy density, equation (1-81), reduces to

$$U_{si}^{SI}(\mathbf{r}_1) = 4\pi\rho_i(\mathbf{r}_1)r_{SI}^2 \quad (1-82)$$

where r_{SI} is the self-exchange Fermi-hole radius generated by the electron density $\rho_i(\mathbf{r}_1)$. Excluding the contributions from all other orbitals except for $\rho_i(\mathbf{r}_1)$, equation (1-59) reduces to

$$r_{SI} = \left(\frac{3}{4\pi}\right)^{1/3}\rho_i^{-1/3}(\mathbf{r}_1) \quad (1-83)$$

equation (1-82) for U^{SI} becomes

$$U_{si}^{SI}(\mathbf{r}_1) = 9c\alpha^{SI}\rho_i^{1/3}(\mathbf{r}_1) \quad (1-84)$$

where c equals $\left(\frac{3}{4\pi}\right)^{1/3}$ and $\alpha^{SI} = \frac{4\pi}{9}\left(\frac{3}{4\pi}\right)^{1/3}$. Finally, the self-exchange energy is

$$E^{SI} = \frac{9}{2}c\alpha^{SI}\int\sum_i \rho_i^{4/3}(\mathbf{r}_1)d\mathbf{r}_1 \quad (1-85)$$

The summation in equation (1-85) is over all electrons in the system, including both spin-up and spin-down electrons.

I-6. The One-Electron Schrödinger Equation

In the self-interaction corrected G-LSD (SIC-G-LSD) theory, the statistical total energy may be written as

$$E = \sum_{i} < u_i(\mathbf{r}_1)|f_1|u_i(\mathbf{r}_1) > + \frac{1}{2} \sum_{i,j(i\neq j)} < u_i(\mathbf{r}_1)u_j(\mathbf{r}_2)||u_i(\mathbf{r}_1)u_j(\mathbf{r}_2) >$$
$$+ \frac{1}{2} \sum_{i}^{s} < u_i(\mathbf{r}_1)|U^G_{si}(\mathbf{r}_1)|u_i(\mathbf{r}_1) > + \frac{1}{2} \sum_{i}^{s'} < u_i(\mathbf{r}_1)|U^G_{s'i}(\mathbf{r}_1)|u_i(\mathbf{r}_1) >$$
$$+ \frac{1}{2} \sum_{i}^{s} < u_i(\mathbf{r}_1)|U^{SI}_{si}(\mathbf{r}_1)|u_i(\mathbf{r}_1) >$$
$$+ \frac{1}{2} \sum_{i}^{s'} < u_i(\mathbf{r}_1)|U^{SI}_{s'i}(\mathbf{r}_1)|u_i(\mathbf{r}_1) > \qquad (1-86)$$

where the one-electron operator $\hat{f}_1$ is

$$\hat{f}_1 = -\nabla_1^2 - \frac{2Z}{r_1} \qquad (1-87)$$

and the two-electron operator

$$|| = \frac{2}{|\mathbf{r}_1 - \mathbf{r}_2|} \qquad (1-88)$$

In equation (1-86), the first term is the sum of the kinetic and nucleus-electron attraction energies. The second term is the electron-electron Coulomb interaction energy excluding the self-Coulomb interaction. The third and forth terms correspond to the exchange energies of the electrons with spin up and spin down, respectively. The last two terms are the self-exchange energy corrections. The electron Coulomb-correlation, the correlation of the electrons with different spins (it will be discussed later), is ignored in equation (1-86). The one-particle exchange energy densities, $U^G_{si}(\mathbf{r}_1)$ and $U^G_{s'i}(\mathbf{r}_1)$, and the one-particle self-exchange energy densities, $U^{SI}_{si}(\mathbf{r}_1)$ and $U^{SI}_{s'i}(\mathbf{r}_1)$ are given in equations (1-69) and (1-84), respectively.

Kohn and Sham[8] obtained the one-electron Schrödinger equation by minimizing the total energy, equation (1-86), with respect to a variation in the one-electron wave functions, $u_i(\mathbf{r}_1)$, and preserving normalization

$$\sum_i^s < u_i(\mathbf{r}_1)|u_i(\mathbf{r}_1) > = \int \rho_s(\mathbf{r}_1)d\mathbf{r}_1 = N_s \qquad (1-89)$$

so that,

$$\left[\hat{f}_1 + V_{c_k}(\mathbf{r}_1) + V_{X_k}^G(\mathbf{r}_1) + V_{X_k}^{SI}(\mathbf{r}_1)\right] u_k(\mathbf{r}_1) = \epsilon_k u_k(\mathbf{r}_1) \qquad (1-90)$$

where ϵ_k is the one-electron eigenvalue of orbital k resulting from the Lagrange multiplier required by the normalization condition of the one-electron wave function; the electron-electron Coulomb-interaction potential, $V_{c_k}(\mathbf{r}_1)$, for the k^{th} orbital, excluding the self-interaction, is

$$V_{c_k}(\mathbf{r}_1) = \int \left[\rho_s(\mathbf{r}_2) - \rho_k(\mathbf{r}_2)\right] \frac{2}{|\mathbf{r}_1 - \mathbf{r}_2|} d\mathbf{r}_2 \qquad (1-91)$$

and the one-electron exchange potential, $V_{X_k}^G(\mathbf{r}_1)$, and the self-exchange potential, $V_{X_k}^{SI}(\mathbf{r}_1)$, are

$$V_{X_k}^{G/SI}(\mathbf{r}_1) = \frac{\delta\left[\sum_i < u_i(\mathbf{r}_1)|U_{s_i}^{G/SI}(\mathbf{r}_1)|u_i(\mathbf{r}_1) >\right]}{2\delta\rho_k(\mathbf{r}_1)} \qquad (1-92)$$

in the LDF theory.

Substituting for U^G from equations (1-69) and U^{SI} from equation (1-84) into equation (1-92) gives

$$\begin{aligned} V_{X_k}^G(\mathbf{r}_1) = -\frac{9}{2}c\alpha^{lim}\Bigg\{ & 2\Big[\rho_s(\mathbf{r}_1) + B_1\rho_k(\mathbf{r}_1)\Big]\rho_s^{2/3}(\mathbf{r}_1) \\ & \Bigg[\sum_j \rho_j(\mathbf{r}_1)\Big(\rho_s(\mathbf{r}_1) + B_2\rho_j(\mathbf{r}_1)\Big)\Bigg]^{-2/3} \\ & + \frac{2}{3}\Bigg[\sum_i \rho_i(\mathbf{r}_1)\Big(\rho_s(\mathbf{r}_1) + B_1\rho_i(\mathbf{r}_1)\Big)\Bigg]\rho_s^{-1/3}(\mathbf{r}_1) \end{aligned}$$

$$\left[\sum_j \rho_j(\mathbf{r}_1)\Big(\rho_s(\mathbf{r}_1)+B_2\rho_j(\mathbf{r}_1)\Big)\right]^{-2/3}$$
$$-\frac{4}{3}\Big[\rho_s(\mathbf{r}_1)+B_2\rho_k(\mathbf{r}_1)\Big]\left[\sum_i \rho_i(\mathbf{r}_1)\Big(\rho_s(\mathbf{r}_1)+B_1\rho_i(\mathbf{r}_1)\Big)\right]\rho_s^{2/3}(\mathbf{r}_1)$$
$$\left[\sum_j \rho_j(\mathbf{r}_1)\Big(\rho_s(\mathbf{r}_1)+B_2\rho_j(\mathbf{r}_1)\Big)\right]^{-5/3}\Bigg\} \qquad (1-93)$$

and

$$V_{X_k}^{SI}(\mathbf{r}_1) = 6c\alpha^{SI}\rho_k^{1/3}(\mathbf{r}_1) \qquad (1-94)$$

which are used in equation (1-90).

I-7. Electronic Correlation Correction

In the G-LSD, GX-LSD, and HF theories, the correlation of the electrons with different spins, the Coulomb-correlation of the last two terms in equation (1-30), is ignored. This is because, firstly, the Coulomb-correlation is much smaller than the Coulomb-repulsion interaction between electron-electron and the Fermi-correlation; secondly, the Coulomb-correlation effect is difficult to describe accurately, although it is important in atomic and molecular calculations.

The Coulomb-hole concept is a fundamental idea developed by Wigner[28] for the electron-correlation correction. The hole volume is directly related to the electron density.

A lot of work has been done to define the Coulomb-correlation expression based on the boundary conditions and sum rule of the Coulomb-correlation factors, $f_{ss'}(\mathbf{r}_1,\mathbf{r}_2)$ and $f_{s's}(\mathbf{r}_1,\mathbf{r}_2)$. For example, Keller and Gázquez[33] assumed the Coulomb-correlation charge density to be

$$\rho_s^{Coul}(\mathbf{r}_2) = -\rho_{s'}(\mathbf{r}_1)exp\left[\frac{-cr_2}{r_a}\right]cos\left[\frac{3\pi r_2}{2r_a}\right] \qquad (1-95)$$

where the constants c and r_a were determined by the sum rule and boundary conditions of the Coulomb-correlation factor. Assuming the radius of the Coulomb-hole equal to the radius of the Fermi-hole in the modified Wigner's Fermi-hole model[26], the Coulomb-correlation energy can be written

$$E_{Corr} = \frac{1}{2}\sum_{i}^{s} < u_i(\mathbf{r}_1)|U_s^{Coul}(\mathbf{r}_1)|u_i(\mathbf{r}_1) > + \frac{1}{2}\sum_{i}^{s'} < u_i(\mathbf{r}_1)|U_{s'}^{Coul}(\mathbf{r}_1)|u_i(\mathbf{r}_1) > \qquad (1-96)$$

where the single-particle Coulomb-correlation energy density is

$$U_s^{Coul}(\mathbf{r}_1) = -0.1538\left[1 + \frac{3.7723}{N_s}\right]^{-2/3} \rho_{s'}(\mathbf{r}_1)\rho_s^{-2/3}(\mathbf{r}_1) \qquad (1-97)$$

Normally, the correlation energy correction can be written[34,35] as

$$E_c = \int [\rho_s(\mathbf{r}) + \rho_{s'}(\mathbf{r})]\epsilon_c[\rho_s(\mathbf{r}), \rho_{s'}(\mathbf{r})]d\mathbf{r} \qquad (1-98)$$

The function $\epsilon_c[\rho_s(\mathbf{r}), \rho_{s'}(\mathbf{r})]$ is the single-particle correlation energy density of the homogeneous electron gas with partial densities $\rho_s(\mathbf{r})$ and $\rho_{s'}(\mathbf{r})$ for the spin-up and spin-down electrons. Before evaluating the Coulomb-correlation energy, equation (1-98), the single-particle correlation energy density must be determined.

Alternative parametrized electron correlation expressions have frequently emerged in the literature. Ceperley[36] calculated the energy of a uniform electron gas over a wide range of densities. He used Monte Carlo techniques to sample a correlated wave function for electrons in a finite volume, subject to periodic boundary conditions, and extrapolated the energy per electron to infinite volume. Letting

$$r_s = \left[\frac{4\pi}{3}\rho(\mathbf{r})\right]^{-1/3} \qquad (1-99)$$

and

$$\zeta = (\rho_s - \rho_{s'})/(\rho_s + \rho_{s'}) \qquad (1-100)$$

with

$$\rho(\mathbf{r}) = \rho_s(\mathbf{r}) + \rho_{s'}(\mathbf{r}) \qquad (1-101)$$

Ceperley's parametrization of the correlation energy for $r_s \geq 1$ is

$$\epsilon_c^i = \gamma_i/(1 + \beta_1^i r_s^{1/2} + \beta_2^i r_s) \qquad (1-102)$$

where i=U (unpolarized, ζ=0) or P (polarized, ζ=1). For atomic calculations, the ϵ_c at high densities ($r_s < 1$) and arbitrary polarization $0 \leq \zeta \leq 1$ is also needed. The leading term of the high-density expansion is

$$\epsilon_c^i = A_i ln r_s + B_i + C_i r_s ln r_s + D_i r_s \qquad (1-103)$$

The parametrized constants γ_i, β_1^i, β_2^i, A_i, B_i, C_i, and D_i for i=U and P were given in Perdew and Zunger's paper[30]. Equations (1-102) and (1-103) were used according to whether $r_s > 1$ or $r_s < 1$.

For intermediate spin polarizations $0 < \zeta < 1$, Barth and Hedin[37] first proposed a standard interpolation formula, in which the correlation energy has the same polarization dependence as the exchange energy:

$$\epsilon_c(r_s, \zeta) = \epsilon_c^P(r_s) + f(\zeta)\left[\epsilon_c^F(r_s) - \epsilon_c^P(r_s)\right] \qquad (1-104)$$

where

$$f(\zeta) = \frac{(1+\zeta)^{4/3} + (1-\zeta)^{4/3} - 2}{2^{4/3} - 2} \qquad (1-105)$$

and the superscripts P and F denoted the para- and ferro-magnetic states according to whether ζ =0 or 1.

Stoll, Pavlidou, and Preuss[38] (SPP) proposed that the single-particle correlation energy density ϵ_c^i for the para- and ferro-magnetic states can be written as

$$\epsilon_c^i(r_s) = -C_i\left[(1+\chi_i^3) ln\left(1 + \frac{1}{\chi_i}\right) + \frac{1}{2}\chi_i - \chi_i^2 - \frac{1}{3}\right], (i = P, F) \qquad (1-106)$$

with

$$\chi_P = r_s/11.4, \chi_F = r_s/15.9, C_P = 0.0666, C_F = 0.0406 \qquad (1-107)$$

Stoll et al.[38] suggested that the correlation energies of electrons with the same spin should be removed from the correlation energy expression, equation (1-98), to give the pure Coulomb correlation energy expression

$$E_c = \int [\rho_s(\mathbf{r}) + \rho_{s'}(\mathbf{r})]\epsilon_c[\rho_s(\mathbf{r}), \rho_{s'}(\mathbf{r})]d\mathbf{r} - \int [\rho_s(\mathbf{r})]\epsilon_c[\rho_s(\mathbf{r}), 0]d\mathbf{r}$$
$$- \int [\rho_{s'}(\mathbf{r})]\epsilon_c[0, \rho_{s'}(\mathbf{r})]d\mathbf{r} \qquad (1-108)$$

Recently, Vosko, Wilk, and Nusir[39] (VWN) emphasized refining the correlation part of the energy functional and pointed out inaccuracies in existing formulas for the correlation energy based on interpolating between para- and ferro-magnetic state results. To improve the correlation terms in the LDF theory, Vosko, Wilk, and Nusir used Ceperley and Alder's[40] accurately determined electron liquid correlation energies which had been extended to cover both para- and ferro-magnetic regimes. These results were combined with a new interpolation procedure to improve the accuracy of the spin dependence of the correlation-energy density $\epsilon_c(r_s, \zeta)$ in the range of metallic densities. In the VWN representation, the single-particle correlation energy density for the para- or ferro-magnetic states is

$$\epsilon_c^{\mathrm{I}}(r_s) = A\left\{ ln\frac{\chi^2}{X(\chi)} + \frac{2b}{Q}F(\chi) - \frac{b\chi_0}{X(\chi_0)} \right.$$
$$\left. \left[ln\frac{(\chi-\chi_0)^2}{X(\chi)} + \frac{2(b+2\chi_0)}{Q}F(\chi) \right] \right\} \qquad (1-109)$$

where A, χ_0, b, and c are parameters determined separately for i=P and F, and

$$Q = (4c - b^2)^{1/2}, X(\chi) = \chi^2 + b\chi + c \qquad (1-110)$$

with

$$F(\chi) = tan^{-1}\frac{Q}{(2\chi + b)} \qquad (1-111)$$

TABLE I-2

Fit parameters determined by Vosko, Wilk and Nusair for interpolation of $\epsilon_c^{P,F}(r_s)$ and and $\alpha_c(r_s)$ over the range of $r_s \leq 6$

	A	b	c	x_0
$\alpha_c(r_s)$	−0.033774	1.13107	13.0045	−0.0047584
$\epsilon_c^P(r_s)$	+0.0621841	3.72744	12.9352	−0.10498
$\epsilon_c^F(r_s)$	+0.0310907	7.06042	18.0578	−0.32500

Here $\chi = r_s^{1/2}$. These parameters are listed in Table I-2.

In the LDF theory, the potential is related to the energy by equation (1-92). The correlation potential is

$$\mu_c^{\pm}(\mathbf{r}) = \frac{\partial}{\partial \rho_{\pm}(\mathbf{r})}\left[\rho(\mathbf{r})\epsilon_c(r_s,\zeta)\right] \qquad (1-112)$$

for the spin-up (+) or spin-down (-) orbital. Hence, the correlation potential for an electron of given spin is

$$\mu_c^{\pm}(\mathbf{r}) = \epsilon_c(r_s,\zeta) - \frac{r_s}{3}\frac{\partial \epsilon_c}{\partial r_s} \pm (1 \mp \zeta)\frac{\partial \epsilon_c}{\partial \zeta} \qquad (1-113)$$

Expressing the r_s differentiation in terms of the χ parametrization of equation (1-109) [$\chi = r_s^{1/2}$], the correlation potentials for spin-up and -down electrons are,

$$\mu_c^{\pm}(\mathbf{r}) = \epsilon_c(r_s,\zeta) - \frac{r_s^{1/2}}{6}\left[[1-\zeta^4 f(\zeta)]\frac{\partial \epsilon_c^P}{\partial \chi} + \zeta^4 f(\zeta)\frac{\partial \epsilon_c^F}{\partial \chi} + (1-\zeta^4)\frac{f(\zeta)}{f''(0)}\frac{\partial \alpha_c}{\partial \chi}\right] \pm 4(1 \mp \zeta)\frac{\alpha_c(r_s)}{f''(0)}$$
$$\left[\zeta^3 f(\zeta)\beta_c(r_s) + \frac{[1+\beta_c(r_s)\zeta^4]}{6(2^{1/3}-1)}[(1+\zeta)^{1/3} - (1-\zeta)^{1/3}]\right] \qquad (1-114)$$

where $\alpha_c(r_s)$, the spin stiffness, is also represented in the form of equation (1-109) with the fit parameters given in Table I-2. Letting g(χ) represent the functions

$\epsilon_c^P(\chi)$, $\epsilon_c^F(\chi)$, and $\alpha_c(\chi)$, then the change in g(χ) with χ is,

$$\frac{dg}{d\chi} = A\Bigg\{2\chi^{-1} - \left[1 - \frac{b\chi_0}{X(\chi_0)}\right]\frac{(2\chi+b)}{X(\chi)} - \frac{2b\chi_0}{(\chi-\chi_0)X(\chi_0)} - 4b\left[1 - \frac{(b+2\chi_0)}{X(\chi_0)}\chi_0\right][Q^2 + (2\chi+b)^2]^{-1}\Bigg\} \qquad (1-115)$$

Equations (1-114) and (1-115) give the correlation potentials with

$$\beta_c(r_s) = \frac{f''(0)}{\alpha_c(r_s)}[\epsilon_c^F(r_s) - \epsilon_c^P(r_s)] - 1 \qquad (1-116)$$

I-8. Relativistic Correction

The relativistic effect is important for high-Z atoms, but the "full" relativistic calculation for atoms and molecules is complicated, because the "large" and "small" components should be calculated simutaneously by solving the Dirac equation[41]. Cowan and Griffin[42] described an approximate solution to the Dirac-Hartree-Fock (DHF) equations for atoms. Wood and Boring[43], and Selvaraj and Gopinathan[44] used this approach in the Dirac-Hartree-Fock-Slater (DHFS) and Ξa theories.

The equations for the Dirac "central-field" problem[45-47] ar-

$$\frac{dP_{nk}(r)}{dr} + \frac{\kappa}{r}P_{nk}(r) - \left\{\frac{2}{\alpha} + \frac{\alpha}{2}\left[\epsilon_{nk} - V_{nk}(r)\right]\right\}Q_{nk}(r) = 0 \qquad (1-117)$$

and

$$\frac{dQ_{nk}(r)}{dr} - \frac{\kappa}{r}Q_{nk}(r) + \left\{\frac{\alpha}{2}\left[\epsilon_{nk} - V_{nk}(r)\right]\right\}P_{nk}(r) = 0 \qquad (1-118)$$

where V_{nk}(r) is the "central-field" potential, ϵ_{nk} is the eigenvalue (minus the rest energy of the electron), and κ is the relativistic quantum number,

$$\kappa = \begin{cases} -(l+1), & \text{when j=l+}\frac{1}{2} \\ l, & \text{when j=l-}\frac{1}{2}. \end{cases} \qquad (1-119)$$

α is the fine-structure constant $\frac{1}{137.036}$. $P_{nk}(r)$ and $Q_{nk}(r)$ are the large and small components, respectively.

The second-order differential equation used by Cowan and Griffin[42] is obtained by substituting $Q_{nk}(r)$ from equation (1-117) into equation (1-118) to give

$$\frac{d^2}{dr^2}P_{nk}(r) = (g + f)P_{nk}(r) \qquad (1-120)$$

with

$$g = -\epsilon_{nk} + \frac{l(l+1)}{r^2} + V_{nk}(r) \qquad (1-121)$$

and

$$\begin{aligned}\hat{f} &= -K\left[\epsilon_{nk} - V_{nk}(r)\right]^2 - KB\frac{dV_{nk}(r)}{dr}\left[\frac{d}{dr} - \frac{1}{r}\right] - KB\left[\frac{k+1}{r}\right]\frac{dV_{nk}(r)}{dr} \\ &= H_m(r) + H_D(r) + H_{SO}(r) \qquad (1-122)\end{aligned}$$

where

$$\begin{aligned}K &= \alpha^2/4, \\ B &= \left[1 + \frac{1}{4}\alpha^2(\epsilon_{nk} - V_{nk})\right]^{-1} \qquad (1-123)\end{aligned}$$

The operator $\hat{f}$ is the sum of the mass-velocity H_m, Darwin $H_D(r)$, and spin-orbital coupling $H_{SO}(r)$ terms. For the present the spin-orbital term in the potential is neglected.

When r approaches zero, the asymptotic form of the potential is

$$V_{nk}(r) = -\frac{2Z}{r} \qquad (1-124)$$

The Darwin correction is positive for all orbitals with $l = 0$, and zero for all others (i.e., $l \neq 0$). The equation used by Cowan and Griffin[42] is

$$\begin{aligned}\Bigg\{ &-\frac{d^2}{dr^2} + \frac{l_k(l_k+1)}{r^2} + V_k(r) - \frac{\alpha^2}{4}\left[\epsilon_k - V_k(r)\right]^2 \\ &- \delta_{l_k 0}\frac{\alpha^2}{4}\left[1 + \frac{\alpha^2}{4}[\epsilon_k - V_k(r)]\right]^{-1}\frac{dV_k(r)}{dr}\left[\frac{dP_k/dr}{P_k} - \frac{1}{r}\right]\Bigg\}P_k(r) \\ &= \epsilon_k P_k(r) \qquad (1-125)\end{aligned}$$

In the SIC-GX-LSD and SIC-G-LSD theories, the potential is

$$V_k(r) = -\frac{2Z}{r} + V_{c_k}(r) + V_{X_k}^{GX/G}(r) + V_{X_k}^{SI}(r) \qquad (1-126)$$

and the Coulomb potential, $V_{c_k}(r)$, excluding the self-Coulomb potential, the generalized exchange potential, $V_{X_k}^{GX/G}(r)$, including the self-exchange potential, and the self-exchange potential, $V_{X_k}^{SI}(r)$, for the orbital i were given by equations (1-93) and (1-94) in the SIC-G-LSD theory. In the SIC-GX-LSD theory, the generalized exchange potential $V_{X_k}^{GX}(\mathbf{r})$ is

$$\begin{aligned} V_{X_k}^{GX}(\mathbf{r}) = -\frac{9c}{2}\alpha^{lim}\Bigg[& \sum_j^s [\rho_s(\mathbf{r}) + B_2\rho_j(\mathbf{r})]^{-2/3}\rho_j(\mathbf{r}) \\ & - \frac{2}{3}\sum_j^s [\rho_s(\mathbf{r}) + B_1\rho_j(\mathbf{r})][\rho_s(\mathbf{r}) + B_2\rho_j(\mathbf{r})]^{-5/3}\rho_j(\mathbf{r}) \\ & + [\rho_s(\mathbf{r}) + 2B_1\rho_k(\mathbf{r})][\rho_s(\mathbf{r}) + B_2\rho_k(\mathbf{r})]^{-2/3} \\ & - \frac{2}{3}B_2[\rho_s(\mathbf{r}) + B_1\rho_k(\mathbf{r})][\rho_s(\mathbf{r}) + B_2\rho_k(\mathbf{r})]^{-5/3}\rho_k(\mathbf{r})\Bigg] \end{aligned} \qquad (1-127)$$

and the self-exchange potential, $V_{X_k}^{SI}(\mathbf{r})$, is

$$V_{X_k}^{SI}(\mathbf{r}) = 6c\alpha^{SI}\rho_k^{1/3}(\mathbf{r}) \qquad (1-128)$$

CHAPTER II

EIGENVALUE AND TOTAL ENERGY

II-1. Eigenvalues and Total Energies for Atoms in the SIC-G-LSD and SIC-GX-LSD Theories

Equation (1-90) for the one-electron eigenvalue and wave function using equations (1-91) for the Coulomb-potential, (1-93) for the exchange-potential, and (1-94) for the self-exchange potential in the SIC-G-LSD theory was solved for each orbital by standard self-consistent-field (SCF) procedures[48]; outward numerical integration of each equation was started by means of a small-r series solution, and inward numerical integration by the analytical exponent wave function. The $(i+1)^{th}$ iteration potential was calculated by mixing electron densities from the i^{th} iteration and the $(i-1)^{th}$ iteration. The SCF procedure was complete, when the difference in the wave function between the i^{th} iteration and the $(i-1)^{th}$ iteration was less than 10^{-7} at all mesh points. The statistical total energy, E, in equation (1-86), was obtained from the converged wave function.

Following conventional LDF calculations, the one-electron densities, $\rho_i(\mathbf{r}_1)$, were spherically averaged and, then, used to evaluate the potentials and statistical total energy for the system. This "central field" approximation is most severe for the $2p$ state, which makes a sizable contribution to the total self-interaction correction. However, Perdew and Zunger[30] showed that the self-Coulomb energy for a hydrogenic $2p$ state (with $m_l = 0$) was only 4 percent larger than it would be for the spherically averaged orbital density in the SIC-LSD theory.

Calculations were performed on atoms helium to krypton by means of (i) the SIC-G-LSD theory with the FEL, Wigner, GWP Fermi-hole parameters (henceforth, the SIC-G-LSD-FEL, SIC-G-LSD-W, and SIC-G-LSD-GWB, respectively);

(ii) the SIC-G-LSD theory with the homogeneous Fermi-hole parameters (SIC-G-LSD-H), which is equivalent to the Xα theory with a α=0.866173; (iii) the original SIC-GX-LSD theory with FEL Fermi-hole parameters[22] (SIC-GX-LSD-FEL); and (iv) the self-interaction corrected exchange-only LSD (SIC-XO-LSD) theory[49], because the correlation of electrons with different spins is ignored in both the SIC-XO-LSD and SIC-G-LSD theories. Calculations (i) and (ii) were performed to test the new SIC-G-LSD theory, and calculations (iii) and (iv) were for comparison.

II-1.1 Exchange Energy

Table II-1 shows the statistical total exchange energies including the self-exchange for the four low-Z closed-shell atoms in the SIC-G-LSD theory and compares with those in the SIC-XO-LSD theory[49], and with the total exchange energies in the HF theory[50]. It is clear that the FEL Fermi-hole parameters in the SIC-G-LSD theory gives the best total exchange energy among all Fermi-hole parameters, although it is slightly bigger than the HF exchange energy, because there is no assumption about the Fermi-hole shape in obtaining the FEL Fermi-hole parameters. The difference in percentage between the total exchange energies in the SIC-G-LSD-FEL theory and in the HF theory decreases as the atomic number increases. The SIC-G-LSD theory with the GWB, Wigner, and homogeneous Fermi-hole parameters, in which the exchange parameters are based on an assumed Fermi-hole shape overestimates the exchange effect. This implies that the GWB, Wigner, and homogeneous models overestimate the Fermi-correlation for real systems. But the SIC-XO-LSD theory, which is equivalent to the SIC-G-LSD-H theory with α^{hm} equal to 2/3, instead of 0.866173, underestimates the exchange effect. It is obvious that the Gáspár[7], and Kohn and Sham[8] model underestimates the Fermi-correlation

for a system with low electron density.

Theoretically, the XO-LSD theory is exact for a system with very high and slowly varying electron density and, therefore, underestimates the Fermi-correlation for real systems with finity electron density, since the exchange parameter α, as proven in the $X\alpha$ theory, increases with the number of total electrons in the system decreases. However, the G-LSD theory with the homogeneous Fermi-hole parameters overestimates the Fermi-correlation, because the exchange parameter, α, decreases as the total electrons increases in the Xα theory.

TABLE II-1

The negative of the total exchange energies (Ry) for some closed-shell atoms calculated using the SIC-G-LSD theory with the FEL, GWB, Wigner, and Homogeneous Fermi-hole parameters, compared with those from the SIC-XO-LSD and HF theories

Z	*Atom*	FEL	GWB	W	H	XO-LSD[a]	HF[b]
2	*He*	2.30	2.30	2.30	2.30	1.77	2.05
10	*Ne*	25.38	26.29	25.84	28.92	22.08	24.22
18	*Ar*	62.21	65.02	63.64	72.85	55.74	60.37
36	*Kr*	190.26	201.74	196.15	231.49	177.27	188.31

a. The XO-LSD exchange energy in the SIC-XO-LSD theory, Ref. 4;
b. The HF exchange energy in HF theory, Ref. 50.

II-1.2 Self-Exchange Energy

The self-exchange energies of the four closed-shell atoms listed in Table II-2 in the SIC-G-LSD theory with the FEL, GWB, Wigner, and homogeneous Fermi-hole parameters are compared with those from the SIC-XO-LSD and HF theories. The self-exchange energies for the same atom in the SIC-G-LSD theory using different Fermi-hole parameters are almost the same. This is reasonable, because the formulas of the self-exchange energy expressions are exactly the same and independent of the Fermi-hole parameters in the SIC-G-LSD theory with the FEL, GWB, Wigner, and homogeneous exchange parameters. It is clear that the SIC-G-LSD theory overestimates the self-exchange energies for these atoms and the SIC-XO-LSD theory underestimates them, in comparison with the HF self-exchange energies[50].

In the present theory, the radius of the self-exchange Fermi-hole for the orbital i, equation (1-83), is only dependent on its own electron density. It is clear that the environment of the self-exchange Fermi-hole disturbs it. As in equation (1-59), the radius of the exchange Fermi-hole, r_F, decreases as the number of total electrons in the system increases. This implies the Fermi-hole is squeezed by increasing the electrons in the system. Hence, the self-exchange Fermi-hole radius also should decreases as the electrons increases. Furthermore, the total self-exchange energy, equation (1-85), is exactly equal to the total exchange energy for the helium isoelectronic systems. Consequently, the present self-exchange correction, equations (1-84) and (1-85) overestimate the self-exchange for the systems other than hydrogen and helium isoelectronic systems. However, in the SIC-XO-LSD theory, the self-exchange may be determined in order to cancel the self-interaction for the helium isoelectronic systems. The exchange effect has been already underestimated by the XO-LSD theory for the low-electron density systems. Hence, the self-exchange correction in the SIC-XO-LSD theory is also underestimated.

The exchange energy is exactly equal to the self-exchange energy for the helium isoelectronic system in both the HF and the self-interaction corrected LDF theories, as shown in Tables II-1 and II-2.

TABLE II-2

Self-exchange energies (Ry) for some closed-shell atoms calculated using the SIC-G-LSD theory with the FEL, GWB, Wigner, and Homogeneous Fermi-hole parameters, compared with those from the SIC-XO-LSD and HF theories

Z	*Atom*	FEL	GWB	W	H	XO-LSD[a]	HF[b]
2	*He*	2.30	2.30	2.30	2.30	1.77	2.05
10	*Ne*	21.98	22.04	22.01	22.23	17.02	19.79
18	*Ar*	50.65	50.75	50.70	51.04	39.13	45.42
36	*Kr*	136.37	136.60	136.49	137.16	105.24	121.55

a. The XO-LSD self-exchange energy in the SIC-XO-LSD theory, Ref. 4;
b. The HF self-exchange energy in the HF theory, Ref. 50.

II-1.3 Pure Exchange Energy

Obviously, the effective contribution of the exchange energy to the total energy is the pure exchange energy, excluding the self-exchange energy in any self-interaction corrected LDF theory. Hence, it is interesting to compare the pure exchange energy in the SIC-G-LSD theory with that in the SIC-XO-LSD and the HF theories. In Table II-3, the pure-exchange energies for these atoms in the SIC-G-LSD theory with the FEL, GWB, and Wigner Fermi-hole parameters are less negative than the corresponding pure HF exchange energy. The total exchange energies and the self-exchange energies for these atoms were overestimated by the SIC-G-LSD-FEL, -GWB, and -W theories. Because of the opposite contributions of the total exchange energy and the self-exchange to the statistical total energy, the total exchange energy without the self-exchange correction decreasing the statistical total energy and the total self-exchange energy increasing it, the overestimation of the energies is partly cancelled. Further, the best prediction of the pure exchange energies among all the Fermi-hole parameters in the SIC-G-LSD theory is given by the GWB Fermi-hole parameters in which the overestimation was well balanced by the overestimation of the self-exchange energy. To give an accurate prediction of the statistical total energy in the SIC-G-LSD-FEL theory in which there is no assumption of a Fermi-hole shape, the description of the self-exchange energy has to be improved. The total exchange and self exchange energies are both underestimated in the SIC-XO-LSD theory. But the cancellation of the underestimation due to the total exchange and the self-exchange is worse in the SIC-XO-LSD theory than in the SIC-G-LSD-GWB theory. Consequently, the SIC-G-LSD-GWB theory gives the best total energies for atoms.

TABLE II-3

The negative of the pure exchange energies (Ry) for some closed-shell atoms calculated using the SIC-G-LSD theory with the FEL, GWB, Wigner, and Homogeneous Fermi-hole parameters, compared with those from the SIC-XO-LSD and HF theories

Z	*Atom*	FEL	GWB	W	H	XO-LSD[a]	HF[b]
2	*He*	0.00	0.00	0.00	0.00	0.00	0.00
10	*Ne*	3.40	4.24	3.82	6.70	5.06	4.43
18	*Ar*	11.56	14.26	12.93	21.81	16.61	14.96
36	*Kr*	53.89	65.15	59.66	94.32	72.30	66.76

a. The XO-LSD exchange energy in the SIC-XO-LSD theory, Ref. 4;
b. The HF exchange energy in the HF theory, ref. 50.

II-1.4 Total Energy

The negative of the total energies for the ground states of the atoms helium to krypton in the SIC-G-LSD theory with the FEL, GWB, Wigner, and homogeneous Fermi-hole parameters is summarized in Table II-4, and compared with the HF total energies[51]. As expected, the SIC-G-LSD theory with the GWB Fermi-hole parameters gives the best total energies for these atoms in the present theory with the FEL, GWB, Wigner, and homogeneous Fermi-hole parameters. The differences between the total energies in the SIC-G-LSD-GWB theory and in the HF theory are very small. For example, this difference is about 1 Ry for krypton whose total energy is about 5504.11Ry.

Fig. 2-1 plots the differences of the total energies of the atoms helium to krypton in the SIC-G-LSD theory with the FEL, GWB, Wigner, and homogeneous Fermi-hole parameters compared to the HF theory, against the atomic number. The effect of the different Fermi-hole parameters is shown in Fig. 2-1. The SIC-G-LSD-FEL theory underestimates the total energies for these atoms, because of

TABLE II-4

The negative of the total energies for the ground state of atoms Helium to Krypton in the SIC-G-LSD theory with the FEL, GWB, Wigner, and Homogeneous Fermi-hole parameters, compared with the HF total energies (Ry)

Z	*Atom*	FEL	GWB	W	H	HF[a]
2	*He*	5.7234	5.7234	5.7234	5.7234	5.7234
3	*Li*	14.8576	14.8623	14.8599	14.8805	14.8655
4	*Be*	29.1209	29.1368	29.1288	29.1970	29.1460
5	*B*	48.9557	49.0168	48.9859	49.2292	49.0581
6	*C*	75.1684	75.3185	75.2435	75.7914	75.3772
7	*N*	108.4442	108.7306	108.5886	109.5749	108.8018
8	*O*	149.0975	149.5020	149.3012	150.7100	149.6187
9	*F*	198.1035	198.6797	198.3941	200.3743	198.8186
10	*Ne*	256.1397	256.9426	256.5457	259.2463	257.0941
11	*Na*	322.5438	323.5099	323.0326	326.2697	323.7178
12	*Mg*	397.8445	398.9804	398.4195	402.2139	399.2292
13	*Al*	482.1055	483.4321	482.7771	487.2063	483.7533
14	*Si*	575.7674	577.3153	576.5514	581.7002	577.7086
15	*P*	679.1633	680.9617	680.0750	686.0222	681.4373
16	*S*	792.4124	794.4526	793.4468	800.1824	795.0097
17	*Cl*	916.0141	918.3294	917.1886	924.8031	918.9637
18	*Ar*	1050.2881	1052.9103	1051.6193	1060.1968	1053.6348
19	*K*	1194.6424	1197.5301	1196.1091	1205.5274	1198.3291
20	*Ca*	1349.5044	1352.6626	1351.1091	1361.3827	1353.5161
21	*Sc*	1515.1127	1518.6101	1516.8909	1528.2208	1519.4710
22	*Ti*	1692.0550	1695.9256	1694.0246	1706.4977	1696.8115
23	*V*	1880.6255	1884.9005	1882.8029	1896.5017	1885.7684
24	*Cr*	2081.2253	2086.0119	2083.6664	2098.8879	2086.7104
25	*Mn*	2293.7767	2298.9525	2296.4182	2312.8157	2299.7314
26	*Fe*	2518.5277	2524.1553	2521.4013	2539.1624	2524.8864
27	*Co*	2755.9982	2762.1096	2759.1209	2778.3283	2762.8284
28	*Ni*	3006.4665	3013.0931	3009.8549	3030.5918	3013.7410
29	*Cu*	3270.2884	3277.5356	3273.9977	3296.5485	3277.9256
30	*Zn*	3547.4991	3555.2510	3551.4687	3575.5198	3555.6954
31	*Ga*	3837.7057	3845.9679	3841.9381	3867.5152	3846.5208
32	*Ge*	4141.2764	4150.0685	4145.7820	4172.9414	4150.7182
33	*As*	4458.3837	4467.7248	4463.1723	4491.9654	4468.4764
34	*Se*	4789.0232	4798.9001	4794.0878	4824.4866	4799.7316
35	*Br*	5133.5323	5143.9697	5138.8857	5170.9579	5144.8816
36	*Kr*	5492.0866	5503.1068	5497.7404	5531.5448	5504.1092

a. Reference 51.

the underestimation of the pure exchange energies; but the SIC-G-LSD-H theory overestimates the total energies of atoms due to the overestimation of the pure exchange energies.

Theoretically, the SIC-G-LSD theory with the FEL Fermi-hole parameters should be better than that with the GWB, Wigner, and homogeneous Fermi-hole parameters in giving the statistical total energies of atoms, because the FEL Fermi-hole parameters were based on the asymptotic trend of the exchange parameters, when the number of the electrons in the system goes to infinity. Also the FEL Fermi-hole has the correct high electron-density limit, and does not assume a specific, approximate shape of the Fermi-hole. Table II-1 also showed that the FEL Fermi-hole parameters in the SIC-G-LSD theory gave the best prediction of the total exchange energies for the closed-shell atoms among all the Fermi-hole parameters. Consequently, the deviation of the SIC-G-LSD-FEL theory from the HF theory is mainly attributed to the self-exchange correction, which overestimated the self-exchange interaction.

The SIC-G-LSD theory with the GWB Fermi-hole parameters, as expected, gives very good statistical total energies for atoms in the agreement with the HF results and should therefore be very useful in molecular calculations where the total energy of a molecule is of interest.

FIGURE 2-1

The differences between the total energies of the atoms helium to krypton in the SIC-G-LSD theory with the FEL, GWB, Wigner, and homogeneous Fermi-hole parameters and in the HF theory vs the atomic number Z

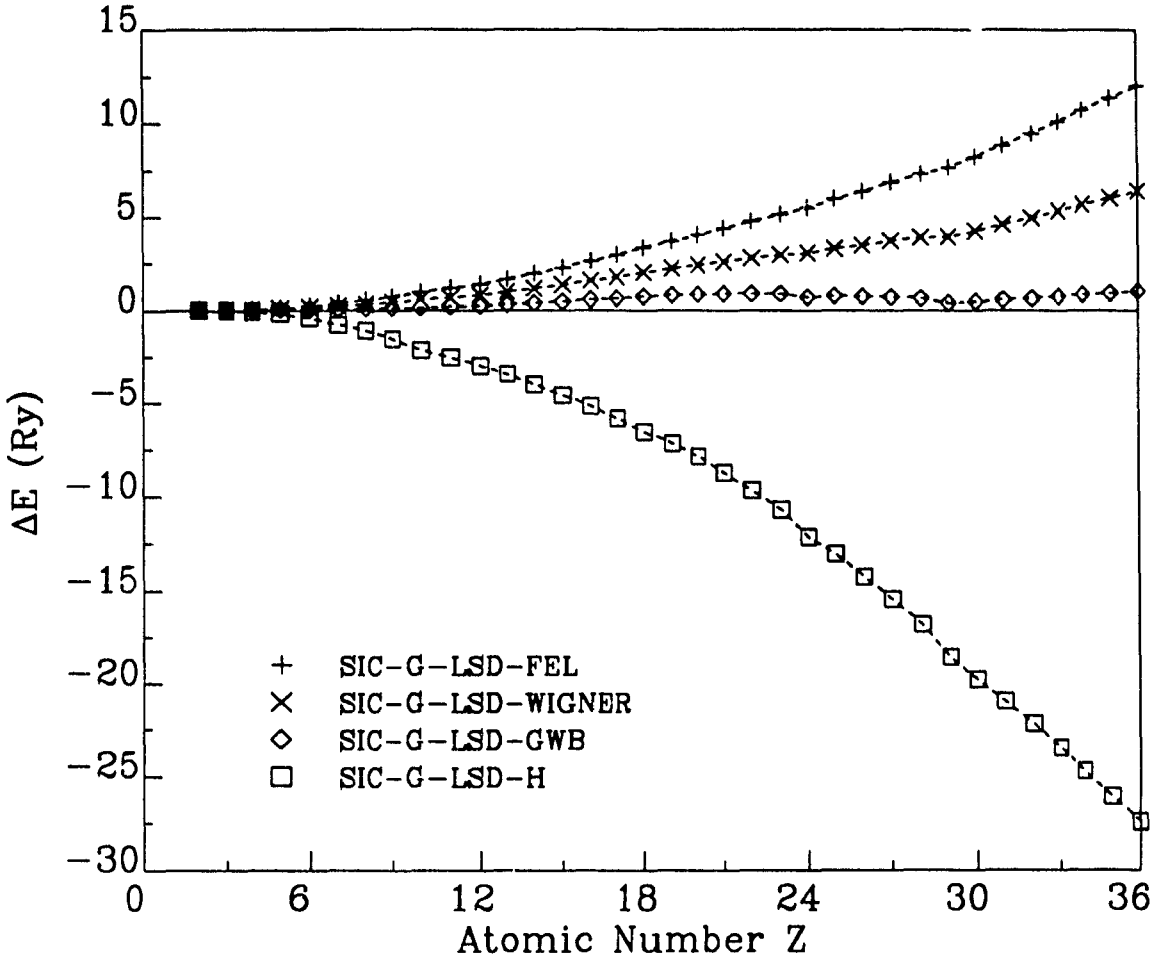

II-1.5 One-Electron Eigenvalue

Tables II-5 and II-6 give the negative of the one-electron eigenvalues for neon and argon, respectively, in the SIC-G-LSD theory with the FEL, GWB, Wigner, and homogeneous Fermi-hole parameters and compares with those in the HF theory. All the one-electron eigenvalues in the SIC-G-LSD theory are less negative than the HF one-electron eigenvalues, except for the 3p orbital in the SIC-G-LSD-H theory. All the 1s- and 2p-orbital eigenvalues are slightly less negative than in the HF theory.

The negative of the one-electron eigenvalue for krypton is presented in Table II-7 and compared with the HF eigenvalues. All the one-electron eigenvalues in the SIC-G-LSD theory with the FEL, GWB, Wigner, and homogeneous Fermi-hole parameters are slightly less negative than those in the HF theory. The one-electron eigenvalues in the SIC-G-LSD-H theory are the most negative among all the Fermi-hole parameters, except for the 1s-orbital. In addition, the one-electron eigenvalues in the SIC-G-LSD-GWB theory are more negative than those in the SIC-G-LSD-FEL and SIC-G-LSD-W theories and less negative than those in the SIC-G-LSD-H theory except for the 1s orbital.

The ionization potential of an atom is exactly equal to the negative of the one-electron eigenvalue of the corresponding orbital in the HF theory, when the frozen orbital approximation is used (Koopmans' theorem). Section II-1.4 has shown that the SIC-G-LSD-GWB theory gives the statistical total energies for atoms in the excellent agreement with the HF total energies. It seems that the one-electron eigenvalues of atoms in the SIC-G-LSD-GWB theory should also be very close to HF, since the self-interaction correction has already been invoked in the SIC-G-LSD theory. But the agreement of the one-electron eigenvalues in the SIC-G-LSD theory with those in the HF theory is not as good as expected. The reason might be as follows.

The ionization potential of the k^{th} orbital of an atom, I_k, can be expressed as

$$I_k \approx -\epsilon_k^{SIC-G-LSD} + \frac{1}{2}\left[\frac{\partial^2}{\partial N_k^2} E_X^G + \frac{\partial^2}{\partial N_k^2} E^{SI}\right] \qquad (2-1)$$

where $\epsilon_k^{SIC-G-LSD}$ is the one-electron eigenvalue of the k^{th} orbital in the SIC-G-LSD theory; E_X^G is the total exchange energy, which is given by the second and third terms in equation (1-86); E^{SI} is the self-exchange energy in equation (1-85); and N_k is the occupation number of the k^{th} orbital. With these substitutions, equation (2-1) becomes

$$I_k \approx -\epsilon_k^{SIC-G-LSD-H} + 0.866173\left(\frac{3}{8\pi}\right)^{1/3} \int \rho_k^2(\mathbf{r})\left\{\left[\rho_k(\mathbf{r})\right]^{-2/3} - \left[\rho(\mathbf{r})\right]^{-2/3}\right\} d\mathbf{r} \qquad (2-2)$$

in the SIC-G-LSD theory with the homogeneous Fermi-hole parameters, under the frozen orbital approximation. The second term in the right-hand side of equation (2-2) is always positive, except for the helium isoelectronic series including helium, that is

$$I_k > -\epsilon_k^{SIC-G-LSD} \qquad (2-3)$$

Consequently, the negative of the one-electron eigenvalue is less than the corresponding ionization potential under the frozen orbital approximation.

TABLE II-5

The negative of the one-electron eigenvalues (Ry) for Neon in the SIC-G-LSD theory with the FEL, GWB, Wigner, and Homogeneous Fermi-hole parameters

Orbital	FEL	GWB	W	H	HF[a]
1s	65.5424	65.4190	65.4792	65.1097	65.5449
2s	3.1170	3.1785	3.1476	3.3744	3.8609
2p	1.4858	1.5512	1.5189	1.7323	1.7009

a. Reference 51.

TABLE II-6

The negative of the one-electron eigenvalues (Ry) for Argon in the SIC-G-LSD theory with the FEL, GWB, Wigner, and Homogeneous Fermi-hole parameters

Orbital	FEL	GWB	W	H	HF[a]
1s	236.7366	236.5968	236.6634	236.3323	237.2208
2s	22.7611	22.9157	22.8384	23.3956	24.6444
2p	18.3898	18.5558	18.4735	19.0303	19.1430
3s	2.0736	2.1158	2.0946	2.2473	2.5547
3p	1.0118	1.0578	1.0352	1.1837	1.1820

a. Reference 51.

II-1.6 Orthogonal Wave Functions

Since the exchange and the self-interaction potentials in the SIC-G-LSD theory are orbital-dependent, the wave functions will be non-orthogonal to those with the same angular quantum number l and different principal quantum number n, at self-consistency. The orthogonalization can be carried out during the SCF procedure. Table II-8 shows the negative of the one-electron eigenvalues for krypton in

TABLE II-7

The negative of the one-electron eigenvalues (Ry)
for Krypton in the SIC-G-LSD theory with the FEL, GWB, Wigner, and
Homogeneous Fermi-hole parameters

Orbital	FEL	GWB	W	H	HF[a]
1s	1038.5165	1038.2977	1038.3972	1038.0930	1040.3306
2s	135.1716	135.5321	135.3505	136.6746	139.8064
2p	123.6149	124.0036	123.8096	125.1497	126.0198
3s	19.4203	19.6063	19.5155	20.0886	21.6990
3p	14.9873	15.1754	15.0841	15.6438	16.6630
3d	7.1007	7.2686	7.1874	7.6768	7.6505
4s	1.9030	1.9443	1.9236	2.0676	2.3058
4p	0.8957	0.9362	0.9163	1.0468	1.0482

a. Reference 51.

the SIC-G-LSD theory with the FEL parameters. Column 2 was obtained without wave function orthogonalization, and column 3 with wave function orthogonalization. The percentage differences of the one-electron eigenvalues between the orthogonal and nonorthogonal calculations are less than 0.03 percent ($2p$-orbital) for krypton. The effect of orthogonalizing the wave function is so small that the one-electron eigenvalues in Tables II-5, II-6, and II-7 were obtained without orthogonalization of the wave function. The same conclusion was reached in Refs. 22 and 30.

II-1.7 Comparison of the Total Energy in the SIC-G-LSD Theory with those in the SIC-GX-LSD and SIC-XO-LSD Theories

Table II-9 compares the total energies of the atoms helium to argon in the SIC-G-LSD-FEL theory with those in the original SIC-GX-LSD theory with the FEL Fermi-hole parameters and the conventional SIC-XO-LSD theory. The results

TABLE II-8

Comparison of the one-electron eigenvalues (Ry) of Krypton calculated using the orthogonal and non-orthogonal wave functions in the SIC-G-LSD theory with the FEL Fermi-hole parameters

Orbital	Nonorthogonal	Orthogonal
1s	1038.5165	1038.6725
2s	135.1716	135.2054
2p	124.6149	124.6585
3s	19.4203	19.4210
3p	14.9873	14.9883
3d	7.1007	7.0997
4s	1.9030	1.9030
4p	0.8957	0.8957

show that there is no significant difference of the total energies between the SIC-G-LSD and SIC-GX-LSD theories, although the SIC-GX-LSD theory was based on a physical restriction to the Fermi correlation correction, equations (1-47) to (1-49). The SIC-G-LSD total energies for these atoms are slightly better than the SIC-GX-LSD results. The agreement of the total energies in the SIC-G-LSD and SIC-GX-LSD theories with the same Fermi-hole parameters are the same up to the fifth digit. The total energies of atoms are slightly underestimated by both the SIC-G-LSD and SIC-GX-SIC theories with the FEL parameters, because of the underestimation of the pure-exchange energy (section II-1.3). The SIC-XO-LSD theory slightly overestimated the total energies for these atoms in comparison with the HF results. This is reasonable, because the SIC-XO-LSD theory overestimated the pure exchange energies listed in Table II-3 for atoms.

Comparing the total energies listed in the column 4 of Table II-4 and the column 5 in Table II-9 with those in the HF theory listed in column 6 of Table II-9 shows that the SIC-G-LSD theory with the GWB Fermi-hole parameters gives

much better results than the SIC-XO-LSD theory, because the SIC-G-LSD theory with the GWB parameters correctly estimates the pure exchange energies for these atoms.

Comparison of the statistical total energies for the atoms in the SIC-G-LSD and SIC-GX-LSD theories shows that the physical restriction made in deriving the GX-LSD theory, equations (1-47) to (1-49) is theoretically and mathematically significant, but does not result in large numerical error. Therefore, the GX-LSD theory is still useful for atomic calculations.

In conclusion, the G-LSD theory was derived based on the general boundary conditions of the Fermi-correlation factor which are from the Hartree-Fock limit, compared to the GX-LSD theory which was based on physically restricted boundary conditions. Consequently, the G-LSD theory is an extension of the GX-LSD theory and more general in describing the inhomogeneous electron-density system theoretically.

The exchange parameters in the G-LSD theory are fixed once the Fermi-hole shape is chosen or by using the free-electron-limit proposed by Manoli and Whitehead[22]. This avoided the time-consuming step in searching the optimal exchange parameters in the $X\alpha$ theory for each atom or ion.

Numerically, the SIC-G-LSD theory gives the statistical total energies for atoms in excellent agreement with the HF theory, and is much better than the SIC-XO-LSD theory, when the GWB exchange parameters are employed. Furthermore, the one-electron eigenvalues in the SIC-G-LSD theory with the GWB Fermi-hole parameters are reasonable good compared with those in the HF theory.

TABLE II-9

Comparison of the negative of the total energies (Ry) for the ground state of atoms (Z=1-18) in the SIC-G-LSD-FEL theory with those in the SIC-GX-LSD-FEL, SIC-XO-LSD, and HF theories

Z	Atom	G-LSD	GX-LSD[a]	XO-LSD[b]	HF[c]
2	*He*	5.7234	5.7234	5.7234	5.7234
3	*Li*	14.8576	14.8565	14.8678	14.8655
4	*Be*	29.1209	29.1173	29.1554	29.1460
5	*B*	48.9557	48.9498	49.0971	49.0581
6	*C*	75.1684	75.1608	75.4894	75.3772
7	*N*	108.4442	108.4352	109.0125	108.8018
8	*O*	149.0975	149.0854	149.9250	149.6187
9	*F*	198.1035	198.0893	199.2707	198.8186
10	*Ne*	256.1397	256.1242	257.7178	257.0941
11	*Na*	322.5438	322.5265	324.4349	323.7178
12	*Mg*	397.8445	397.8260	400.0554	399.2292
13	*Al*	482.1055	482.0864	484.6824	483.7533
14	*Si*	575.7674	575.7495	578.7554	577.7086
15	*P*	679.1633	679.1471	682.5983	681.4373
16	*S*	792.4124	792.3985	796.2969	795.0097
17	*Cl*	916.0141	916.0037	920.3935	918.9637
18	*Ar*	1050.2881	1050.2816	1055.1990	1053.6348

a. The statistical total energy in the SIC-GX-LSD theory, Ref. 22;
b. The statistical total energy in the SIC-XO-LSD theory, Ref. 30;
c. The HF total energy, Ref. 51.

II-2. Eigenvalues and Total Energies for Negative Ions

The investigation of negative ions is very interesting topic, because it not only leads to understanding the microscopic electronic structure and to understanding the stability of the matter[52], but it also tests the theory itself. The accurate description for the electron structure of negative ions is much more difficult than that of neutral atoms and positive ions, because it is very sensitive to the exchange and self-interaction potentials and the electron-correlation.

Theoretically, the G-LSD theory is more rigorous than the GX-LSD theory in deriving their single-particle exchange energy-density expressions. But, numerically, as shown in the above section, the statistical total energies of atoms in the G-LSD theory and the GX-LSD theory are very close (up to the first five digits). All the following calculations were done by the GX-LSD theory and preceded the development of the G-LSD theory.

The SCF calculation for the negative ions B^-, C^-, O^-, F^-, Na^-, Al^-, Si^-, S^-, and Cl^- and the corresponding neutral atoms were performed using the SIC-GX-LSD theory, equation (1-90) combining equations (1-91), (1-127), and (1-128), with the FEL, Wigner, GWB, and homogeneous Fermi-hole parameters (henceforth called the GX-FEL, GX-W, GX-GWB, and GX-H, respectively). The results are as follows.

II-2.1 One-Electron Eigenvalues

Table II-10 gives the one-electron eigenvalues and averaged one-electron eigenvalues of each orbital; the averaged one-electron eigenvalue was defined as

$$\epsilon_{nl_{av}} = (\epsilon_{nl\uparrow} N_{nl\uparrow} + \epsilon_{nl\downarrow} N_{nl\downarrow})/(N_{nl\uparrow} + N_{nl\downarrow}) \qquad (2-4)$$

They are compared to the Ξa eigenvalues of Sen[53] and the HF eigenvalues of Clementi and Roetti[51].

The GX-FEL, GX-W, GX-GWB, and GX-H eigenvalues of the 1s electrons for all the negative ions are in very good agreement with those of HF. Almost all the eigenvalues of the 2s orbital are slightly higher than those of HF as are the eigenvalues of the 2p electron which are not in the outermost electron. The GX-H eigenvalues of the 2p electron are very close to the HF eigenvalues. They are

better than those calculated with the Ξa theory[53]. For the outermost electrons, the GX-FEL, GX-W, and GX-GWB eigenvalues are greater than those of HF, while the GX-H eigenvalues are closer to those of HF except for Na^-. All of the GX eigenvalues are closer to those of HF than the Ξa eigenvalues.

According to Koopmans' approximation[54], the one-electron eigenvalues in the HF theory are equal to the binding energies of the electrons, under the frozen orbital approximation Table II-10 shows that the SIC-GX-LSD theory is the best in describing the electron binding energies of negative ions.

In both the SIC-GX-LSD and Ξa theories, the self-interaction of the electron has been removed; therefore, the one-electron eigenvalue in both theories should approximately equal the corresponding one-electron energy (i.e. the orbital energy) in the HF theory. However, this is not true for the negative ions. The accuracy of the self-interaction correction is measured by comparing the one-electron eigenvalues. From Table II-10, the one-electron eigenvalues for the $1s$ and np electrons are in much better agreement with those of the HF than those in the Ξa theory. For the $2s$ and $3s$ electrons, the Ξa theory is a little better than the SIC-GX-LSD theory. Table II-10 shows that the self-interaction correction in both the SIC-GX-LSD and Ξa theories is not perfect for the negative ions. Nevertheless, the self-interaction correction in the SIC-GX-LSD theory is more accurate than that in the Ξa theory.

TABLE II-10

The negative of the one-electron eigenvalues (Ry) of the ground states of several negative ion calculated using the SIC-GX-LSD theory with the FEL, Wigner, GWB, and H Fermi-hole parameters, compared to the results from the Ξa and HF theories.

Ion	$(nl)_\sigma$	FEL	W	GWB	H	Ξ_a^a	HF[b]
B^-	$1s\uparrow$	14.9855	14.9406	14.8982	14.6855		
	$1s\downarrow$	14.9675	14.9197	14.8741	14.6372		
	$1s_{av}$	14.9765	14.9302	14.8861	14.6614		14.8494
	$2s\uparrow$	0.5536	0.5416	0.5321	0.5250		
	$2s\downarrow$	0.4575	0.4289	0.4021	0.2777		
	$2s_{av}$	0.5055	0.4853	0.4671	0.4014		0.4847
	$2p\uparrow$	0.0186	0.0228	0.0276	0.0700		0.0526
C^-	$1s\uparrow$	22.0403	21.9910	21.9447	21.7125		
	$1s\downarrow$	21.9856	21.9292	21.8757	21.5947		
	$1s_{av}$	22.0129	21.9601	21.9102	21.6536		21.9122
	$2s\uparrow$	0.7392	0.7425	0.7475	0.8096		
	$2s\downarrow$	0.5304	0.5032	0.4781	0.3605		
	$2s_{av}$	0.6348	0.6228	0.6128	0.5850		0.7454
	$2p\uparrow$	0.0792	0.0906	0.1025	0.1815		0.1538
O^-	$1s\uparrow$	40.5383	40.4786	40.4209	40.1102		
	$1s\downarrow$	40.4919	40.4271	40.3646	40.0257		
	$1s_{av}$	40.5151	40.4528	40.3928	40.0679	39.417	40.3963
	$2s\uparrow$	1.3457	1.3595	1.3731	1.4610		
	$2s\downarrow$	1.2304	1.2302	1.2309	1.2592		
	$2s_{av}$	1.2881	1.2948	1.3020	1.3605	1.574	1.6265
	$2p\uparrow$	0.2651	0.2813	0.2970	0.3862		
	$2p\downarrow$	0.0795	0.0875	0.0961	0.1573		
	$2p_{av}$	0.1908	0.2038	0.2167	0.2946	0.479	0.2585
F^-	$1s\uparrow\downarrow$	51.7489	51.6768	51.6080	51.2429	50.529	51.6590
	$2s\uparrow\downarrow$	1.6171	1.6306	1.6445	1.7417	2.009	2.1489
	$2p\uparrow\downarrow$	0.2504	0.2675	0.2846	0.3860	0.628	0.3617
Na^-	$1s\uparrow\downarrow$	80.5681	80.5084	80.4511	80.1506		80.6628
	$2s\uparrow\downarrow$	4.3615	4.4027	4.4429	4.6777		5.2995
	$2p\uparrow\downarrow$	2.4311	2.4697	2.5077	2.7253		2.7418
	$3s\uparrow\downarrow$	0.0273	0.0277	0.0280	0.0295		0.0249
Al^-	$1s\uparrow$	116.4973	116.4254	116.3568	116.0076		
	$1s\downarrow$	116.4945	116.4223	116.3533	116.0014		
	$1s_{av}$	116.4959	116.4238	116.3550	116.0045		116.6161
	$2s\uparrow$	8.2902	8.3316	8.3721	8.6207		
	$2s\downarrow$	8.2858	8.3267	8.3669	8.6123		
	$2s_{av}$	8.2880	8.3291	8.3697	8.6165		9.4323
	$2p\uparrow$	5.7088	5.7474	5.7858	6.0172		
	$2p\downarrow$	5.7035	5.7414	5.7791	6.0068		
	$2p_{av}$	5.7062	5.7444	5.7824	6.0120		6.9503
	$3s\uparrow$	0.4878	0.4801	0.4735	0.4611		
	$3s\downarrow$	0.4374	0.4209	0.4052	0.3281		
	$3s_{av}$	0.4626	0.4505	0.4394	0.3946		0.4176
	$3p\uparrow$	0.0163	0.0191	0.0222	0.0479		0.0397

TABLE II-10 (Continued)

The negative of the one-electron eigenvalues (Ry) of the ground states of several negative ion calculated using the SIC-GX-LSD theory with the FEL, Wigner, GWB, and H Fermi-hole parameters, compared to the results from the Ξa and HF theories

Ion	$(nl)_s$	FEL	W	GWB	H	Ξ_a^a	HF[b]
Si^-	$1s\uparrow$	136.9239	136.8526	136.7849	136.4491		
	$1s\downarrow$	136.9138	136.8414	136.7728	136.4302		
	$1s_{av}$	136.9188	136.8470	136.7789	136.4396		137.1058
	$2s\uparrow$	10.5079	10.5561	10.6041	10.8968		
	$2s\downarrow$	10.4926	10.5395	10.5862	10.8724		
	$2s_{av}$	10.5002	10.5478	10.5951	10.8846		11.7933
	$2p\uparrow$	7.5867	7.6326	7.6785	7.9565		
	$2p\downarrow$	7.5684	7.6126	7.6569	7.9260		
	$2p_{av}$	7.5776	7.6226	7.6677	7.9416		7.9957
	$3s\uparrow$	0.6223	0.6233	0.6255	0.6602		
	$3s\downarrow$	0.5069	0.4906	0.4756	0.4050		
	$3s_{av}$	0.5646	0.5570	0.5505	0.5326		0.6030
	$3p\uparrow$	0.0619	0 0697	0.0778	0.1297		0.1230
S^-	$1s\uparrow$	183.0350	182.9661	182.9006	182.5783		
	$1s\downarrow$	183.0265	182.9568	182.8907	182.5637		
	$1s_{av}$	183.0308	182.9615	182.8956	182.5710		183.3519
	$2s\uparrow$	15.7820	[illegible]8446	15.9062	16.2721		
	$2s\downarrow$	15.7703	15 8320	15.8927	16.2547		
	$2s_{av}$	15.7762	15.8383	15.8995	16.2634		17.3503
	$2p\uparrow$	12.1556	12 2168	12.2774	12.6335		
	$2p\downarrow$	12.1414	12.2014	12.2610	12.6123		
	$2p_{av}$	12.1485	12.2091	12.2692	12.6229		12.7099
	$3s\uparrow$	0.9662	0.9746	0.9833	1.0451		
	$3s\downarrow$	0.9088	0.9099	0.9118	0.9395		
	$3s_{av}$	0.9375	0.9423	0.9476	0.9923		1.1586
	$3p\uparrow$	0.1671	0 1794	0.1916	0.2615		
	$3p\downarrow$	0.1004	0.1069	0.1138	0.1608		
	$3p_{av}$	0.1404	0 1504	0.1604	0.2213		0.2148
Cl^-	$1s\uparrow\downarrow$	208.6252	208.5544	208.4875	208.1638	207.647	209.0103
	$2s\uparrow\downarrow$	18.7515	18.8182	18.8842	19.2790	20.203	20.4578
	$2p\uparrow\downarrow$	14.7599	14.8258	14.8912	15.2790	16.165	15.3907
	$3s\uparrow\downarrow$	1.1256	1.1347	1.1442	1.2123	1.386	1.4659
	$3p\uparrow\downarrow$	0.2008	0.2139	0.2267	0.3031	0.468	0.2998

a. Reference 53;
b. Reference 51.

II-2.2 Difference of Total Energies

Table II-11 gives the negative of the statistical total energies of the ground state for several atoms and negative ions and the HF energies[51]. The total energies of the atoms and the corresponding negative ions are calculated separately by using equation (1-86) in the SIC-GX-LSD theory. The binding energies of the outermost electron for these negative ions in the corresponding ground states calculated by using the difference of the statistical total energies between the atoms and the corresponding negative ions, and those obtained using experimental methods given by Refs. 55 and 56 are listed in Table II-11.

It can be seen that the GX-GWB and GX-H results are closer to the experimental values than those of the GX-FEL and GX-W. But the GX-GWB binding energies are smaller, and the GX-H binding energies larger, than the corresponding experiment; they are better than the HF and Xα results. It is difficult to estimate the binding energies of the negative ions by using the HF and Xα theories, since they are unreliable; for example, the binding energy for B^- is negative in the HF and Xα theories, and therefore B^- is unstable; but experimentally B^- is stable.

The differences between the theoretical and experimental values in Table II-11 occur for two reasons. First, the binding energy is expressed as a small difference between two large quantities, one is the total energy for the neutral atom, and another is for the corresponding negative ion, and therefore subject to numerical errors; secondly, the correlation effects between electrons of different spin directions are neglected. Raghavachari[57] has used Moller-Plessert perturbation theory to calculate the binding energies for the first row negative ions and discussed the electron correlation effects on the negative ions. The electron correlation correction has to be considered in calculating negative ions of atoms.

TABLE II-11

The negative of the statistical total energies of the ground states for several atoms and negative ions, calculated using the SIC-GX-LSD theory with the FEL, Wigner, GWB, and H, Fermi-hole, and the energy differences Δ_{SCF}, compared to the results obtained using the HF and Xα, and experiment (Ry).

Z	FEL	Wigner	GWB	H	HF[a]	Xα[b]	Expt.[c]
B^-	48.9294	48.9759	49.0222	49.3103	49.0384		
B	48.9506	48.9841	49.0180	49.2292	49.0581		
Δ_{SCF}	−0.0212	−0.0082	0.0042	0.0811	−0.0197	−0.054	0.0204
C^-	75.1910	75.2944	75.3854	75.9832	75.4176		
C	75.1615	75.2417	75.3209	75.7914	75.3772		
Δ_{SCF}	0.0295	0.0527	0.0745	0.1918	0.0404	−0.013	0.0932
O^-	149.0626	149.2973	149.5257	150.8395	149.5790		
O	149.0859	149.2999	149.5083	150.7101	149.6187		
Δ_{SCF}	−0.0233	−0.0026	0.0174	0.1294	−0.0397	0.098	0.1075
F^-	198.1983	198.5355	198.8624	200.7074	198.9187		
F	198.0899	198.3934	198.6884	200.3743	198.8186		
Δ_{SCF}	0.1084	0.1421	0.1740	0.3331	0.1001	0.168	0.2498
Na^-	322.5245	323.0327	323.5237	326.2713	323.7093		
Na	322.5269	323.0341	323.5246	326.2697	323.7178		
Δ_{SCF}	−0.0025	−0.0014	−0.0009	0.0016	−0.0085	0.012	0.0401
Al^-	482.0873	482.7921	483.4724	487.2719	483.7556		
Al	482.0869	482.7835	483.4561	487.2063	483.7534		
Δ_{SCF}	0.0004	0.0086	0.0163	0.0656	0.0022	−0.028	0.0325
Si^-	575.8010	576.6279	577.4252	581.8577	577.7789		
Si	575.7500	576.5619	577.3450	581.7002	577.7086		
Δ_{SCF}	0.0510	0.0660	0.0802	0.1575	0.0703	0.022	0.1018
S^-	792.4631	793.5459	794.5879	800.3543	795.0764		
S	792.3992	793.4676	794.4957	800.1825	795.0097		
Δ_{SCF}	0.0639	0.0783	0.0922	0.1718	0.0667	0.147	0.1527
Cl^-	916.1712	917.4046	918.5906	925.1231	919.1534		
Cl	916.0045	917.2156	918.3801	924.8032	918.9637		
Δ_{SCF}	0.1667	0.1890	0.2105	0.3199	0.1897	0.221	0.2657

a. Reference 51;
b. Reference 55;
c. References 56 and 58.

CHAPTER III

IONIZATION POTENTIAL AND ELECTRON AFFINITY

III-1. Introduction

The local-density functional (LDF) theory is often used to calculate atoms, molecules, and the solid state, and has been successful in describing the molecular bonding[59,60], magnetism[61-63], cohesion[61-64], surface electronic properties of metals[65,66] and semiconductors[67-69]. However, the calculation of accurate electron affinities and the stability of negative ions has proved difficult[57]: most stable negative ions, such as H^-,[70] O^-,[71] F^-, and Cl^-[53] are unstable in the Xα and other LDF theories. The correlation effect of the electrons with different spins is often neglected in these theories and consequently, the results are not in good agreement with experiment. Schwarz[71] compared the Xα and HF exchange potentials for some stable negative ions, and showed that the stability of the negative ions is related to the one-electron energies in the two theories. Sen[53] calculated the one-electron eigenvalues for the negative ions O^-, F^-, and Cl^- with the Ξa theory, and suggested that the instability of the stable negative ions arises from too crude a treatment of the self-interaction potential.

The existence of stable negative ions is well known[58,72]. Most neutral atoms in the periodic table bind an extra electron to form stable negative ions. Theoretical investigation of the structures is difficult because the contribution of the electron correlation correction to the electron affinity of an atom might be larger than the kinetic, Coulomb, and exchange energies[57,73,74]. Therefore the HF theory, which is an accurate and simple procedure but does not include electron correlation, usually gives wrong electron affinities for atoms[74].

Since the papers which dealt with the self-interaction correction[29-31,75] and electron correlation correction[38,39,75] in the LDF theory, the SIC-LDF theory with electron correlation correction has successfully predicted electronic structures of negative ions[30,49]. The calculated electron affinities for most atoms are in excellent agreement with experiment.

The ionization potentials and electron affinities for atoms have attracted experimental measurements and theoretical calculations using the HF and LDF theories, especially using the accurate multiconfiguration self-consistent field (MC-SCF) and configuration interaction (CI) methods. Most of these methods have been quite successful in describing ionization potentials for atoms, but the HF, Xα, spin-polarized Xα (SP-Xα), Hyper-Hartree-Fock (HHF), and the SIC-GX-LSD theories cannot describe the negative ions exactly, because the Coulomb correlation is neglected.

Obviously, the ionization potential and electron affinity are the very important concepts in understanding the microscopic structure of matter. Theoretical calculations of ionization potentials and electron affinities can be used to test the theory itself. Therefore, the SIC-GX-LSD theory will be applied to evaluate the ionization potentials and electron affinities for the ordinary atoms.

By the definition, the ionization potential is

(i) approximately the negative of the one-electron eigenvalue in the self-interaction corrected LDF (SIC-LDF) theory under the frozen orbital approximation, that is

$$I_k \approx -\epsilon_k^{SIC-LDF} \qquad (3-1)$$

(ii) the difference between the total energies, which include the statistical total energy from equation (1-86) and the electron-correlation energy from equation

(1-98), of the original system and the ionized system, under the frozen orbital approximation is,

$$I_k = E_{tot}^{unrel}(N_k = 0) - E_{tot}^{unrel}(N_k = 1) \qquad (3-2)$$

(iii) the negative of one-electron eigenvalue generated by removing a half-electron from the corresponding orbital to infinity in the self-interaction uncorrected LDF theory (Slater transition state theory) is,

$$I_k \approx -\epsilon_k|_{N_k=1/2} \qquad (3-3)$$

and finally, (iv) the ionization potential equals the difference between two statistical total energies, one for the non-ionized system and another for the ionized system obtained by two separated self-consistent-field calculations

$$I_k = E_{tot}^{rel}(N_k = 0) - E_{tot}^{rel}(N_k = 1) \qquad (3-4)$$

The electron affinity is identical to the ionization potential for the corresponding negative ion of an atom. Each method has its own advantages and disadvantages. For example, although (i), (ii), and (iii) are computationally easier than (iv), the relaxation effect in the ionization process is totally neglected in (i) and (ii) and partly ignored in (iii). Method (iv) is computationally expensive and can have numerical errors, since the ionization potential and electron affinity are small differences of two large numbers, although the relaxation of the ionization process is fully considered.

The self interaction uncorrected GX-LSD (GX-LSD) theory and self interaction corrected GX-LSD (SIC-GX-LSD) theory will be applied for atoms, and tested for the efficiency for atoms.

III-2. Ionization Potential and Electron Affinity under the Frozen-Orbital Approximation

In the LDF theory, the statistical total energy of an atom is a function of the occupation number, N_i. A Taylor-series expansion of the energy around the neutral atom value is

$$\begin{aligned} E(N_1, N_2, ..., N_i, ..., N_r) - E(N_1, N_2, ..., N_{i_0}, ..., N_r) \\ = (N_i - N_{i_0})\frac{\partial E}{\partial N_i}|_{N_i=N_{i_0}} \\ + \frac{(N_i - N_{i_0})^2}{2!}\frac{\partial^2 E}{\partial N_i^2}|_{N_i=N_{i_0}} + ... \end{aligned} \qquad (3-5)$$

The first term in the right-hand side of equation (3-5) is the electronegativity[76] and the second term, the hardness[77] of the atom. Because the electronegativity and hardness are related to the chemical potential and the hardness and softness of acids and bases, they have received much attention[55,78-80]. Equation (3-5) gives the ionization potential of the atom for $N_i - N_{i_0} = -1$ and the electron affinity for $N_i - N_{i_0} = 1$ under the frozen orbital approximation.

In the GX-LSD theory, the statistical total energy for an atom is given in equation (1-86). The total energy of the system is a function of the occupation number N_i; therefore, the first through fourth derivatives with respect to the occupation number are[81]

$$\begin{aligned} \left[\frac{\partial E}{\partial N_j}\right]_{N_i \neq N_j} &= < u_j(\mathbf{r})|f|u_j(\mathbf{r}) > + \sum_i N_i < u_i(\mathbf{r})u_j(\mathbf{r}')||u_i(\mathbf{r})u_j(\mathbf{r}') > \\ &- \frac{9}{2}c\alpha^{lim} < u_j(\mathbf{r})|[f_j(\mathbf{r}) + B_1\rho_j(\mathbf{r})]g_j^{-2/3}(\mathbf{r}) + \sum_i N_i\rho_i(\mathbf{r})g_i^{-2/3}(\mathbf{r}) \\ &- \frac{2}{3}\sum_i N_i\rho_i(\mathbf{r})(1 + B_2\delta_{ij})f_i(\mathbf{r})g_i^{-5/3}(\mathbf{r})|u_j(\mathbf{r}) > \\ &= \epsilon_j \end{aligned} \qquad (3-6)$$

$$\left[\frac{\partial^2 E}{\partial N_j^2}\right]_{N_i \neq N_j} = < u_j(\mathbf{r})u_j(\mathbf{r}')||u_j(\mathbf{r})u_j(\mathbf{r}') > -9c\alpha^{lim} < u_j^2(\mathbf{r})|(1 + B_1)g_j^{-2/3}(\mathbf{r})$$

$$- \frac{2}{3}[(1+B_2)f_j(\mathbf{r}) + (B_1+B_2+B_1B_2)\rho_j(\mathbf{r})]g_j^{-5/3}(\mathbf{r})$$
$$+ \frac{5}{9}B_2(2+B_2)\rho_j(\mathbf{r})f_j(\mathbf{r})g_j^{-8/3}(\mathbf{r}) - \frac{2}{3}\sum_i N_i\rho_i(\mathbf{r})g_i^{-5/3}(\mathbf{r})$$
$$+ \frac{5}{9}\sum_i N_i\rho_i(\mathbf{r})f_i(\mathbf{r})g_i^{-8/3}(\mathbf{r})|u_j^2(\mathbf{r}) > \qquad (3-7)$$

$$\left[\frac{\partial^3 E}{\partial N_j^3}\right]_{N_i\neq N_j} = -9c\alpha^{lim} < u_j^3(\mathbf{r})| - 2(1+B_1)(1+B_2)g_j^{-5/3}(\mathbf{r})$$
$$+ \frac{5}{9}\Big\{3(1+B_2)^2 f_j(\mathbf{r}) + \Big[3B_2(1+B_1)(1+B_2) + 2B_1$$
$$+ 3B_1B_2 + B_2\Big]\rho_j(\mathbf{r})\Big\}g_j^{-8/3}(\mathbf{r})$$
$$- \frac{40}{27}B_2(1+B_2)(2+B_2)\rho_j(\mathbf{r})f_j(\mathbf{r})g_j^{-11/3}(\mathbf{r})$$
$$+ \frac{5}{9}\sum_i N_i\rho_i(\mathbf{r})\Big[3 + (B_1+2B_2)\delta_{ij}\Big]g_j^{-8/3}(\mathbf{r})$$
$$- \frac{40}{27}\sum_i N_i\rho_i(\mathbf{r})(1+B_2\delta_{ij})f_i(\mathbf{r})g_i^{-11/3}(\mathbf{r})|u_j^3(\mathbf{r}) > \qquad (3-8)$$

and

$$\left[\frac{\partial^4 E}{\partial N_j^4}\right]_{N_i\neq N_j} = -9c\alpha^{lim} < u_j^4(\mathbf{r})|\frac{20}{3}(1+B_1)(1+B_2)^2 g_j^{-8/3}(\mathbf{r})$$
$$- \frac{80}{27}(1+B_2)\Big\{2(1+B_2)^2 f_j(\mathbf{r}) + \Big[2B_2(1+B_1)(1+B_2)$$
$$+ B_1 + 2B_1B_2 + B_2\Big]\rho_j(\mathbf{r})\Big\}g_j^{-11/3}(\mathbf{r})$$
$$+ \frac{440}{81}B_2(2+B_2)(1+B_2)^2\rho_j(\mathbf{r})f_j(\mathbf{r})g_j^{-14/3}(\mathbf{r})$$
$$- \frac{80}{27}\sum_i N_i\rho_i(\mathbf{r})\Big\{2 + \Big[2B_2 + (1+B_2)(B_1+B_2)\Big]\delta_{ij}\Big\}g_i^{-11/3}(\mathbf{r})$$
$$+ \frac{440}{81}\sum_i N_i\rho_i(\mathbf{r})(1+B_2\delta_{ij})^2 f_i(\mathbf{r})g_i^{-14/3}(\mathbf{r})|u_j^4(\mathbf{r}) > \qquad (3-9)$$

In equations (3-6)-(3-9)

$$f_i(\mathbf{r}) = \rho_s(\mathbf{r}) + B_1\rho_i(\mathbf{r}) \qquad (3-10)$$

and

$$g_i(\mathbf{r}) = \rho_s(\mathbf{r}) + B_2\rho_i(\mathbf{r}) \qquad (3-11)$$

Using the definitions of the electronegativity and hardness[76,77] gives

$$\chi = -\left[\frac{\partial E}{\partial N_j}\right]_{N_i \neq N_j} = -\epsilon_j \qquad (3-12)$$

and

$$\eta = \frac{1}{2}\left[\frac{\partial^2 E}{\partial N_j^2}\right]_{N_i \neq N_j} \qquad (3-13)$$

and if

$$\mu = \frac{1}{6}\left[\frac{\partial^3 E}{\partial N_j^3}\right]_{N_i \neq N_j} \qquad (3-14)$$

and

$$\lambda = \frac{1}{24}\left[\frac{\partial^4 E}{\partial N_j^4}\right]_{N_i \neq N_j} \qquad (3-15)$$

then the ionization potential and electron affinity can be written as

$$I \approx \chi + \eta \quad \mu + \lambda \qquad (3-16)$$

and

$$A \approx \chi - \eta - \mu - \lambda \qquad (3-17)$$

Usually, the third and fourth derivatives are neglected in equations (3-16) and (3-17), and the ionization potential and electron affinity become[55,82]

$$I \approx \chi + \eta \qquad (3-18)$$

and

$$A \approx \chi - \eta \qquad (3-19)$$

This is because the third and fourth derivatives are very small in the Xα and SP-Xα theories, and equations (3-18) and (3-19) are essentially correct. This might be not true in the GX-LSD theory with the FEL Fermi-hole parameters, the GX-LSD-FEL theory, particularly for the calculation of the electron affinity. Table III-1 gives the absolute values of the second, third, and fourth derivatives of the exchange energy in the GX-LSD-FEL theory and the SP-Xα theory, with respect to the occupation number. The third and fourth derivatives in the GX-LSD-FEL theory effect the ionization potential and electron affinity more than in the SP-Xα theory. In the GX-LSD-FEL theory the fifth, sixth, etc. terms rapidly decrease to zero both absolutely and when divided by N!.

When the electron-correlation energy correction is considered, equations (3-16) and (3-17) become

$$I = \chi + \eta - \mu + \lambda + E^{+}_{Corr} - E^{0}_{Corr} \qquad (3-20)$$

and

$$EA = \chi - \eta - \mu - \lambda + E^{0}_{Corr} - E^{-}_{Corr} \qquad (3-21)$$

where E^{+}_{Corr}, E^{0}_{Corr}, and E^{-}_{Corr} are the Coulomb-correlation energy corrections of the positive ion, neutral atom, and negative ion, respectively, given by equations (1-96) of Keller and Gázquez's[33] Coulomb-correlation formula.

The elements were classified into two categories: (i) elements which involved one-orbital in going from the positive ion to the negative ion, and (ii) elements which involved two orbitals in going from the positive ion to the negative ion. The electronegativities, hardnesses, second ionization potentials and electron affinities for the first category elements of $Z \leq 36$ were calculated using the GX-LSD-FEL theory. The first ionization potentials for some atoms (Z=2 - 20, 31, 32, 34, 35) were calculated using the same theory. The results are listed in Tables III-2 to III-6.

TABLE III-1

The absolute values of the second, third, and fourth derivatives of the exchange energy with respect to the occupation number (Ry) in the SP-Xα and GX-LSD-FEL theories

Atom	N_s	SP-Xα 2nd	SP-Xα 3rd	SP-Xα 4th	GX-LSD 2nd	GX-LSD 3rd	GX-LSD 4th
B	3	0.0876	0.0269	0.0216	0.1693	0.0924	0.1210
Ne	5	0.1348	0.0210	0.0083	0.3117	0.0951	0.0328
Ar	9	0.0745	0.0116	0.0047	0.1699	0.0513	0.0183
Ge	17	0.0506	0.0108	0.0062	0.1073	0.0431	0.0376

III-2.1 Ionization Potential

In Table III-2, column 3 gives the results using the approximation equation (3-18). Column 4 lists the results including the third and fourth derivatives, equation (3-16), column 5 presents the results involving the Coulomb-correlation correction, equation (3-20). Other theoretical[55] and experimental[83] values are also given.

Comparing columns 3 and 6 with the experimental results in column 7 (six comparisons), shows that the first ionization potentials using (3-18) in the GX-LSD-FEL theory are better than those in the Xα theory.

Columns 3 and 4 compared with experiment show that the effects of the third and fourth derivatives of the total energy with respect to the occupation number are too large to be neglected in the GX-LSD theory.

Mathematically, equation (3-16) is more accurate than equation (3-18) under the frozen-orbital approximation. But the results in column 4 of Table III-2 are not overall better, some are better and some worse than those from (3-16). Compar-

ing column 5 with experiment shows that all the results including the Coulomb-correlation correction and the frozen-orbital approximation are bigger than experiment. The real total energies for the neutral atom, positive, and negative ion are shown as solid lines in Fig. 3-1; and the positive and negative ions calculated by using the wave functions of the neutral atom under the frozen-orbital approximation are shown as dotted lines in Fig. 3-1. The relaxation effect is neglected corresponding to Koopmans' theorem in the HF theory From the variation principle, the minimum value of the total energy for the many-body system corresponds to the self-consistent solution of the Schrodinger equation Relaxation lowers the total energy of the system; therefore, going from the positive ion to neutral atom decreases the total energy of the positive ion, and going from the neutral atom to the negative ion decreases the total energy of the negative ion. Therefore, the real statistical total energy for the positive and negative ions, the solid line of Fig 3-1, are lower than those without relaxation. The calculated ionization potentials are thus higher than experiment. Therefore, the results which include the Coulomb-correlation correction and the frozen orbital approximation are higher than experiment In order to obtained more accurate results, the relaxation and correlation must both be included in calculating the ionization potential.

Comparing columns 3-5 with experiment shows that the third and fourth derivative correction to the ionization potential are almost the same as the Coulomb-correlation correction in absolute values. However, the correction of the third and fourth derivatives decreases the ionization potential, whereas the Coulomb-correlation increases it, consequently (3-18) is a useful approximation for calculating the ionization potentials.

Table III-3 shows the second ionization potentials for the second category elements with $Z < 36$ from the GX-LSD-FEL theory with equation (3-18) and

experiment. Equation (3-18) is very good approximation for calculating the second ionization potentials for the low-Z atoms in the GX-LSD-FEL theory.

TABLE III-2

The first ionization potentials (Ry) for some atoms in the GX-LSD-FEL theory under the frozen-orbital approximation, compared with other calculations and experiment

Z	Atom	This Work I^a	I^b	I^c	Xα I^d	I^e_{Expt}
2	*He*	2.0716	1.9897	2.0160		1.8067
3	*Li*	0.4450	0.4272	0.4368		0.3962
4	*Be*	0.6890	0.6635	0.6882		0.6850
5	*B*	0.6131	0.5927	0.6141	0.6313	0.6098
6	*C*	0.8679	0.8515	0.8743	0.8725	0.8279
7	*N*	1.1317	1.1199	1.1442		1.0687
8	*O*	1.0677	1.0329	1.1029	1.3723	1.0007
9	*F*	1.4032	1.3777	1.4483	1.6325	1.2804
10	*Ne*	1.7430	1.7258	1.7985		1.5846
11	*Na*	0.4280	0.4122	0.4344		0.3777
12	*Mg*	0.5773	0.5577	0.5869		0.5619
13	*Al*	0.4126	0 3997	0.4301		0.4398
14	*Si*	0.5822	0.5722	0.6040		0.5990
15	*P*	0.7551	0.7483	0.8099		0.8085
16	*S*	0.7496	0.7293	0.7909		0.7613
17	*Cl*	0.9539	0.9396	1.0003	1.0716	0.9563
18	*Ar*	1.1618	1.1525	1.2139		1.1580
19	*K*	0.3517	0.3394	0.3639		0.3189
20	*Ca*	0.4519	0.4373	0.4729		0.4492
31	*Ga*	0.4219	0.4101	0.4447		0.4410
32	*Ge*	0.5695	0.5607	0.5974		0.5792
34	*Se*	0.7011	0 6842	0.7465		0.7166
35	*Br*	0.8636	0.8520	0.9136	0.9460	0.8703

a. Eq. (3-18);
b. Eq. (3-16);
c. Eq. (3-20);
d. Eq. (3-18) in the Xα theory (Ref. 55);
e. Reference 83.

FIGURE 3-1

The ground-state energy levels for the neutral atom, and positive and negative ions with (solid lines) and without (dotted lines) relaxation

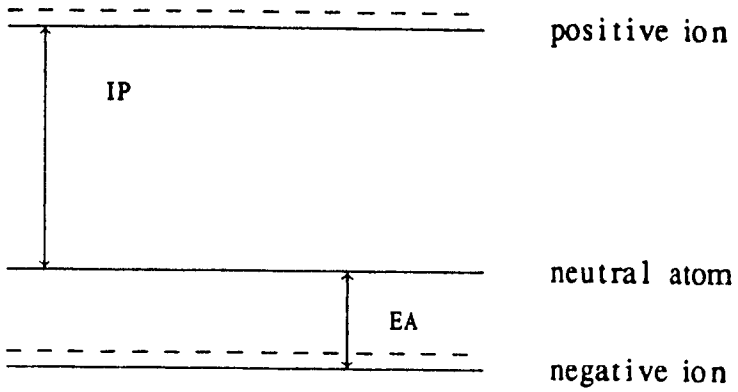

TABLE III-3

The second ionization potentials (Ry) for the second category elements with Z < 36 in the GX-LSD-FEL theory, compared with experiment

Z	*Atom*	I^a	I^b_{Expt}
5	*B*	1.8473	1.8485
6	*C*	1.8079	1.7971
8	*O*	2.6294	2.5833
9	*F*	2.6355	2.5711
13	*Al*	1.4010	1.3835
14	*Si*	1.1685	1.2010
16	*S*	1.6818	1.7200
17	*Cl*	1.7242	1.7494
31	*Ga*	1.5228	1.5075
32	*Ge*	1.1414	1.1709
34	*Se*	1.5361	1.5803
35	*Br*	1.5516	1.5877

a. Eq. (3-18);
b. Reference 83.

III-2.2 Electron Affinity

Table III-4 gives the electron affinities for the second category elements with Z < 36 calculated using equation (3-19), column 3, (3-17), and column 4, which involve the third and fourth derivatives, (3-19) plus the Coulomb-correlation correction, column 5, and (3-17) plus the correlation-energy correction, column 6, together with other theoretical values[74,76] and experimental results[56,58].

The Coulomb-correlation correction is very important in calculating the electron affinity for an atom, although its absolute value is very small For some atoms, say Al and Ga, the contribution is bigger than that of the kinetic energy, Coulomb interaction, and exchange energies. Almost all the theoretical values of the electron

TABLE III-4

The electron affinities (Ry) for the second category elements with Z < 36 in the GX-LSD-FEL theory, compared with other calculations and experiment

Z	Atom	This Work EA[a]	EA[b]	EA[c]	EA[d]	Other Work EA[e]	EA[f]	EA^{g}_{Expt}
5	*B*	−0.0308	−0.0412	−0.0114	−0.0233	−0.0823	−0.0212	0.0204
6	*C*	0.0015	−0.0091	0.0233	0.0111	−0.0272	0 0295	0.0932
8	*O*	−0.0454	−0.0632	0.0154	−0.0024	0.1176	−0 0233	0.1075
9	*F*	0.0407	0.0214	0.1049	0.0883	0.2065	0.1084	0 2198
13	*Al*	0.0103	0 0039	0.0357	0.0293	--0.0529	0 0004	0 0325
14	*Si*	0.0551	0 0487	0.0829	0.0761	0.0007	0 0510	0 1018
16	*S*	0.0744	0.0642	0.1288	0.1184	0.1338	0.0639	0.1527
17	*Cl*	0.1574	0.1482	0.2129	0.2037	0.2132	0.1667	0 2657
31	*Ga*	0.0050	−0 0009	0.0370	0 0311	−0.0669		0.0222
32	*Ge*	0.0551	0.0494	0.0897	0 0840	−0.0074		0.0897
34	*Se*	0.0838	0.0753	0 1404	0 1319	0.1213		0.1485
35	*Br*	0.1616	0.1541	0.2195	0 2120	0.1926		0.2473

a. Eq. (3-19);
b. Eq. (3-17);
c. Eq. (3-19) plus the correlation energy contribution;
d. Eq. (3-17) plus the correlation energy contribution;
e. Reference 76, calculated from eq. A = 2χ - I in the Xα theory;
f. Reference 74;
g. References 56 and 58.

affinities are smaller than experiment. This is because the relaxation effect has been neglected. As shown in Fig. 3-1, the relaxation lowers the total energy of the negative ions and increases the difference between the total energies of the neutral atom and the negative ion.

TABLE III-5

The electronegativities (Ry) for the second category elements with Z < 36 calculated by using GX-LSD-FEL theory, compared with other theoretical values

Z	Atom	This work[a]	HHF[b]	Xα[c]	SP-Xα[d]
5	*B*	0.2912	0.2168	0.2506	0.2999
6	*C*	0.4347	0.3021	0.3778	0.4734
8	*O*	0.5112	0.5079	0.6571	0.7064
9	*F*	0.7219	0.6314	0.8093	0.8181
13	*Al*	0.2114			0.1977
14	*Si*	0.3186			0.3234
16	*S*	0.4120			0.5057
17	*Cl*	0.5556	0.5380	0.5968	0.6005
31	*Ga*	0.2135			0.1867
32	*Ge*	0.3123			0.3014
34	*Se*	0.3925			0.4572
35	*Br*	0.5126	0.5020	0.5329	0.5358

a. Eq. (3-12);
b. Reference 55;
c. Reference 55;
d. Reference 84.

III-2.3 Electronegativity and Hardness

Table III-5 gives the electronegativities for the second category elements with Z < 36 calculated by equation (3-12) in the GX-LSD-FEL theory. The electronegativities from the GX-LSD-FEL theory are larger than those from HHF, and the electronegativities for the atoms in which the valence-electron is spin-up are larger than those in the Xα theory. The electronegativities for atoms in which the valence-electron is spin-down are smaller than those in both the Xα and SP-Xα theories.

Orsky and Whitehead[78] developed definitions of hardnesses for acids A and bases B by using the original definition of η which is equal to $\frac{1}{2}\frac{\partial^2 E}{\partial N^2}$. The hardness

can be written

$$\eta_A = \frac{1}{4}(I_{A+} - A_{A^0}) \qquad (3-22)$$

and

$$\eta_B = \frac{1}{4}(I_{B^0} - A_{B-}) \qquad (3-23)$$

where η_A and η_B are the hardnesses for acids A and bases B. I_{B^0} and I_{A+} are the first and second ionization potentials and A_{A^0} and A_{B-} are the first and second electron affinities for atom A. Orsky and Whitehead claimed that A_{B-}, the second electron affinity of A, is very small and can be neglected in equation (3-23). Then, η_B reduces to

$$\eta_B = \frac{1}{4}I_{B^0} \qquad (3-24)$$

The hardnesses for the second category elements with Z < 36 calculated with equations (3-13), (3-22), and (3-24) in the GX-LSD-FEL theory are given in Table III-6. The values given in the last two columns are obtained with equations (3-22) and (3-24), using the experimental first and second ionization potentials and electron affinities, other theoretical values obtained with equation (3-13) in the HHF and Xα theories are also listed. The hardnesses for these atoms in the GX-LSD-FEL theory are smaller than those in both the HHF and Xα theories. Comparing the results in columns 4 and 5 with those in the last two columns, shows that the hardnesses for acid A and base B in the GX-LSD-FEL theory are very close to experiment.

TABLE III-6

The hardnesses (Ry) for the second category elements with Z < 36 calculated by using GX-LSD-FEL Theory compared with other calculated values

Z	Atom	This Work[a] η	η_A	η_B	Other Work[b] η^{HHF}	$\eta^{X\alpha}$	Expt.[c] η_A	η_B
5	*B*	0.3219	0.4647	0.1533	0.4027	0.3807	0.4570	0.1525
6	*C*	0.4332	0.4462	0.2170	0.5123	0.4947	0.4246	0.2070
8	*O*	0.5566	0.6539	0.2669	0.7240	0.7152	0.6190	0.2502
9	*F*	0.6813	0.6327	0.3508	0.8291	0.8232	0.5803	0.3201
13	*Al*	0.2012	0.3413	0.1032			0.3378	0.1100
14	*Si*	0.2636	0.2714	0.1461			0.2748	0.1498
16	*S*	0.3376	0.3883	0.1874			0.3918	0.1903
17	*Cl*	0.3983	0.3778	0.2385	0.4741	0.4748	0.3709	0.2391
31	*Ga*	0.2084	0.3715	0.1055			0.3713	0.1103
32	*Ge*	0.2572	0.2629	0.1423			0.2703	0.1448
34	*Se*	0.3086	0.3489	0.1752			0.3580	0.1792
35	*Br*	0.3510	0.3330	0.2159	0.4142	0.4131	0.3351	0.2176

a. η is equal to the second derivative of the total energy. $\eta_A = \frac{1}{4}(I_{A+} - A_{A^0})$, and $\eta_B = \frac{1}{4} I_{B^0}$; I_{B^0}, I_{A+}, and I_{A^0} were taken from Table III-2 (column 3), III-3 (column 3), and III-4 (column 5) respectively;

b. Reference 55. η^{HHF} and $\eta^{X\alpha}$ are equal to the second derivative of the total energy in the HHF and Xα theories, respectively.

c. The values are calculated with eqs. (3-22) and (3-24), using the experimental first and second ionization potentials and electron affinities.

III-3. Ionization Potential and Electron Affinity Calculated from the Relaxed Total Energies

As shown in Table II-11, the SIC-GX-LSD theory combining the GWB Fermi-hole parameters gives the best prediction to the statistical totle energies for the atoms among all the Fermi-hole shapes in comparison with HF. Therefore, the SIC-GX-LSD theory with the GWB parameters is expected to give good ionization

potentials and electron affinities for atoms, when they are calculated by the differences of the relaxed statistical total energies. Consequently, the self-interaction corrected GX-LSD theory with the GWB[27] Fermi-hole parameters (henceforth called the SIC-GX-LSD-GWB theory) has been used to calculate the statistical total energies of the neutral atoms and positive ions of elements helium to strontium, and the stable negative ions of elements hydrogen to potassium and copper to rubidium separately. The wave functions are used to calculate the corresponding self-interaction corrected SPP[38] (SPP-SIC) and the self-interaction corrected VWN[39] (VWN-SIC) correlation energy corrections, equation (1-108), for these atoms and positive and negative ions. The effect of the correlation potential on the one-electron eigenvalue, ionization potential, and electron affinity is very small[85], so that it is neglected in the present calculation. The ionization potentials and electron affinities for these atoms are obtained by equation (3-4).

Table III-7 gives the ionization potentials of the atoms helium to titanium, chromium to iron, and copper to strontium. In Table III-7, column 3 gives the results including the relaxation without correlation correction, columns 4 and 5 show the values involved in the SPP-SIC and VWN-SIC correlation-energy correction; other theoretical[51,84,86,87] values and experiment[83] are listed in columns 6, 7, 8, and 9, respectively.

From Table III-7, it may be seen that although the relaxation is involved in the calculation, the ionization potentials in the SIC-GX-LSD-GWB theory (column 3) are still far away from experiment, unless the correlation-energy correction is included. The differences between these results and the experimental values are almost equal to those in the HF theory in which the relaxation effect is also included. Comparing the results in columns 3, 6, 7, and 9 shows that the ionization potentials did not improve much, even though the relaxation effect in the process of ionization

TABLE III-7

Ionization potentials (Ry) for atoms in the SIC-GX-LSD-GWB theory with correlation correction (The value in parentheses are equal to $100 \cdot (I^{theor} - I^{expt})/I^{expt}$)

Z	Atom	No Correl.	With SPP-SIC	With VWN-SIC	SP-Xα[a]	HF[b]	HF or CI	Expt.[c]
2	*He*	1.722	1.823	1.839	1.994	1.724		1.807
		(−4.7)	(0.9)	(1.8)	(10.3)	(−4.6)		
3	*Li*	0.390	0.392	0.393	0.416	0.393		0.396
		(−1.5)	(−1.0)	(−0.8)	(5.1)	(−0.8)		
4	*Be*	0.592	0.649	0.661	0.670	0.591		0.685
		(−13.6)	(−5.3)	(−3.5)	(−2.2)	(−13.7)		
5	*B*	0.564	0.591	0.598	0.615	0.584		0.610
		(−7.5)	(−3.1)	(−2.0)	(0.8)	(−4.3)		
6	*C*	0.801	0.820	0.827	0.868	0.794		0.828
		(−3.3)	(−1.0)	(−0.1)	(4.8)	(−4.1)		
7	*N*	1.045	1.059	1.066	1.117	1.022		1.069
		(−2.2)	(−0.9)	(−0.3)	(4.5)	(−4.4)		
8	*O*	0.867	0.964	0.971	1.285	0.875		1.001
		(−13.4)	(−3.7)	(−3.0)	(28.4)	(−12.6)		
9	*F*	1.190	1.265	1.271	1.435	1.154		1.280
		(−7.0)	(−1.2)	(−0.7)	(12.1)	(−9.8)		
10	*Ne*	1.510	1.571	1.579	1.638	1.463		1.585
		(−4.7)	(−0.9)	(−0.4)	(3.3)	(−7.7)		
11	*Na*	0.382	0.387	0.389	0.385	0.368		0.378
		(1.1)	(2.4)	(2.9)	(1.9)	(−2.6)		
12	*Mg*	0.506	0.555	0.566	0.554	0.485		0.562
		(−10.0)	(−1.2)	(0.7)	(−1.4)	(−13.7)		
13	*Al*	0.386	0.407	0.412	0.406	0.404		0.440
		(−12.3)	(−7.5)	(−6.4)	(−7.7)	(−8.2)		
14	*Si*	0.554	0.570	0.575	0.583	0.559		0.590
		(−7.5)	(−4.8)	(−4.0)	(−2.7)	(−6.7)		
15	*P*	0.793	0.805	0.810	0.757	0.742		0.808
		(−1.9)	(−0.4)	(0.2)	(−6.3)	(−8.2)		
16	*S*	0.661	0.739	0.748	0.878	0.662		0.761
		(−13.1)	(−2.9)	(−1.7)	(15.4)	(−13.0)		
17	*Cl*	0.874	0.935	0.942	0.993	0.867		0.956
		(−8.6)	(−2.2)	(−1.5)	(3.9)	(−9.3)		
18	*Ar*	1.085	1.136	1.143	1.141	1.088		1.158
		(−6.3)	(−1.9)	(−1.3)	(−1.5)	(−6.0)		
19	*K*	0.317	0.324	0.326	0.317	0.294		0.319
		(−0.6)	(1.6)	(2.2)	(−0.6)	(−7.8)		
20	*Ca*	0.401	0.443	0.452	0.432	0.375		0.449
		(−10.7)	(−1.3)	(0.7)	(−3.8)	(−16.5)		
21	*Sc*	0.420	0.470	0.480	0.476	0.390		0.482
		(−12.9)	(−2.5)	(−0.4)	(−1.2)	(−19.1)		
22	*Ti*	0.434	0.489	0.500	0.504	0.404		0.502
		(−13.5)	(−2.6)	(−0.4)	(1.0)	(−19.5)		

TABLE III-7 (Continued)

Ionization potentials (in Ry) for atoms in the SIC-GX-LSD-GWB theory with correlation correction (The value in parentheses are equal to $100 \cdot (I^{theor} - I^{expt})/I^{expt}$)

24	*Cr*	0.517	0.516	0.516	0.533	0.434		0.497
		(4.0)	(3.8)	(3.8)	(7.2)	(−12.7)		
25	*Mn*	0.467	0.532	0.545	0.579	0.434		0.546
		(−14.5)	(−2.6)	(−0.2)	(6.0)	(−20.5)		
26	*Fe*	0.512	0.569	0.579	0.603	0.463		0.581
		(−11.9)	(−2.1)	(−0.3)	(3.8)	(−20.3)		
29	*Cu*	0.561	0.578	0.583	0.576	0.470	0.541[d]	0.568
		(−1.2)	(1.8)	(2.6)	(1.4)	(−17.3)	(−4.8)	
							0.562[e]	
							(−1.0)	
30	*Zn*	0.640	0.688	0.696	0.677	0.559	0.673[d]	0.690
		(−7.2)	(−0.3)	(0.9)	(−1.9)	(−19.0)	(−2.5)	
							0.693[e]	
							(0.5)	
31	*Ga*	0.395	0.416	0.421	0.399	0.404		0.441
		(−10.4)	(−5.7)	(−4.5)	(−9.5)	(−8.4)		
32	*Ge*	0.543	0.559	0.564	0.553	0.544		0.579
		(−6.2)	(−3.5)	(−2.6)	(−4.5)	(−6.0)		
33	*As*	0.689	0.701	0.706	0.699	0.698		0.721
		(−4.4)	(−2.8)	(−2.1)	(−3.1)	(−3.2)		
34	*Se*	0.627	0.701	0.710	0.795	0.610		0.717
		(−12.6)	(−2.2)	(−1.0)	(10.9)	(−14.9)		
35	*Br*	0.802	0.859	0.867	0.883	0.794		0.870
		(−7.8)	(−1.3)	(−0.3)	(1.5)	(−8.7)		
36	*Kr*	0.971	1.018	1.026	1.003	0.978		1.029
		(−5.6)	(−1.1)	(−0.3)	(−2.5)	(−5.0)		
37	*Rb*	0.301	0.309	0.311				0.307
		(−2.0)	(0.7)	(1.3)				
38	*Sr*	0.372	0.410	0.420				0.418
		(−11.0)	(−1.9)	(0.5)				
ave[f]		(7.5)	(2.3)	(1.6)	(5.4)	(10.3)		

a. Reference 84;
b. Reference 51;
c. Reference 83;
d. Ref. 86, with the *ab initio* SCF-CI procedure.
e. Ref. 87, using the HF theory with correlation and relativistic correction.
f. $[\sum_i^N |I_i^{Theor} - I_i^{Expt}|/I_i^{Expt} X100]/N$.

is considered. This means that the relaxation effect is not a major one.

The results in columns 4 and 5 show that once the correlation-energy correction is introduced into the calculation of ionization potentials, the results are improved and are in excellent agreement with experiment. Columns 4, 5, and 9 show that the results with the VWN-SIC correlation-energy correction are closer to experiment than those with the SPP-SIC correction. The differences between the results in the SIC-GX-LSD-GWB theory with the VWN-SIC and experiment are less than 5 percent for all atoms except for Al. The average difference is equal to 1.6 percent in the SIC-GX-LSD-GWB theory with the VWN-SIC correlation-energy correction less than 2.3 percent with SPP-SIC, 5.4 percent in the SP-Xα theory, 7.5 percent in the SIC-GX-LSD-GWB theory without correlation correction, and 10 percent in the HF theory.

In Table III-7, column 8 gives several other results for Cu and Zn given by Sunil and Jordan[86] using an *ab-initio* SCF-CI procedure and by Jankowski and Polasik[87] using the HF theory with correlation and relativistic corrections. The differences between the theoretical results for these three theories with experiment are almost the same. But it is worth pointing out that the SIC-GX-LSD theory is the simplest and cheapest theory and has been applied to a wide range of atoms successfully.

From column 5, it may be seen that for the transition-metal atoms, the ionization potentials are a little bigger than experiment for the atoms which involved two orbitals in going from the neutral atom to the positive ion, i.e., Cr, and a little smaller for the atoms which involved one orbital in going from the neutral atom to the positive ion, i.e., Sc, Ti, Mn, and Fe. The ionization potentials are a little bigger than experiment for those atoms in which the outermost electrons are s electrons, except for Li and Be, and are a little smaller than experiment for others. The differences between the present results with experiment, as shown in Fig. 3-2,

FIGURE 3-2

The deviations of the ionization potentials for the low-Z atoms
in the SIC-GX-LSD-GWB theory and in experiment
decrease as the occupation number of
p_σ orbital increases

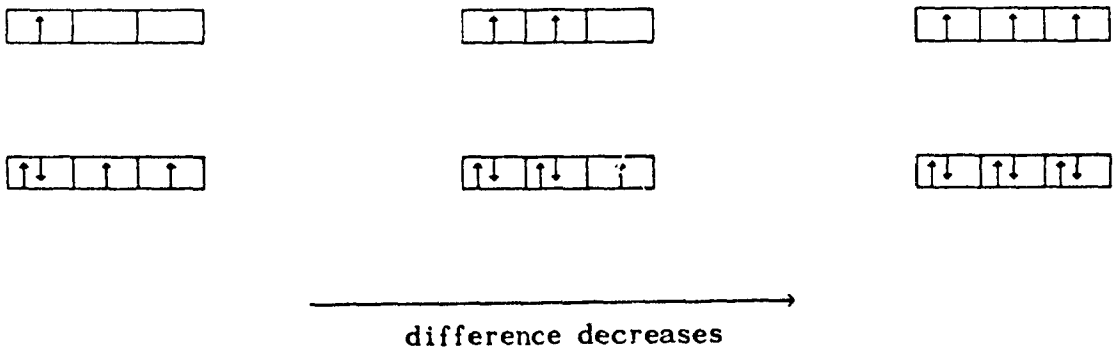

decrease as the occupation number of the p_s orbital increases. This is because the fuller the orbital, the more accurate the spherical approximation in the SIC-GX-LSD theory.

TABLE III-8

Ionization potential (Ry) for Vanadium, Cobalt and Nickel calculated using the SIC-GX-LSD-GWB theory with correlation correction (The value in parentheses are equal to $100 \cdot (I^{theor} - I^{expt})/I^{expt}$)

Z	Electron Atom	Config. Ion	No Correl.	With SPP-SIC	With VWN-SIC	Other SP-Xα[a]	Expt.[b]
23	V $3d^{3.4}4s^2$	$3d^2 4s^2$	0.867	0.894	0.901		
23	V $3d^3 4s^2$	$3d^4$	0.369	0.411	0.418	0.512	0.495
			(−25.5)	(−17.1)	(−15.6)	(3.3)	
23	V $3d^3 4s^2$	$3d^3 4s^1$	0.446	0.505	0.517		0.519
			(−14.1)	(−2.7)	(−0.4)		
27	Co $3d^7 4s^2$	$3d^6 4s^2$	0.910	0.983	0.989		0.949
			(−4.1)	(−3.6)	(4.2)		
27	Co $3d^7 4s^2$	$3d^8$	0.531	0.530	0.537	0.558	0.578
			(−8.1)	(−8.2)	(−7.1)	(−3.4)	
27	Co $3d^7 4s^2$	$3d^7 4s^1$	0.550	0.603	0.612		0.609
			(−9.7)	(−1.0)	(0.5)		
28	Ni $3d^8 4s^2$	$3d^7 4s^1$	1.041	1.107	1.114		
28	Ni $3d^8 4s^2$	$3d^9$	0.468	0.475	0.481	0.565	0.561
			(−16.6)	(−15.4)	(−14.3)	(0.8)	
28	Ni $3d^8 4s^2$	$3d^8 4s^1$	0.583	0.633	0.642		0.638
			(−8.6)	(−0.8)	(0.7)		

a. Reference 84;
b. Reference 83.

Table III-8 shows the ionization potentials for the transition-metal atoms vanadium, cobalt, and nickel from the neutral atoms to three different final states. In the process of ionization, if one 4s electron is removed to infinity and another one is relaxed to a 4d electron, the ionization potentials in the SIC-GX-LSD-GWB

theory with or without correlation-energy correction for these atoms are smaller than experiment, and if one 4s electron is removed and another one still stays in a 4s orbital, the ionization potentials are bigger than experiment except for V. However, the averaged value of these two situations almost equals experiment. This shows that the two final states interact strongly, and thus the Slater transition-state theory gives good results.

The electron affinities for several atoms calculated using the SIC-GX-LSD-GWB theory with and without correlation-energy correction are listed in Table III-9. Column 6 gives the results obtained by means of the GX-LSD-FEL theory with the correlation-energy correction under the frozen orbital approximation (from column 6 of Table III-4). Columns 7 and 8 list other theoretical values evaluated using the HF theory with Moller-Plesset perturbation theory through complete fourth order using several large basis sets[57], CI[86,88,90], and MCSCF[89], the fixed-node quantum Monte Carlo method[91]. The experimental results[56,58] are listed in the last column.

Comparing the results in column 3 (including the relaxation without the correlation energy correction) with experiment shows that although the relaxation effect is perfectly calculated, the electron affinities for these atoms are not much improved. But once the correlation-energy correction is included, the results are in very good agreement with experiment.

From columns 4 and 5, one can see that the results with the VWN-SIC correction-energy correction are better than these with the SPP-SIC correction. The average difference in the SIC-GX-LSD-GWB theory for these atoms is 8.9 percent with the VWN-SIC, 16.9 percent with the SPP-SIC, and 57.2 percent without correlation-energy correction. Comparing the results from the SIC-GX-LSD-GWB theory with the VWN-SIC correlation-energy correction and other theoretical val-

TABLE III-9

Electron affinities (Ry) for atoms in the SIC-GX-LSD-GWB theory with correlation correction (The value in parentheses are equal to $100 \cdot (I^{theor} - I^{expt})/I^{expt}$)

Z	Atom	No Correl.	With SPP-SIC	With VWN-SIC	Unrel.[a]	EA	EA	Expt.[b]
1	*H*	−0.0240 (−141.6)	0.0389 (−32.6)	0.0521 (−9.7)				0.0577
3	*Li*	−0.0055 (−112.1)	0.0296 (−35.1)	0.0397 (−12.9)				0.0456
5	*B*	0.0042 (−79.4)	0.0128 (−37.3)	0.0160 (−21.6)	−0.0233 (−214.2)	0.0162[c] (−20.7)	0.0110[d] (−46.1)	0.0204
6	*C*	0.0745 (−20.1)	0.0833 (−10.6)	0.0876 (−6.0)	0.0111 (−88.1)	0.0897[c] (−3.8)	0.0816[d] (−12.5)	0.0932
						0.0794[e] (−14.8)	0.0838[f] (−10.1)	
8	*O*	0.0180 (−83.3)	0.0753 (−30.0)	0.0815 (−24.2)	−0.0024 (−102.2)	0.1000[c] (−7.0)	0.0831[d] (−22.7)	0.1075
							0.0801[e] (−25.5)	
9	*F*	0.1742 (−30.3)	0.2231 (−10.7)	0.2301 (−7.9)	0.0883 (−64.7)	0.2462[c] (−1.4)	0.2293[d] (−8.2)	0.2498
						0.2337[e] (−6.4)	0.2535[g] (−1.5)	
11	*Na*	−0.0009 (−102.2)	0.0319 (−20.4)	0.0413 (3.0)				0.0401
13	*Al*	0.0163 (−49.8)	0.0211 (−35.1)	0.0230 (−29.2)	0.0293 (−9.9)			0.0325
14	*Si*	0.0802 (−21.2)	0.0864 (−15.1)	0.0890 (−12.6)	0.0761 (−25.3)			0.1018
16	*S*	0.0925 (−39.4)	0.1419 (−7.1)	0.1487 (−2.6)	0.1184 (−22.5)			0.1527
17	*Cl*	0.2107 (−20.7)	0.2521 (−5.1)	0.2591 (−2.5)	0.2037 (−23.3)			0.2657
19	*K*	0.0019 (−94.8)	0.0300 (−18.5)	0.0384 (4.3)				0.0368
29	*Cu*	0.0453 (−49.8)	0.0807 (−10.6)	0.0883 (−2.2)		0.0856[h] (−5.0)	0.0713[i] (−21.0)	0.0903
31	*Ga*	0.0148 (−33.3)	0.0192 (−13.5)	0.0208 (−6.3)	0.0311 (40.1)			0.0222
32	*Ge*	0.0796 (−11.3)	0.0854 (−4.8)	0.0877 (−2.2)	0.0840 (−6.4)			0.0897

TABLE III-9 (Continued)

Electron affinities (in Ry) for atoms in the SIC-GX-LSD-GWB theory with correlation correction (The value in parentheses are equal to $100 \cdot (I^{theor} - I^{expt})/I^{expt}$)

Z	Atom	No Correl.	With SPP-SIC	With VWN-SIC	Unrel.[a] EA	EA	Expt.[b]
34	*Se*	0.0989	0.1460	0.1531	0.1319		0.1485
		(−33.4)	(−1.7)	(3.1)	(−11.2)		
35	*Br*	0.2042	0.2437	0.2506	0.2120		0.2470
		(−17.3)	(−1.3)	(1.5)	(−14.2)		
37	*Rb*	0.0035	0.0302	0.0384			0.0357
		(−90.2)	(−15.4)	(7.6)			
ave[j]		(57.2)	(16.9)	(8.9)			

a. The values were calculated by using the GX-LSD-FEL with KG's (Reference 33) correlation-energy correction under the frozen orbital approximation (Table III-4);

b. Experiment values (References 56 and 58);
c. Reference 57;
d. Reference 88;
e. Reference 89;
f. Reference 90;
g. Reference 91;
h. Reference 87;
i. Reference 86.
j. ave $= \sum_i^N [I_i^{theor} - I_i^{Expt}|/I_i^{Expt} X100]/N$.

ues in columns 7 and 8 with experiment shows that, although the SIC-GX-LSD theory is simple relative to the other *ab-initio* methods listed, the electron affinities in this theory for these atoms are equal to those in any more complicated methods.

Consequently, it can be seen that the SIC-GX-LSD-GWB theory with the VWN-SIC correlation-energy correction is a powerful method for calculating ionization potentials and electron affinities for atoms. The results from this theory are so close to experiment that it can be used to predict the ionization potential of any atom which is unknown experimentally. The agreement of the present results

with experiment increases with atomic number for these atoms. Therefore it might be possible to get good results for the high-Z atoms by using the SIC-GX-LSD-GWB theory with the correlation-energy correction, if the relativistic effect were considered in the calculation of ionization potential and electron affinity.

III-4. Ionization Potential and Electron Affinity from the Relaxed Quasi-Relativistic SIC-GX-LSD Calculation

Equation (1-125) combining equations (1-126), (1-127), and (1-128) is solved by means of the standard self-consistent procedures[48]; outward numerical integration of each equation is started in the usual manner by means of a small-r series solution described in the Ref. 45. The relativistic-correction terms in equation (1-125) are treated as a part of the potential; that is, the radial function P_k(r) and one-electron eigenvalue ϵ_k in the (i-1)th iteration are used to calculate the relativistic terms of the potential of equation (1-125) for the ith iteration, so the relativistic-correction terms in equation (1-125) are completely neglected in the first iteration[45].

First of all, to test the reliability of the present relativistic correction[92], Table III-10 lists the relativistic energy contributions to the ns, np, and $(n-1)d$ electron removal energies, $\Delta E_{rel}(QR)$ in the quasi-relativistic SIC-GX-LSD (QR-SIC-GX-LSD) theory[45] and compares these with the ΔE_{rel} obtained by the (2J+1) weighted Dirac-Fock (DF) results, $\Delta E_{rel}(DF)$, and the ΔE_{rel} from the relativistic perturbed HF theory, $\Delta E_{rel}(pert)$, for the alkaline metals[35,93] and the elements in group IIIB[94]. Table III-10 shows that the QR-SIC-GX-LSD theory slightly overestimates the relativistic contribution to the ns electron removal energies, except for Fr ($6p^6 7s^1$) and slightly underestimates the relativistic contribution to the np and (n-1)d electrons except Sc ($4s^2 4p^1$). The agreement between the relativistic

TABLE III-10

Comparison of the QR-SIC-GX-LSD relativistic energy contributions to the ns, np, and $(n-1)d$ electron removal energies with the DF and perturbation calculation in DFT (Ry)

Elements	Configuration	ΔE_{rel}(QR)[a]	ΔE_{rel}(DF)[b,d]	ΔE_{rel}(DF)[c]	ΔE_{rel}(pert)[e]
		ns			
K	$(3p^6 4s^1)$	0.0013	0.0010	0.0011	
Rb	$(4p^6 5s^1)$	0.0053	0.0040	0.0041	
Cs	$(5p^6 6s^1)$	0.0107	0.0094	0.0078	
Fr	$(6p^6 7s^1)$	0.0357		0.018	
		np			
Sc	$(4s^2 4p^1)$	−0.0011	−0.0010		−0.0012
Y	$(5s^2 5p^1)$	−0.0030	−0.0034		−0.0032
La	$(6s^2 6p^1)$	−0.0058	−0.0058		−0.0054
Ac	$(7s^2 7p^1)$	−0.0121	−0.0152		−0.0116
		$(n-1)d$			
Sc	$(3d^1 4s^2)$	−0.0134	−0.0140		−0.0136
Y	$(4d^1 5s^2)$	−0.0295	−0.0316		−0.0310
La	$(5d^1 6s^2)$	−0.0547	−0.0590		−0.0572
Ac	$(6d^1 7s^2)$	−0.1166	−0.1324		−0.1222

a. This work;
b. Reference 35;
c. Reference 93;
d. Reference 94;
e. Reference 94.

contributions in the QR-SIC-GX-LSD and DF theories is comparable with that in the HF theory including relativistic shift correction and the DF theory.

The relativistic contribution to the removal energy for the 7s orbital of Fr, 0.0357 Ry, is overestimated in this theory, compared to the DF value of 0.0180 Ry. To check whether this contribution came strictly from the quasi-relativistic effect, the Fr calculations [i.e., Fr $(6p^6 7s^1)$ and Fr^+ $(6p^6)$] were repeated without

TABLE III-11

Ionization potentials (Ry) for the high-Z atoms in the SIC-GX-LSD-GWB theory, compared to other work and experiment (The value in parentheses are equal to $100 \cdot (I^{theor} - I^{expt})/I^{expt}$)

Z	Atom	With Relax. No Correl.	With SPP-SIC	With VWN-SIC	No Relax. Correl.	Other Work	Expt.[a]
37	*Rb*	0.300 (2.2)	0.308 (−0.4)	0.311 (−1.3)	0.313 (−2.0)	0.275[b] (10.4) 0.284[c] (7.5) 0.283[d] (7.8)	0.307
38	*Sr*	0.371 (11.3)	0.410 (2.0)	0.419 (−0.1)	0.392 (6.3)		0.418
39	*Y*	0.452 (5.4)	0.484 (−1.3)	0.491 (−2.8)	0.437 (8.5)		0.478
40	*Zr*	0.408 (20.1)	0.464 (9.2)	0.476 (6.8)	0.464 (9.2)		0.511
41	*Nb*	0.495 (0.5)	0.494 (0.7)	0.494 (0.7)	0.512 (−2.9)		0.498
42	*Mo*	0.515 (1.3)	0.514 (1.5)	0.514 (1.5)	0.532 (−1.9)		0.522
43	*Tc*	0.432 (19.3)	0.500 (6.6)	0.514 (3.9)	0.517 (3.4)		0.535
44	*Ru*	0.520 (3.9)	0.530 (2.1)	0.534 (1.3)	0.532 (1.7)		0.541
45	*Rh*	0.521 (5.0)	0.535 (2.4)	0.539 (1.7)	0.532 (3.0)		0.548
47	*Ag*	0.521 (6.4)	0.541 (2.8)	0.546 (1.9)	0.530 (4.8)	0.434[b] (22.1) 0.459[c] (17.6) 0.456[d] (18.1)	0.557
48	*Cd*	0.589 (10.9)	0.633 (4.2)	0.641 (3.0)	0.607 (8.1)		0.661
49	*In*	0.380 (10.6)	0.400 (5.9)	0.406 (4.5)	0.393 (7.6)		0.425
50	*Sn*	0.506 (6.2)	0.521 (3.5)	0.526 (2.5)	0.526 (2.5)		0.540
51	*Sb*	0.627 (1.3)	0.640 (−0.8)	0.645 (−1.6)	0.656 (−3.3)		0.635
52	*Te*	0.574 (13.3)	0.641 (3.2)	0.651 (1.7)	0.613 (7.4)		0.662
53	*I*	0.717 (6.7)	0.770 (−0.2)	0.776 (−1.0)	0.760 (1.1)		0.768
54	*Xe*	0.853 (4.3)	0.896 (−0.5)	0.904 (−1.4)	0.904 (−1.4)		0.891

TABLE III-11 (Continued)

Ionization potentials (in Ry) for the high-Z atoms in the SIC-GX-LSD-GWB theory and comparing with other work and experiments (The value in parentheses are equal to $100 \cdot (I^{theor} - I^{expt})/I^{expt}$)

55	*Cs*	0.272 (4.9)	0.278 (2.8)	0.281 (1.8)	0.284 (0.7)	0.246[b] (14.0) 0.255[c] (10.8) 0.254[d] (11.2)	0.286
56	*Ba*	0.330 (13.8)	0.366 (4.4)	0.375 (2.1)	0.351 (8.3)		0.383
72	*Hf*	0.566 (−10.0)	0.592 (−15.1)	0.600 (−16.6)	0.471 (8.5)		0.515
73	*Ta*	0.420 (27.5)	0.484 (16.4)	0.498 (14.0)	0.490 (15.4)		0.579
74	*W*	0.426 (27.4)	0.494 (15.8)	0.510 (13.0)	0.519 (11.5)		0.586
75	*Re*	0.432 (25.3)	0.502 (13.2)	0.516 (10.8)	0.535 (7.5)		0.578
76	*Os*	0.475 (25.7)	0.533 (16.7)	0.545 (14.8)	0 541 (15.4)		0.640
77	*Ir*	0.508 (23.2)	0.563 (14.9)	0.574 (13.2)	0.560 (15.3)		0.661
78	*Pt*	0.527 (20.3)	0.543 (17.9)	0.551 (16.7)	0.538 (18.7)		0.661
79	*Au*	0.523 (22.8)	0.547 (19.3)	0.551 (18.7)	0.535 (21.1)	0.436[b] (35.7) 0.464[c] (31.6) 0.460[d] (32.2)	0.678
80	*Hg*	0.586 (23.6)	0.629 (17.9)	0.637 (16.9)	0.604 (21.2)		0.767
ave[e]		(12.6)	(7.2)	(6.3)	(7.8)		

a. Reference 83;
b. These values were obtained by using the HF theory, Ref. 35;
c. Obtained by using the HF theory with the SPP-SIC under the frozen-orbital approximation, Ref. 35;
d. The values were calculated by using the HF theory with the SPP-SIC and relaxation correction, Ref. 35;
e. ave = $[\sum_i^N |I_i^{Expt} - I_i^{Theor}| / I_i^{Expt} \times 100] / N$

any VWN correlation energy functional; the $7s$ removal energy in that case was 0.0358 Ry. Thus the deviation of the removal energy for the $7s$ orbital in the QR-SIC-GX-LSD and DF theories is not caused by the correlation energy functional. The overestimation may be caused by the underlying $4f$ orbital, which strongly affects the $7s$ removal energy in the QR-SIC-GX-LSD theory for Fr; further study of the interaction between the f and s orbitals is needed.

Expression (1-86), the statistical total energy, has been used to calculate the positive ions and neutral atoms of elements rubidium to barium and hafnium to mercury, the negative ions of some high-Z elements, by means of the wave functions in the QR-SIC-GX-LSD-GWB and SIC-GX-LSD-GWB theories. The wave functions in both the QR-SIC-GX-LSD-GWB and SIC-GX-LSD-GWB theories are also used to calculate the SPP and VWN correlations with the self-interaction correction[34] (SPP-SIC and VWN-SIC, respectively) for the corresponding neutral atoms, positive and negative ions. Finally, the ionization potentials and electron affinities for these atoms are obtained in terms of the energy difference between the positive ion and neutral atom for the ionization potential, and between the neutral atom and negative ion for the electron affinity, equation (3-4). The ionization potentials for these atoms in both the QR-SIC-GX-LSD-GWB and SIC-GX-LSD-GWB theories are also calculated under the frozen-approximation equation (3-2). All results are given in Tables III-11 to III-14.

Table III-11 contains the ionization potentials for some high-Z atoms in the SIC-GX-LSD-GWB theory without and with the correlation-energy correction (columns 3, 4, and 5, respectively). Column 6 gives the results without relaxation or correlation-energy correction. Columns 7 and 8 list other work given by Savin et al.[35] using the HF theory and experimental values[83]. The table shows that (i) the results are greatly improved by the correlation-energy correction; (ii) the non-

relativistic results are in very good agreement with experiment for the atoms of the atomic number from 37 to 56. The differences for these atoms are less than 5 percent, except for Zr. But the SIC-GX-LSD-GWB theory cannot accurately describe the atoms for which the atomic numbers are bigger than 72 (the differences exceed 10 percent); (iii) the SIC-GX-LSD-GWB results are much better than the HF results in describing ionization potentials for the high-Z atoms whether the correlation-energy correction is included or not.

Table III-12 gives the ionization potentials for some high-Z atoms obtained by using the QR-SIC-GX-LSD-GWB theory without and with the correlation-energy correction (columns 3-6), other theoretical values given by Savin et al.[35] using the Dirac-Fock (DF) theory[95]. From columns 4 and 5, it may be seen that the results in the QR-SIC-GX-LSD-GWB with the SPP-SIC and VWN-SIC correlation-energy correction are in excellent agreement with experiment, particularly for atoms of atomic number from 72 to 80: the percentage differences in the SIC-GX-LSD-GWB theory are greater than 10 percent, but they are less than 3.5 percent in the QR-SIC-GX-LSD-GWB theory. Generally speaking, the results without relaxation and correlation-energy corrections are better than those with relaxation and without correlation-energy correction. The results with correlation and relaxation corrections, as expected, are much better than those with relaxation but without correlation-energy correction or with correlation but without relaxation correction. This is because in the process of ionization, the effect of relaxation adjusts the ion structure in the lowest-energy state, the relaxation decreases the ionization potential of an atom, but the correlation effect increases the ionization potential. However, the decrease in the relaxation and increase in the correlation are not equal. Comparing the present work in columns 3-6 and other work in column 7 with experiment in column 8 shows that the QR-SIC-GX-LSD-GWB theory is much better than the DF method in calculating ionization potentials for the high-Z atoms. It

TABLE III-12

Ionization potentials (Ry) for the high-Z atoms in the QR-SIC-GX-LSD-GWB theory, compared with other work and experiment (The value in parentheses are equal to $100 \cdot (I^{theor} - I^{expt})/I^{expt}$)

Z	Atom	With Relax. No Correl.	With SPP-SIC	With VWN-SIC	No Relax. Correl.	Other Work	Expt.[a]
37	*Rb*	0.306 (0.3)	0.313 (−2.0)	0.315 (−2.6)	0.318 (−3.6)	0.279[b] (9.1) 0.289[c] (5.9) 0.288[d] (6.2)	0.307
38	*Sr*	0.377 (9.9)	0.416 (0.6)	0.425 (−1.6)	0.398 (4.9)		0.418
39	*Y*	0.423 (11.5)	0.455 (4.8)	0.462 (3.3)	0.448 (6.2)		0.478
40	*Zr*	0.418 (18.2)	0.477 (6.6)	0.489 (4.3)	0.477 (6.6)		0.511
41	*Nb*	0.519 (−4.3)	0.518 (−4.1)	0.518 (−4.1)	0.539 (−8.3)		0.498
42	*Mo*	0.543 (−4.0)	0.542 (−3.9)	0.542 (−3.9)	0.562 (−7.7)		0.522
43	*Tc*	0.446 (16.7)	0.518 (3.2)	0.532 (0.6)	0.538 (−0.5)		0.535
44	*Ru*	0.553 (−2.2)	0.563 (−4.0)	0.567 (−4.7)	0.567 (−4.7)		0.541
45	*Rh*	0.555 (−1.2)	0.570 (−4.0)	0.575 (−4.9)	0.568 (−3.6)		0.548
47	*Ag*	0.559 (−0.4)	0.580 (−4.2)	0.585 (−5.1)	0.570 (−2.4)	0.466[b] (16.3) 0.495[c] (11.1) 0.491[d] (11.8)	0.557
48	*Cd*	0.626 (5.3)	0.671 (−1.5)	0.678 (−2.6)	0.646 (2.2)		0.661
49	*In*	0.378 (11.1)	0.399 (6.2)	0.403 (5.2)	0.390 (8.3)		0.425
50	*Sn*	0.504 (6.6)	0.520 (3.7)	0.524 (2.9)	0.525 (2.7)		0.540
51	*Sb*	0.627 (1.3)	0.640 (−0.8)	0.644 (−1.4)	0.655 (−3.1)		0.635
52	*Te*	0.573 (13.5)	0.641 (3.2)	0.651 (1.7)	0.612 (7.6)		0.662
53	*I*	0.716 (6.8)	0.770 (−0.2)	0.776 (−1.0)	0.761 (1.0)		0.768
54	*Xe*	0.853 (4.3)	0.896 (−0.5)	0.905 (−1.5)	0.905 (−1.5)		0.891

TABLE III-12 (Continued)

Ionization potentials (in Ry) for the high-Z atoms in the QR-SIC-GX-LSD-GWB theory and comparing with other work and experiments (The value in parentheses are equal to $100 \cdot (I^{theor} - I^{expt})/I^{expt}$)

55	*Cs*	0.282 (1.4)	0.290 (−1.4)	0.293 (−2.4)	0.294 (−2.8)	0.256[b] (10.5) 0.266[c] (7.0) 0.265[d] (7.3)	0.286
56	*Ba*	0.343 (10.4)	0.379 (1.0)	0.388 (−1.3)	0.362 (5.5)		0.383
72	*Hf*	0.475 (7.7)	0.502 (2.4)	0.508 (1.3)	0.525 (−2.0)		0.515
73	*Ta*	0.477 (17.6)	0.545 (5.9)	0.561 (3.1)	0.556 (4.0)		0.579
74	*W*	0.484 (17.5)	0.561 (4.3)	0.576 (1.8)	0.600 (−2.3)		0.586
75	*Re*	0.488 (15.6)	0.574 (0.8)	0.590 (−2.0)	0.623 (−7.7)		0.578
76	*Os*	0.551 (13.8)	0.617 (3.5)	0.629 (1.6)	0.634 (0.9)		0.640
77	*Ir*	0.602 (9.0)	0.660 (0.2)	0.668 (−1.0)	0.666 (−0.7)		0.661
78	*Pt*	0.656 (0.8)	0.680 (−2.8)	0.684 (−3.4)	0.676 (−2.2)		0.661
79	*Au*	0.664 (2.0)	0.691 (−2.0)	0.691 (−2.0)	0.678 (0.0)	0.565[b] (16.7) 0.604[c] (10.9) 0.597[d] (11.9)	0.678
80	*Hg*	0.719 (6.2)	0.762 (0.6)	0.770 (−0.4)	0.741 (3.3)		0.767
ave[e]		(7.8)	(2.8)	(2.6)	(3.8)		

a. Reference 83;
b. These values were obtained by using the DF theory, Ref. 35;
c. Obtained by using the DF theory with the SPP-SIC under the frozen-orbital approximation approximation, Ref. 35;
d. The values were calculated by using the DF theory with the SPP-SIC and relaxation correction, Ref. 35;
e. ave = $[\ \sum_i^N |I_i^{Expt} - I_i^{Theor}|/I_i^{Expt} \text{X } 100\ ] / \text{N}$

is worth pointing out again that the QR-SIC-GX-LSD-GWB theory is much easier and cheaper to use than the DF theory.

The electron affinities for some high-Z atoms obtained using the QR-SIC-GX-LSD-GWB theory without and with the SPP-SIC and VWN-SIC are given in Table III-13. Corresponding to the elements in Table III-12, some atoms are missing in Table III-13, because for these atoms some of the negative ions are not stable experimentally[58] and some are not convergent for the experimental electron configurations (e.g., excited-electron configuration of negative ions) in the QR-SIC-GX-LSD-GWB theory. From Table III-13, it can be seen that the results without correlation-energy correction are very far from experiment[56,58], i.e., the theoretical values are much smaller than experiment, except for Zr. Once the correlation-energy correction is added, the electron affinities for those atoms are improved. Especially for the atoms Sb and W, the contribution of the correlation-energy correction to the electron affinity is much bigger than that of the kinetic energy, Coulomb and exchange interaction energies of the electrons. Comparing columns 4 and 5 with experiment, column 6, it is clear that the results with the SPP-SIC and VWN-SIC are in very good agreement with experiment: the results with the VWN-SIC are a slightly better than those with the SPP-SIC for those atoms, on the average difference are 6.6 percent for the former, 6.9 percent for the latter, and 47.8 percent for those without correlation correction.

Table III-14 gives the ionization potentials of the ground and first excited-electron configurations of the atom palladium and electron affinity in the QR-SIC-GX-LSD-GWB theory. The results show that both the SPP-SIC and VWN-SIC overestimate the correlation-energy correction of the electron configuration $4d^{10}$ for the neutral atom palladium. The multiconfiguration interaction has to be applied in order to describe the correlation correction accurately.

TABLE III-13

Electron affinities (Ry) for the high-Z atoms in the QR-SIC-GX-LSD-GWB theory, compared with experiment (The value in parentheses are equal to $100 \cdot (I^{theor} - I^{expt})/I^{expt}$)

Z	Atom	No Correl.	With SPP-SIC	With VWN-SIC	Expt[a]
37	*Rb*	0.0039	0.0308	0.0391	0.0357
		(89.1)	(13.8)	(−9.4)	
40	*Zr*	0.0469	0.0337	0.0342	0.0313
		(−49.8)	(−7.6)	(−9.2)	
44	*Ru*	0.0313	0.0674	0.0752	0.0773
		(59.6)	(12.8)	(2.7)	
45	*Rh*	0.0440	0.0801	0.0879	0.0836
		(47.4)	(4.2)	(−5.1)	
47	*Ag*	0.0645	0.0996	0.1064	0.0958
		(32.7)	(−4.0)	(−11.1)	
49	*In*	0.0205	0.0254	0.0273	0.0235
		(12.7)	(−8.0)	(−16.4)	
50	*Sn*	0.0840	0.0898	0.0908	0.0897
		(6.4)	(−0.2)	(−1.2)	
51	*Sb*	0.0107	0.0645	0.0752	0.0790
		(86.4)	(18.4)	(4.8)	
52	*Te*	0.1035	0.1475	0.1543	0.1448
		(28.5)	(−1.8)	(−6.6)	
53	*I*	0.1934	0.2314	0.2383	0.2249
		(14.0)	(−2.9)	(−5.9)	
55	*Cs*	0.0049	0.0303	0.0371	0.0347
		(85.9)	(12.8)	(−6.9)	
72	*Hf*	−0.0117	−0.0039	0.0020	≈ 0
74	*W*	0.0098	0.0566	0.0684	0.0600
		(83.7)	(5.6)	(−13.9)	
76	*Os*	0.0273	0.0820	0.0859	0.0823
		(66.8)	(0.3)	(−4.4)	
78	*Pt*	0.1133	0.1484	0.1563	0.1564
		(27.6)	(5.1)	(0.1)	
79	*Au*	0.1250	0.1602	0.1719	0.1697
		(26.3)	(5.6)	(−1.3)	
ave[b]		(47.8)	(6.9)	(6.6)	

a. References 56 and 58;

b. ave = $[\ \sum_i^N |I_i^{Expt} - I_i^{Theor}|/I_i^{Expt} \times 100\ ]\ /\ N$

The SIC-GX-LSD-GWB theory with the VWN-SIC correlation-energy correction can describe the ionization potential accurately for the atoms for which the atomic number Z is less than 56, but the relativistic effect has to be considered for the atoms of atomic number Z > 72. The ionization potentials and electron affinities for the high-Z atoms in the QR-SIC-GX-LSD-GWB theory are in reasonably good agreement with experiment, so that this theory can be used to predict the ionization potentials of any high-Z atoms which are unknown experimentally.

TABLE III-14

Ionization potentials and electron affinities (Ry) for palladium in different electron configurations in the QR- and SIC-GX-LSD-GWB theories with correlation correction (The value in parentheses are equal to $100 \cdot (I^{theor} - I^{expt})/I^{expt}$)

Z	Electron Atom	Config. Ion	No Correl.	With SPP-SIC	With VWN-SIC	Expt.[a]
			I_R			
46	Pd $4d^{10}$	$4d^9$	0.6182 (−1.0)	0.6631 (−8.3)	0.6709 (−9.6)	0.6122
46	Pd $4d^9 5s^1$	$4d^9$	0.5566 (−0.6)	0.5762 (−4.1)	0.5811 (−5.0)	0.5533
			I_{NR}			
46	Pd $4d^{10}$	$4d^9$	0.6289 (−2.7)	0.6738 (−10.1)	0.6816 (−11.3)	0.6122
46	Pd $4d^9 5s^1$	$4d^9$	0.5205 (5.9)	0.5381 (2.7)	0.5430 (1.9)	0.5533
			EA_R			
46	Pd $4d^{10}$	$4d^9 5s^2$	−0.0068 (122.1)	0.0029 (90.5)	0.0078 (74.8)	0.0310

a. References 56, 58 and 83.

TABLE III-15

Ionization potentials (Ry) for the multiply charged ions of carbon, compared with other calculations and experiment

Degree of Ionization	GX-LSD Without Corre.[a]	GX-LSD With VWN[b]	HF Rel.[c]	HF Unrel.[d]	Xα[e]	Expt[f]
0	0.801	0.827	0.793	0.867	0.809	0.828
1	1.772	1.814	1.767	1.808	1.817	1.792
2	3.316	3.411	3.365	3.388	3.617	3.518
3	4.689	4.699	4.730	4.733	4.630	4.739
ave[g]	(2.8)	(1.3)	(2.5)	(2.4)	(2.2)	

a. The difference of the statistical total energies for the i^{th} and $(i+1)^{th}$ ions in the two separate calculation Δ_{SCF};
b. Δ_{SCF} plus the VWN correlation-energy correction;
c. Δ_{SCF} in the HF theory, reference 102;
d. Orbital energy in HF theory, reference 102;
e. Transition-state calculation in the Xα method with theoretically determined parameter α, reference 97;
f. Reference 103;
g. ave $= [\sum_i^N |I_i^{Theor} - I_i^{Expt}|/I_i^{Expt} X100]/N$.

III-5. Ionization Potentials of Multiply-Charged Ions

Investigation of ionization potentials for multiply-charged ions has attracted attention[96,97], because of the interest in these ionization potentials for interpreting stellar spectra. Other properties of multiply charged ions, e.g. photoionization cross-section, have also attracted some attention[98,99] experimentally. Theoretical calculation for them might be interesting.

Few publications dealing with the ionization potentials of ions using the LDF theory occur in the literature, even for the multiply-charged ions, although the LDF theory has been widely used in the calculations of atoms and molecules and solid state. The reason might be that the values of the exchange parameters, e.g., α

TABLE III-16

Ionization potentials (Ry) for the multiply charged ions of aluminium, compared with other calculations and experiment

Degree of Ionization	GX-LSD Without Corre.[a]	GX-LSD With VWN[b]	HF Rel.[c]	HF Unrel.[d]	Xα[e]	Expt[f]
0	0.386	0.412	0.404	0.419	0.378	0.440
1	1.316	1.386	1.288	1.308	1.364	1.384
2	2.093	2.108	2.060	2.065	2.043	2.090
3	8.734	8.822	8.715	8.967	9.019	8.817
4	11.195	11.304	11.191	11.539	11.704	11.302
5	13.707	13.854	13.858	14.479	14.607	13.996
6	17.892	17.932	17.776	17.860	17.716	17.782
7	20.891	20.942	20.921	21.020	21.018	20.958
8	24.102	24.171	24.252	24.328	24.488	24.263
9	29.007	29.144	28.915	28.885	29.250	29.291
ave[g]	(2.4)	(1.0)	(2.1)	(2.1)	(3.0)	

a. The difference of the statistical total energies for the i^{th} and $(i+1)^{th}$ ions in the two separate calculation Δ_{SCF};
b. Δ_{SCF} plus the VWN correlation-energy correction;
c. Δ_{SCF} in the HF theory, ref. 102;
d. Orbital energy in the HF theory, ref. 102;
e. Transition-state calculation in the Xα method with theoretically determined parameter α, ref. 97;
f. Reference 103;
g. ave $= [\sum_i^N |I_i^{Theor} - I_i^{Expt}|/I_i^{Expt} X100]/N$.

in the Xα theory and a in the Ξa theory, have been missing in the literature for ions. Also it is time-consuming to search for the optimal exchange parameters for all multiply charged ions of all atoms in the periodic table.

In 1987, Gáspár and Nagy[97] published the ionization potentials for some multiply-charged ions evaluated by means of the Xα theory in which the value of α was determined by the electron charge density self-consistently; their results are comparable with those from the HF theory and agree with experiment. The

TABLE III-17

Ionization potentials (Ry) for the multiply charged ions of chlorine compared with other calculations and experiment

Degree of Ionization	GX-LSD Without Corre.[a]	GX-LSD With VWN[b]	HF Rel.[c]	HF Unrel.[d]	Expt[e]
0	0.874	0.942	0.867	1.013	0.956
1	1.633	1.728	1.645	1.878	1.749
2	2.842	2.868	2.875	2.917	2.933
3	3.830	3.865	3.854	3.885	3.932
4	4.870	4.918	4.904	4.922	4.983
5	7.009	7.100	6.958	6.972	7.108
6	8.383	8.406	8.332	8.334	8.399
7	25.503	25.606	25.517	25.741	25.601
8	29.315	29.440	29.336	29.801	29.452
9	33.218	33.382	33.338	34.207	33.466
10	38.957	39.003	39.011	39.120	
11	43.430	43.487	43.480	43.560	
12	47.980	48.057	48.132	48.181	
ave[f]	(2.6)	(0.8)	(2.5)	(2.3)	

a. The difference of the statistical total energies for the i^{th} and $(i+1)^{th}$ ions in the two separate calculation Δ_{SCF};
b. Δ_{SCF} plus the VWN correlation-energy correction;
c. Δ_{SCF} in the HF theory, ref. 102;
d. Orbital energy in the HF theory, ref. 102;
e. Reference 103;
f. ave $= [\sum_i^N |I_i^{Theor} - I_i^{Expt}|/I_i^{Expt} X100]/N$.

advantage of Gáspár and Nagy's Xα theory is that the exchange parameter α can be optimized in each iteration according to the electron density during the self-consistents-field process, unlike that in the traditional Xα theory in which the α was determined by fitting the total Xα energy to the HF total energy, or by fitting the total energy to satisfy the virial theorem.

The SIC-GX-LSD theory is somewhat analogous to Gáspár and Nagy's Xα

TABLE III-18

Ionization potentials (Ry) for the multiply charged ions of argon, compared with other calculations and experiment

Degree of Ionization	GX-LSD Without Corre.[a]	GX-LSD With VWN[b]	HF Rel.[c]	HF Unrel.[d]	Expt[e]
0	1.085	1.192	1.086	1.181	1.158
1	1.938	2.064	1.940	2.093	2.031
2	2.861	3.013	2.879	3.135	2.995
3	4.269	4.359	4.311	4.352	4.396
4	5.406	5.504	5.433	5.463	5.514
5	6.589	6.699	6.624	6.643	6.689
6	9.010	9.159	8.956	8.969	9.138
7	10.526	10.606	10.470	10.473	10.544
8	30.955	31.151	30.977	31.201	31.050
ave[f]	(−2.6)	(0.6)	(−2.4)	(0.6)	

a. The difference of the statistical total energies for the i^{th} and $(i+1)^{th}$ ions in the two separate calculation Δ_{SCF};
b. Δ_{SCF} plus the VWN correlation-energy correction;
c. Δ_{SCF} in the HF theory, ref. 102;
d. Orbital energy in the HF theory, ref. 102;
e. Reference 103;
f. ave $= [\sum_i^N |I_i^{Theor} - I_i^{Expt}|/I_i^{Expt} X100]/N$.

theory[97] in determining the optimal exchange parameters for atoms and ions. However obtaining the exchange parameters is much easier and simpler in the SIC-GX-LSD theory than in Gáspár and Nagy's Xα theory. The exchange parameters in the SIC-GX-LSD theory are fixed once the Fermi-hole shape is chosen. Therefore one set of parameters applies to all atoms and ions.

This section tests the reliability of the SIC-GX-LSD theory in predicting ionization potentials of multiply-charged ions which have been experimentally measured. The SIC-GX-LSD theory is much easier to use than the HF theory, because the local exchange potential is used, and even easier to use than the Xα theory,

TABLE III-19

Ionization potentials (Ry) for the multiply charged ions of calcium, compared with other calculations and experiment

Degree of Ionization	GX-LSD Without Corre.[a]	GX-LSD With VWN[b]	HF Rel.[c]	HF Unrel.[d]	Xα[e]	Expt[f]
0	0.401	0.452	0.376	0.389	0.417	0.45
1	0.867	0.881	0.833	0.830	0.825	0.87
2	3.645	3.714	3.668	3.748	3.726	3.74
3	4.820	4.905	4.833	4.998	4.997	4.93
4	6.043	6.155	6.068	6.372	6.341	6.20
5	7.830	7.864	7.883	7.923	7.761	8.00
6	9.254	9.296	9.284	9.312	9.246	9.39
7	10.714	10.770	10.751	10.767	10.789	10.82
8	13.685	13.786	13.630	13.641	13.860	13.84
9	15.477	15.504	15.422	15.435	15.432	15.53
10	43.624	43.734	43.403	43.658	43.961	43.46
11	47.574	47.708	48.218	48.729	49.150	48.24
12	53.428	53.602	53.214	54.241	54.535	53.36
13	59.658	59.707	60.197	60.268	60.105	60.02
14	66.407	66.468	65.656	65.707	65.842	65.79
15	71.491	71.573	71.295	71.366	71.714	71.59
16	77.980	78.139	78.984	78.937	79.547	79.75
ave[g]	(1.8)	(0.8)	(2.0)	(1.9)	(1.6)	

a. The difference of the statistical total energies for the i^{th} and $(i+1)^{th}$ ions in the two separate calculation Δ_{SCF};
b. Δ_{SCF} plus the VWN correlation-energy correction;
c. Δ_{SCF} in the HF theory, ref. 102;
d. Orbital energy in the HF theory, ref. 102;
e. Transition-state calculation in the Xα method with theoretically determined parameter α, ref. 93;
f. Reference 103;
g. ave = $[\sum_i^N |I_i^{Theor} - I_i^{Expt}|/I_i^{Expt} X100]/N$.

because there is a unique set of parameters for all atoms once the Fermi-hole shape is selected.

Therefore, the SIC-GX-LSD theory is used to calculate the ionization poten-

TABLE III-20

Ionization potentials (Ry) for the multiply charged ions of iron, compared with other calculations and experiment

Degree of Ionization	GX-LSD Without Corre.[a]	GX-LSD With VWN[b]	HF Rel.[c]	HF Unrel.[d]	Xα[e]	Expt[f]
0	0.512	0.579		0.514	0.588	0.58[f]
1	1.205	1.217			1.134	1.19
2	2.221	2.321	2.084	2.631	2.488	2.25
3	4.071	4.112	3.979	4.145	3.888	4.03
4	5.632	5.681	5.483	5.689	5.469	5.51
5	7.336	7.393	7.249	7.423	7.211	7.28
6	8.896	8.961	9.156	9.261	9.100	9.19
7	11.393	11.468	11.052	11.172	11.127	11.10[g]
8	17.036	17.123	17.104	17.198	17.221	17.20
9	19.070	19.174	19.104	19.330	19.389	19.26
10	21.125	21.257	21.165	21.608	21.622	21.31
11	23.982	24.026	22.069	24.107	23.912	24.33
12	26.232	26.285	28.278	26.312	25.257	26.53
13	28.499	28.567	28.546	28.591	28.644	28.81
14	33.123	33.239	33.040	33.074	33.431	33.59
15	35.733	35.765	35.649	35.646	35.682	35.94
16	92.629	92.751	92.711	92.901	93.492	93.05
17	99.437	99.583	99.508	100.173	100.801	99.81
18	106.263	106.452	106.484	107.821	108.295	107.00
19	115.960	116.014	116.080	116.200	115.961	116.30
20	123.569	123.636	123.513	123.550	123.775	124.10
21	130.914	131.003	131.127	131.194	131.700	132.20
22	141.417	141.590	141.403	141.440	142.926	143.30
ave[h]	(1.6)	(1.2)	(1.6)	(2.2)	(1.6)	

a. The difference of the statistical total energies for the i^{th} and $(i+1)^{th}$ ions in the two separate calculation Δ_{SCF};
b. Δ_{SCF} plus the VWN correlation-energy correction;
c. Δ_{SCF} in the HF theory, ref. 102;
d. Orbital energy in the HF theory, ref. 102;
e. Transition-state calculation in the Xα method with theoretically determined parameter α, ref. 97;
f. Reference 103;
g. Reference 104;
h. ave $= [\sum_i^N |I_i^{Theor} - I_i^{Expt}|/I_i^{Expt} X100]/N$.

TABLE III-21

Ionization potentials (Ry) for the multiply charged ions of bromine, compared with other calculations and experiment

Degree of Ionization	GX-LSD Without Corre.[a]	GX-LSD With VWN[b]	HF Unrel.[c]	Xα[d]	Expt[e]
0	0.802	0.867	0.911	0.859	0.87
1	1.480	1.570	1.676	1.608	1.60
2	2.522	2.549	2.580	2.433	2.65
3	3.379	3.414	3.410	3.322	3.48
4	4.276	4.323	4.292	4.261	4.39
5	6.318	6.397	6.196	6.370	6.51
6	7.521	7.557	7.350	7.457	7.57
7	14.237	14.327	14.040	14.255	14.41
ave[f]	(3.8)	(1.5)	(3.3)	(2.8)	

a. The difference of the statistical total energies for the i^{th} and $(i+1)^{th}$ ions in the two separate calculation Δ_{SCF};
b. Δ_{SCF} plus the VWN correlation-energy correction;
c. Δ_{SCF} in the HF theory, ref. 102;
d. Orbital energy in the HF theory, ref. 102;
e. Reference 103;
f. ave $= [\sum_i^N |I_i^{Theor} - I_i^{Expt}|/I_i^{Expt} X100]/N$.

tials of multiply-charged ions for C, Al, Ca, Fe, and Br to compare the results with those from the Xα calculations[97] and Cl and Ar which are interesting to chemists and astrophysicists. The effect of the correlation correction proposed by Vosko et al.[39] on the ionization potential is considered.

The SIC-GX-LSD theory with the GWB Fermi-hole parameters was applied to calculate the wave functions of the neutral atoms together with the corresponding multiply-charged ion wave functions. These numerical wave functions were then used to calculate the corresponding statistical total energies, equation (1-86), and the VWN correlation energy corrections, equation (1-108), for the atoms and ions.

The VWN has not been treated self-consistently, becaused it is not very important in calculating ionization potentials[100], although it is essential in predicting electron affinities for the alkaline-earth elements, rare gasses, and actinides[92,94,101], which will be discussed later in detail. The ionization potentials were obtained from the differences of the statistical total energies which included the VWN correlation-energy corrections for the k^{th} and $(k+1)^{th}$ ions, equation (3-4). Results in Table III-15 to III-21 are compared to the HF results[102] and experiment[83,103,104].

Relaxation lowers the total energy and decreases as the number of electron increases. The HF results in columns 4 and 5 of Tables III-15 to III-20 show the ionization potentials of the multiply-charged ions without relaxation to be mostly larger than experiment. In addition, correlation lowers the total energy but increases as the number of electrons increases and therefore, the correlation correction increases the ionization potential; all the values in column 3 are bigger than those in columr 2.

The electron correlation-energy correction plays an important role in the first ionization potentials and electron affinities mentioned earlier, because the contribution of the correlation correction to the electron affinity is comparable to that of the kinetic, Coulomb and exchange interaction energies. Comparing the results of the SIC-GX-LSD-GWB theory with the VWN correlation correction in column 3 of Tables III-15 to III-21 with those excluding the VWN correlation correction in column 2 shows that the correlation-energy correction also plays a role in the ionization potentials of the multiply-charged ions.

In Tables III-15, III-16, and III-19 to III-21, the calculation of the multiply-charged ions obtained by using a Slater transition-state calculation in the $X\alpha$ theory[97] with theoretically determined parameter α are also presented. The data show that the results in the SIC-GX-LSD-GWB theory and in the transition-state

of $X\alpha$ theory with theoretically determined parameter α are comparable with the results from the HF theory. But the ionization potentials of the multiply-charged ions in SIC-GX-LSD-GWB theory with the VWN correlation energy correction are much better than all others. Their agreement with experiment is excellent.

The deviation of each calculated ionization potential, Tables III-15 to III-21, from the experimental values is expressed as a percentage. These percentages are averaged for all multiply-charged ions of the same element to give the average percentage deviations for the theories discussed in this work, the relaxed and unrelaxed HF, and the recent $X\alpha$ transition state results. The results using SIC-GX-LSD-GWB theory with the VWN correlation correction are the best. The average percentage deviation for all these elements in this theory are less than 1.5 percent. Furthermore the percentage deviation for each value is about one.

One may expect to calculate the ionization potentials of the multiply charged ions by means of the traditional $X\alpha$ theory with the corresponding optimal α values of the neutral atoms. In order to compare the SIC-GX-LSD results with those in the traditional $X\alpha$ theory, the relaxed $X\alpha$ calculations for the ionization potentials of these multiply-charged ions were carried out using Schwarz's α values[10] for neutral atoms and corresponding α values of the atoms which are of the same number of electrons as the multiply-charged ions. The results (not listed here) are much worse than those in the HF and SIC-GX-LSD theories which agree with experiment. The average percentage deviations are around 3.5[105].

From the results listed in Tables III-15 to III-21 and the comparison above, it can be seen that the ionization potentials of multiply-charged ions calculated by means of the difference between two statistical total energies in the SIC-GX-LSD theory with the GWB Fermi-hole exchange parameters are comparable with that in the HF theory. The SIC-GX-LSD theory is much easier and cheaper to use than the

HF theory. The correlation energy correction of the electrons with different spin is important, so that the SIC-GX-LSD-GWB theory with the VWN correlation correction gives excellent ionization potentials for the multiply-charged ions in the agreement with experiment. It can be expected that the quasi-relativistic SIC-GX-LSD theory with the GWB Fermi-hole parameters and the VWN correlation energy correction should give very good ionization potentials of the multiply-charged ions for the high-Z elements, even for the actinides, with acceptable computational time, because there is no need to search for the optimal exchange parameters α for each atom or ion. Based on the excellent agreement between the calculated and experimental values, the SIC-GX-LSD theory with the GWB exchange parameters and the VWN correlation energy correction can be used to predict the ionization potentials of multiply-charged ions which are unknown experimentally.

CHAPTER IV

STABILITY OF SINGLE- AND DOUBLE-CHARGED NEGATIVE IONS

IV-1. Introduction

Hotop and Lineberger[58,72] summarized the binding energies in atomic negative ions and showed that most single-charged negative ions of atoms are stable, except for the rare gases, alkaline-earth elements, and some transition metals. The alkali-metal elements get a second electron in the outermost s orbital to form a stable negative ion, with a positive binding energy, whereas the alkaline-earth elements have the electron in another p or d orbital and therefore have negative values for the electron affinities, so that the negative ions of these elements do not exist.

Fischer et al.[106] reported a positive electron affinity for the alkaline-earth element Ca by the multiconfiguration HF (MCHF) method, with relativistic correction. The prediction was confirmed in an elegant experiment by Pegg et al.[107] Vosko et al.[94] found the negative ions for other alkaline-earth elements Sr^-, Ba^-, and Ra^- are also stable by a HF calculation with relativistic shift and electron correlation correction, when the electron configurations were ns^2np (n = 4, 5, 6, and 7) and not (n-1)d ns^2. Fischer[108] studied the electron affinities of alkaline-earth elements by the MCHF theory, and also predicted positive electron affinities for the alkaline-earth elements Ca, Sr, and Ba in electron configuration ns^2np and not (n-1)dns^2. The Fischer et al.[106] and Vosko et al.[94] prediction was confirmed by Guo and Whitehead[101] and Fuentealba et al.[109] in the correlation corrected LDF theory.

The probability that stable negative ions exist for rare gases has been investigated theoretically and experimentally. Kuyatt et al.[110] calculated electron affinities within ± 0.03eV for the rare gases from resonances observed in the elastic scattering of electrons. Zollweg[111] estimated negative electron affinities for the rare gases by horizontal analysis. In contrast the excited state of rare-gas negative ions are predicted to be stable experimentally and theoretically with respect to the excited state of the corresponding neutral atoms[111-115]. The electron affinity, for example, is 0.51 eV from He ($1s\ 2s^3S$) to He^- ($1s\ 2s^22S$).

There are few reliable results of the electron affinities for the elements with $Z \geq 87$ which are missing in Hotop and Lineberger's papers[58,72]. Bratsch and Lagowski[116] obtained electron affinities for the actinides by considering the energy variations associated with changes in the $5f$ orbital population, while Sen and Politzer[117] calculated electron affinities by using the SIC-LSD theory[118] with the relativistic and correlation corrections. Bratsch and Lagowski[116] predicted the ground-state electron affinities of the actinides with the range +1.0 to -0.3 eV, with an estimated uncertainty of ± 0.3 eV for the elements whose electron affinities were +0.3 to -0.3eV and ± 1 eV for Fm and Md (the electron affinities are 1.0 eV for Fm and -0.1 eV for Md). Sen and Politzer[117] predicted the electron affinities for the actinides more accurately than Bratsch and Lagowski, but obtained converged values for only half the actinides. It is essential to attempt to get more reliable electron affinities for these elements by calculation.

The first aim[92,101] of this chapter is to test the reliability of the GX-LSD theory, with the self-interaction correction, the electron correlation correction, and the relativistic correction, to predict the stability of the negative ions for the alkaline-earth elements and the electron affinities for them, because accurate calculations[106] and experimental results[107] exist. If the LDF theory works for the negative ions

of the alkaline-earth elements, it will be extended to predict the stability of the negative ions for the rare gases and actinides and the electron affinities for them, since the LDF theory is much more efficient than the HF, MCHF, CI, et al.

Attention has also been paid to investigating the doubly charged negative ions experimentally[119-127] and some evidence for the existence of doubly charged negative ions, such as, O^{2-}, Te^{2-}, Bi^{2-}, F^{2-}, Cl^{2-}, Br^{2-}, and I^{2-} was found[122]. Theoretically, the stability of doubly charged negative ions of atoms has been of interest for a long time. Baughan[128] calculated the first, second, and third electron affinities for atoms using lattice-energy data of ionic crystals, and the spectroscopic data of the corresponding molecules, and estimated the values of the second electron affinities for elements O, S, and Se and the third electron affinity for N by the extrapolation, starting from the first, second and third ionization potentials of the corresponding atom. Gáspár and Csavinszky[129] presented the solution of O^{2-}; Watson[130] published O^{2-} results which are the analytic forms of the wave functions, one-electron eigenvalues, two electron integrals, and total energy for the doubly charged negative ion, O^{2-}, in the Hartree-Fock (HF) theory using an artificial positively charged sphere surrounding the doubly charged negative ion. Clementi and McLean[131] reported the results for N^{2-} and O^{2-} and concluded that they were unstable because the second electron affinities were -0.454 Ry for N and -0.444 Ry for O in the electron-correlation corrected HF theory. Ahlrichs[132] pointed out that HF calculations which yield $\epsilon_k > 0$ for an occupied orbital do not minimize the HF energy. He calculated some multiply charged negative ions, O^{2-}, N^{3-}, C^{4-}, S^{2-}, O_2^{2-}, and C_2^{2-} in the HF theory by an appropriate admixture of a continuum function to the corresponding orbital, but could not find any evidence of stable multiply charged negative ions, although he arrived at much lower total energies than Robb and Csizmadia[133]. Recently, Kalcher[134] studied the stability of the doubly charged negative ions of the second-period elements, Si, P, S, and Cl in a configuration-

interaction (CI) calculation using systematically different substitutions from any configuration of the reference wave functions. He reported that the doubly charged negative ions of Si, P, S, and Cl were unstable with negative electron affinities between -0.0494 Ry and -0.0612 Ry.

There is no report in the literature about the investigation of the stability of doubly charged negative ions of atoms in the gas phase in the LDF theory, although the LDF theory has been widely used to study molecular bonding, magnetism, cohesion, the surface electronic properties of metals, and semiconductors[74] and to predict the stability of singly charged negative ions. The reason is obvious if one focuses on the details of the numerical self-consistent-field (SCF) procedure in the LDF theory[48]. Following the numerical approach of Herman and Skillman[48], the wave function is obtained by outward numerical integration starting from r=0 and inward numerical integration starting from r=∞. The wave functions at the first several mesh points in both directions are calculated by solving the one-electron Schrödinger equation analytically with the asymptotic forms of the potential $V^{hm}(r)$ for each orbital, when r approaches zero and infinity. The radial function is of the form

$$P_{nl}(r) = c_0 e^{-[q_{nl}(r)]^{1/2} r} \qquad (4-1)$$

when r approaches infinity; where c_0 is a normalization constant and $q_{nl}(r)$ is

$$q_{nl}(r) = V^{\infty}(r) - \epsilon_{nl} \qquad (4-2)$$

where ϵ_{nl} is the one-electron eigenvalue. In the self-interaction corrected (SIC) LDF theory, e.g., the SIC-LSD theory[30], the asymptotic potential, $V^{\infty}(r)$, when r approaches infinity, is

$$V^{\infty}(r) = -\frac{2(Z-N+1)}{r} \qquad (4-3)$$

with the atomic number Z and the number of total electrons N in Rydberg atomic units. $V^{\infty}(r)$ is positive for a doubly charged negative ion, because of N=Z+2. With this feature, the orbital energy is positive[132].

In the SIC-LSD theory, the one-electron eigenvalue ϵ_{nl} is approximately equal to the orbital energy[30,49]. This implies that $q_{nl}(r)$ in equation (4-2) is negative when r approaches infinity. The wave function (4-1) is continuous. Consequently, no bound wave function can be obtained in the SIC-LSD theory for a doubly charged negative ion.

The second aim of this chapter is to investigate the stability of the doubly charged negative ions of atoms in crystals and the stability of the doubly charged negative ions of the second and third period elements which involve one orbital in going from the neutral atom to its doubly charged negative ion in the gas phase by the SIC-GX-LSD theory with the GWB Fermi-hole parameters and the VWN electron correlation energy functional and by means of a special convergence technique. As mentioned above, no bound solution can be found by directly solving the Schrödinger equation in the SIC-LSD theory. Consequently, a positively charged artificial sphere, which was proposed by Watson[130] (henceforth called the Watson sphere) and usually used in the molecular anion calculations[135-137], is invoked to surround the doubly charged negative ion and ensure the one-electron Schrödinger equation has a bound solution. Obviously, the statistical total energy and the electron-density distribution of a doubly charged negative ion are dependent on the size of the Watson sphere and the charge on the Watson sphere. However, if the charge on the Watson sphere is fixed, and the radius of the Watson sphere is gradually increased, the calculated statistical total energy and the electron-density distribution of the doubly charged negative ion should then gradually approach the real statistical total energy and the electron-density distribution of the system. On the other hand, the VWN correlation corrected SIC-GX-LSD theory with the GWB Fermi-hole parameters has been previously established to be excellent for predicting the ionization potentials and electron affinities of atoms[92,101] compared to experiment.

IV-2. Alkaline-Earth Elements and Actinides

The one-electron Schrödinger equation (1-90) in the SIC-GX-LSD theory and equation (1-125) in the QR-SIC-GX-LSD theory both with the GWB Fermi-hole parameters have been used and attempt made to get converged values for the negative ions of the alkaline-earth and actinide elements. It failed to converge for all the negative ions of the alkaline-earth elements including both the electron configurations ns^2np and (n-1)d ns^2 and for most negative ions of the actinide elements; the SCF procedure was not convergent.

The elements are classified in two categories again: (i) elements which involve one orbital in going from the neutral atom to the negative ion and (ii) elements involving two orbitals going from the neutral atom to the negative ion. In Hotop and Lineberger's paper[58], all the negative ions involving one orbital are stable, whereas almost all the negative ions involving two orbitals are unstable except for the transition-metal elements Sc, Y, and Pd. Previous calculations of the electron affinities of atoms (in Chapter III)[45,73] also showed that equations (1-90) and (1-125) worked very well in predicting the electron affinities for the first category elements and failed for the second category. In the Roothaan-Hartree-Fock theory, Clementi and Roetti[51] reported the calculation of negative ions for the elements $Z < 54$ except for the alkaline-earth elements and rare gases (which they either did not calculate or found non-convergency). Recently, Vosko et al. [94] reported the results for the negative ions of the alkaline-earth elements by the HF theory with the density-functional correlation correction potential. The electron-correlation correction energy and potential which were given in equations (1-98) and (1-114), respectively, proposed by Vosko, Wilk, and Nusair[39] (VWN), have been included in their calculation.

Equations (1-90) and (1-125) combined with equation (1-114), the VWN correlation correction potential[138], have been tested on the alkaline-earth and actinide

elements. The calculations showed that the SIC-GX-LSD-GWB theory with the VWN correlation correction potential works very well for all the negative ions of the alkaline-earth elements whose electron configurations are ns^2np, but not for configurations (n-1)d ns^2, and very well for most of the negative ions of the actinides. Probably, because of auto-ionization effect, the neutral atoms of the alkaline-earth elements may not stably bind an extra electron in their (n-1)d orbitals.

Therefore, equations (1-90) and (1-125) with the GWB parameters and the VWN correlation correction potential have been used to calculate the wave functions and eigenvalues of the neutral atoms and the negative ions for the alkaline-earth and actinide elements. The calculated wave functions were then used to calculate the statistical total energies, equation (1-86), and the VWN correlation energy corrections, equation (1-98), for the corresponding atoms and negative ions using the SIC-GX-LSD theory. To compare the VWN correlation correction with that proposed by Stoll, Pavlidou, and Preuss[38] (SPP), the wave functions in equations (1-90) and (1-125) with the GWB parameters and the VWN correlation correction were used to evaluate the SPP correlation energy corrections. Finally, the electron affinities of the alkaline-earth and the actinide elements were obtained by means of the difference of the statistical total energies between the neutral atoms and the corresponding negative ions, equation (3-4). These results are listed in Tables IV-1 to IV-3.

TABLE IV-1

Electron affinities (Ry) for Mg, Ca, Sr, Ba, and Ra calculated by the SIC-GX-LSD-GWB theory with the VWN correlation, compared with other non-relativistic calculations and experiment

Z	Elec. Atom	Confi. Ion	GX-LSD No Corr.	GX-LSD SPP	GX-LSD VWN	HF[a] VWN	MCHF[b]	Expt[c]
12	Mg	$3s^2$	$3s^2 3p^1$	−0.0059	0.0079	0.0056			
20	Ca	$4s^2$	$4s^2 4p^1$	−0.0112	0.0150	0.0105	0.0102	0.140	0.0032 ± 0.0005
38	Sr	$5s^2$	$5s^2 5p^1$	−0.0113	0.0163	0.0117	0.0142	0.256	
56	Ba	$6s^2$	$6s^2 6p^1$	−0.0117	0.0209	0.0156	0.0194	0.554	
88	Ra	$7s^2$	$7s^2 7p^1$	−0.0112	0.0220	0.0168	0.0206		

a. Reference 94;
b. Reference 108;
c. Reference 107.

IV-2.1 Alkaline-Earth Elements

Tables IV-1 to IV-2 summarize the electron affinities for the alkaline-earth elements in the SIC-GX-LSD and QR-SIC-GX-LSD theories with the GWB Fermi-hole parameters and with and without the SPP and VWN correlation-energy correction compared with other theoretical calculations[94,108] and experiment[107]. Tables IV-1 and IV-2 show that (i) the contributions of the kinetic, Coulomb, and exchange energies to the electron affinities are negative, and almost equal except in Mg; (ii) the electron affinities become positive once the correlation-energy correction is added; the electron correlation makes the negative ions stable; and (iii) the relativistic contribution to the electron affinities is negative, which is opposite to the relativistic contribution to the ionization potential of atoms which is usually positive. These features parallel HF theory[94].

Comparing the present results with the HF (Ref. 94) and MCHF (Ref. 108)

calculations shows that the QR-SIC-GX-LSD theory with the VWN correlation correction results in excellent agreement with HF, whereas the QR-SIC-GX-LSD theory with the SPP correlation-energy correction overestimates the electron affinities. The MCHF theory obviously overestimates the electron affinities compared to HF, the present work, and experiment.

TABLE IV-2

Electron affinities (Ry) for Mg, Ca, Sr, Ba, and Ra calculated by the QR-SIC-GX-LSD theory with the VWN correlation, compared with other calculations and experiment

Z	Elec. Atom	Confi. Ion	GX-LSD No Corr.	GX-LSD SPP	GX-LSD VWN	HF[a] VWN	MCHF[b]	Expt[c]
12 Mg	$3s^2$	$3s^2 3p^1$	−0.0058	0.0078	0.0056			
20 Ca	$4s^2$	$4s^2 4p^1$	−0.0110	0.0146	0.0102	0.0096	0.124	0.0032 ± 0.0005
38 Sr	$5s^2$	$5s^2 5p^1$	−0.0106	0.0146	0.0104	0.0118	0.212	
56 Ba	$6s^2$	$6s^2 6p^1$	−0.0105	0.0175	0.0129	0.0146	0.296	
88 Ra	$7s^2$	$7s^2 7p^1$	−0.0090	0.0121	0.0085	0.0092		

a. Reference 94;
b. Reference 108;
c. Reference 107.

It is interesting that the predicted values for the electron affinity of Mg in both the SIC-GX-LSD and QR-SIC-GX-LSD theories with the SPP and VWN correlation-energy correction are positive. Subtracting the overestimated value for Mg, in contrast with Ca, the electron affinity for Mg is probably around zero.

IV-2.2 Actinides

The electron affinities of the actinides with and without the SPP and VWN correlation energy correction in the QR-SIC-GX-LSD theory with the GWB Fermi-hole parameters are listed in Table IV-3 and compared with the results calculated by the SIC-LSD theory[117] and the values estimated by using the energy variation extrapolation[116]. The present results in the SIC-GX-LSD theory with the SPP and VWN correlation-energy correction are larger than those in the SIC-LSD theory and also larger than the extrapolated values, except for Cm, Md, and Lr. However, the results in the SIC-GX-LSD theory with the VWN correlation energy correction are within the estimated uncertainty of the extrapolated results, except for Th and Lr.

As mentioned before, the electron affinities are usually positive for elements involving a single orbital, according to the previous calculations[45,73] and Hotop and Lineberger's paper[58] for the elements $Z < 87$. Therefore the negative ions are usually stable for the first category elements. The few exceptions in the actinide elements are shown in Table IV-3, that is, Pu, Bk, Cf, and Es, the first-category elements have negative electron affinities.

Am belongs the second category element using two orbitals, but its negative ion is stable according to the present calculation. Other electron configurations of the negative ion, like $5f^7 6d^1 7s^2$ and $5f^8 7s^2$, have been tried, but no converged results have been obtained. The extra electron of Am^- goes to the $7p$ orbital instead of $5f$ and $6d$. From Table IV-3, one may see that Th^- and Md^- are the most stable negative ions according to the present calculation, in agreement with Bratsch and Lagowski's estimation[116].

Although the electron correlation correction potential is very small compared to the Coulomb, exchange, and SIC potentials, it is very important in the present

TABLE IV-3

Electron affinities (Ry) for actinides calculated using the QR-SIC-GX-LSD-GWB theory with the VWN and SPP correlation corrections, compared with other calculations and experiment

Z	Electron Atom	Config. Ion	GX-LSD No Cor.	GX-LSD SPP	GX-LSD VWN	LSD[a]	Extra.[b]
89 Ac	$6d^1 7s^2$	$6d^2 7s^2$	−0.0156	0.0437	0.0322	0.0206	0.022
90 Th	$6d^2 7s^2$	$6d^3 7s^2$	0.0361	0.1005	0.0863	0.0706	0.037
91 Pa	$5f^2 6d^1 7s^2$	$5f^2 6d^2 7s^2$	−0.0071	0.0530	0.0406	0.0243	0.022
92 U	$5f^3 6d^1 7s^2$	$5f^3 6d^2 7s^2$	−0.0086	0.0516	0.0390	0.0213	0.022
93 Np	$5f^4 6d^1 7s^2$	$5f^4 6d^2 7s^2$	−0.0123	0.0477	0.0351	0.0176	0.022
94 Pu	$5f^6 7s^2$	$5f^7 7s^2$	−0.0986	−0.0203	−0.0370		
94		$5f^6 6d^1 7s^2$	*	*	*	*	−0.022
95 Am	$5f^7 7s^2$	$5f^7 7s^2 7p^1$	−0.0068	0.0104	0.0076		
95		$5f^7 6d^1 7s^2$	*	*	*	*	−0.022
95		$5f^8 7s^2$	*	*			
96 Cm	$5f^7 6d^1 7s^2$	$5f^7 6d^2 7s^2$	−0.0255	0.0330	0.0208	0.0022	0.022
97 Bk	$5f^9 7s^2$	$5f^{10} 7s^2$	−0.2215	−0.1096	−0.1265		
97		$5f^9 6d^1 7s^2$	*	*	*	*	−0.022
98 Cf	$5f^{10} 7s^2$	$5f^{11} 7s^2$	−0.1687	−0.0571	−0.0745		
98		$5f^{10} 6d^1 7s^2$	*	*	*	*	−0.022
99 Es	$5f^{11} 7s^2$	$5f^{12} 7s^2$	−0.1146	−0.0042	−0.0219		
99		$5f^{11} 6d^1 7s^2$	*	*	*	*	−0.022
100 Fm	$5f^{12} 7s^2$	$5f^{13} 7s^2$	−0.0651	0.0439	0.0260	*	−0.007
101 Md	$5f^{13} 7s^2$	$5f^{14} 7s^2$	−0.0175	0.0900	0.0719	*	0.074
102 No	$5f^{14} 7s^2$	$5f^{14} 7s^2 7p^1$	−0.1803	−0.1692	−0.1709		
102		$5f^{14} 6d^1 7s^2$	*	*	*	*	−0.022
103 Lr	$5f^{14} 6d^1 7s^2$	$5f^{14} 6d^2 7s^2$	−0.0503	−0.0156	−0.0230	*	0.022

* No convergence obtained;
a. Reference 117;
b. Reference 116.

calculations. This correlation correction determines whether the negative ions for the alkaline-earth and most of the actinide elements converge.

The QR-SIC-GX-LSD theory with correlation correction potential can be used to predict the electron affinities of the alkaline-earth and actinide elements.

The electron affinities are as good as the HF theory with density-functional correlation correction potential, and are much easier and cheaper to use. The present results of the alkaline-earth elements strongly support the prediction of the stable negative ions Ca^-, Sr^-, Ba^-, and Ra^- made by Fischer et al.[106] and Vosko et al.[94], if their electron configurations are ns^2np.

IV-3. Rare Gases and Actinides

The calculation of the negative ions for the actinide elements has not been completed because of the non-convergence problem for some of them. They will be discussed in this section. Furthermore, the probability of the stable negative ions for the rare-gas elements will be discussed in the SIC-GX-LSD theory with the VWN correlation correction potential and a special convergence technique[92].

IV-3.1 Adiabatic Convergence Technique

Starting with the converged potential of the neutral atom from a Herman and Skillman[48] calculation and the electron configuration for the corresponding negative ion, neither gave converged values for any of the rare gases, nor for the actinides. The converged potential deviates too much from the real negative ion potential to be stable to bind an extra electron. However, starting with the converged potential and the electron configuration of the neutral atom, 10 percent of an electron was added in each following iteration until a total of one electron was included in the extra orbital; for the rare gases, convergence was then achieved from this negative-ion state. In the SCF processes of actinide negative ions, adding 10 percent of an electron in the extra orbital in the following iteration turned out to be too big for the

SCF process to stabilize. In order to increase the occupation number smoothly, the function 0.051×1.05^{-i}, in which i is the iteration number, was used to add the new fractional electron in the first 81 iterations. This slow, adiabatic change from the neutral atom allows the system to remain in its ground state. The mixture factor was chosen to be 0.25 for the negative ions of the rare gases, so that 75 percent of electron density from the $(i-1)^{th}$ iteration and 25 percent of electron density from the i^{th} iteration were combined together and used to calculate the new potential for the $(i+1)^{th}$ iteration. The mixture factor for the actinide elements was reduced to 0.05 for the negative ions. The SCF was then performed until the differences of the wave functions between the i^{th} and the $(i+1)^{th}$ iterations were less than 10^{-8} at all the calculated mesh points.

TABLE IV-4

The negative of the one-electron eigenvalues (Ry) of the extra electrons for the negative ions of rare gases

Z	Atom	nl	SIC-GX-LSD	QR-SIC-GX-LSD
2	*He*	2*s*	00738	0.00738
10	*Ne*	3*s*	00805	0.00806
18	*Ar*	4*s*	00862	0.00865
36	*Kr*	5*s*	00904	0.00919
54	*Xe*	6*s*	00916	0.00957
86	*Rn*	7*s*	00932	0.01090

IV-3.2 Rare Gases

The existence of stable negative ions of atoms in nature is mainly caused by the quantum effect; because of the negative contribution of the exchange correlation effect of the electron to the energy functional, the neutral system (neutral atom) can bind an extra electron and form a stable system. The contribution of the nuclear attraction to forming the stable system is very small because each electron partially screens the nucleus from all other electrons. Furthermore, the exchange-correlation potential is approximately proportional to the electron number, so that the exchange-correlation effect increases with the number of electrons. The Coulomb repulsion between electrons, of course, increases with the number of total electrons. The exchange-correlation effect competes with the Coulomb repulsion; if the exchange correlation is bigger than the Coulomb repulsion, the negative ion is stable.

TABLE IV-5

Electron affinities (Ry) for the rare gases calculated by the SIC-GX-LSD and QR-SIC-GX-LSD theories with the GWB Fermi-hole parameters and the VWN correction

Z	Elec. Atom	Confi. Ion	GX-LSD No Corr.	GX-LSD VWN	QR-GX-LSD No Corr.	QR-GX-LSD VWN
2	He $1s^2$	$1s^2 2s^1$	−0.0029	0.0054	−0.0029	0.0054
10	Ne $2p^6$	$2p^6 3s^1$	−0.0035	0.0061	−0.0035	0.0061
18	Ar $3p^6$	$3p^6 4s^1$	−0.0040	0.0071	−0.0040	0.0071
36	Kr $4p^6$	$4p^6 5s^1$	−0.0043	0.0079	−0.0043	0.0081
54	Xe $5p^6$	$5p^6 6s^1$	−0.0043	0.0082	−0.0043	0.0091
86	Rn $6p^6$	$6p^6 7s^1$	−0.0045	0.0085	−0.0038	0.0126

Table IV-4 lists the negative of the one-electron eigenvalue of the extra orbital for the negative ions of rare gases in the SIC-GX-LSD theory, both nonrelativistic and quasi-relativistic (QR). The GWB exchange parameters and the VWN energy-correlation functional were employed in both cases. Table IV-5 gives the corresponding electron affinities. These tables show (i) that all the negative ions of the rare gases are stable, the electron affinities being several milli-rydbergs. The stability of these negative ions is caused by the correlation between the extra electron and all the other electrons. The Coulomb repulsion is much bigger than the exchange-only effect; (ii) the relativistic effect of the electrons increases the binding energy and the electron affinity. This is the reverse of the relativistic contribution to the negative ions of the alkaline-earth elements[101] in which the relativistic effect decreases the binding energies; (iii) the binding energies and electron affinities increase with atomic number, because of the increase in the Coulomb repulsion as the number of electrons increase.

TABLE IV-6

The negative of the one-electron eigenvalues (Ry) of the extra electrons for the negative ions of some actinides

Z	Atom	nl	SIC-GX-LSD	QR-SIC-GX-LSD
94	*Pu*	6*d*	0.0710	0.00288
95	*Am*	6*d*	0.0682	0.00291
97	*Bk*	6*d*	0.0473	0.00297
98	*Cf*	6*d*	0.0369	0.00299
99	*Es*	6*d*	0.0267	0.00299

IV-3.3 Actinides

Tables IV-6 and IV-7 summarize the results of some actinide elements for which no converged results had previously been obtained (in Section IV-2)[101,117]. Therefore the present results are compared with the estimated values obtained by energy extrapolation analysis[116]. Table IV-6 shows the one-electron eigenvalues of the negative ions for some actinide elements. The numbers decrease in absolute value with the occupation number of the $5f$ orbital in the SIC-GX-LSD theory, excluding the relativistic effect. When the relativistic effect is included the extra-electron eigenvalues are almost constant for these negative ions. The electron affinities for these actinide atoms are summarized in Table IV-7 and compared with the estimated values. With the relativistic term the extra electron is bound in the neutral system and forms a stable negative ion. The present prediction of the stability for the negative ions of these actinide elements is opposite to that by the energy-extrapolation analysis[116] in which the estimated uncertainty is $\pm$ 0.022Ry in the results. Previously[101], the electron affinities have been calculated for the electron configuration $5f^N 7s^2$ (N=7, 10, 11, and 12 for Pu^-, Bk^-, Cf^-, and Es^-, respectively) and yielded negative electron affinities. Consequently the extra electron in these negative ions favour the $6d$ orbital and not the $5f$ orbital.

The present results for the rare gases and some actinides show that their negative ions are still stable, even when the relativistic correction to the electron removal energy is overestimated for the rare gases and underestimated for the actinides as in the QR-SIC-GX-LSD theory (see Table III-10, because the spin-orbital coupling term is neglected in the QR-SIC-GX-LSD theory), except for the negative ions of Bk, Cf, and Es with electron configurations $5f^N\ 7s^2$. Further investigation of the stability for the negative ions of the rare gases and actinides is certainly

needed experimentally.

TABLE IV-7

Electron affinities (Ry) for some actinides calculated by the SIC-GX-LSD and QR-SIC-GX-LSD theories with the GWB Fermi-hole parameters and the VWN correlation correction *

Z		Elec. Atom	Confi. Ion	GX-LSD No Corr.	GX-LSD VWN	QR-GX-LSD No Corr.	QR-GX-LSD VWN
94	Pu	$5f^6 7s^2$	$5f^6 6d^1 7s^2$	0.0068	0.0596	0.0180	0.0272
95	Am	$5f^7 7s^2$	$5f^7 6d^1 7s^2$	0.0036	0.0564	0.0195	0.0278
97	Bk	$5f^9 7s^2$	$5f^9 6d^1 7s^2$	−0.0165	0.0386	0.0094	0.0154
98	Cf	$5f^{10} 7s^2$	$5f^{10} 6d^1 7s^2$	−0.0253	0.0303	0.0088	0.0140
99	Es	$5f^{11} 7s^2$	$5f^{11} 6d^1 7s^2$	−0.0340	0.0217	0.0061	0.0108

* The extrapolated values are -0.022 Ry for all these elements.

IV-4. Double-Charged Negative Ions in Crystals

Baughan[128] calculated the first, second, and third electron affinities of atoms using the lattice-energy data of some ionic crystals, and the spectroscopic data of the corresponding molecules; he also estimated the values of the second electron affinities for elements O, S, and Se and the third electron affinity for N by extrapolation, starting from the first, second, and third ionization potentials of the corresponding atom.

The HF calculations of double-charged negative ions in crystal have been performed by Gáspár and Csavinszky[129] who presented the solution of O^{2-}, and Watson[130] who published the analytic form of wave functions, the one-electron eigenvalues, the two-electron integrals, and the total energy for the double-charged negative ion, O^{2-}. The SCF calculation for a double-charged negative ion is much more difficult than that for a neutral atom, positive ion, or even single-charged negative ion, since the asymptotic form of the potential function becomes positive when the atomic radial variable r approaches infinity.

The study on the stability of doubly charged negative ions of atoms might be interesting; firstly, because there is no report dealing with the doubly changed negative ions from the LDF theory; secondly, the LDF theory is successful in describing the atomic and molecular structures. Hence, the SIC-GX-LSD theory with the GWB Fermi-hole parameters and the VWN correlation functional is used to calculate the doubly charged negative ions in crystals[139].

IV-4.1 Convergence Technique

In the SIC-LDF theory, the asymptotic form of the potential is

$$V(r) = -\frac{2(Z - N + 1)}{r} \qquad (4-4)$$

as r approaches infinity; Z and N are the atomic number and the number of electrons in an atom. For the double-charged negative ion, N=Z+2, and equation (4-4) becomes

$$V(r) = \frac{2}{r} \qquad (4-5)$$

This is a repulsive interaction. Physically, the second extra electron might not be bound stably by a single-charged negative ion in its free state because of the repulsive potential surrounding the isolated negative ion. Numerically, there is a continuous solution of the Schrödinger equation with the asymptotic potential of equation (4-5), instead of a bound wave function.

Stable double-charged negative ions exist in crystals, because of the surrounding environment. To simulate such an environment for the double-charged negative ions in crystals and to ensure a bound solution to the Schrödinger equation, Watson proposed a sphere of charge +1 or +2 with a defined radius surrounding the free single- or double-charged negative ion. The charged sphere forces the asymptotic form of the potential to be negative and the Schrödinger equation to give a bound solution.

The extra potential generated by the Watson sphere with charge +1 or +2 (the environment of the double-charged negative ion in crystal) is combined within the SIC-GX-LSD theory. The one-electron Schrödinger equation (1-90) is solved self-consistently with the pure Coulomb potential (1-91), the exchange potential (1-127), the self-exchange correction (1-128), and the VWN correlation energy

functional (1-114). The statistical total energy and the VWN correlation energy correction are calculated by equations (1-86) and (1-98) with the converged wave functions.

IV-4.2 Estimation of Electron Affinity

The calculation of the double-charged negative ion of oxygen, O^{2-} , was carried out using the SIC-GX-LSD theory with the GWB Fermi-hole parameters and the VWN correlation energy functional, and a Watson sphere of charge +1 and +2. The calculated SIC-GX-LSD statistical total energy (including the energy contribution of the Watson sphere but excluding the VWN correlation energy correction) for O^{2-} was -156.2137Ry for the +1 Watson sphere and -163.5574 Ry for the +2 Watson sphere, compared to Watson's HF calculation[130] in which the total ionic energy (including Watson sphere energy) was -156.1194 Ry for the +1 Watson sphere and -163.4968 Ry for the +2 Watson sphere. The same radius (1.4 $\AA$ or 2.66 a.u.) of Watson sphere[130] was used in both calculations. The excellent agreement of the total energies for the double-charged negative ion from the SIC-GX-LSD theory and from the HF theory parallels that for the neutral atoms, positive ions, and the single-charged negative ions[74]. Therefore the SIC-GX-LSD theory predicts double-charged negative ions as reliably as the HF theory.

The statistical total energy of a negative ion from the Watson sphere aided SIC-GX-LSD theory is dependent on the charge on Watson sphere. There are several choices of the charges on the Watson sphere, +2, +1, or 0 for the single- and double-charged negative ions. The calculation shows that there is no difficulty in getting convergent results for the single- and double-charged negative ions with the Watson sphere of charge +1 and +2, but, as mentioned in section IV-4.1, it

might be impossible to obtain a convergent value for a double-charged negative ion using the Watson sphere of charge 0, which is equivalent to a calculation without any Watson sphere.

TABLE IV-8

The total energies (Ry) including the statistical total energy and the VWN correlation energy contribution for the single- and double-charged negative ions of O without and with the Watson sphere energy contribution in the Watson sphere aided SIC-GX-LSD theory with the VWN correlation correction

Degree of Ion	Without[a] +2	+1	0	With[b] +2	+1	0
-1	−150.0894	−150.1131	−150.1310	−163.5258	−156.8166	−150.1310
-2	−149.4502	−149.5549	– – ––	−164.2259	−156.8741	– – ––
EA	−0.6392	−0.5582		+0.7001	+0.0575	

a. Without the energy contribution of the Watson sphere;
b. With the energy contribution from the Watson sphere.

Table IV-8 summarizes the VWN correlation energy corrected statistical total energies without and with the energy contribution from the Watson sphere for the single- and double-charged negative ions of oxygen, O^- and O^{2-}, in the SIC-GX-LSD theory with the Watson sphere of charge +2, +1, and 0 and radius 2.66 a.u. The last line gives the corresponding energy differences of the single- and double-charged negative ions, that is,

$$EA = E^-_{tot} - E^{2-}_{tot} \qquad (4-6)$$

the second electron affinity of O, where E^-_{tot} and E^{2-}_{tot} are the total energy with the energy contribution from the VWN correlation correction excluding the Watson

sphere energy (corresponding to columns 2, 3, and 4 in Table IV-8) or the total energy including the Watson sphere energy (columns 5, 6, and 7), respectively Compared to the experimental second electron affinity, -0.60Ry for O, it is clear that the difference of the statistical total energies (excluding the Watson sphere energy) with both +1 and +2 charges for the single- and double-charged negative ions (columns 2 and 3) can be used to fit the experimental value of the second electron affinity for O by slightly adjusting the radius of the Watson sphere. However, the difference of the statistical total energy including the Watson sphere energy(columns 5 and 6) cannot be fitted to experiment. The best prediction of the second electron affinity for O is with the Watson sphere of charge +2.

The difference of the statistical total energies between the single-charged negative ion O^- with the Watson sphere of charge +1 and the double-charged negative ion O^{2-} with the Watson sphere of charge +2, is -0.6629Ry, close to experiment. It can be used to fit the experimental value by adjusting the radius of Watson sphere. However, this method was not used to predict any other second electron affinity because (i) the best fit of the second electron affinity is obtained from the difference of the statistical total energies, with the Watson spheres of charge +2 and radius 2.66a.u. (which is interestingly close to the lattice-distance); (ii) physically, the second electron affinity should be the total energy difference between the single- and double-charged negative ions in the same environment, it is possible to obtain a positive second electron affinity for an atom by using a different environment for the single- and double-charged negative ions.

The statistical total energy of the negative ion in the Watson sphere aided SIC-GX-LSD theory depends on the Watson sphere radius. Therefore the difference between the statistical total energies for the single- and double-charged ions, equation (4-6), depends on the choice of Watson sphere radius. Watson suggested using

the ionic radius of the double-charged negative ion for the artificial charged sphere. This suggestion was tested in the present work for O, S, and Se using the Watson sphere of charge +2. The second electron affinity in the SIC-GX-LSD theory with the VWN correlation energy correction is -0.6655 Ry for O, -0.3858 Ry for S, and -0.3462 Ry for Se, compared to the averaged experimental values which are -0.595 Ry for O, -0.45 Ry for S, and -0.39 Ry for Se. Obviously, the agreement between the calculated and experimental values is not consistent for these three elements; the second electron affinity is underestimated for O and overestimated for S and Se using the ionic radii of the double-charged negative ions for the Watson spheres.

To find the Watson sphere radius which is best for calculating the second electron affinity of an atom, the second electron affinities, the difference of the total energies (including the VWN correlation energy correction but excluding the Watson sphere energy) between the single- and double-charged negative ions, with a Watson sphere of charge +2 are plotted in Fig. 4-1 against the radii of Watson sphere for O, S, and Se in the SIC-GX-LSD theory with VWN correlation energy functional and GWB Fermi-hole parameters. Fig. 4-2 has a Watson sphere of charge +1. The experimental values of the second electron affinities for $O^{128,140}$, S, and $Se^{128,141}$ are also marked on the corresponding curves of these figures. From Figs. 4-1 and 4-2, it is obvious that the calculated second electron affinities of O, S, and Se are much less negative with a Watson sphere of charge +1 than with a sphere of charge +2 for the same Watson sphere radius. Physically, the Watson sphere of charge +2 is more reasonable, because the net charge provided by the remainder of a crystal would be +2 for an equilibrium situation. The Watson sphere has to be very small to give an acceptable second electron affinity with a +1 charge sphere so that it is far from the lattice-distance found in the crystal.

Fig. 4-1 illustrates the calculated second electron affinity for O equal to

FIGURE 4-1

The difference of the statistical total energies between the single- and double-charged negative ions, with a Watson sphere of charge +2 vs the radius of the Watson sphere

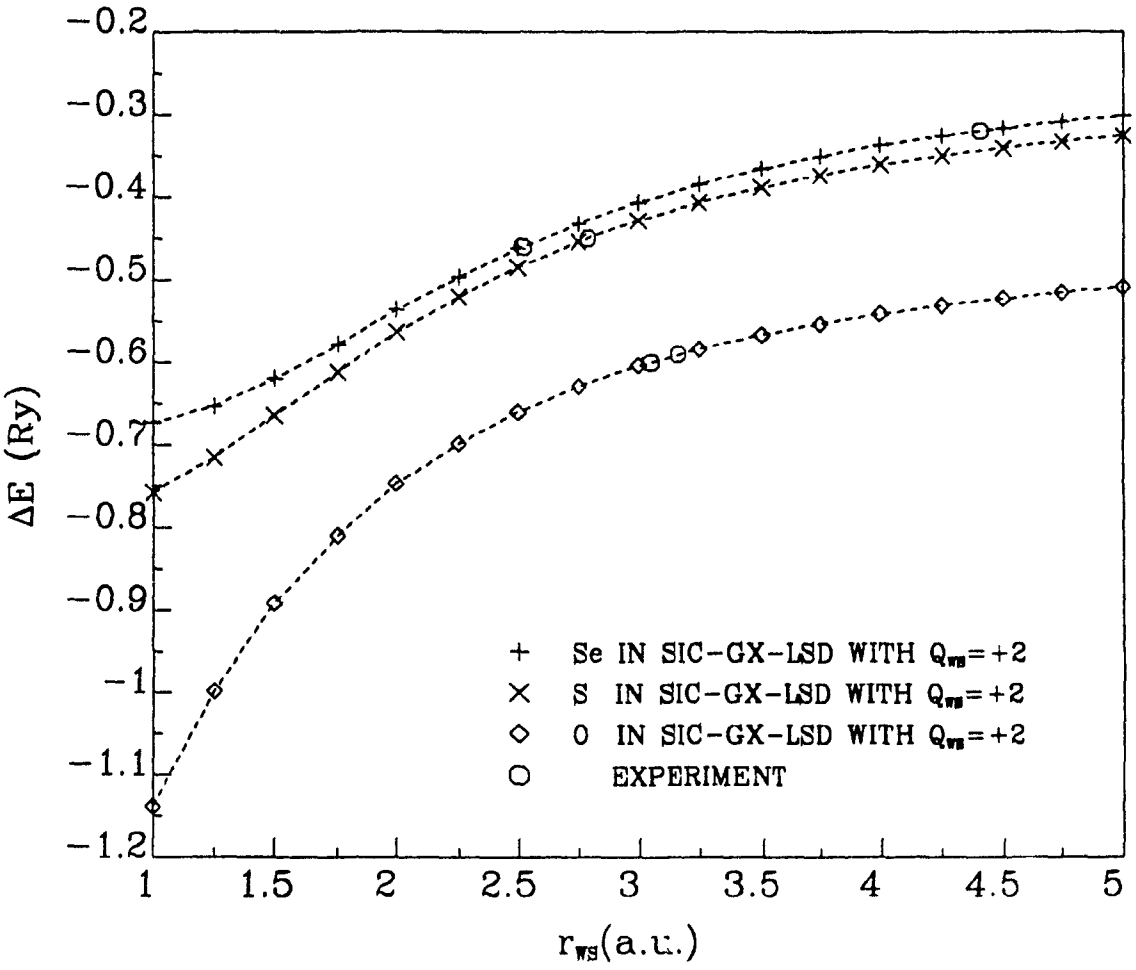

experiment at a Watson sphere radius of approximately 3.0 a.u.; approximately 2.8 a.u. for S and 2.6 a.u. for Se or 4.37 a.u., since two different experimental values of the second electron affinity for Se are given[128,141]. The "best" Watson sphere radius, suitable for the three double-charged negative ions to give correct second electron affinities, compared to experiment, is approximately 3.0 a.u.

Table IV-9 lists the negative of the second electron affinities for atoms helium to krypton calculated using equation (4-6), in which the total energies are the statistical total energies (including the VWN correlation energy correction and excluding the energy generated by the Watson sphere) with the Watson sphere of charge +2 and radius 3.0 a.u. using the SIC-GX-LSD theory with the VWN correlation energy functional and the GWB Fermi-hole parameters. These results are compared with other estimates[128,141], for which extrapolation was used, and with experiment[128,140,141]. Columns 3 and 4 give the electron configurations of the single- and double-charged negative ions, chosen according to the ground-state electron configurations of the atoms, in which the total number of electrons is the same as in the negative ion. Column 5 and 6 give the present results without and with the VWN correlation energy correction.

Table IV-9 shows that all the double-charged negative ions are unstable (the negative values of the second electron affinities) which supports the physical fact that they exist only in crystals (section IV-4.1). The statistical total energy of the single-charged negative ion is lower than that of the double-charged negative ion for all these elements.

It may be seen that the second electron affinities for the same group elements become less negative as the atomic number Z increases, except for the first row elements, H and He, where the average Watson sphere radius of 3.0 a.u. is too far from the ideal for these atoms. The second electron affinities, EA(2), of the same

FIGURE 4-2

The difference of the statistical total energies between the single- and double-charged negative ions, with a Watson sphere of charge +1 vs the radius of the Watson sphere

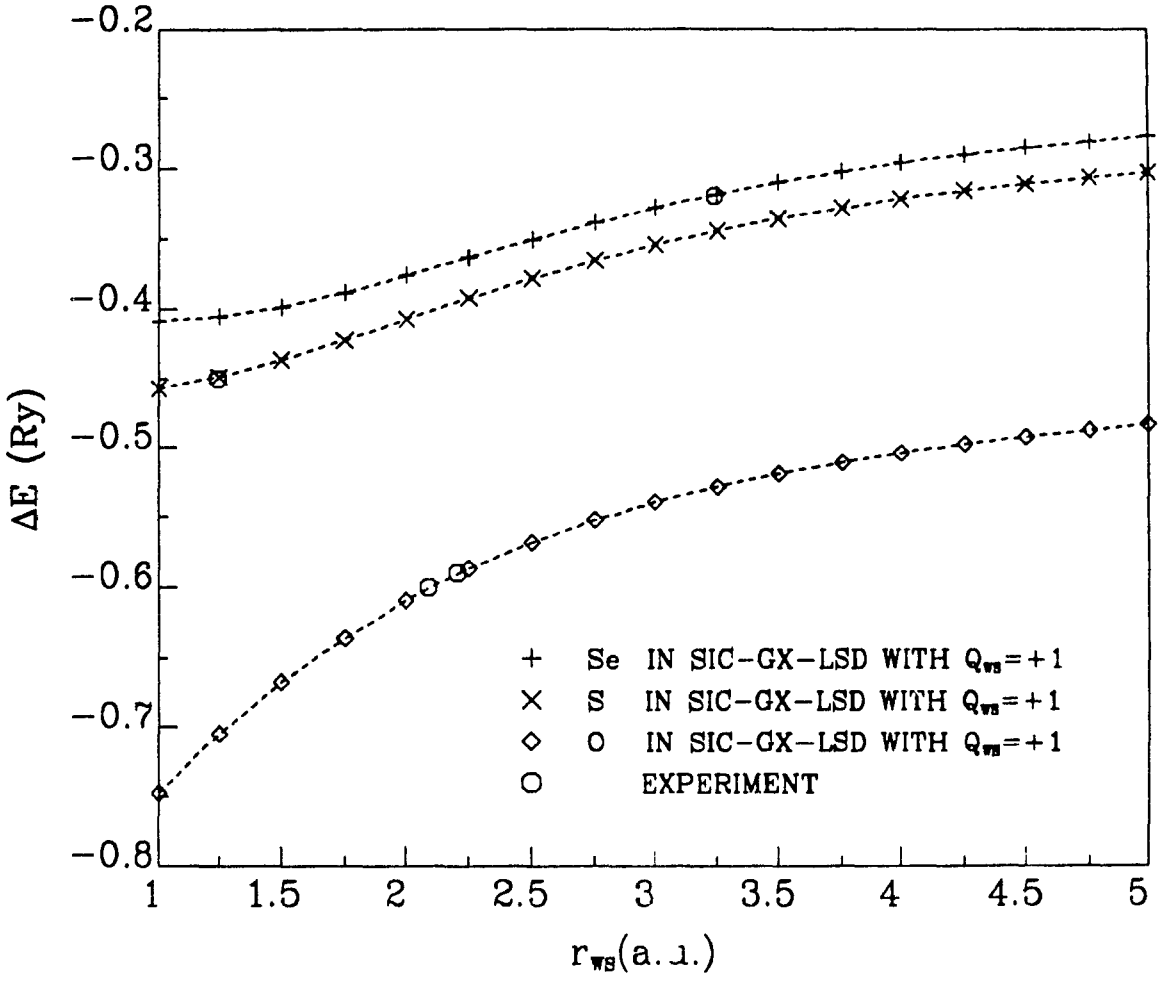

row elements in which the outermost orbitals are $2p$ also become less negative as the occupation number of their spin quantum number m_s increases, that is

$$EA(2)_{Li} < EA(2)_{Be} < EA(2)_B$$

and

$$EA(2)_C < EA(2)_N < EA(2)_O$$

etc., as is true for the elements in which the outermost orbitals are $3p$ and $4p$. The calculated results parallel experiment. These trends are reasonable; as the total number of electrons increases, the exchange-correlation which is approximately proportional to the number of electrons, also increases. The existence of the stable negative ions of atoms in nature is mainly caused by the quantum effect, which is the negative contribution of the exchange-correlation effect of the electrons to the energy functional, therefore the results should parallel the exchange-correlation.

Table IV-10 summarizes the second electron affinities for the elements rubidium to lawrencium in the QR-SIC-GX-LSD theory with the GWB Fermi-hole parameters and the VWN correlation energy correction, and a Watson sphere of radius 3.0 a.u. with a cha of +2. The trend is similar to that in Table IV-9.

In conclusion, it has been shown that the Watson sphere is an effective technique for calculating the double-charged negative ions in the SIC-GX-LSD theory. The second electron affinities of atoms are acceptable when a correct radius of Watson sphere is chosen, the method has been illustrated and the trends established using a fairly accurate average Watson sphere radius of 3.0 a.u. Specific choice of radius would yield slightly more accurate numerical results but not alter the trends.

TABLE IV-9

The negative of the second electron affinities (Ry) of the atoms Helium to Krypton in the SIC-GX-LSD theory with the VWN correlation energy functional, compared with other calculations and experiment

Z	Atom	Electron Config. 1^{st}	2^{nd}	GX-LSD No Corr.	GX-LSD With VWN	Other Calc.	Expt.
1	*H*	$1s^2$	$1s^2 2s^1$	0.4373	0.4303		
2	*He*	$1s^2 2s^1$	$1s^2 2s^2$	0.5092	0.4583		
3	*Li*	$2s^2$	$2s^2 2p^1$	0.5977	0.5712		
4	*Be*	$2s^2 2p^1$	$2s^2 2p^2$	0.5754	0.5564		
5	*B*	$2s^2 2p^2$	$2s^2 2p^3$	0.5573	0.5428		
6	*C*	$2s^2 2p^3$	$2s^2 2p^4$	0.7431	0.6635		
7	*N*	$2s^2 2p^4$	$2s^2 2p^5$	0.6993	0.6383	0.61[a]	
8	*O*	$2s^2 2p^5$	$2s^2 2p^6$	0.6534	0.6041	0.61[a]	0.60[b] 0.59[c]
9	*F*	$2p^6$	$2p^6 3s^1$	0.5754	0.5649		
10	*Ne*	$2p^6 3s^1$	$2p^6 3s^2$	0.5561	0.5048		
11	*Na*	$3s^2$	$3s^2 3p^1$	0.5721	0.5478		
12	*Mg*	$3s^2 3p^1$	$3s^2 3p^2$	0.5376	0.5196		
13	*Al*	$3s^2 3p^2$	$3s^2 3p^3$	0.4992	0.4846		
14	*Si*	$3s^2 3p^3$	$3s^2 3p^4$	0.6077	0.5312		
15	*P*	$3s^2 3p^4$	$3s^2 3p^5$	0.5414	0.4828		
16	*S*	$3s^2 3p^5$	$3s^2 3p^6$	0.4769	0.4282	0.40[b]	0.45[b] 0.45[a]
17	*Cl*	$3p^6$	$3p^6 4s^1$	0.5190	0.5054		
18	*Ar*	$3p^6 4s^1$	$3p^6 4s^2$	0.5048	0.4589		
19	*K*	$4s^2$	$3d^1 4s^2$	0.5049	0.4814		
20	*Ca*	$3d^1 4s^2$	$3d^2 4s^2$	0.4741	0.4558		
21	*Sc*	$3d^2 4s^2$	$3d^3 4s^2$	0.6282	0.6034		
22	*Ti*	$3d^3 4s^2$	$3d^5 4s^1$	0.6908	0.7546		
23	*V*	$3d^5 4s^1$	$3d^5 4s^2$	0.5781	0.4844		
24	*Cr*	$3d^5 4s^2$	$3d^6 4s^2$	0.8363	0.7657		
25	*Mn*	$3d^6 4s^2$	$3d^7 4s^2$	0.7978	0.7343		
26	*Fe*	$3d^7 4s^2$	$3d^8 4s^2$	0.7635	0.7053		
27	*Co*	$3d^8 4s^2$	$3d^{10} 4s^1$	1.0075	0.9570		
28	*Ni*	$3d^{10} 4s^1$	$3d^{10} 4s^2$	0.5352	0.4877		
29	*Cu*	$4s^2$	$4s^2 4p^1$	0.6316	0.6058		
30	*Zn*	$4s^2 4p^1$	$4s^2 4p^2$	0.5665	0.5478		
31	*Ga*	$4s^2 4p^2$	$4s^2 4p^3$	0.5106	0.4957		
32	*Ge*	$4s^2 4p^3$	$4s^2 4p^4$	0.5986	0.5235		
33	*As*	$4s^2 4p^4$	$4s^2 4p^5$	0.5246	0.4669		
34	*Se*	$4s^2 4p^5$	$4s^2 4p^6$	0.4549	0.4066		0.46[b] 0.32[a]
35	*Br*	$4p^6$	$4p^6 5s^1$	0.5004	0.4861		
36	*Kr*	$4p^6 5s^1$	$4p^6 5s^2$	0.4839	0.4397		

a. Reference 141; b. Reference 128; c. Reference 140.

IV-5. Double-Charged Negative Ions in gas phase

Equation (1-90) for the one-electron eigenvalue and wave function using equation (1-91) for the Coulomb-interaction potential, (1-127) for the exchange potential, (1-128) for the self-exchange potential, and (1-114) for the electron-correlation potential in the electron-correlation corrected SIC-GX-LSD theory with the GWB Fermi-hole parameters[27] was solved for each orbital by standard SCF procedure[48]. The statistical total energy, E, in equation (1-86), and the electron-correlation energy, E_c, in equation (1-98), for a doubly charged negative ion were obtained from the converged wave function[142].

The SCF procedure in the electron-correlation corrected SIC-GX-LSD theory was achieved easily for the doubly charged negative ions of the first category elements in the second and third periods with a small size of Watson sphere ($r_{WS} < 10$ a_0), whereas it is increasely difficult when the radius of the Watson sphere increases. The electronic structures of these doubly charged negative ions are very sensitive to the potential with a large Watson sphere. No converged results were obtained by starting with the converged potential of the neutral atom from a Herman and Skillman calculation[48] and the electron configuration for the corresponding doubly charged negative ions, when the radii of the Watson spheres are bigger than 10 a_0. Hence, an adiabatic convergence technique[92] was used: starting with the converged potential and electron configuration of the neutral atom, 1 percent of an electron was added in each following iteration until a total of two electrons was included in the extra orbitals. This slow, adiabatic change from the neutral atom allows the system to remain in its ground state. The mixture factor was chosen to be 0.01 to 0.001 when the radii of the Watson spheres increase from 10 a_0 to 62 a_0, the largest radius of the Watson sphere in the present work, for B^{2-} and Al^{2-}, 10 a_0 to 74 a_0 for C^{2-}, 10 a_0 to 60 a_0 for Si^{2-}, 10 a_0 to 70 a_0 for N^{2-} and P^{2-}, and 10 a_0 to 36

TABLE IV-10

The electron affinities (Ry) for the high-Z elements in the QR-SIC-GX-LSD theory with the aid of Watson sphere of radius 3 a.u. and the VWN correlation energy Functional

Z	Atom	Electron Configuration 1^{st}	2^{nd}	SIC-GX-LSD No Corr.	SIC-GX-LSD With VWN
37	*Rb*	$5s^2$	$4d^1 5s^2$	−0.6646	−0.6323
38	*Sr*	$4d^1 5s^2$	$4d^2 5s^2$	−0.6141	−0.5869
39	*Y*	$4d^2 5s^2$	$4d^4 5s^1$	−0.6499	−0.7024
40	*Zr*	$4d^4 5s^1$	$4d^5 5s^1$	−0.5591	−0.5528
41	*Nb*	$4d^5 5s^1$	$4d^5 5s^2$	−0.5521	−0.4533
43	*Tc*	$4d^7 5s^1$	$4d^8 5s^1$	−0.6889	−0.6241
44	*Ru*	$4d^8 5s^1$	$4d^{10}$	−0.8464	−0.7720
45	*Rh*	$4d^{10}$	$4d^{10} 5s^1$	−0.5045	−0.4749
46	*Pd*	$4d^{10} 5s^1$	$4d^{10} 5s^2$	−0.5086	−0.4620
47	*Ag*	$4d^{10} 5s^2$	$4d^{10} 5s^2 5p^1$	−0.6165	−0.5895
48	*Cd*	$5s^2 5p^1$	$5s^2 5p^2$	−0.5499	−0.5299
49	*In*	$5s^2 5p^2$	$5s^2 5p^3$	−0.4919	−0.4758
50	*Sn*	$5s^2 5p^3$	$5s^2 5p^4$	−0.5646	−0.4922
51	*Sb*	$5s^2 5p^4$	$5s^2 5p^5$	−0.4928	−0.4365
52	*Te*	$5s^2 5p^5$	$5s^2 5p^6$	−0.4258	−0.3781
53	*I*	$5p^6$	$5p^6 6s^1$	−0.4667	−0.4522
54	*Xe*	$5p^6 6s^1$	$5p^6 6s^2$	−0.4522	−0.4098
55	*Cs*	$6s^2$	$5d^1 6s^2$	−0.6024	−0.5686
56	*Ba*	$5d^1 6s^2$	$4f^2 6s^2$	−0.9907	−0.9606
57	*La*	$4f^2 6s^2$	$4f^3 6s^2$	−0.8143	−0.7868
58	*Ce*	$4f^3 6s^2$	$4f^4 6s^2$	−0.8759	−0.8457
59	*Pr*	$4f^4 6s^2$	$4f^5 6s^2$	−0.9035	−0.8725
60	*Nd*	$4f^5 6s^2$	$4f^6 6s^2$	−0.9180	−0.8870
61	*Pm*	$4f^6 6s^2$	$4f^7 6s^2$	−0.9272	−0.8964
62	*Sm*	$4f^7 6s^2$	$4f^7 5d^1 6s^2$	−0.6485	−0.6212
63	*Eu*	$4f^7 5d^1 6s^2$	$4f^8 5d^1 6s^2$	−1.0244	−0.9515
64	*Gd*	$4f^8 5d^1 6s^2$	$4f^{10} 6s^2$	−1.3033	−1.2253
65	*Tb*	$4f^{10} 6s^2$	$4f^{11} 6s^2$	−1.0922	−1.0439
66	*Dy*	$4f^{11} 6s^2$	$4f^{12} 6s^2$	−1.1178	−1.0679
67	*Ho*	$4f^{12} 6s^2$	$4f^{13} 6s^2$	−1.1234	−1.0744
68	*Er*	$4f^{13} 6s^2$	$4f^{14} 6s^2$	−1.1183	−1.0714
69	*Tm*	$4f^{14} 6s^2$	$4f^{14} 5d^1 6s^2$	−0.6993	−0.6683
70	*Yb*	$4f^{14} 5d^1 6s^2$	$5d^2 6s^2$	−0.6451	−0.6192
71	*Lu*	$5d^2 6s^2$	$5d^3 6s^2$	−0.6040	−0.5812

TABLE IV-10 (Continued)

The electron affinities (Ry) for the high-Z elements in the QR-SIC-GX-LSD theory with the aid of Watson sphere of radius 3 a.u. and the VWN correlation energy Functional

Z	Atom	Electron Configuration 1^{st}	2^{nd}	SIC-GX-LSD No Corr.	SIC-GX-LSD With VWN
72	Hf	$5d^3 6s^2$	$5d^4 6s^2$	−0.5672	−0.5469
73	Ta	$5d^4 6s^2$	$5d^5 6s^2$	−0.5308	−0.5127
74	W	$5d^5 6s^2$	$5d^6 6s^2$	−0.7020	−0.6265
75	Re	$5d^6 6s^2$	$5d^7 6s^2$	−0.6438	−0.5778
76	Os	$5d^7 6s^2$	$5d^9 6s^1$	−0.7737	−0.7127
77	Ir	$5d^9 6s^1$	$5d^{10} 6s^1$	−0.5955	−0.5432
78	Pt	$5d^{10} 6s^1$	$5d^{10} 6s^2$	−0.4398	−0.3929
79	Au	$6s^2$	$6s^2 6p^1$	−0.6225	−0.5950
80	Hg	$6s^2 6p^1$	$6s^2 6p^2$	−0.5538	−0.5335
81	Tl	$6s^2 6p^2$	$6s^2 6p^3$	−0.4934	−0.4772
82	Pb	$6s^2 6p^3$	$6s^2 6p^4$	−0.5581	−0.4862
83	Bi	$6s^2 6p^4$	$6s^2 6p^5$	−0.4868	−0.4310
84	Po	$6s^2 6p^5$	$6s^2 6p^6$	−0.4201	−0.3729
85	At	$6s^2 6p^6$	$6p^6 7s^1$	−0.4667	−0.4503
86	Rn	$7s^1$	$7s^2$	−0.4495	−0.4074
87	Fr	$7s^2$	$6d^1 7s^2$	−0.6017	−0.5694
88	Ra	$6d^1 7s^2$	$6d^2 7f^2$	−0.5538	−0.5264
89	Ac	$6d^2 7f^2$	$5f^2 6d^1 7s^2$	−1.0068	−0.9656
90	Th	$5f^2 6d^1 7s^2$	$5f^3 6d^1 7s^2$	−0.7620	−0.7321
91	Pa	$5f^3 6d^1 7s^2$	$5f^3 7s^2$	−0.9487	−0.9145
92	U	$5f^3 7s^2$	$5f^6 7s^2$	−0.7900	−0.7629
93	Np	$5f^6 7s^2$	$5f^7 7s^2$	−0.7871	−0.7602
94	Pu	$5f^7 7s^2$	$5f^7 6d^1 7s^2$	−0.6308	−0.6078
95	Am	$5f^7 6d^1 7s^2$	$5f^8 6d^1 7s^2$	−0.8777	−0.8039
96	Cm	$5f^8 6d^1 7s^2$	$5f^{10} 7s^2$	−1.0907	−0.9907
97	Bk	$5f^{10} 7s^2$	$5f^{11} 7s^2$	−0.9200	−0.8636
98	Cf	$5f^{11} 7s^2$	$5f^{12} 7s^2$	−0.8963	−0.8422
99	Es	$5f^{12} 7s^2$	$5f^{13} 7s^2$	−0.8716	−0.8199
100	Fm	$5f^{13} 7s^2$	$5f^{14} 7s^2$	−0.8466	−0.7972
101	Md	$5f^{14} 7s^2$	$5f^{14} 6d^1 7s^2$	−0.7023	−0.6714
102	No	$6d^1 7s^2$	$6d^2 7s^2$	−0.6456	−0.6200
103	Lr	$6d^2 7s^2$	$6d^3 7s^2$	−0.6034	−0.5808

a_0 for O^{2-} and S^{2-}. This means 99.9 percent of electron density from the (i-1)th iteration and 0.1 percent of electron density from the ith iteration were combined together and used to produce the new potential for the (i+1)th iteration, when the mixture factor is 0.001. The SCF procedure was completed when the difference in the wave functions of electrons between the ith and the (i+1)th iterations were less than 10^{-8} at all mesh points. Obviously, the speed of convergence is very slow and decreases, when the radius of the Watson sphere increases. In all this work, the net charge on the Watson sphere is +1 e. When the radius of the Watson sphere is bigger than the largest radius of the Watson sphere of the corresponding doubly charged negative ion, no converged results were obtained. The largest radius of the Watson sphere which can be used to produce the converged electronic structure of the corresponding doubly charged negative ion differs for different doubly charged negative ions and depends on the electronic structure and electron configuration. For example, the largest radius is 62 a_0 for both B^{2-} and Al^{2-}, which are of the same valence electron configurations with a half occupied p orbital, $p^3_\uparrow$.

The additional potential produced by the introduction of a Watson sphere in the doubly charged negative ions is

$$V_{WS}(r) = \begin{cases} -\frac{2}{r_{WS}}, & \text{when } r < r_{WS}; \\ -\frac{2}{r}, & \text{when } r \geq r_{WS}. \end{cases} \qquad (4-7)$$

The total potential including the Coulomb interactions between the nucleus and electron, electron and electron, and positive charge on the Watson sphere and electron, the exchange and correlation potentials is certainly a continuous function of radial r. But its derivative is not a continuous function, because of the use of the Watson sphere potential. The left-hand derivative of the Watson sphere potential, $V_{WS}(r)$, is zero and its right-hand derivative is $\frac{2}{r^2_{WS}}$ at $r = r_{WS}$. Fig. 4-3 plots the product of the potential and the radial r for the outermost orbital, $2p\downarrow$, of the doubly charged negative ion of carbon, C^{2-}, against the modified radial x (the re-

lationship of the modified radial x and the ordinary radial r is $r = \frac{1}{2}(\frac{3\pi}{4})^{2/3} Z^{-1/3} x$ with the atomic number Z) and demonstrates the discontinuous behaviour of the first derivative of the total potential at $r = r_{WS}$. It is very interesting that there is a total potential barrier with positive total potential inside the Watson sphere. The total potential of the outermost orbital gradually increases passing the $rV(r) = 0$ value with a zero total potential and then becomes positive arriving its peak. As the radial r continuously increases, the total potential gradually decreases and passes the $rV(r) = 0$ value again and becomes negative outside the Watson sphere. This implies that the electron-electron interaction potential, which is the only positive contribution to the potential in the total potential expression, is larger than the negative potential, which includes the contribution from the nucleus-electron and Watson sphere charge-electron interaction and the exchange-correlation effect.

Fig. 4-4 plots the dependence of the electron density distribution for the electron in the outermost orbital, $2p\downarrow$, of the doubly charged negative ion of carbon, C^{2-}, on the radius of the Watson sphere. It is clear that the electron density is gradually shifted toward a large radius, when the radius of the Watson sphere is increasing. In order to keep the normalization restriction of the wave function, the peak of the curve is reduced and the electron density gradually spreads, as the Watson sphere size increases. The electron density distribution of a core orbital, such as the 1s orbital in C^{2-}, is not affected by changing the radius of the Watson sphere.

Comparing Figs. 4-3 and 4-4 shows that the electron density of the outermost orbital is mainly distributed outside of the Watson sphere, when the radius of the Watson sphere is less than 70 a_0. Hence, the barrier of the total potential is not caused by the charge density of the electron in the outermost orbital, but created by the constant potential generated by the charge on the Watson sphere inside the

FIGURE 4-3

The potential of the outermost orbital, $2p\downarrow$, of the doubly charged negative ion of carbon, C^{2-}, vs the modified radial x

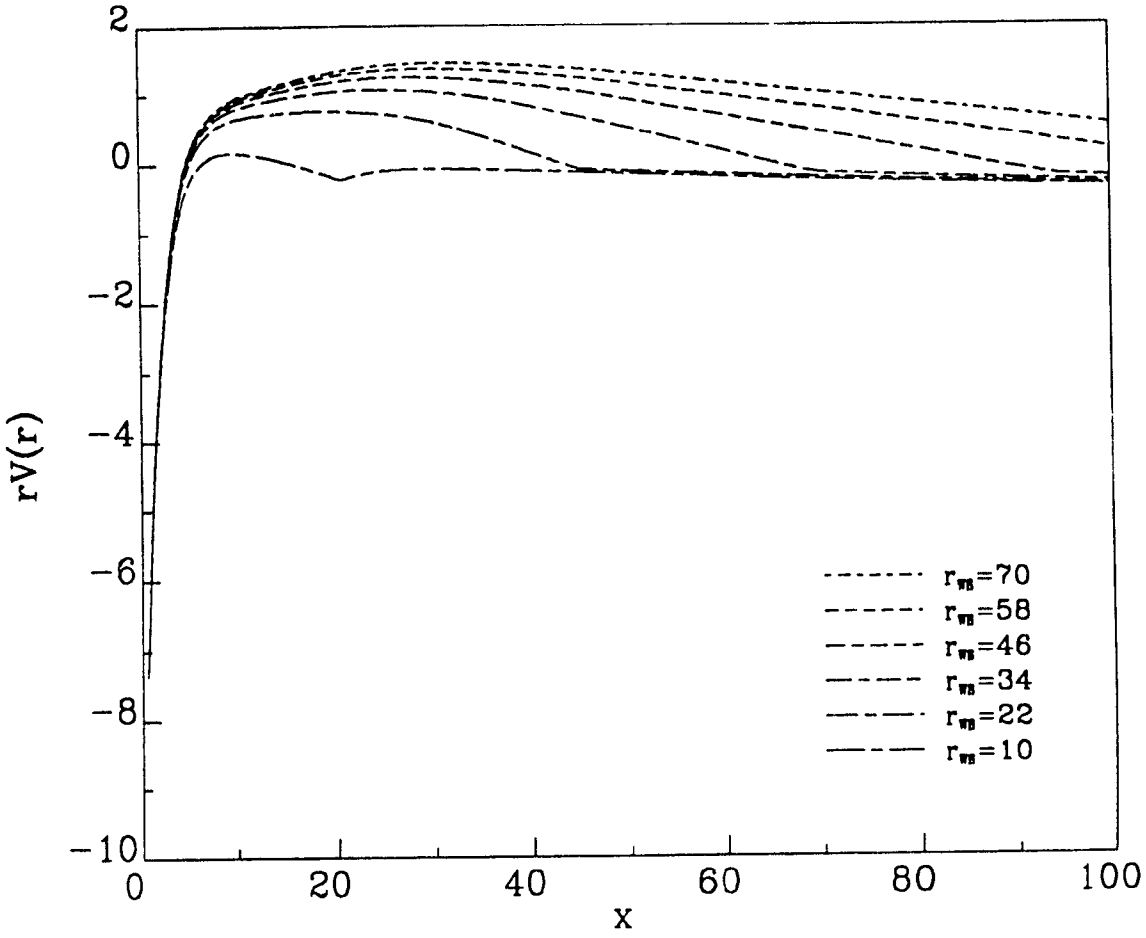

Watson sphere.

Obviously, the statistical total energy and the one-electron eigenvalue of a doubly charged negative ion in the electron-correlation corrected SIC-GX-LSD theory with the GWB Fermi-hole parameters are dependent on the Watson sphere size, when it is not large enough. Table IV-11 shows the dependence of the total energy including the statistical total energy and the VWN correlation energy contribution but excluding the energy contribution from the Watson sphere, the one-electron eigenvalue, and the expectation value of the Watson sphere potential for the electron in the outermost orbital of the doubly charged negative ion of carbon, C^{2-}, on the radius of the Watson sphere. When the radius of the Watson sphere increases, the electron density spreads toward the large radial. Therefore, the electron-electron repulsive energy decreases and the nucleus-electron attractive energy decreases. Because the contribution of the former to the statistical total energy is positive and the contribution of the latter is negative, they partly cancel. The total energy excluding the Watson sphere energy (Table IV-11) depends slightly on the radius of the Watson sphere and increases in size as the radius of the Watson sphere increases. Furthermore, the dependence of the total energy on the radius of the Watson sphere decreases as the radius of the Watson sphere increases. For example for C^{2-} the difference of the total energies calculated by using the Watson spheres with $r_{WS} = 14a_0$ and $r_{WS} = 18a_0$ is 0.0017 Ry, whereas the difference of the total energies calculated by using the Watson spheres with $r_{WS} = 54a_0$ and $r_{WS} = 58a_0$ is 0.0010 Ry. However the one-electron eigenvalue for the outermost orbital of the doubly charged negative ion is strongly dependent on the radius of the Watson sphere and decreases in magnitude as the radius of the Watson sphere increases. The dependence of the expectation value of the Watson sphere potential for the electron in the outermost orbital of C^{2-} is shown in column 4 of Table IV-11. The value decreases as the radius of the Watson sphere increases, because

FIGURE 4-4

The dependence of the electron density distribution for the electron in the outermost orbital, $2p\downarrow$, of the doubly charged negative ion of carbon, C^{2-}, on the radius of the Watson sphere

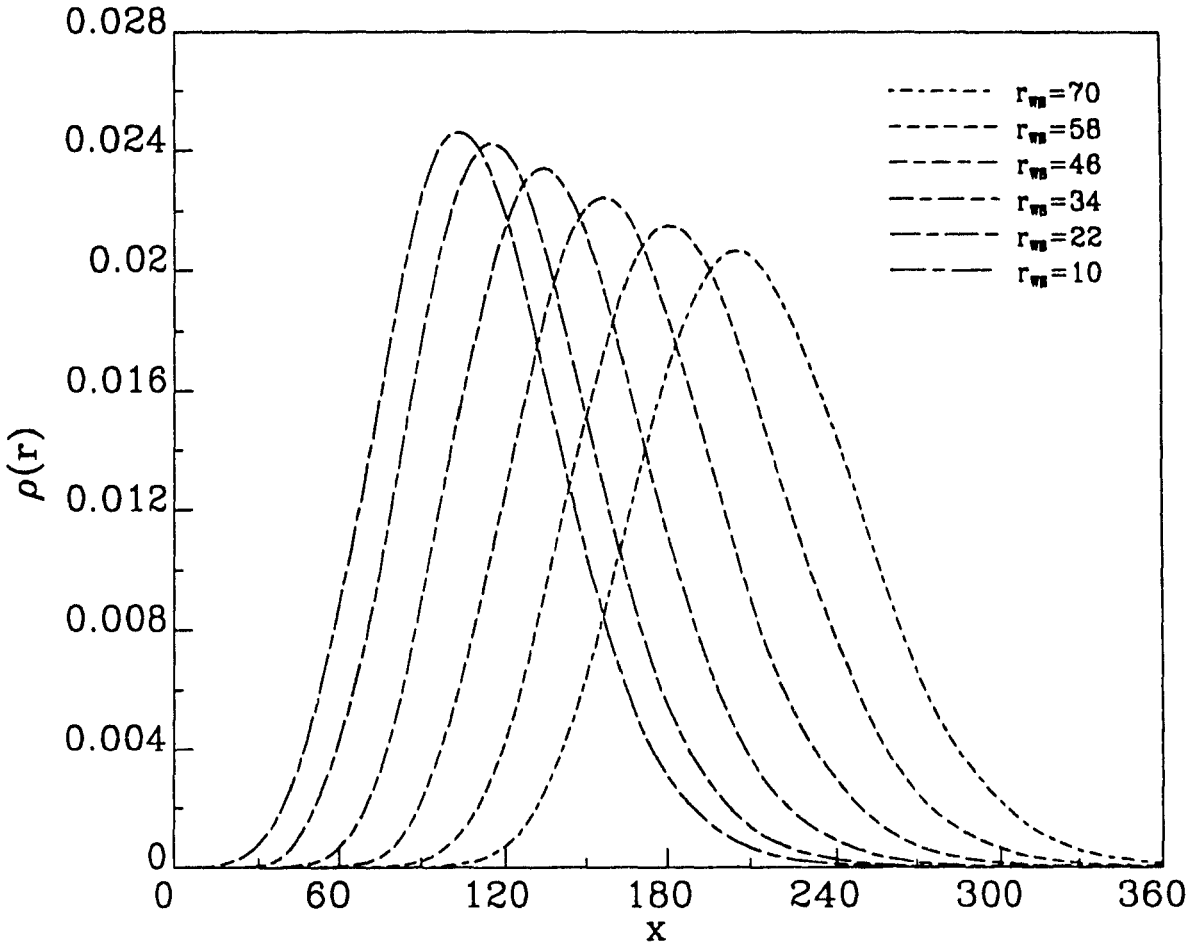

the potential contribution of the Watson sphere is gradually reduced by increasing the radius of the Watson sphere. The real one-electron eigenvalue can be obtained by subtracting the expectation value of the Watson sphere potential, column 4 in Table IV-11, from the calculated one-electron eigenvalue of the corresponding orbital, in column 3 in Table IV-11. Hence the real one-electron eigenvalue excluding the contribution from the Watson sphere is positive and gradually decreases when the radius of the Watson sphere increases.

TABLE IV-11

The dependence of the total energy and the one-electron eigenvalue and the expectation value of the Watson sphere potential for the outermost orbital of the doubly charged negative ion of carbon, C^{2-} (Ry)

r_{WS}	E_{tot}	$\epsilon_{2p\downarrow}$	$< 2p\downarrow \|V_{WS}\|2p\downarrow >$
10	−76.1276	−0.004366	−0.04175
14	−76.1292	−0.004320	−0.04009
18	−76.1309	−0.004265	−0.03838
22	−76.1327	−0.004197	−0.03654
26	−76.1346	−0.004119	−0.03462
30	−76.1364	−0.004033	−0.03274
34	−76.1381	−0.003943	−0.03094
38	−76.1398	−0.003853	−0.02927
42	−76.1413	−0.003763	−0.02772
46	−76.1426	−0.003675	−0.02629
50	−76.1439	−0.003590	−0.02500
54	−76.1450	−0.003508	−0.02380
58	−76.1460	−0.003429	−0.02271
62	−76.1470	−0.003353	−0.02170
66	−76.1479	−0.003280	−0.02079
70	−76.1487	−0.003211	−0.01994

Since the total energy excluding the energy contribution of the Watson sphere for a doubly charged negative ion increases in magnitude as the radius of the Watson

sphere increases, the difference of the total energies for the doubly charged negative ion and the singly charged negative ion, in which no Watson sphere was used, should decrease in magnitude. Table IV-12 lists the dependence of the second electron affinities for the B and Al on the radius of the Watson sphere in the electron-correlation corrected SIC-GX-LSD theory with the GWB Fermi-hole parameters. The difference in the electron affinities become smaller and smaller, when the radius of the Watson sphere becomes bigger and bigger. For instance, the difference of the electron affinity for B is -0.2437 Ry, when the Watson sphere size is increased from 2 a_0 to 4 a_0, -0.0020 Ry when the size is increased from 30 a_0 to 32 a_0, and -0.0006 Ry when the size is increased from 60 a_0 to 62 a_0. The electron affinity in the electron-correlation corrected SIC-GX-LSD theory is not significantly changed by increasing the Watson sphere radius when the Watson sphere radius is large enough and approaches a constant value. Unfortunately, no converged values were obtained for B, when the radius of the Watson sphere was bigger than 62 a_0. This raises the question of what is the asymptotic value of the electron affinity for B when the Watson sphere radius goes to infinity? Is it possible to fit the calculated value and then estimate its asymptotic electron affinity using any function? The behaviour of the calculated electron affinity for B is inversely proportional to the radius of the Watson sphere.

The simpliest function worthwhile testing is

$$A = A_0 - \frac{a}{r_{WS}} \qquad (4-8)$$

where A_0 and a are constants to be determined. If the equation can fit the electron affinities calculated in the electron-correlation corrected SIC-GX-LSD theory with a large size of Watson sphere, the asymptotic value should correspond to the real electron affinity, when r_{WS} approaches infinity, that is A_0.

This approach was tested for B first. It was found that when A_0 = -0.1147

Ry and a = 1 Ry/a_0, the electron affinities calculated by using the Watson spheres whose radii are bigger than 30 a_0 were perfectly fitted by equation (4-8). The calculated and fitted results are listed in the columns 2 and 3 of Table IV-12, respectively, and plotted in Fig. 4-5. The dependence of calculated electron affinities for Al on the radius of the Watson sphere is of the same behaviour as those for B. The calculated electron affinities by using different radii of the Watson spheres also can be fitted by equation (4-8) with A_0 = -0.1344 Ry and a = 1 Ry/a_0. The calculated and fitted electron affinities are summarized in the columns 4 and 5 of Table IV-12, respectively, and plotted in Fig. 4-6.

The same behaviour can be applied to other doubly charged negative ions of the first category elements in the second and third periods. Figs. 4-7 to 4-12 plot the electron affinities calculated in the electron correlation corrected SIC-GX-LSD theory with the GWB Fermi-hole parameters and the fitted electron affinities by using equation (4-8) with A_0 = -0.0047 Ry and a = 0.9 Ry/a_0 for C, A_0 = -0.0083 Ry and a = 0.7 Ry/a_0 for Si, A_0 = -0.0237 Ry and a = 1.425 Ry/a_0 for N, A_0 = -0.0458 Ry and a = 1.395 Ry/a_0 for P, A_0 = -0.3606 Ry and a = 0.6353 Ry/a_0 for O, and A_0 = -0.2012 Ry and a = 0.56 Ry/a_0 for S. The electron affinities are presented in Table IV-13 and compared with the HF calculation given by Clementi and McLean[131] and the configuration interaction calculations with the single and double substitutions obtained by Kalcher[134]. The calculated results are very different. But the present results are the only ones which are part of a large body of established results and should be correct. Unfortunately, there are no experimental values to be available for comparison. But, at least, all these calculations show that the doubly charged negative ions of the first category elements in the second and third periods are unstable in gas phase.

It might be impossible to achieve the SCF calculation for the doubly charged

TABLE IV-12

The dependence of the second electron affinities (Ry) of B and Al on the Watson sphere radius (a_0), and fitting by a function of $A = A_0 - \frac{a}{r_{WS}}$ with A_0=-0.1147 Ry and a=1 Ry a_0^{-1} for B and -0.1344 Ry and a=1 Ry a_0^{-1} for Al

r_{WS}	B GX-LSD	Fitting	Al GX-LSD	Fitting
2	−0.5835	−0.6147	−0.5839	−0.6344
4	−0.3398	−0.3647	−0.3577	−0.3844
6	−0.2613	−0.2814	−0.2771	−0.3011
8	−0.2248	−0.2397	−0.2397	−0.2594
10	−0.2040	−0.2147	−0.2193	−0.2344
12	−0.1903	−0.1980	−0.2063	−0.2177
14	−0.1805	−0.1861	−0.1971	−0.2058
16	−0.1730	−0.1772	−0.1902	−0.1969
18	−0.1671	−0.1703	−0.1846	−0.1900
20	−0.1623	−0.1647	−0.1802	−0.1844
22	−0.1583	−0.1602	−0.1765	−0.1799
24	−0.1547	−0.1564	−0.1733	−0.1761
26	−0.1501	−0.1532	−0.1706	−0.1729
28	−0.1489	−0.1504	−0.1676	−0.170[illegible]
30	−0.1474	−0.1480	−0.1666	−0.167[illegible]
32	−0.1454	−0.1459	−0.1647	−0.1656
34	−0.1437	−0.1441	−0.1630	−0.16[illegible]8
36	−0.1421	−0.1425	−0.1615	−0.1622
38	−0.1407	−0.1410	−0.1600	−0.1607
40	−0.1394	−0.1397	−0.1587	−0.1594
42	−0.1384	−0.1385	−0.1577	−0.1582
44	−0.1373	−0.1374	−0.1566	−0.1571
46	−0.1364	−0.1364	−0.1557	−0.1561
48	−0.1354	−0.1355	−0.1546	−0.1552
50	−0.1347	−0.1347	−0.1543	−0.1544
52	−0.1339	−0.1339	−0.1535	−0.1536
54	−0.1332	−0.1332	−0.1528	−0.1529
56	−0.1325	−0.1326	−0.1521	−0.1523
58	−0.1319	−0.1319	−0.1516	−0.1516
60	−0.1314	−0.1314	−0.1510	−0.1511
62	−0.1308	−0.1308	−0.1505	−0.1505

negative ions of atoms directly applying the LDF theory, but with the aid of a Watson sphere, the SCF procedure can be carried out properly, when the radius

of the Watson sphere is not very big. The total energy for the doubly charged negative ion in the electron correlation corrected SIC-GX-LSD theory with the GWB Fermi-hole parameters is of the same behaviour as equation (4-8). The second electron affinities of atoms calculated by the differences of the total energies can be approximated by the asymptotic values of equation (4-8) as the radius of the Watson sphere goes to infinity.

TABLE IV-13

The second electron affinities (Ry) of B, C, N, O, Al, Si, P and S obtained by fitting the calculated values in the electron correlation corrected SIC-GX-LSD theory with the GWB Fermi-hole parameters, compared with other theoretical calculations

Atom	SIC-GX-LSD[a]	HF[b]	CI(SD)[c]
B	−0.1147		
C	−0.0047		
N	−0.0237	−0.4540	
O	−0.3606	−0.4440	
Al	−0.1344		−0.0542
Si	−0.0083		−0.0612
P	−0.0458		−0.0612
S	−0.2012		−0.0499

a. The present work;
b. Reference 131;
c. Reference 134.

Qualitatively, the signs of the second electron affinities in the electron correlation corrected SIC-GX-LSD theory with the GWB parameters are the same as obtained by the HF and CI(SD) calculations. The doubly charged negative ions in their ground states are unstable in gas phase for the first category elements in the second and third periods.

FIGURE 4-5

The dependence of calculated second electron affinities for B on the radius of the Watson sphere

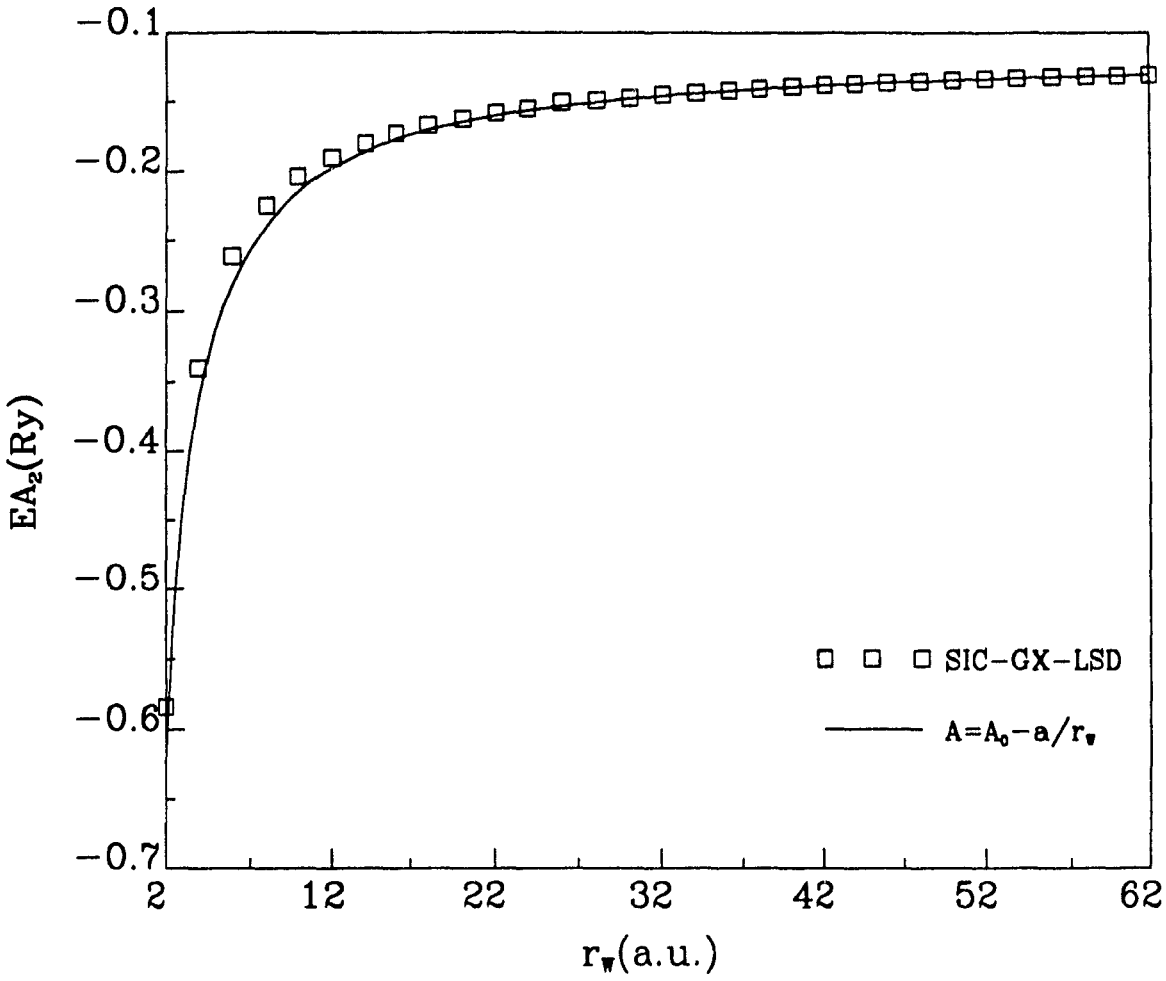

FIGURE 4-6

The dependence of calculated second electron affinities for Al on the radius of the Watson sphere

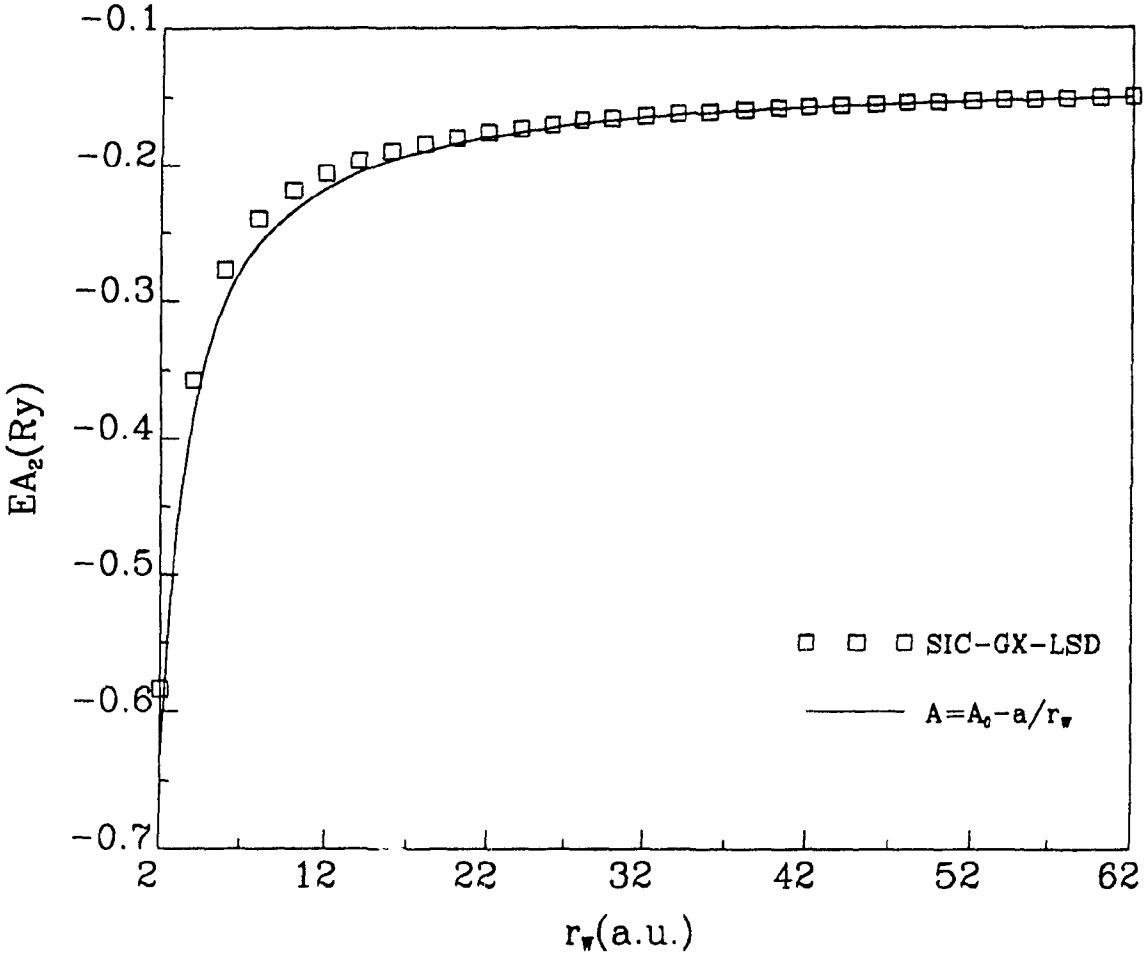

FIGURE 4-7

The dependence of calculated second electron affinities for C on the radius of the Watson sphere

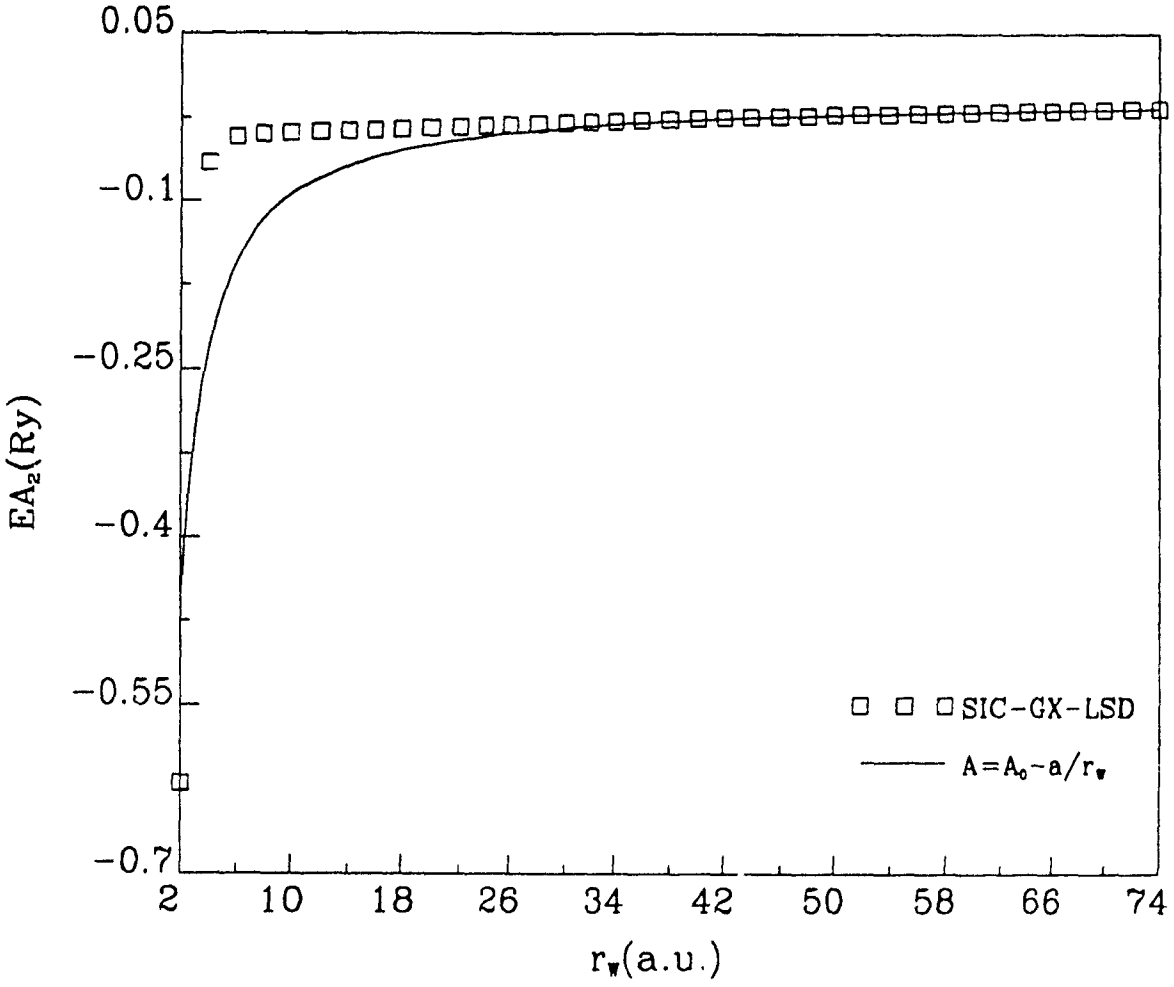

FIGURE 4-8

The dependence of calculated second electron affinities for Si on the radius of the Watson sphere

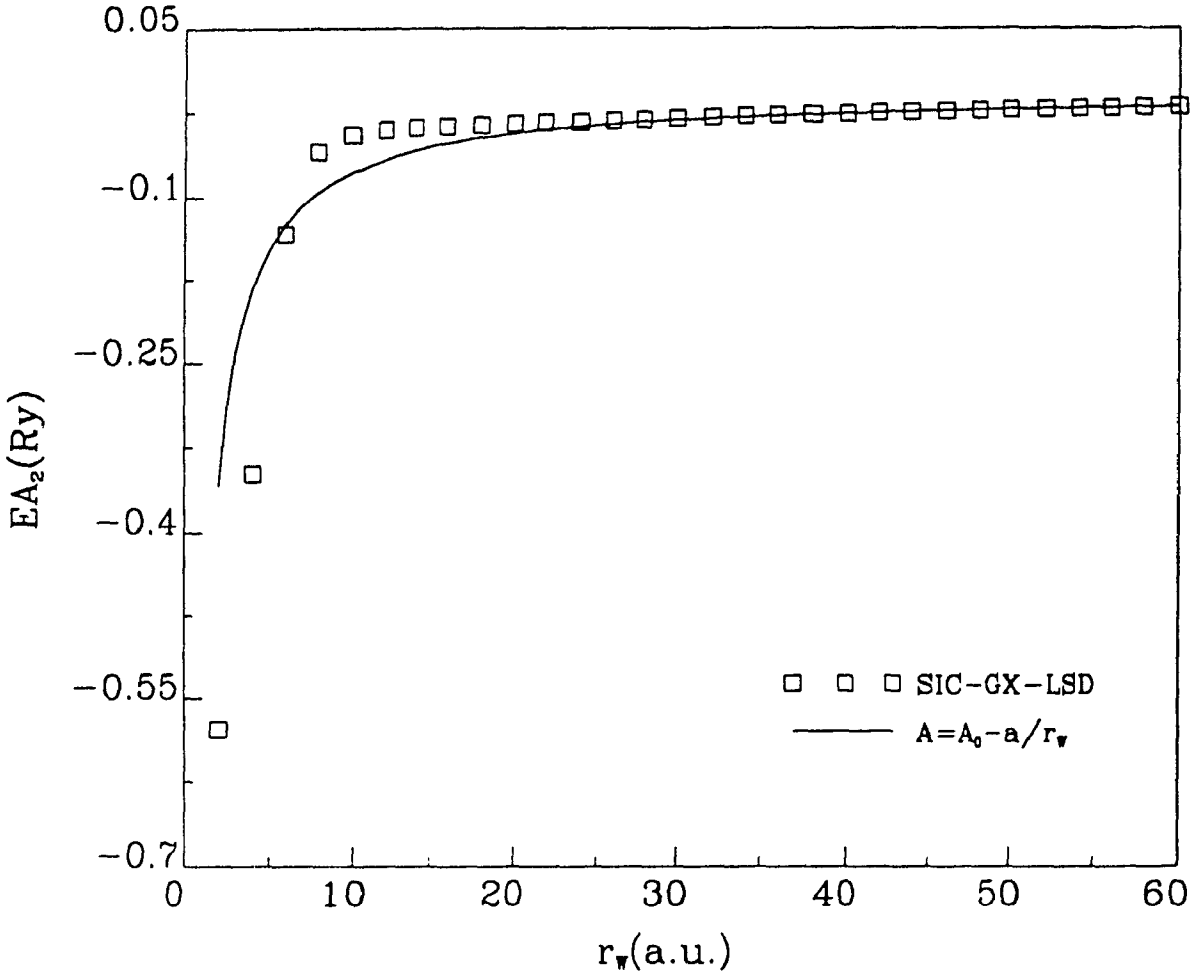

FIGURE 4-9

The dependence of calculated second electron affinities for N on the radius of the Watson sphere

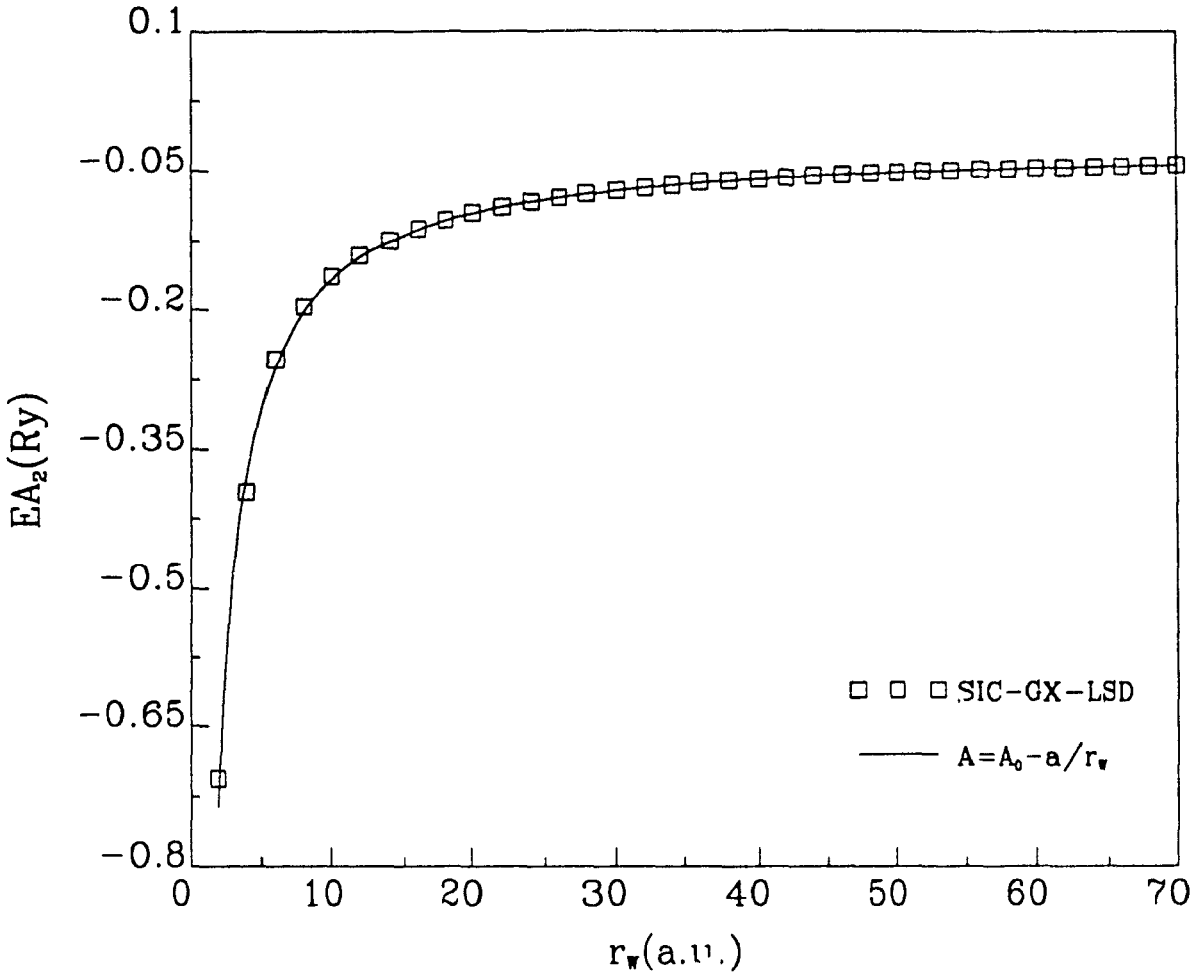

FIGURE 4-10

The dependence of calculated second electron affinities for P on the radius of the Watson sphere

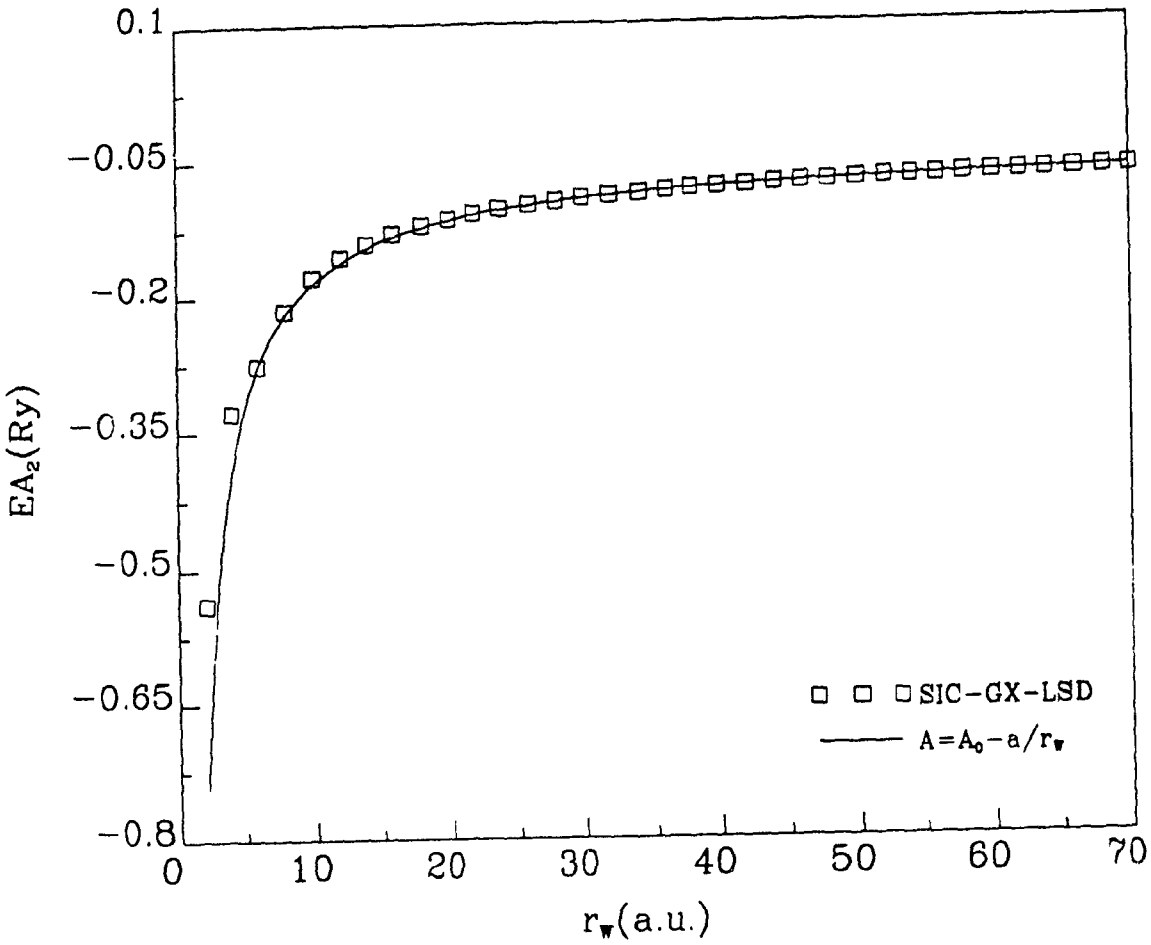

FIGURE 4-11

The dependence of calculated second electron affinities for O on the radius of the Watson sphere

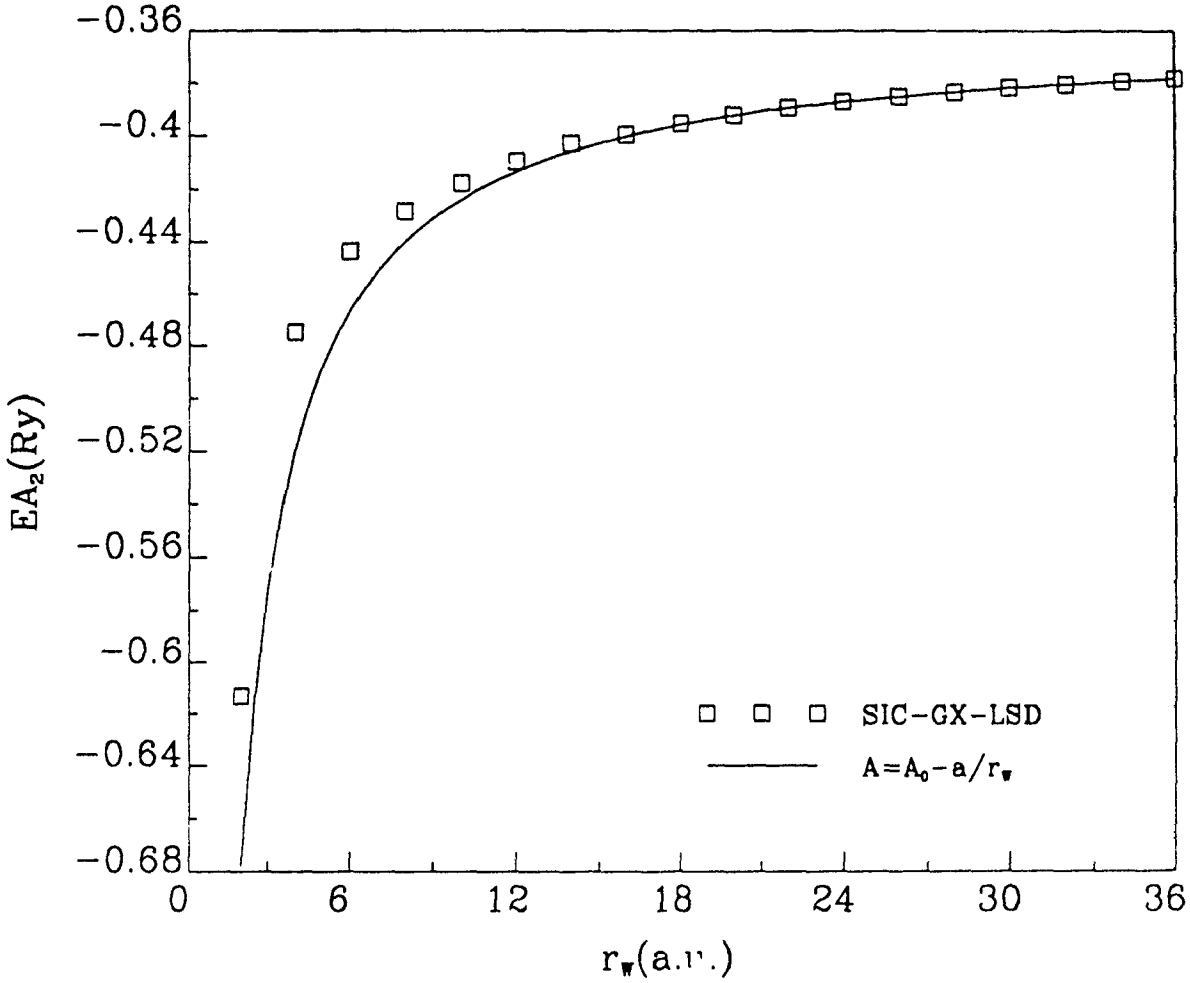

FIGURE 4-12

The dependence of calculated second electron affinities
for S on the radius of the Watson sphere

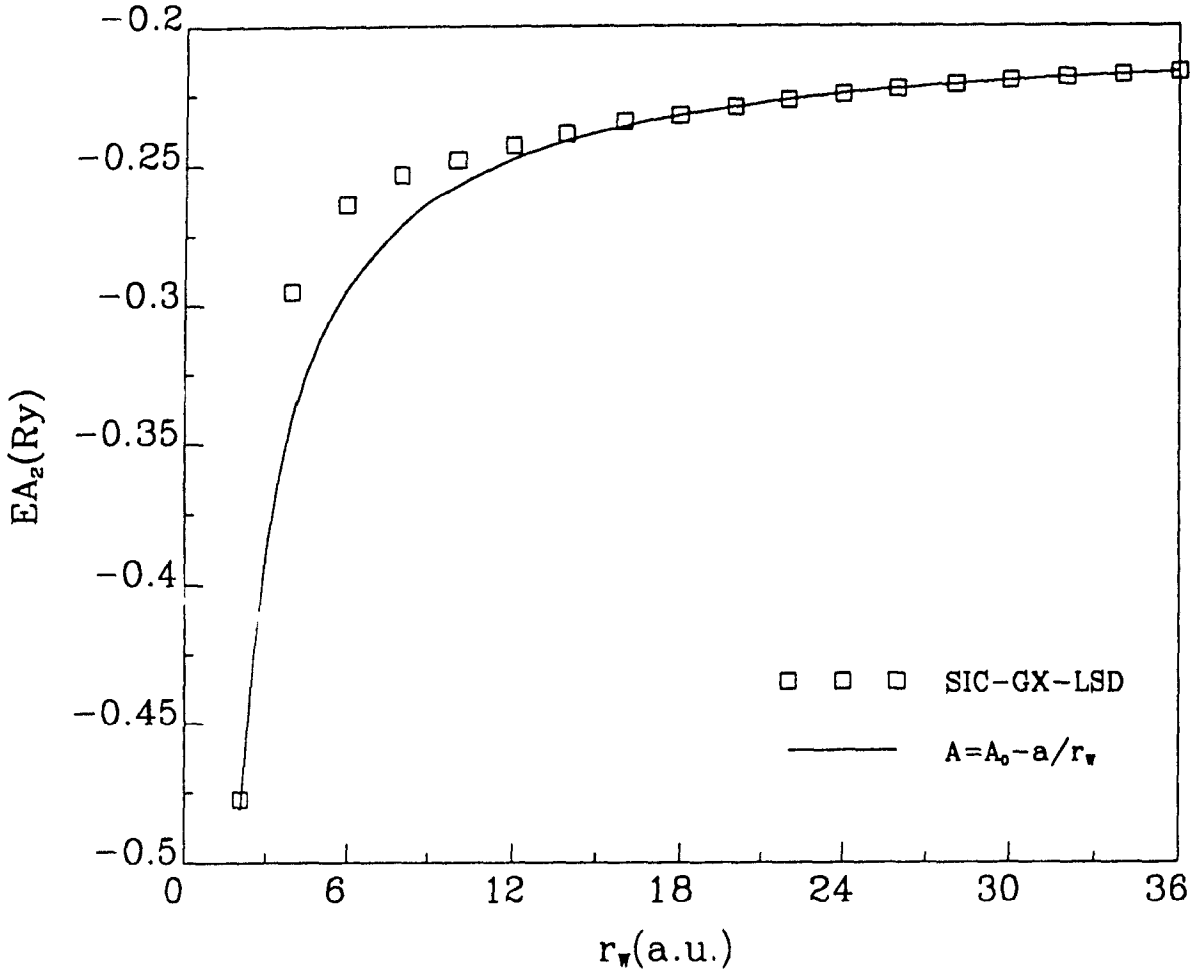

CHAPTER V

FRACTIONAL CHARGED ATOMS AND IONS

V-1. Introduction

The electronegativity of an atom is an important concept in understanding many molecular properties[141,143], such as the screened nuclear charge seen by the outer electrons, the radius of electron clouds, the work function of metals, the bond energy of molecules, the dipole moment of molecules, the force constants of molecules, etc. It has been related with the dipole polarizability in atoms[144,145] and the electronic distribution in molecules[116]. Therefore, much attention has been focused on predicting the electronegativities of atoms and atomic groups[55,76,78,144-154]. Electronegativity is the power of an atom in a molecule to attract electrons to itself[143].

Many definitions of the electronegativity occur[141]. A widely used definition of atomic electronegativity was given by Mulliken[155]

$$\chi = \frac{(I + A)}{2} \qquad (5 - 1)$$

The electronegativity, χ, is equal to the average value of the ionization potential, I, and electron affinity, A, of the atom in the ground state.

The electronegativity concept in the density-functional theory of Parr et al.[147] is

$$\chi = -\left[\frac{\partial E}{\partial N}\right]_Z \qquad (5 - 2)$$

where E is the statistical total energy treated as a continuous function[156] of electron number, N, and the nuclear charge, Z. Parr and Pearson[77] defined the absolute hardness η of an atom to be

$$\eta = \frac{1}{2}\left[\frac{\partial^2 E}{\partial N^2}\right]_Z \qquad (5-3)$$

If the derivation in equation (5-3) is replaced by its finite difference, the absolute hardness η can be expressed by

$$\eta = \frac{(I-A)}{2} \qquad (5-4)$$

The electronegativity and hardness of an atom provide the relationship to quantify the amount of charge transferred in the formation of a molecule because the electronegativity must be constant everywhere in equilibrium. When two atoms A and B are brought together, electrons will flow from the atom with lower electronegativity to that with higher electronegativity until the electronegativities become equal. The charge transferred during the formation is

$$\Delta q = \frac{\chi_A - \chi_B}{2(\eta_A + \eta_B)} \qquad (5-5)$$

Recently, the definition of hardness of an atom was generalized by Orsky and Whitehead[78] to

$$\eta_A = \frac{(I_{A+} - A_{A0})}{4} \qquad (5-6a)$$

and

$$\eta_B = \frac{(I_{B0} - A_{B-})}{4} \qquad (5-6b)$$

where η_A and η_B are the hardnesses for the acid A and base B; I_{B0} and I_{A+} are the first and second ionization potentials, and A_{A0} and A_{B-} the first and second

electron affinities for the atom. This theory was developed and used in atom and atomic group calculations[81,152].

Calculations of electronegativity and hardness need accurate values of ionization potentials and electron affinities. The experimental ionization potentials and electron affinities are missing for many atoms. Semi-empirical inter-extrapolation[153] compensates for the lack of experimental values, but was based on existing experimental values of atoms and molecules.

Fortunately, the self-interaction and electron-correlation corrected LDF theory has proved powerful in predicting the ionization potentials and electron affinities of atoms[30,45,49,73,81,92,101,105]. The self-interaction and electron-correlation corrected LDF theory does not depend on any experimental values.

Lackner and Zweig[153,157] generalized the concept of electronegativity and hardness to fractionally charged atoms. They obtained the ionization potentials and electron affinities of quark atoms for all elements with $Z < 93$ in the periodic table by isoelectronic interpolation of the experimental ionization potentials and electron affinities of the ordinary atoms. They reported the electronegativities and hardnesses of quark atoms with fractional nuclear charge $Z=N\pm\frac{1}{3}$ and $Z=N\pm\frac{2}{3}$. Sen et al.[158] published the electronegativities and the eletronegativity differences for the quark atoms of halogens, having nuclear charge $Z=N\pm\frac{1}{3}$ by using equations (5-1) and (5-2) in the SIC-LSD theory. The SIC-LSD results are in agreement with the Lackner and Zweig[153] empirical results. But Sen et al [158] only dealt with the halogens, because of convergence problems in calculating the negative ions of the quark atoms of other elements with fractional nuclear charge $Z=N-\frac{1}{3}$.

In this chapter[159], the ionization potentials and electron affinities for calculating the electronegativities and hardnesses, the first and second ionization potentials and electron affinities of the quark atoms with fractional nuclear charges

$Z=N\pm\frac{1}{3}$ and $Z=N\pm\frac{2}{3}$ for the elements with $Z < 37$ will be calculated by the SIC-GX-LSD theory with the GWB Fermi-hole parameters and the Vosko, Wilk, and Nusair[39,138] (VWN) correlation energy functional. A special convergence technique performs the self-consistent-field (SCF) calculation for the electron affinities, to avoid severe convergence problems in calculating the negative ions of quark atoms.

By means of the method introduced in section III-1, equation (3-4), the first ionization potential, I, and electron affinity, A, are given by

$$I = E^{+}_{tot} - E^{0}_{tot} \qquad (5-7a)$$

and

$$A = E^{0}_{tot} - E^{-}_{tot} \qquad (5-7b)$$

where E^{+}_{tot}, E^{0}_{tot}, and E^{-}_{tot} are sum of the statistical total energy in the SIC-LDF theory, E, and correlation energy contribution, E_c, for the positive ion, neutral atom, and negative ion, respectively, that is

$$E^{I}_{tot} = E^{I} + E^{I}_{c} \qquad (5-8)$$

where I stands for +, 0, or -. The statistical total energy in the correlation corrected SIC-GX-LSD theory is calculated by equation (1-86), and the correlation energy correction, E_c, is obtained by equation (1-98) in the VWN correlation procedure.

The electron-correlation corrected SIC-GX-LSD theory with the GWB[27] exchange parameters is used in this calculation, because previously[45,73,74,81,101,105], it gave very good statistical total energies for the neutral atoms E^0, positive and negative ions E^I (where I stands for + or -) of the ordinary atoms in agreement with Hartree-Fock (HF)[102]. The first and second ionization potentials and the first electron affinities for the quark atoms (hydrogen to krypton) with fractional nuclear charge $Z=N\pm\frac{1}{3}$ and $Z=N\pm\frac{2}{3}$ and the second electron affinities for the quark

atoms with $Z=N\pm\frac{1}{3}$ and $Z=N+\frac{2}{3}$ are evaluated from the difference in total energies which are the sums of the statistical total energies and the corresponding VWN correlation-energy corrections of the quark atom and first order quark ion (equations (5-7a) and (5-7b)) or the first and second order quark ions. The results are shown in Tables V-1 to V-4, V-7 and V-8 and compared to the isoelectronic interpolated values given by Lackner and Zweig[153]. The ionization potentials and electron affinities are employed to calculate the electronegativities and the hardnesses by equation (5-4) and the equations (5-6a) and (5-6b). The results are summarized in Tables V-1 to V-4.

V-2. Ionization Potential

The first and second ionization potentials are listed in columns 3 and 4 of Table V-1 to V-4 for the quark atoms with fractional nuclear charge $Z=N\pm\frac{1}{3}$ and $Z=N\pm\frac{2}{3}$, respectively, for the elements hydrogen to krypton in the electron-correlation corrected SIC-GX-LSD theory with the GWB Fermi-hole parameters. The electron-configurations for the quark atoms and the first and second order positive ions were taken from Moore's table[83], the electron-configuration of an quark atom or positive ion is the same as that of the neutral atom or positive ion of the corresponding element in Moore's table.

To compare the present values with the empirical interpolated first ionization potentials of Lackner and Zweig[153] based on the experimental ionization potentials of isoelectronic consequences of the ordinary neutral atoms and positive ions, Figs. 5-1 to 5-4 plot the first ionization potentials of the quark atoms with fractional nuclear charge $Z=N\pm\frac{1}{3}$ and $Z=N\pm\frac{2}{3}$ against the nuclear charge. The agreement of the first ionization potentials for the quarks with fractional nuclear $Z=N\pm\frac{1}{3}$

and $Z=N+\frac{2}{3}$ between the present calculated values and the Lackner and Zweig results is excellent, except for the transition-metals elements. The deviation for the transition-metal elements might be caused by the different electron-configurations considered in the present work and in the interpolation. Furthermore, the present results are slightly bigger than Lackner and Zweig's results. From Fig. 5-4, it can be seen that this agreement for the quark atoms with $Z=N-\frac{2}{3}$ is worse than that of the quark atoms with $Z=N\pm\frac{1}{3}$ and $Z=N+\frac{2}{3}$. Because the net charge for these quark atoms with $Z=N-\frac{2}{3}$ is $-\frac{2}{3}e$, and consequently, the outermost electrons are less bound than in the quark atoms with $Z=N\pm\frac{1}{3}$ and $Z=N+\frac{2}{3}$. In the numerical calculation, the quark atoms with $Z=N-\frac{2}{3}$ are strongly dependent on the electron-correlation, like that of the ordinary negative ions[92,94,106,109]. Hence, the correlation-energy contribution to the ionization potentials is very important for the quark atoms with $Z=N-\frac{2}{3}$.

From Figs. 5-1 to 5-4 and Tables V-1 to V-4, it can be seen that the first and second ionization potentials of the quark atoms have the same trend as the ordinary atoms; the ionization potential increases as the occupation number of the subshell increases. The rare gas elements are of the highest first ionization potentials in the same row, and the alkaline-metal elements possess the lowest first ionization potentials.

FIGURE 5-1

The first ionization potentials of the quark atoms with fractional nuclear charge Z=N + $\frac{1}{3}$ in the electron-correlation corrected SIC-GX-LSD-GWB theory, compared with Lackner and Zweig's interpolation

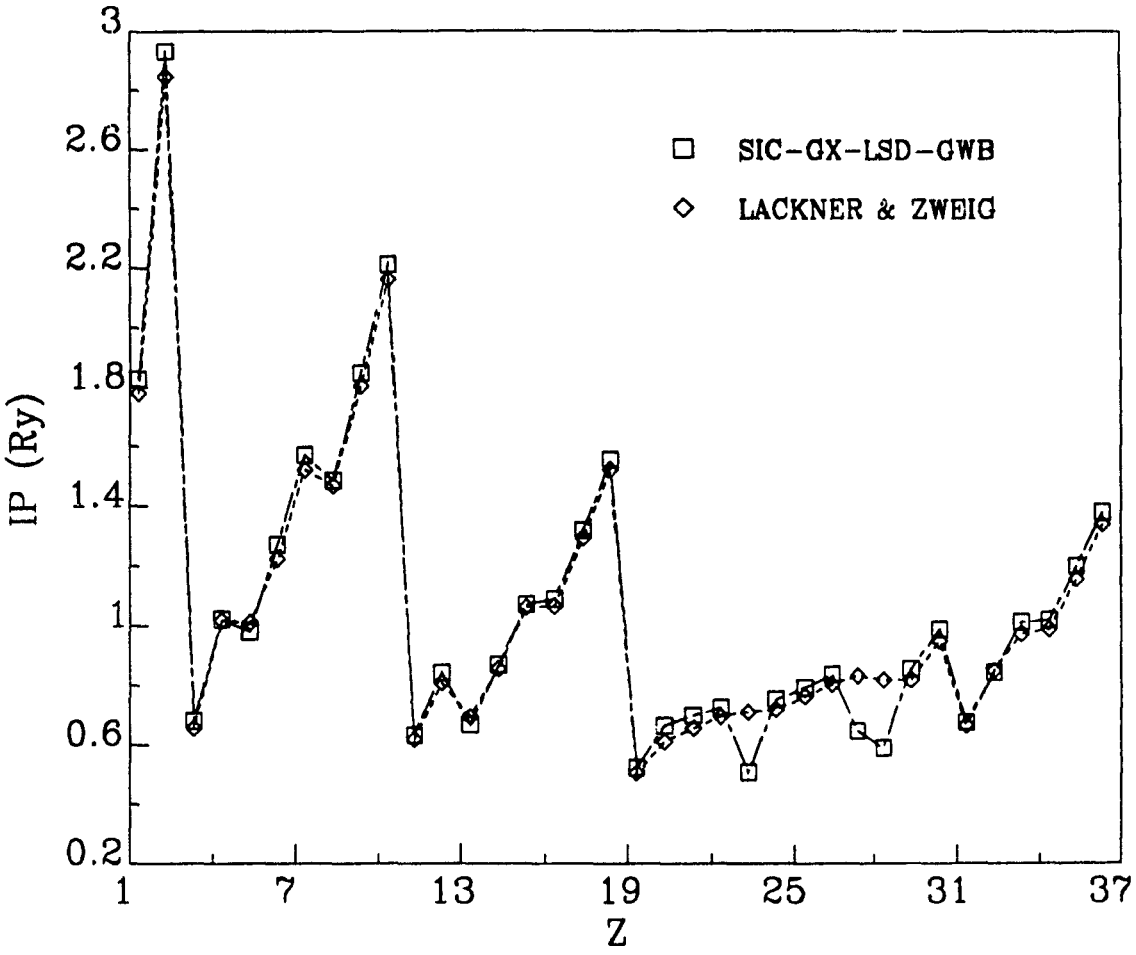

V-3. Electron Affinity

Equation (1-90) for the one-electron eigenvalue and wave function using equation (1-91) for the Coulomb-interaction potential, (1-127) for the exchange potential, (1-128) for the self-exchange potential, and (1-114) for the electron-correlation potential in the electron-correlation corrected SIC-GX-LSD theory was solved for each orbital by standard SCF procedure[48] self-consistently. The SCF process was achieved easily for the ordinary quark atoms and their negative ions with fractional nuclear charge Z=N+$\frac{1}{3}$ and Z=N+$\frac{2}{3}$, because of the attractive asymptotic forms of potential

$$V(r) = -\frac{2(1+\frac{a}{3})}{r} \qquad (5-9)$$

when r approaches infinity, for the quark atoms with a = 1 for Z = N + $\frac{1}{3}$ and a = 2 for Z = N + $\frac{2}{3}$. The results are listed in Tables V-1 and V-3.

The electron affinities of the quark atoms with fractional nuclear charge Z=N+$\frac{1}{3}$ listed in column 5 of Table V-1 are actually equivalent to the first ionization potentials of the quark atoms with Z=N-$\frac{2}{3}$ (in Table V-4), and the electron affinities of the quark atoms with Z=N+$\frac{2}{3}$ in column 5 of Table V-3 are equivalent to the first ionization potentials of the quark atoms with Z=N-$\frac{1}{3}$ (column 3 of Table V-2), but belonging to different quark atoms. For example, the electron affinity of 0.47 Ry for the quark atom H with Z=N+$\frac{1}{3}$=1$\frac{1}{3}$ is equal to the first ionization potential of He with Z=N-$\frac{2}{3}$=1$\frac{1}{3}$, because they have the same number of electrons, the same nuclear charge, and the same electron configuration; and the electron affinity of 1.07 Ry for H with Z=N+$\frac{2}{3}$=1$\frac{2}{3}$ in Table V-3 is equal to the first ionization potential of He with Z=N-$\frac{1}{3}$=1$\frac{2}{3}$ in Table V-2.

The SCF calculation was achieved for the negative ions of the quark atoms related to the elements in group VII A, having fractional nuclear charge Z=N-$\frac{1}{3}$,

TABLE V-1

The first and second ionization potentials, electron affinities, electronegativities, and hardnesses (Ry) calculated by the electron-correlation corrected SIC-GX-LSD-GWB theory for some quark elements whose net charge is +e/3 (Z=N+1/3)

	Z	I_1^a	I_2^b	A_1^c	χ^d	η_A^e	η_B^f	η^g
H	$1\frac{1}{3}$	1.83		0.47	1.15		0.46	0.68
He	$2\frac{1}{3}$	2.93	5.51	0.08	1.51	1.36	0.73	1.43
Li	$3\frac{1}{3}$	0.68	7.38	0.21	0.45	1.79	0.17	0.23
Be	$4\frac{1}{3}$	1.02	1.79	0.14	0.58	0.41	0.26	0.44
B	$5\frac{1}{3}$	0.98	2.34	0.26	0.62	0.52	0.24	0.36
C	$6\frac{1}{3}$	1.27	2.34	0.40	0.83	0.49	0.32	0.44
N	$7\frac{1}{3}$	1.57	2.80	0.27	0.92	0.63	0.39	0.65
O	$8\frac{1}{3}$	1.48	3.26	0.46	0.97	0.70	0.37	0.51
F	$9\frac{1}{3}$	1.85	3.23	0.67	1.26	0.64	0.46	0.59
Ne	$10\frac{1}{3}$	2.21	3.76	0.09	1.15	0.92	0.55	1.06
Na	$11\frac{1}{3}$	0.63	4.29	0.20	0.42	1.02	0.16	0.22
Mg	$12\frac{1}{3}$	0.84	1.46	0.10	0.47	0.34	0.21	0.37
Al	$13\frac{1}{3}$	0.67	1.76	0.20	0.44	0.39	0.17	0.23
Si	$14\frac{1}{3}$	0.87	1.52	0.31	0.59	0.30	0.22	0.28
P	$15\frac{1}{3}$	1.07	1.81	0.28	0.68	0.38	0.27	0.40
S	$16\frac{1}{3}$	1.09	2.10	0.42	0.75	0.42	0.27	0.33
Cl	$17\frac{1}{3}$	1.32	2.16	0.57	0.94	0.40	0.33	0.38
Ar	$18\frac{1}{3}$	1.55	2.48	0.09	0.82	0.60	0.39	0.73
K	$19\frac{1}{3}$	0.52	2.80	0.17	0.35	0.66	0.13	0.17
Ca	$20\frac{1}{3}$	0.67	1.14	0.15	0.41	0.25	0.17	0.26
Sc	$21\frac{1}{3}$	0.70	1.22	0.11	0.41	0.28	0.17	0.29
Ti	$22\frac{1}{3}$	0.73	1.29	0.34	0.53	0.24	0.18	0.20
V	$23\frac{1}{3}$	0.51	1.60	0.42	0.46	0.30	0.13	0.04
Cr	$24\frac{1}{3}$	0.75	1.73	0.21	0.48	0.38	0.19	0.27
Mn	$25\frac{1}{3}$	0.79	1.48	0.03	0.41	0.36	0.20	0.38
Fe	$26\frac{1}{3}$	0.84	1.52	0.34	0.59	0.30	0.21	0.25
Co	$27\frac{1}{3}$	0.65	1.80	0.44	0.54	0.34	0.16	0.11
Ni	$28\frac{1}{3}$	0.59	1.94	0.53	0.56	0.35	0.15	0.03
Cu	$29\frac{1}{3}$	0.86	2.07	0.29	0.57	0.44	0.21	0.28
Zn	$30\frac{1}{3}$	0.99	1.69	0.10	0.54	0.40	0.25	0.41

TABLE V-1 (Continued)

The first and second ionization potentials, electron affinities, electronegativities, and hardnesses (Ry) calculated by the electron-correlation corrected SIC-GX-LSD-GWB theory for some quark elements whose net charge is +e/3 (Z=N+1/3)

	Z	I_1^a	I_2^b	A_1^c	χ^d	η_A^e	η_B^f	η^g
Ga	$31\frac{1}{3}$	0.68	1.87	0.20	0.44	0.42	0.17	0.24
Ge	$32\frac{1}{3}$	0.84	1.47	0.30	0.57	0.29	0.21	0.27
As	$33\frac{1}{3}$	1.01	1.69	0.28	0.65	0.35	0.25	0.36
Se	$34\frac{1}{3}$	1.02	1.91	0.40	0.71	0.38	0.25	0.31
Br	$35\frac{1}{3}$	1.20	1.94	0.53	0.86	0.35	0.30	0.34
Kr	$36\frac{1}{3}$	1.38	2.18	0.09	0.73	0.52	0.34	0.65

a. The first ionization potential;
b. The second ionization potential;
c. The first electron affinity;
d. Electronegativity, $\chi = \frac{(I+A)}{2}$,
e. Hardness of acid A, $\eta_A = \frac{(I_{A+}-A_{A0})}{4}$;
f. Hardness of base B, $\eta_B = \frac{(I_{B0}-A_{B-})}{4}$;
g. Absolute hardness, $\eta = \frac{(I-A)}{2}$.

although the asymptotic forms of the potentials are repulsive, the value of a in equation (5-9) is -1. The calculations in the electron-correlation corrected SIC-GX-LSD theory and in the electron-correlation corrected quasi-relativistic SIC-GX-LSD (QR-SIC-GX-LSD) theory show that the negative ions of these quark atoms with Z=N-$\frac{1}{3}$ are stable except for F^-, when the VWN correlation energy contribution is invoked The electron affinity is -0.0451Ry for F, 0.0711Ry for Cl, 0.0815Ry for Br, 0.0945Ry for I, and 0.0975Ry for At with Z=N-$\frac{1}{3}$ in the electron-correlation corrected SIC-GX-LSD theory, and it is -0.0455Ry for F, 0.0702Ry for Cl, 0.0789Ry for Br, 0.0901Ry for I, and 0.0895Ry for At in the electron-correlation corrected QR-SIC-GX-LSD theory. The relativistic effect is to decrease the binding energy

TABLE V-2

The first and second ionization potentials, electron affinities, electronegativities, and hardnesses (Ry) calculated by the electron-correlation corrected SIC-GX-LSD-GWB theory for some quark elements whose net charge is -e/3 (Z=N-1/3)

	Z	I_1^a	I_2^b	A_1^c	χ^d	η_A^e	η_B^f	η^g
H	$\frac{2}{3}$	0.48		−0.09	0.19		0.12	0.29
He	$1\frac{2}{3}$	1.07	2.83	−0.01	0.53	0.71	0.27	0.54
Li	$2\frac{2}{3}$	0.22	4.19	−0.03	0.10	1.06	0.06	0 13
Be	$3\frac{2}{3}$	0.42	1.00	−0.01	0.21	0.25	0.11	0.22
B	$4\frac{2}{3}$	0.36	1.40	−0.08	0.14	0.37	0.09	0.22
C	$5\frac{2}{3}$	0.54	1.38	−0.07	0.23	0.36	0.13	0.30
N	$6\frac{2}{3}$	0.73	1.73	−0.02	0.35	0.44	0.18	0.38
O	$7\frac{2}{3}$	0.61	2.08	−0.13	0.24	0.55	0.15	0.37
F	$8\frac{2}{3}$	0.86	2.01	−0.05	0 41	0 51	0.22	0.45
Ne	$9\frac{2}{3}$	1.12	2.43	−0.02	0.55	0.61	0 28	0.57
Na	$10\frac{2}{3}$	0.24	2.85	−0.03	0.10	0.72	0.06	0.13
Mg	$11\frac{2}{3}$	0.38	0.88	−0.02	0.18	0.22	0 10	0.20
Al	$12\frac{2}{3}$	0.26	1.12	−0.05	0.10	0.29	0.06	0.15
Si	$13\frac{2}{3}$	0.39	0.92	−0.02	0.19	0.24	0.10	0.21
P	$14\frac{2}{3}$	0.53	1.15	−0.04	0.25	0.30	0.13	0.29
S	$15\frac{2}{3}$	0.52	1.39	−0.01	0.25	0.35	0.13	0.26
Cl	$16\frac{2}{3}$	0.69	1.42	0.07	0.38	0.34	0.17	0.31
Ar	$17\frac{2}{3}$	0.86	1.68	−0.02	0.42	0.42	0.22	0.44
K	$18\frac{2}{3}$	0.21	1.94	−0.02	0.09	0.49	0.05	0.12
Ca	$19\frac{2}{3}$	0.32	0.71	−0.05	0.14	0.19	0.08	0.18
Sc	$20\frac{2}{3}$	0.34	0.93	−0.04	0.15	0.24	0.09	0.19
Ti	$21\frac{2}{3}$	0.35	1.57	−0.09	0.13	0.41	0.09	0.22
V	$22\frac{2}{3}$	0.36	1.83	−0.03	0.16	0.47	0.09	0.20
Cr	$23\frac{2}{3}$	0.37	2.12	−0.03	0.17	0.54	0.09	0.20
Mn	$24\frac{2}{3}$	0.38	2.30	−0.29	0.04	0.65	0.10	0.34
Fe	$25\frac{2}{3}$	0.41	1.18	−0.16	0.12	0.33	0.10	0.29
Co	$26\frac{2}{3}$	0.47	1.92	−0.10	0.19	0.51	0.12	0.29
Ni	$27\frac{2}{3}$	0.42	2.25	−0.04	0.19	0.57	0.10	0.23
Cu	$28\frac{2}{3}$	0.41	2.57	−0.03	0.19	0.65	0.10	0.22
Zn	$29\frac{2}{3}$	0.50	2.69	−0.04	0.23	0.68	0.13	0.27
Ga	$30\frac{2}{3}$	0.26	1.26	−0.05	0.11	0.33	0.07	0.16

TABLE V-2 (Continued)

The first and second ionization potentials, electron affinities, electronegativities, and hardnesses (Ry) calculated by the electron-correlation corrected SIC-GX-LSD-GWB theory for some quark elements whose net charge is -e/3 (Z=N-1/3)

	Z	I_1^a	I_2^b	A_1^c	χ^d	η_A^e	η_B^f	η^g
Ge	$31\frac{2}{3}$	0.39	0.92	−0.02	0.18	0.24	0.10	0.21
As	$32\frac{2}{3}$	0.51	1.11	−0.04	0.24	0.29	0.13	0.28
Se	$33\frac{2}{3}$	0.50	1.29	0.00	0.25	0.32	0.13	0.25
Br	$34\frac{2}{3}$	0.65	1.30	0.08	0.36	0.31	0.16	0.28
Kr	$35\frac{2}{3}$	0.79	1.50	−0.04	0.38	0.39	0.20	0.41

a. The first ionization potential;
b. The second ionization potential;
c. The first electron affinity;
d. Electronegativity, $\chi = \frac{(I+A)}{2}$;
e. Hardness of acid A, $\eta_A = \frac{(I_{A+}-A_{A0})}{4}$;
f. Hardness of base B, $\eta_B = \frac{(I_{B0}-A_{B-})}{4}$;
g. Absolute hardness, $\eta = \frac{(I-A)}{2}$.

of the extra electron for the quark atoms related to the elements in group VII A. The convergence in the SCF procedure for the negative ions of these quark atoms might be attributed to the negative contribution of the exchange-correlation energy functional.

Unfortunately, the SCF procedure failed in calculating the negative ions of the quark atoms with Z=N-$\frac{1}{3}$ for the remaining elements, and no convergence was obtained. Presumably the exchange-correlation potential approaches zero faster for these elements, than for the halogens, when r approaches infinity.

To converge the one-electron Schrödinger equation for the negative ions of the quark atoms with Z=N-$\frac{1}{3}$, an artificial positively charged sphere, introduced by Watson[130] in calculating an oxygen double-charged negative ion, was used. Pre-

TABLE V-3

The first and second ionization potentials, electron affinities, electronegativities, and hardnesses (Ry) calculated by the electron-correlation corrected SIC-GX-LSD-GWB theory for some quark elements whose net charge is +2e/3 (Z=N+2/3)

	Z	I_1^a	I_2^b	A_1^c	A_1^d	χ^e	η_A^f	η_B^g	η^h
H	$1\frac{2}{3}$	2.83		1.07	−0.01	1.95		0.71	0.88
He	$2\frac{2}{3}$	4.19	7.18	0.22	−0.03	2.21	1.74	1.06	1.99
Li	$3\frac{2}{3}$	1.00	9.30	0.42	−0.01	0.71	2.72	0 25	0.29
Be	$4\frac{2}{3}$	1.40	2.28	0.36	−0.08	0.88	0.48	0 37	0 52
B	$5\frac{2}{3}$	1.38	2.89	0.54	−0.07	0.96	0.59	0.36	0.42
C	$6\frac{2}{3}$	1.73	2.91	0.73	−0.02	1.23	0.55	0.44	0.50
N	$7\frac{2}{3}$	2.08	3.43	0.61	−0.13	1.34	0.70	0.55	0 73
O	$8\frac{2}{3}$	2.01	3.94	0.86	−0.05	1.44	0.77	0.51	0.57
F	$9\frac{2}{3}$	2.43	3.93	1.12	−0.02	1.77	0.70	0.61	0.65
Ne	$10\frac{2}{3}$	2.85	4.52	0.24	−0.03	1.54	1.07	0.72	1.30
Na	$11\frac{2}{3}$	0.88	5.10	0.38	−0.02	0.63	1.18	0.22	0.25
Mg	$12\frac{2}{3}$	1.12	1.79	0.26	−0.05	0.69	0 38	0.29	0.43
Al	$13\frac{2}{3}$	0.92	2.12	0.39	−0.02	0.66	0.43	0.24	0.27
Si	$14\frac{2}{3}$	1.15	1.86	0.53	−0.04	0.84	0.33	0.30	0.31
P	$15\frac{2}{3}$	1.39	2.18	0.52	−0.01	0.95	0.41	0.35	0.43
S	$16\frac{2}{3}$	1.42	2.50	0.69	0.07	1.05	0.45	0.34	0.36
Cl	$17\frac{2}{3}$	1.68	2.57	0.86	−0.02	1.27	0.43	0.42	0.41
Ar	$18\frac{2}{3}$	1.94	2.92	0.21	−0.02	1.07	0.68	0.49	0.87
K	$19\frac{2}{3}$	0.71	3.27	0.32	−0.05	0.51	0 74	0.19	0.20
Ca	$20\frac{2}{3}$	0.93	1.38	0.34	−0.04	0.64	0.26	0.24	0.30
Sc	$21\frac{2}{3}$	1.07	1.47	0.35	−0.09	0.71	0.28	0.29	0.36
Ti	$22\frac{2}{3}$	1.21	1.55	0.36	−0.03	0.78	0 30	0.31	0.42
V	$23\frac{2}{3}$	0.99	2.01	0.37	−0.03	0.68	0.41	0.25	0.31
Cr	$24\frac{2}{3}$	0.97	2.15	0.38	−0.29	0.68	0.44	0.32	0.30
Mn	$25\frac{2}{3}$	1.18	1.76	0.41	−0.16	0.79	0.34	0.33	0.38
Fe	$26\frac{2}{3}$	1.28	1.81	0.47	−0.10	0.88	0.33	0.35	0.40
Co	$27\frac{2}{3}$	1.10	2.25	0.42	−0.04	0.76	0.46	0.29	0.34
Ni	$28\frac{2}{3}$	1.20	2.40	0.41	−0.03	0.81	0.50	0 31	0.40
Cu	$29\frac{2}{3}$	1.11	2.55	0.50	−0.04	0.81	0.51	0.29	0.31
Zn	$30\frac{2}{3}$	1.26	2.00	0.26	−0.05	0.76	0 43	0.33	0.50

TABLE V-3 (Continued)

The first and second ionization potentials, electron affinities, electronegativities, and hardnesses (Ry) calculated by the electron-correlation corrected SIC-GX-LSD-GWB theory for some quark elements whose net charge is +2e/3 (Z=N+2/3)

	Z	I_1^a	I_2^b	A_1^c	A_2^d	χ^e	η_A^f	η_B^g	η^h
Ga	$31\frac{2}{3}$	0.92	2.20	0.39	−0.02	0.65	0.45	0.24	0.27
Ge	$32\frac{2}{3}$	1.11	1.77	0.51	−0.04	0.81	0.31	0.29	0.30
As	$33\frac{2}{3}$	1.29	2.01	0.50	0.00	0.90	0.38	0.32	0.39
Se	$34\frac{2}{3}$	1.30	2.25	0.65	0.08	0.98	0.40	0.31	0.33
Br	$35\frac{2}{3}$	1.50	2.29	0.79	−0.04	1.15	0.38	0.39	0.36
Kr	$36\frac{2}{3}$	1.70	2.54	0.20	−0.02	0.95	0.59	0.43	0.75

a. The first ionization potential;
b. The second ionization potential;
c. The first electron affinity;
d. The second electron affinity;
e. Electronegativity, $\chi = \frac{(I+A)}{2}$;
f. Hardness of acid A, $\eta_A = \frac{(I_{A+}-A_{A0})}{4}$;
g. Hardness of base B, $\eta_B = \frac{(I_{B0}-A_{B-})}{4}$;
h. Absolute hardness, $\eta = \frac{(I-A)}{2}$.

viously (section IV-4)[139,142], the total energy including the statistical total energy and the VWN correlation energy in the electron-correlation corrected SIC-GX-LSD theory was a function of both the charge on and the radius of the Watson sphere, when a Watson sphere with radius between 1 and 5 a.u. were used. Fortunately, both the statistical total energy and the VWN correlation energy are not changed by the Watson sphere, when the sphere radius is large enough. Table V-5 shows the total energies (equation (5-8)), including the statistical total energy and the VWN correlation energy correction, of the quark atom and its negative ion for fluorine with fractional nuclear charge Z=N-$\frac{1}{3}$ in the electron-correlation corrected SIC-GX-

TABLE V-4

The first and second ionization potentials, electronegativities, and hardnesses (Ry) calculated by the electron-correlation corrected SIC-GX-LSD-GWB theory for some quark elements whose net charge is -2e/3 (Z=N-2/3)

	Z	I_1^a	I_2^b	χ^c	η_A^d	η_B^e	η^f
H	$\frac{1}{3}$	0.12		0.06		0.03	0.06
He	$1\frac{1}{3}$	0.47	1.83	0.23	0.46	0.14	0.23
Li	$2\frac{1}{3}$	0.08	2.93	0.04	0.73	0.03	0.04
Be	$3\frac{1}{3}$	0.21	0.68	0.11	0.17	0.07	0.11
B	$4\frac{1}{3}$	0.14	1.02	0.07	0.26	0.06	0.07
C	$5\frac{1}{3}$	0.26	0.98	0.13	0.24	0.06	0.13
N	$6\frac{1}{3}$	0.40	1.27	0.20	0.32	0.13	0.20
O	$7\frac{1}{3}$	0.27	1.57	0.13	0.39	0.07	0 13
F	$8\frac{1}{3}$	0.46	1.48	0.23	0.37	0.13	0.23
Ne	$9\frac{1}{3}$	0.67	1.85	0.33	0.46	0.18	0.33
Na	$10\frac{1}{3}$	0.09	2.21	0.05	0.55	0.02	0.05
Mg	$11\frac{1}{3}$	0.20	0.63	0.10	0.16	0.07	0.10
Al	$12\frac{1}{3}$	0.10	0.84	0.05	0.21	0.02	0.05
Si	$13\frac{1}{3}$	0.20	0.67	0.10	0.17	0.06	0 10
P	$14\frac{1}{3}$	0.31	0.87	0.16	0.22	0.07	0.16
S	$15\frac{1}{3}$	0.28	1.07	0.14	0.27	0.06	0.14
Cl	$16\frac{1}{3}$	0.42	1.09	0.21	0.27	0.10	0.21
Ar	$17\frac{1}{3}$	0.57	1.32	0.28	0.33	0.15	0.28
K	$18\frac{1}{3}$	0.09	1.55	0.04	0.39	0.03	0.04
Ca	$19\frac{1}{3}$	0.17	0.52	0.09	0.13	0.06	0.09
Sc	$20\frac{1}{3}$	0.15	0.67	0.08	0.17	0.13	0.08
Ti	$21\frac{1}{3}$	0.11	0.70	0.06	0.17	0.13	0.06
V	$22\frac{1}{3}$	0.34	0.73	0.17	0.18	0.17	0.17
Cr	$23\frac{1}{3}$	0.42	0.51	0.21	0.13	0.12	0.21
Mn	$24\frac{1}{3}$	0.21	0.75	0.10	0.19	0.13	0.10
Fe	$25\frac{1}{3}$	0.03	0.79	0.01	0.20	0.13	0.01
Co	$26\frac{1}{3}$	0.34	0.84	0.17	0.21	0.21	0.17
Ni	$27\frac{1}{3}$	0.44	0.65	0.22	0.16	0.21	0.22
Cu	$28\frac{1}{3}$	0.53	0.59	0.26	0.15	0.07	0.26
Zn	$29\frac{1}{3}$	0.29	0.86	0.15	0.21	0.09	0.15
Ga	$30\frac{1}{3}$	0.10	0.99	0.05	0.25	0.04	0.05

TABLE V-4 (Continued)

The first and second ionization potentials, electronegativities, and hardnesses (Ry) calculated by the electron-correlation corrected SIC-GX-LSD-GWB theory for some quark elements whose net charge is -2e/3 (Z=N-2/3)

	Z	I_1^a	I_2^b	χ^c	η_A^d	η_B^e	η^f
Ge	$31\frac{1}{3}$	0.20	0.68	0.10	0.17	0.07	0.10
As	$32\frac{1}{3}$	0.30	0.84	0.15	0.21	0.08	0.15
Se	$33\frac{1}{3}$	0.28	1.01	0.14	0.25	0.07	0.14
Br	$34\frac{1}{3}$	0.40	1.02	0.20	0.25	0.11	0.20
Kr	$35\frac{1}{3}$	0.53	1.20	0.26	0.30	0.15	0.26

a. The first ionization potential;
b. The second ionization potential,
c. Electronegativity, $\chi = \frac{(I+A)}{2}$;
d. Hardness of acid $\eta_A = \frac{(I_{A+} - A_{A0})}{4}$;
e. Hardness of base . alculated by the Lagrange extrapolation formula $\eta(Z=N-\frac{2}{3}) = 2\,[\,\eta(Z \; -\frac{1}{3}) - \eta(Z=N+\frac{1}{3})\,] + \eta(Z=N+\frac{2}{3})$, and $\eta(Z=N+\frac{1}{3})$, $\eta(Z=N-\frac{1}{3})$, and $\eta(Z=N+\frac{2}{3})$ were taken from Tables V-1 to V-3;
f. Absolute hardness, $\eta = \frac{(I-A)}{2}$.

LSD theory versus the radius of the Watson sphere with charge +4/3 a.u. Table V-5 shows that the total energies of the fluorine quark atom with different radii of the Watson sphere are the same as without a Watson sphere, when the radii are larger than 5 a.u. Its negative ion has the same trend as the quark atom, but it converges rather slowly, and when the sphere radii are bigger than 7 a.u., the total energy is the same as without any Watson sphere.

Fluorine and chlorine are special cases, for which the negative ions of their quark atoms can be solved by the SCF procedure perfectly. To show that the convergence trend of the total energy with the radius of Watson sphere increases is also true for other quark atoms and their negative ions, Table V-6 presents the

FIGURE 5-2

The first ionization potentials of the quark atoms with fractional nuclear charge Z=N - $\frac{1}{3}$ in the electron-correlation corrected SIC-GX-LSD-GWB theory, compared with Lackner and Zweig's interpolation

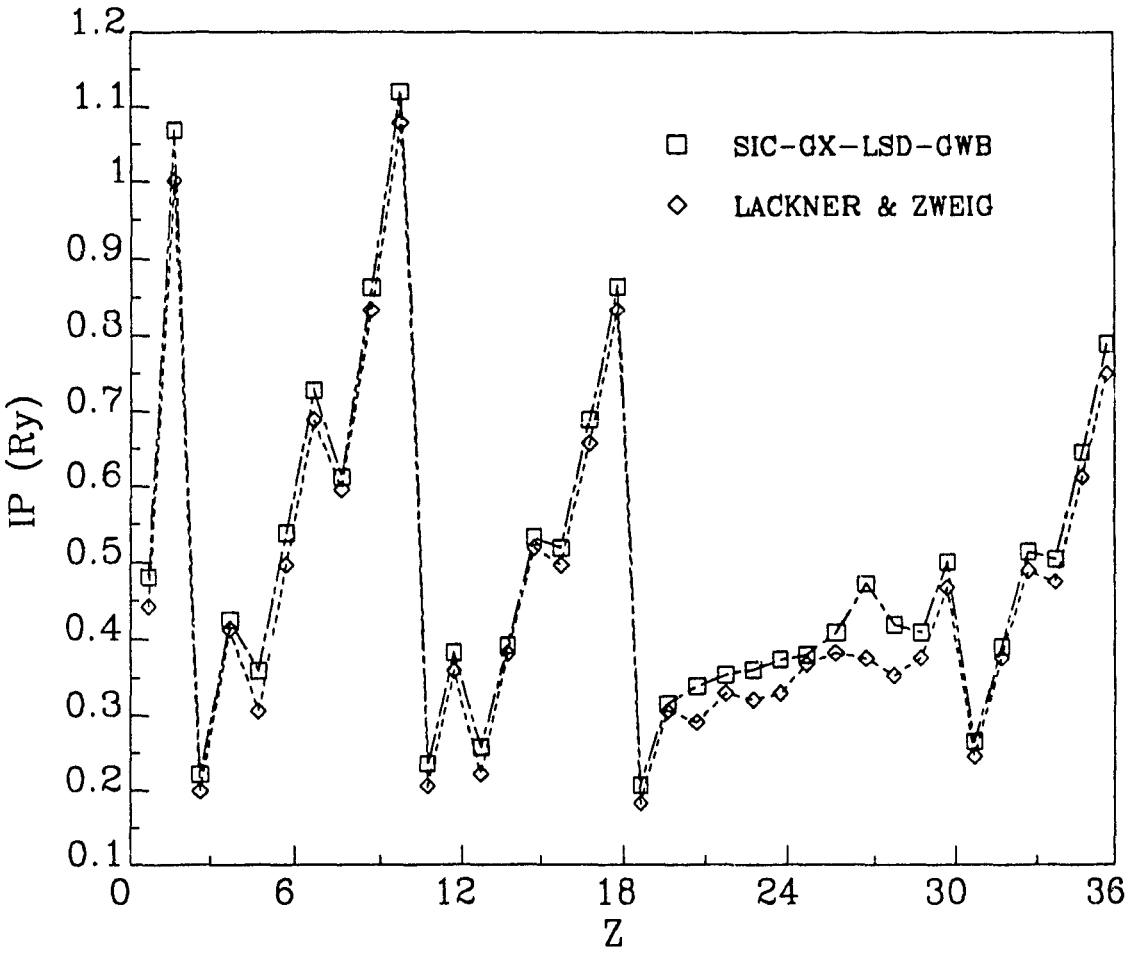

results for carbon. The total energy of carbon negative ion converges slowly , but when the Watson sphere radius is bigger than 18 a.u., the total energy converges to -66.4977Ry, and the electron affinity converges to -0.0699Ry. The total energy of the carbon quark atom converges as fast as the quark atom of fluorine. The different convergence speeds of the total energies between the negative ions of the quark atoms for fluorine and carbon is because the electrons in fluorine are paired.

The present work tested all the quark atoms and their negative ions for elements from hydrogen to krypton with Z=N-$\frac{1}{3}$. The total energy convergence speeds are the same for all quark atoms but differ for their negative ions. The radius of the Watson sphere to get the converged total energy is around 7 a.u. for the elements in group VII A, 50 a.u. for those in group VIII A, 40 a.u. for group II A, and 20 a.u. for all others. The SCF procedure works very well with the aid of large Watson sphere. Actually, if one is only interested in the first two digits behind the decimal point, the convergence is much faster than that listed above. Therefore, the Watson sphere radii are fixed to be 20 a_0 in calculating the first electron affinities of the transition-metal quark elements with Z=N-$\frac{1}{3}$.

Column 5 of Table V-2 summarizes the converged electron affinities of the quark atoms with fractional nuclear charge Z=N-$\frac{1}{3}$. The electron configurations of the first order negative ions were chosen to be the same as the corresponding single-charge negative ions of the ordinary atoms reported by Hotop and Lineberger[58]. To compare the present results with the empirical interpolated values[153], Fig. 5-5 plots the first electron affinities for the quark atoms with Z=N-$\frac{1}{3}$. It may be seen that there are not only large differences between the present calculated values and Lackner and Zweig's results[153], but also a different trend. In the present calculated results, the first electron affinity, -0.01 Ry, for Be with Z=4-$\frac{1}{3}$ is bigger than -0.03 Ry, the electron affinity for Li with Z=3-$\frac{1}{3}$, which is of the same trend as He to H.

FIGURE 5-3

The first ionization potentials of the quark atoms with fractional nuclear charge Z=N + $\frac{2}{3}$ in the electron-correlation corrected SIC-GX-LSD-GWB theory, compared with Lackner and Zweig's interpolation

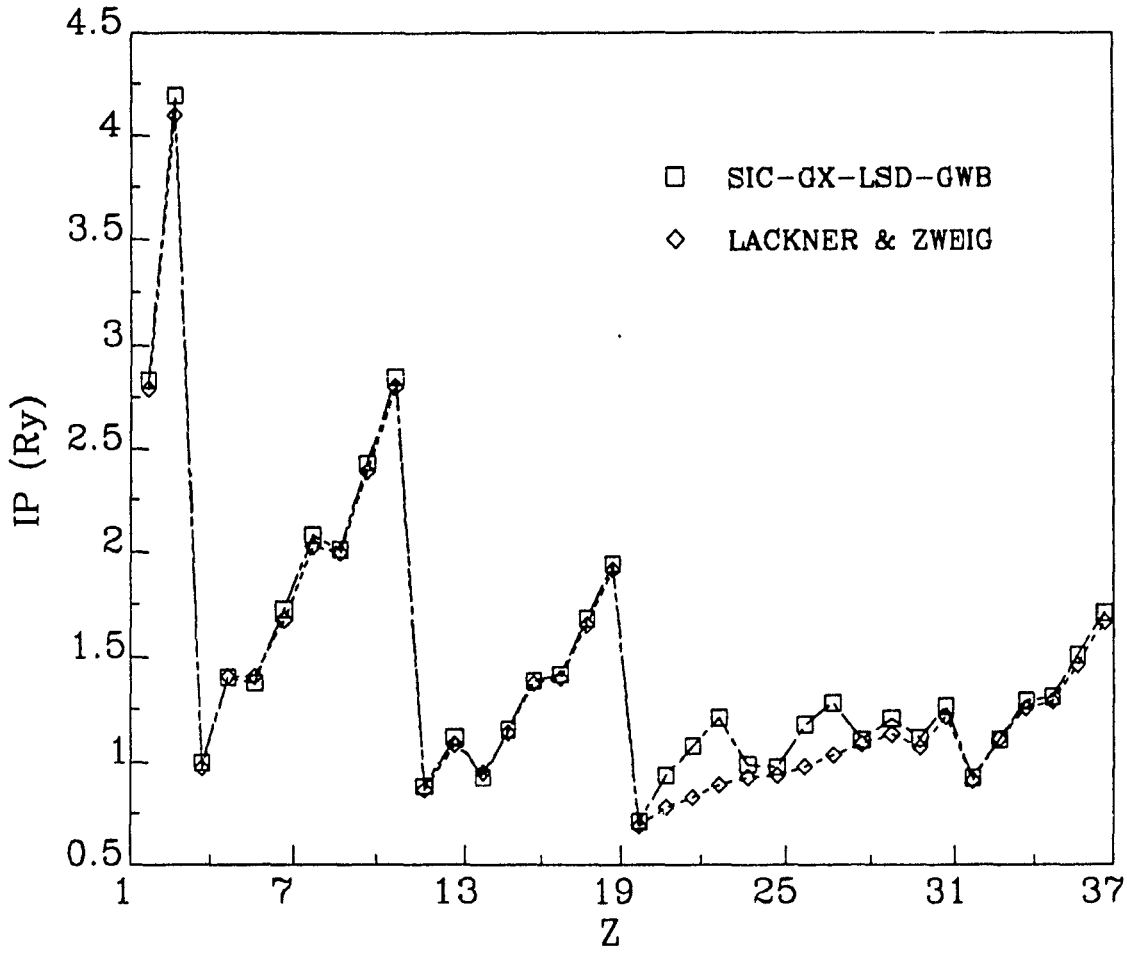

However the electron affinity for Be with Z=4-$\frac{1}{3}$ in Lackner and Zweig's interpolation is -0.36 Ry which is much smaller than the electron affinity, -0.05 Ry, for Li with Z=3-$\frac{1}{3}$. The same deviations occur for N, Ne, Mg, and etc. with Z=N-$\frac{1}{3}$. The reason of the deviation is probably the following. Lackner and Zweig's results were isoelectronic interpolation based on existing experimental electron affinities. They also interpolated the electron affinities of some ordinary atoms, for which the experimental electron affinities were not available, as input data to get the electron affinities of the quark atoms. This "double" interpolation causes uncertainty in the electron affinities of quark atoms. Furthermore, some of the existing electron affinities were not accurate, e.g., for the alkaline-earth elements, rare gasses[92,94,101,106,107]. The present calculation is based on the local-density functional model which has well defined approximations and shows no lack of predictability for other properties. Therefore the theoretical predictions are correct.

TABLE V-5

The effect of the Watso sphere radius on the statistical total energies of F(Z=N-1/3) and F^-(Z=N-1/3) (Ry)

r_W	E_{tot}[F]	$E_{tot}[F^-]$	EA
3.	−182.7040	−182.6444	−0.0596
4.	−182.7054	−182.6565	−0.0489
5.	−182.7055	−182.6594	−0.0461
6.	−182.7056	−182.6602	−0.0454
7.	−182.7056	−182.6604	−0.0452
No	−182.7056	−182.6605	−0.0451

The first electron affinities of the quark atoms with Z=N-$\frac{2}{3}$ are equivalent to the second electron affinities of the quark atoms with Z=N-$\frac{1}{3}$. The second or-

FIGURE 5-4

The first ionization potentials of the quark atoms with fractional nuclear charge Z=N - $\frac{2}{3}$ in the electron-correlation corrected SIC-GX-LSD-GWB theory, compared with Lackner and Zweig's interpolation

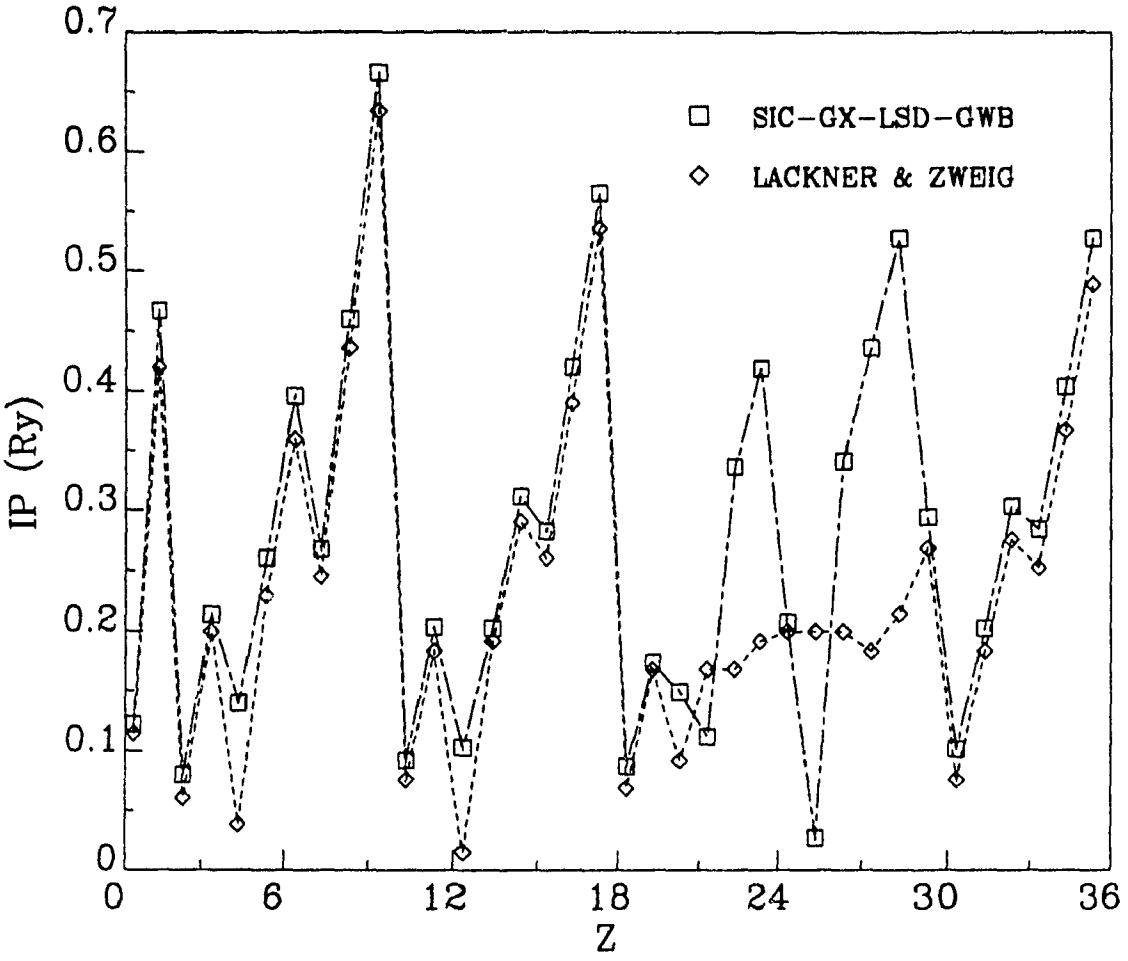

der negative ions of the selected quark atoms with Z=N$\pm\frac{1}{3}$ were calculated using the electron-correlation corrected SIC-GX-LSD theory with the GWB Fermi-hole parameters and Watson spheres. The results are summarized in Tables V-7 and V-8.

TABLE V-6

The effect of the Watson sphere radius on the statistical total energies of C(Z=N-1/3) and C^-(Z=N-1/3)

r_W	E_{tot}[F]	$E_{tot}[F^-]$	EA
3.	−66.5563	−66.4307	−0.1256
6.	−66.5676	−66.4911	−0.0765
9.	−66.5676	−66.4964	−0.0712
12.	−66.5676	−66.4973	−0.0703
15.	−66.5676	−66.4976	−0.0700
18.	−66.5676	−66.4977	−0.0699
21.	−66.5676	−66.4977	−0.0699
24.	−66.5676	−66.4977	−0.0699

Obviously, the second electron affinities calculated by the difference of the total energies between the first order negative ion and the second order negative ion are strongly dependent on the radius of the Watson sphere, when no Watson sphere was used for the first order negative ions with Z=N+$\frac{1}{3}$ or a very large Watson sphere was employed for those with Z=N-$\frac{1}{3}$, and the radius of the Watson sphere for the second order negative ions is gradually increased. As mentioned before, the total energy of the first order negative ion should be not affected by the Watson sphere for quark atoms with Z=N-$\frac{1}{3}$. Hence, the dependence of the second electron affinities on the Watson sphere is caused by the second order negative ion. Table V-7 lists the dependence of the second electron affinities of selected quark

atoms with Z=N+$\frac{1}{3}$ on the radii of the Watson spheres used in the SCF calculation for calculating the second order negative ions. Gradually increasing the radius of the Watson sphere, the total energies of the second order negative ions gradually decrease (more negative). Therefore, the difference of the total energies between the first and second order negative ions gradually increases (less negative). Obviously, when the Watson sphere radius goes to infinity, the total energy of the second order negative ion approaches the total energy of the real system. The results in Table V-7 show the trend. The second electron affinities of the selected quark atoms with Z=N+$\frac{1}{3}$ gradually approach very small values or zero as the radius of the Watson sphere with the net charge +1 increases. The second electron affinities of the selected quark atoms with Z=N-$\frac{1}{3}$ listed in Table V-8 show the same trend as Table V-7; the second electron affinities approach very small values or zero as the radius of the Watson sphere with the net charge +2$\frac{1}{3}$e increases. The speed of approach to the real values is different in Tables V-7 and V-8, because of the difference of the net charges in the second order negative ions with Z=N+$\frac{1}{3}$ and Z=N-$\frac{1}{3}$, the net charge is -1$\frac{2}{3}$e for the former and -2$\frac{1}{3}$e for the latter, and the difference of the net positive charge on the Watson spheres.

The second electron affinities of the quark atoms with fractional nuclear charge Z=N-$\frac{2}{3}$ are much more slowly approaching to their real values, because the net charge of the second order negative ions for them is -2$\frac{2}{3}$e.

The second electron affinities of the quark atoms with Z=N+$\frac{2}{3}$ are listed in column 6 of Table V-3. Actually, they are equivalent to the first electron affinities of the quark atoms with Z=N-$\frac{1}{3}$ shown in column 5 of Table V-2, e.g., the second electron affinity of H with Z=N+$\frac{2}{3}$=1$\frac{2}{3}$, which is -0.01 Ry, equal to the first electron affinity of He with Z=N-$\frac{1}{3}$=1$\frac{2}{3}$ in Table V-2, and so on.

FIGURE 5-5

The first electron affinities for the quark atoms with Z=N-$\frac{1}{3}$ in the electron-correlation corrected SIC-GX-LSD-GWB theory, compared with Lackner and Zweig's interpolation

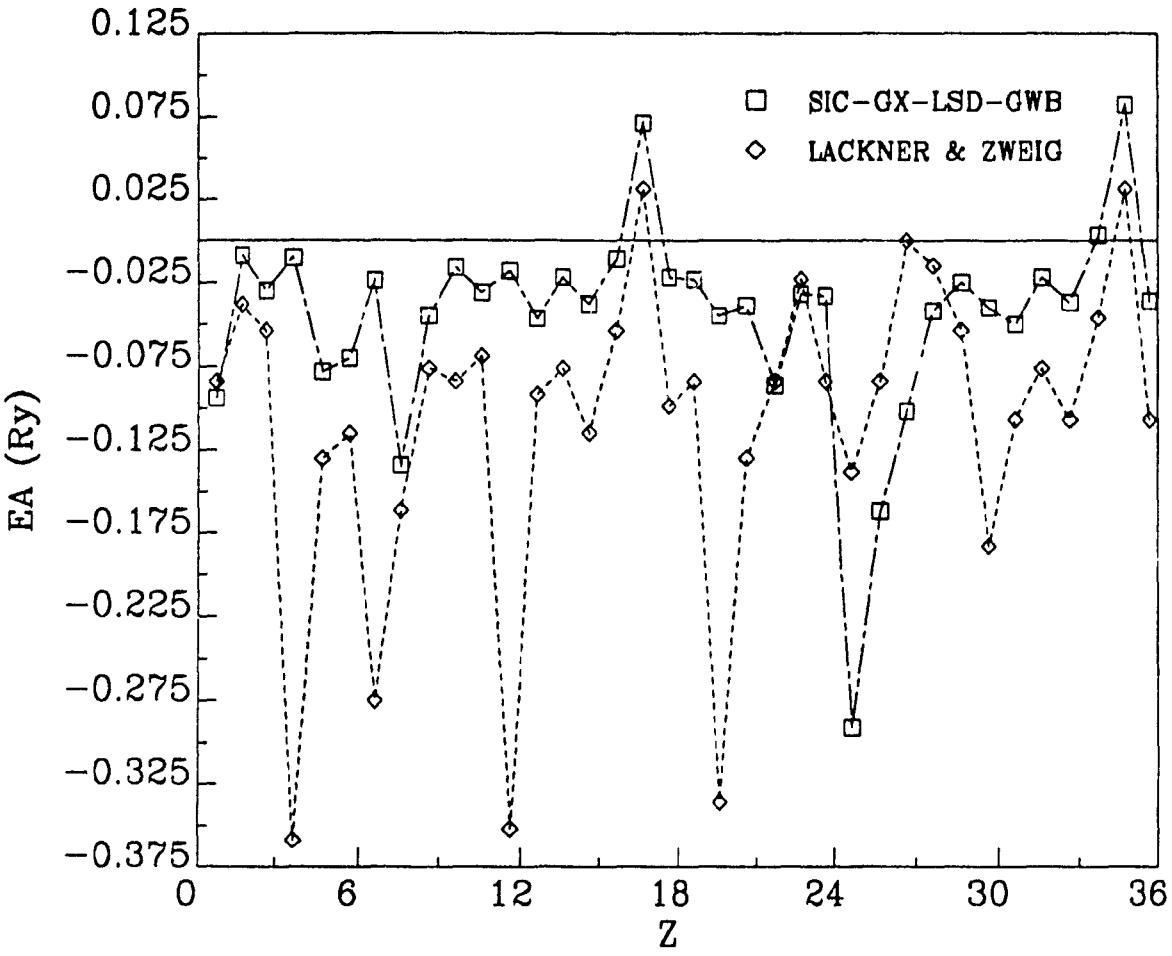

TABLE V-7

Electron affinities (Ry) with different Watson sphere radius (a_0) of some quark elements whose net charge is +e/3 (Z=N+1/3)

	Z	$r_w = 15$	$r_w = 20$	$r_w = 25$	$r_w = 35$	$r_w = 45$	$r_w = 55$	$r_w = 65$
H	$1\frac{1}{3}$	−0.041	−0.033	−0.028	−0.021	−0.017	−0.015	
He	$2\frac{1}{3}$	−0.067	−0.058	−0.053	−0.030	−0.023	−0.019	−0.016
Li	$3\frac{1}{3}$	−0.068	−0.051	−0.042	−0.030	−0.024	−0.019	−0.016
C	$6\frac{1}{3}$	−0.065	−0.051	−0.041	−0.030	−0.024	−0.019	−0.016
F	$9\frac{1}{3}$	−0.067	−0.051	−0.042	−0.030	−0.023	−0.019	−0.016
Ne	$10\frac{1}{3}$	−0.072	−0.063	−0.044	−0.030	−0.023	−0.019	−0.016
Na	$11\frac{1}{3}$	−0.069	−0.052	−0.042	−0.030	−0.024	−0.019	−0.016
Si	$14\frac{1}{3}$	−0.067	−0.051	−0.042	−0.030	−0.024	−0.019	−0.016
Cl	$17\frac{1}{3}$	−0.068	−0.052	−0.042	−0.030	−0.023	−0.019	−0.016
Ar	$18\frac{1}{3}$	−0.068	−0.059	−0.055	−0.030	−0.023	−0.019	−0.016

V-4. Electronegativity and Hardness

The electronegativities of the quark atoms with fractional nuclear charge $Z=N\pm\frac{1}{3}$ and $Z=N\pm\frac{2}{3}$ were calculated by averaging the ionization potential and electron affinity of the corresponding quark atom, equation (5-4), and are reported in column 6 of Tables V-1 and V-2, column 7 of Table V-3, and column 5 of Table V-4. The trend of the electronegativities is similar to Lackner and Zweig's calculation[153], except for the quark atoms with $Z=N-\frac{2}{3}$. Lackner and Zweig reported the negative electronegativities for the quark atoms with $Z=N-\frac{2}{3}$ in group IA - IVA and N and O and the positive electronegativities for others. The electronegativity distributions are random. However the electronegativities in the present calculation follow the same trend as those for the quark atoms with $Z=N\pm\frac{1}{3}$ and $Z=N+\frac{2}{3}$. The deviation between the present electronegativities and the Lackner and Zweig's results is

caused by the difference of the electron affinities of these quark atoms. Lackner and Zweig gave negative electron affinities which in absolute value are larger than the ionization potentials of the corresponding quark atoms. However, the second electron affinities approach some very small negative values or zero in the electron-correlation corrected SIC-GX-LSD theory which is excellently predictable.

TABLE V-8

Electron affinities (Ry) with different Watson sphere radius (a_0) of some quark elements whose net charge is -e/3 (Z=N-1/3)

	Z	r_w = 10	15	20	30	40	50	60	70	80
H	$\frac{2}{3}$	−0.220	−0.111	−0.059	−0.007					
He	$1\frac{2}{3}$	−0.258	−0.159	−0.135	−0.085	−0.057	−0.042	−0.032	−0.026	−0.021
Be	$3\frac{2}{3}$	−0.317	−0.201	−0.144	−0.087	−0.060	−0.044	−0.034	−0.027	−0.022
N	$6\frac{2}{3}$	−0.308	−0.188	−0.130	−0.073	−0.046	−0.030	−0.020	−0.013	−0.008
F	$8\frac{2}{3}$	−0.242	−0.162	−0.122	−0.081	−0.061	−0.049	−0.040	−0.034	−0.030
Ne	$9\frac{2}{3}$	−0.293	−0.183	−0.129	−0.076	−0.051	−0.036	−0.026	−0.019	
Na	$10\frac{2}{3}$	−0.251	−0.166	−0.115	−0.064	−0.038	−0.023	−0.012	−0.006	

From the values of the electronegativities listed in Tables V-1 to V-4, it can be seen that: (i) the electronegativity increases as the occupation number of the subshell increases, except for the quark atoms in the group VIII A with Z=N+$\frac{1}{3}$; (ii) the electronegativity increases with nuclear charge increases; for example, the electronegativity of F is 0.23 Ry with Z=N-$\frac{1}{3}$, 0.41 Ry with Z=N-$\frac{1}{3}$, 1.26 Ry with Z=N+$\frac{1}{3}$, and 1.77 Ry with Z=N+$\frac{2}{3}$. It is quite reasonable that the nuclear attractive force increases with the nuclear charge and that the ability to get an extra-electron increases, when the electron-configuration is fixed.

The hardnesses of acids and bases in terms of definitions (5-6a) and (5-6b) and the absolute hardnesses by definition (5-4) were calculated by using the first and second ionization potentials and electron affinities in Tables V-1 to V-4 for the quark atoms with Z=N$\pm\frac{1}{3}$ and Z=N$\pm\frac{2}{3}$. The results are summarized in Tables V-1 to V-4. The hardnesses of bases, η_B, listed in column 7 of Table V-4 were calculated by the Lagrange extrapolation formula

$$\eta\left(Z=N-\frac{2}{3}\right)=2\left[\eta\left(Z=N-\frac{1}{3}\right)-\eta\left(Z=N+\frac{1}{3}\right)\right]+\eta\left(Z=N+\frac{2}{3}\right) \qquad (5-10)$$

for the quark atoms with Z=N-$\frac{2}{3}$, where η(Z=N+$\frac{1}{3}$), η(Z=N-$\frac{1}{3}$), and η(Z=N+$\frac{2}{3}$) were taken from Tables V-1 to V-3; because no second electron affinities were obtained for them in the SCF procedure by the electron-correlation corrected SIC-GX-LSD theory. Furthermore, the second affinities used in equation (5-6b) in calculating the hardnesses of bases for the quark atoms with Z=N$\pm\frac{1}{3}$ were treated as zero, because the second electron affinities (in Tables V-7 and V-8) go to very small values or zero, when the Watson sphere radius approaches infinity.

The absolute hardnesses of the quark atoms with Z=N$\pm\frac{1}{3}$ and Z=N$\pm\frac{2}{3}$ are of the similar trend as predicted by Lackner and Zweig[153]: the absolute hardnesses increase, when the number of electrons in the subshell (nlm_s) increases. For example, N is harder than O and F, P is harder than S and Cl for the quark atoms with Z=N+$\frac{1}{3}$ and Z=N+$\frac{2}{3}$, displaying the similar behaviour as the ordinary atoms[151]; and N is harder than O and softer than F, and P is harder than S and softer than Cl for the quark atoms with Z=N-$\frac{1}{3}$ and Z=N-$\frac{2}{3}$, which possesses the same feature as the hardnesses (η^+) of the ordinary atoms in Goycoolea et al.'s work[151].

The trend of the absolute hardnesses differs from that obtained by equation (5-3) for the ordinary atoms. As mentioned by Vinayagam and Sen[149], O is harder

than N, F is harder than O, S is harder than P, and Cl is harder than S for the ordinary atoms by definition (5-3). The different trend is caused by the replacement of the derivative in equation (5-3) by the finite difference in equation (5-4).

The hardnesses of bases calculated by equation (5-6b) for the quark atoms with $Z=N\pm\frac{1}{3}$ and $Z=N+\frac{2}{3}$ and extrapolated by equation (5-10) for the quark atoms with $Z=N-\frac{2}{3}$ have the same behaviour as calculated by equation (5-3) for the atoms[149], except for O with $Z=N\pm\frac{1}{3}$ and $Z=N+\frac{2}{3}$. The hardnesses of O with $Z=N\pm\frac{1}{3}$ and $Z=N+\frac{2}{3}$ are smaller than those for N with $Z=N\pm\frac{1}{3}$ and $Z=N+\frac{2}{3}$, respectively. This implies that equation (5-6b) leads to the proper empirical trends in the hardness parameters.

The hardnesses of acids obtained using equation (5-6a) leads to the same dependence of the electron-configuration as the hardnesses of bases. The hardnesses of bases increase, as the number of the electrons in a subshell increases, except for the elements in group VII A, the halogens.

The values of the hardnesses, η_A and η_B of acids and bases and the values of the absolute hardnesses, η, increase as the nuclear charge increases for all these quark atoms, when the electron-configuration is fixed. The effect of increasing the nuclear charge is to enlarge the Coulomb attractive force between the nucleus and the electrons, the removal energy of the electron in the outermost orbital is, then, increased and the ability of binding an extra-electron increases. But the former increases much faster than the latter.

The present calculations show that the ionization potentials for quark atoms and electron affinities for the well-bound quark atoms obtained by the empirical isoelectronic interpolation technique is in excellent agreement with those from the electron-correlation SIC-GX-LSD theory with the GWB Fermi-hole parameters, when the accurate experimental results are employed in the interpolation. The

convergence technique using a very large Watson sphere surrounding the negative ion in the SCF calculation for the first order negative ions of the quark atoms with fractional nuclear charge $Z=N-\frac{1}{3}$ and the second order negative ions of the quark atoms with $Z=N\pm\frac{1}{3}$ and $Z=N+\frac{2}{3}$ is efficient.

The electronegativities and hardnesses of the quark atoms with fractional nuclear charge $Z=N\pm\frac{1}{3}$ and $Z=N\pm\frac{2}{3}$ possesses a similar trend to that of ordinary atoms. The dependence of the electron-configuration for the electronegativities and hardnesses of the quark atoms is the same as for the ordinary atoms.

CHAPTER VI

THE SELF-INTERACTION CORRECTED MULTIPLE-SCATTERING Xα METHOD

VI-1. Introduction

Molecular calculations are interesting to chemists. However, most methods are computationally tedious The cheapest s the multiple-scattering Xα (MS-Xα) method[160,161], except for the semi-empirical methods. The MS-Xα method is excellent in predicting the photoelectron spectra of molecules, clusters of relatively heavy atoms of interest in solid state physics and chemistry, and other molecular properties[162-172]. The introduction of the overlapping sphere approximation[173] showed that good ionization potentials could be obtained from the negative of the one-electron eigenvalue calculated by the Slater transition-state theory[174,175]. Case and Karplus[176] introduced a charge-partitioning algorithm which distributes the "muffin-tin" wave function contribution from the interatomic region among the atomic spheres. The MS-Xα method gives reasonably good expectation values for the one-electron operators from the Xα wave function and has been used to calculate molecular properties, such as dipole moments, quadrupole moments, diamagnetic susceptibilities, and nuclear quadrupole coupling constants[171,177,178].

The "muffin-tin" approximation makes the molecular one-electron eigenvalues and electron-density distributions differ from experiment The deviation can be reduced by using overlapping spheres. Then, the one-electron eigenvalues and electron-density distribution are sensitive to the percentage of overlapping sphere. The most reliable results are produced by means of the atomic sphere radii in the Norman criterion[168] scaling by a factor between 0.8 - 0.88[171,177,179-181].

Recently, some other theoretical methods have been developed, such as the LCAO-Xα method[181-183], the discrete variational Xα (DV-Xα) method[184-186], and the completely numerical local-density approximation (LDA) method[187]. They are more theoretically rigorous than the MS-Xα method and their results are better than MS-Xα. They are also much easier to use than the *ab-initio* Hartree-Fock method. But they are expensive for large molecules containing heavy atoms and complicated to wield in practise. The numerical results depend on the choice of the basis set in the LCAO-Xα method, the selection of the mesh points and the basis set (when the basis set is employed, instead of using the numerical integration) in the DV-Xα method, and the restricted application, e.g., only applying to diatomic molecules in the completely numerical LDA method. A powerful method in chemistry must be applicable to all molecules large and small containing light or heavy atoms and predict all properties with the same accuracy.

Because of the statistical approximate exchange energy functional in the Xα method, unlike the HF method, the self-exchange term does not cancel completely the self-Coulomb term. Hence the one-electron eigenvalue in the Xα method does not have the same theoretical or numerical value as in the HF method. The Xα one-electron eigenvalue corresponds to the electronegativity of the atom or molecule, equation (3-12), as defined by Parr et al.[77], whereas the HF one-electron eigenvalue equals the negative of the ionization potential for the corresponding orbital when the frozen orbital approximation is used (Koopmans' theorem)[54].

Slater[174,175] introduced the transition state theory, in which the ionization potential can be calculated from the negative of the one-electron eigenvalue obtained by removing a half-electron from the corresponding orbital to infinity in the self-consistent-field (SCF) procedure. Obviously, because the transition state is one between the initial and final states in the ionization process, the relaxation effect is partly included. However, the wave function given in the transition state SCF

procedure does not give correct expectation values for other one-electron operators in calculating other molecular properties, such as dipole moments, diamagnetic susceptibilities, etc. To obtain both the ionization potential and other one-electron operator expectation values, the SCF procedure has to be carried out twice for the same system, one for the transition state, and another for the ground state or excited state. This is an inefficient and expensive procedure, especially when the MS-Xα method is applied to large systems containing heavy atoms.

The self-interaction problem can be avoided by the direct removal of the exact self-Coulomb term and the approximate self-exchange term from the energy functional[29-32]. Application of this self-interaction correction (SIC) in the LDF theory, the SIC-LDF theory, to atomic calculations gave significant improvement over the uncorrected LSD results[29-32,45,49,81]. Theoretically, for atomic systems, the SIC-LSD theory leads to a potential with the correct asymptotic behaviour 1/r for the neutral atom.

The SIC has been successfully applied to small molecules and solids. The SIC-LSD theory has been used to calculate the electronic structures of diatomic molecules and solids[188,189] and gives excellent one-electron eigenvalues and total energies for some small molecules in the agreement with those in the multiconfiguration self-consistent-field (MCSCF) calculation. But the full numerical SIC-LSD theory might be impossible to apply to large and heavy molecules, because of the computational time.

In this chapter[190], to give the photoelectronic spectra and the correct wave function at the same time for a molecule by a single SCF calculation, the SIC is introduced into the MS-Xα theory. Section VI-2 will give a brief description about the MS-Xα method; and, then, the SIC in the MS-Xα will be introduced in Section VI-3. Since the SIC energy functional depends on the individual orbital densities,

the SIC total energy is not invariant under the orbital transformation[189]. To give the minimized total energy, Edmiston and Ruedenberg's method[191], developed by Pederson et al.[189,192], is used. The detail of the minimization of the SIC energy will be discussed in Section VI-4.

VI-2. Multiple-Scattering Xα Method

Details of the MS-Xα method can be found in the literature[193,194]. Only a brief description is given to introduce the SIC into the MS-Xα method.

The MS-Xα method is based on the division of molecular space into non-overlapping atomic, interatomic, and extramolecular regions, with a spherically averaged potential for the atomic and extramolecular regions and a volume-averaged potential for the interatomic region, including the conventional Xα approximation to the exchange-correlation. The spherically averaged potential in "muffin-tin" spheres is centred on each atomic site, with a constant potential elsewhere. The volume-averaged potential in the interatomic region significantly simplifies the molecular calculation.

Consider a system with N atomic spheres of radii b_α (α=1,2,...,N). The one-electron Schrödinger equations in the atomic, interatomic, and extramolecular regions are different, because of the different potentials,

$$V(\mathbf{r}) = \begin{cases} V^\alpha(r_\alpha), & \text{when } r_\alpha = |\mathbf{r} - \mathbf{R}_\alpha| \le b_\alpha \text{ (atomic region);} \\ V^0(r_0), & \text{when } r_0 = |\mathbf{r} - \mathbf{R}_\alpha| > b_0 \text{ (outer sphere);} \\ \bar{V}, & \text{otherwise (interatomic region).} \end{cases} \qquad (6-1)$$

where R_α is the distance of an atomic site from the origion of the system, and b_α and b_0 are the radii of the atom α and outer sphere. In the atomic sphere α, the

one-electron Schrödinger equation is

$$[-\nabla^2 + V^\alpha(r_\alpha)]\psi_i^I(\mathbf{r}_\alpha) = \epsilon_i \psi_i^I(\mathbf{r}_\alpha) \qquad (6-2)$$

in Rydberg atomic units, where the index I stands for the wave function in the atomic region and $V^\alpha(r_\alpha)$ is the total potential including the Coulomb interaction potentials between the nucleus and electron, electron and electron, and the exchange-correlation potential. The wave function, $\psi_i^I(\mathbf{r}_\alpha)$, may be expressed in terms of the single-centre partial wave expansion,

$$\psi_i^I(\mathbf{r}_\alpha) = \sum_L C_{iL}^\alpha R_{il}^\alpha(r_\alpha) Y_L(\mathbf{\Omega}_\alpha), (0 \leq r_\alpha \leq b_\alpha) \qquad (6-3)$$

where L = (l,m) is the partial wave index, $Y_L(\mathbf{\Omega}_\alpha)$ are real spherical harmonics and the expansion coefficients C_{iL}^α are to be determined.

In the extramolecular region, the one-electron Schrödinger equation is of the same form as equation (6-2),

$$[-\nabla^2 + V^0(r_0)]\psi_i^{III}(\mathbf{r}_0) = \epsilon_i \psi_i^{III}(\mathbf{r}_0) \qquad (6-4)$$

The wave function is also expanded into

$$\psi_i^{III}(\mathbf{r}_0) = \sum_L C_{iL}^0 R_{il}^0(r_0) Y_L(\mathbf{\Omega}_0), (b_0 \leq r_0 < \infty) \qquad (6-5)$$

In the interatomic region, equation (6-2) reduces to

$$[-\nabla^2 + \kappa_i^2]\psi_i^{II}(\mathbf{r}) = 0 \qquad (6-6)$$

where

$$\kappa_i^2 = \bar{V} - \epsilon_i \qquad (6-7)$$

The one-electron Schrödinger equations (6-2) and (6-4) in the atomic and extramolecular regions are easily solved numerically in each region in the partial wave

representation. The solution of equation (6-6) can be written in the multicenter partial-wave representation

$$\psi_i^{II}(\mathbf{r}) = \sum_\alpha \sum_L a_{iL}^\alpha n_l(k_i r_\alpha) Y_L(\mathbf{\Omega}_\alpha) + \sum_L a_{iL}^0 j_l(k_i r_0) Y_L(\mathbf{\Omega}_0) \qquad (6-8)$$

when

$$\epsilon_i > \bar{V} \qquad (6-9)$$

or

$$\psi_i^{II}(\mathbf{r}) = \sum_\alpha \sum_L a_{iL}^\alpha k_l^{(1)}(k_i r_\alpha) Y_L(\mathbf{\Omega}_\alpha) + \sum_L a_{iL}^0 i_l(k_i r_0) Y_L(\mathbf{\Omega}_0) \qquad (6-10)$$

when

$$\epsilon_i < \bar{V} \qquad (6-11)$$

The expansion coefficients C_{iL}^α, C_{iL}^0, a_{iL}^α, and a_{iL}^0 in equations (6-3), (6-5), and (6-8) or (6-10) are determined in terms of the continuous wave functions and their derivatives on all the sphere boundaries.

Furthermore, the Coulomb and exchange potentials in the SCF calculation are constructed from the electron densities in the differen' regions. The total potentials which include the Coulomb and exchange potentials in the spin-restricted MS-Xα method are

$$\begin{aligned} V^\alpha(r_\alpha) = & -\frac{2Z_\alpha}{r_\alpha} + \frac{2}{r_\alpha}\int_0^{r_\alpha} 4\pi r^2 \rho_\alpha(r) dr \\ & + 2\int_{r_\alpha}^{b_\alpha} 4\pi r^2 \frac{1}{r}\rho_\alpha(r) dr - 6\alpha\left[\frac{3}{8\pi}\rho_\alpha(r_\alpha)\right]^{1/3} \\ & + 2\left[\sum_{\beta(\neq\alpha)} \frac{1}{R_{\alpha\beta}}(Q_\beta - Z_\beta) + \int_{b_0}^{\infty} 4\pi r^2 \frac{1}{r}\rho_0(r) dr\right] \\ & + 4\pi\rho_{int}\left[b_0^2 - b_\alpha^2 - \frac{R_\alpha^2}{3} - \frac{2}{3}\sum_{\beta(\neq\alpha)} \frac{b_\beta^3}{R_{\alpha\beta}}\right] \end{aligned} \qquad (6-12)$$

in the atomic sphere α,

$$V^0(r_0) = \frac{2}{r_0}\left\{\sum_\beta (Q_\beta - Z_\beta) + Q_{int} + \int_{b_0}^{r_0} 4\pi r^2 \rho_0(r) dr\right\}$$
$$+ 2\int_{r_0}^{\infty} 4\pi r^2 \frac{1}{r}\rho_0(r)dr - 6\bar{\alpha}\left[\frac{3}{8\pi}\rho_0(r_0)\right]^{1/3} \qquad (6-13)$$

in the extramolecular region, and

$$\bar{V} = 4\pi\rho_{int}\left\{b_0^2 - \frac{4\pi}{3V}\left[\frac{1}{5}b_0^5 - \sum_\alpha (\frac{1}{3}b_\alpha^3 R_\alpha^2 + \frac{1}{5}b_\alpha^5)\right]\right\}$$
$$+ \frac{4\pi}{V}\sum_\alpha \left[Q_\alpha - Z_\alpha - \frac{4}{3}\pi b_\alpha^3 \rho_{int}\right]\left[b_0^2 - b_\alpha^2 - \frac{1}{3}R_\alpha^2 - \frac{2}{3}\sum_{\beta(\neq\alpha)} \frac{b_\beta^3}{R_{\alpha\beta}}\right]$$
$$- 6\bar{\alpha}\left[\frac{3}{8\pi}\rho_{int}\right]^{1/3} + 2\int_{b_0}^{\infty} 4\pi r^2 \frac{1}{r}\rho_0(r)dr \qquad (6-14)$$

in the interatomic region; $\rho_\alpha(r_\alpha)$ and $\rho_0(r_0)$ are the spherically averaged electron densities in the atomic sphere α and the outer sphere; ρ_{int} is the constant electron density in the interatomic region; $R_{\alpha\beta}$ is the distance between the centres of the atomic spheres α and β; Q_α and Z_α are the electron charge and the atomic number in the atomic sphere α; V is the volume of the interatomic region,

$$V = \frac{4}{3}\pi\left[b_0^3 - \sum_\alpha b_\alpha^3\right] \qquad (6-15)$$

Q_{int} is the total electron charge in the interatomic region, and the constant α in the exchange potential term of equation (6-12) is the exchange parameter of the atomic sphere α, and $\bar{\alpha}$ the parameter for both the extramolecular and interatomic regions.

The one-electron Schrödinger equations (6-2) and (6-4) are solved by the SCF procedure, until the differences of the potentials between the (i+1)th and the ith iterations are less than a defined value. The one-electron eigenvalues and the wave function are considered to be self-consistent in the MS-Xα method.

VI-3. Self-Interaction Correction in the Multiple-Scattering Xα Method

When the SIC carried out by removing the exact self-Coulomb from the Coulomb repulsive functional and the approximate self-exchange from the local electron density functional, is applied to the MS-Xα method, the one-electron Schrödinger equation (6-2) becomes

$$\left[-\nabla^2 + V^{\alpha}(r_\alpha) + V_i^{SIC-\alpha}(r_\alpha) \right] \psi_i^I(\mathbf{r}_\alpha) = \sum_j \epsilon_{ij} \psi_j^I(\mathbf{r}_\alpha) \qquad (6-16)$$

for the atomic sphere α, while equation (6-4) becomes

$$\left[-\nabla^2 + V^{0}(r_0) + V_i^{SIC-0}(r_0) \right] \psi_i^{III}(\mathbf{r}_0) = \sum_j \epsilon_{ij} \psi_j^{III}(\mathbf{r}_0) \qquad (6-17)$$

for the extramolecular region, and equation (6-6) becomes

$$\left[-\nabla^2 + \kappa_i'^2 \right] \psi_i^{II}(\mathbf{r}) = \sum_j \epsilon_{ij} \psi_j^{II}(\mathbf{r}) \qquad (6-18)$$

for the interatomic region. In equations (6-16) and (6-17), $V_i^{SIC-\alpha}$ and V_i^{SIC-0} are the total self-interaction potentials including the exact self-Coulomb and the approximate self-exchange potentials for orbital i. κ_i' in equation (6-18) changes from equation (6-7) to

$$\kappa_i'^2 = \bar{V} + \bar{V}_i^{SIC} \qquad (6-19)$$

where $\bar{V}_i^{SIC}$ is the total self-interaction potential in the interatomic region.

The self-interaction potential for the atomic sphere α is, in contrast to equation (6-12),

$$\begin{aligned} V_i^{SIC-\alpha}(r_\alpha) = -2\Bigg\{ & \frac{1}{r_\alpha} \int_0^{r_\alpha} 4\pi r^2 \rho_i^{\alpha}(r) dr + \int_{r_\alpha}^{b_\alpha} 4\pi r^2 \frac{1}{r} \rho_i^{\alpha}(r) dr \\ & + \left[\sum_{\beta(\neq\alpha)} \frac{1}{R_{\alpha\beta}} Q_{i\beta} + \int_{b_0}^{\infty} 4\pi r^2 \frac{1}{r} \rho_i^{0}(r) dr \right] \\ & + 2\pi \rho_i^{int} \left[b_0^2 - b_\alpha^2 - \frac{1}{3} R_\alpha^2 - \frac{2}{3} \sum_{\beta(\neq\alpha)} \frac{b_\beta^3}{R_{\alpha\beta}} \right] \Bigg\} \\ & + 6\alpha \left[\frac{3}{8\pi} \rho_i^{\alpha}(r_\alpha) \right]^{1/3} \end{aligned} \qquad (6-20)$$

The first term is the exact self-Coulomb potential produced by the electron in orbital i and the second term is the approximate self-exchange potential. In the self-Coulomb potential, the $\left\{...\right\}$ of equation (6-20), the first two terms are the self-Coulomb potentials generated by the electron density in the atomic sphere α, and by the electron densities in all other atomic spheres treated as point charges except for the atomic sphere α, and in the outer sphere region; the third term is the potential contribution from the interatomic region. ρ_i^α and ρ_i^0 are the electron densities of electron i in the atomic and extramolecular regions, respectively. $Q_{i\beta}$ is the total fractional charge of electron i in the interatomic region.

The self-interaction potential for the extramolecular region is modified from equation (6-13) to

$$V_i^{SIC-0}(r_0) = -2\left\{ \frac{1}{r_0}\left(\sum_\beta Q_{i\beta} + Q_i^{int} \right) + \frac{1}{r_0}\int_{b_0}^{r_0} 4\pi r^2 \rho_i^0(r)dr + \int_{r_0}^{\infty} 4\pi r^2 \frac{1}{r}\rho_i^0(r)dr \right\} + 6\bar{\alpha}\left[\frac{3}{8\pi}\rho_i^0(r_0) \right]^{1/3} \qquad (6-21)$$

Here the first and second terms are the self-Coulomb and self-exchange interaction corrections to the potential in the extramolecular region. In the self-Coulomb potential, the first term is from the atomic and interatomic regions, and the second and third terms are the self Coulomb potentials from the outer sphere itself.

In the interatomic region, the self-interaction potential is modified from equation (6-14) to

$$\bar{V}_i^{SIC} = -4\pi\rho_i^{int}\left\{ b_0^2 - \frac{4\pi}{3V}\left[\frac{1}{5}b_0^5 - \sum_\alpha \left(\frac{1}{3}b_\alpha^3 R_\alpha^2 + \frac{1}{5}b_\alpha^5 \right) \right] \right\} - \frac{4\pi}{V}\sum_\alpha \left[Q_{i\alpha} - \frac{4\pi}{3}b_\alpha^3\rho_i^{int} \right]\left[b_0^2 - b_\alpha^2 - \frac{1}{3}R_\alpha^2 - \frac{2}{3}\sum_{\beta(\neq\alpha)} \frac{b_\beta^3}{R_{\alpha\beta}} \right] - 2\int_{b_0}^{\infty} 4\pi r^2 \frac{1}{r}\rho_i^0(r)dr + 6\bar{\alpha}\left[\frac{3}{8\pi}\rho_i^{int} \right]^{1/3} \qquad (6-22)$$

This is a volume-averaged potential. The first term is the volume-averaged potential obtained by assuming that the atomic and interatomic regions were covered by the

constant electron density ρ_i^{int}. But, in fact, this is not true for the atomic spheres, so the second term is the averaged potential generated by all the atomic spheres in the atomic region with the real electron densities subtracted from the potential produced by the constant electron density ρ_i^{int}. The third term is the Coulomb interaction potential produced by the electron charge on the outer sphere, and the last term is the self-exchange potential which only relates to the local electron density.

VI-4. Minimization of the Total Self-Interaction-Correction Energy

In the SIC-MS-Xα method, the energy functional depends on individual orbital electron densities, unlike the MS-Xα method where the energy functional depends on the total electron density. The total SIC energy is not invariant under orbital transformation. The orbital transformation leaves the statistical total energy in the MS-Xα method invariant, because the orbital transformation is unitary, but it alters the SIC energy.

Let $\left\{\phi\right\}$ be a set of orbitals corresponding to the minimized value of the total SIC energy and $\left\{\psi\right\}$ a set of orbitals in the symmetric representation. Usually, $\left\{\psi\right\}$ is not identical to $\left\{\phi\right\}$, and consequently the transformation

$$\phi_\mu = \sum_i M_{\mu i}\psi_i \qquad (6-23)$$

is used to minimize the total SIC energy when the orbital densities from $\left\{\phi\right\}$ has be found.

Following the Edmiston and Ruedenberg[191] localization procedure, which minimized the self-Coulomb energy and was extended to minimize the total SIC energy in the SIC-LSD theory by Pederson et al.[189,192].

Consider an infinitesimal orthogonal transformation T which takes a set of orbital $\left\{\phi\right\}$ to a new set $\left\{\phi'\right\}$, that is

$$\phi'_i = \phi_i + \delta\phi_i = \sum_j \phi_i T_{ij} \qquad (6-24)$$

with

$$\sum_n T_{in} T_{jn} = \delta_{ij} \qquad (6-25)$$

Let

$$T_{ij} = \delta_{ij} + t_{ij} \qquad (6-26)$$

gives

$$t_{ij} + t_{j\cdot} + \sum_n t_{in} t_{jn} = 0 \qquad (6-27)$$

where t_{ij} is an infinitesimal value. Keeping the first order terms, equation (6-27) reduces to

$$t_{ij} + t_{ji} = 0 \qquad (6-28)$$

The minimization of the total self-interaction correction energy requires

$$\left(\frac{\partial E_{SIC}}{\partial t_{\mu\nu}}\right)_{t_{ij}=0} = 0 \qquad (6-29)$$

for all μ, ν, i, j with $\mu > \nu$, j>i. Writing the SIC energy expression in terms of the primed orbitals and carrying out the differential of equation (6-29) leads to

$$< \phi_\mu | V_\mu^{SIC} - V_\nu^{SIC} | \phi_\nu > = 0 \qquad (6-30)$$

for all μ and ν. Equation (6-30) has to be satisfied for all orbitals by successively minimizing each pair of orbitals. An iteration technique is used to find an appropriate new orbital set $\left\{\phi\right\}$. Consider a given pair of orbitals (ϕ_μ, ϕ_ν), and that the new pair of orbitals can be written as

$$\begin{pmatrix} \phi_\mu \\ \phi_\nu \end{pmatrix} = \begin{pmatrix} cos\gamma & -sin\gamma \\ sin\gamma & cos\gamma \end{pmatrix} \begin{pmatrix} \phi'_\mu \\ \phi'_\nu \end{pmatrix} \qquad (6-31)$$

Constraint condition equation (6-30) determines the γ value in equation (6-31). The self-exchange potential in equation (6-30) may make it impossible to solve analytically for the γ value in equation (6-31) by using equation (6-30). Therefore, an iteration technique is employed to find the γ value satisfying equation (6-30). In detail, starting with the orbital set $\left\{\psi\right\}$, equations (6-30) and (6-31) may be rewritten as

$$< \phi_{\mu}^{(i+1)} | V_{\mu i}^{SIC} - V_{\nu i}^{SIC} | \phi_{\nu}^{(i+1)} > = 0 \qquad (6-32)$$

and

$$\begin{pmatrix} \phi_{\mu}^{(i+1)} \\ \phi_{\nu}^{(i+1)} \end{pmatrix} = \begin{pmatrix} cos\gamma^{(i+1)} & -sin\gamma^{(i+1)} \\ sin\gamma^{(i+1)} & cos\gamma^{(i+1)} \end{pmatrix} \begin{pmatrix} \phi_{\mu}^{(i)} \\ \phi_{\nu}^{(i)} \end{pmatrix} \qquad (6-33)$$

during the (i+1)th iteration. In equation (6-32), the total SIC potentials for orbitals μ and ν were calculated from the orbitals $\phi_{\mu}^{(i)}$ and $\phi_{\nu}^{(i)}$, respectively. Substituting equation (6-33) into (6-32) gives

$$tan2\gamma^{(i+1)} = \frac{2 < \phi_{\mu}^{(i)} | \Delta V_{\mu\nu i}^{SIC} | \phi_{\nu}^{(i)} >}{< \phi_{\mu}^{(i)} | \Delta V_{\mu\nu i}^{SIC} | \phi_{\mu}^{(i)} > - < \phi_{\nu}^{(i)} | \Delta V_{\mu\nu i}^{SIC} | \phi_{\nu}^{(i)} >} \qquad (6-34)$$

Where $\Delta V_{\mu\nu i}^{SIC}$ is the difference of the SIC potentials between orbitals μ and ν in the ith iteration, i.e.

$$\Delta V_{\mu\nu i}^{SIC} = V_{\mu i}^{SIC} - V_{\nu i}^{SIC} \qquad (6-35)$$

The process continues, until the new γ from equation (6-34) is less than 10^{-5}, when equation (6-30) is considered to have been satisfied for orbitals ϕ_{μ} and ϕ_{ν}. But, when ϕ_{μ} and ϕ_{ν} are paired and satisfy equation (6-30), they probably do not satisfy equation (6-30), when paired with any other orbitals ϕ_{η} separately. Therefore this procedure has to be applied to all pairs. A check is made that the total SIC energy does not change, compared to the last cycle. The cycle is repeated until the total SIC energy is changed less than 10^{-8} a.u.

In the MS-Xα method, because of the division of molecular space, the calculation of the matrix elements of $\Delta V_{\mu\nu}^{SIC}$ is rather complicated, e.g.,

$$< \phi_\mu | \Delta V_{\mu\nu}^{SIC} | \phi_\nu > = \sum_\alpha < \phi_\mu^I(\mathbf{r}_\alpha) | \Delta V_{\mu\nu}^{SIC-\alpha}(r_\alpha) | \phi_\nu^I(\mathbf{r}_\alpha) > + < \phi_\mu^{III}(\mathbf{r}_0) | \Delta V_{\mu\nu}^{SIC-0}(r_0) | \phi_\nu^{III}(\mathbf{r}_0) > + < \phi_\mu^{II}(\mathbf{r}) | \Delta \bar{V}_{\mu\nu}^{SIC} | \phi_\nu^{II}(\mathbf{r}) > \qquad (6-36)$$

where the iteration index i has been dropped. In equation (6-36), the first term is the contribution from all the atomic spheres, the second term from the extramolecular region, and the third term from the interatomic region.

It is impossible to calculate exactly the third term in equation (6-36) because of the irregular shape of the interatomic region, although the wave functions and constant potentials for all the orbitals are known before calculating the matrix elements.

To overcome the irregular shape in the interatomic region, the charge partitioning algorithm proposed by Case and Karplus[176] in the calculation of the expectation value of one-electron operators was used. The electron charge in the interatomic region is partitioned into individual atomic spheres and the wave functions of the individual atomic spheres expanded into the interatomic region including the extra electron charge contributed from the interatomic region.

After applying the charge partitioning algorithm, equation (6-36) becomes

$$< \phi_\mu | \Delta V_{\mu\nu}^{SIC} | \phi_\nu > = \sum_\alpha < \phi_\mu'^{II}(\mathbf{r}_\alpha) | \Delta V_{\mu\nu}^{SIC-\alpha}(r_\alpha) | \phi_\nu'^{II}(\mathbf{r}_\alpha) > + < \phi_\mu^{III}(\mathbf{r}_0) | \Delta V_{\mu\nu}^{SIC-0}(r_0) | \phi_\nu^{III}(\mathbf{r}_0) > \qquad (6-37)$$

Obviously, the second term on the right hand side of equation (6-37) is the same as the second term in equation (6-36). $\phi_\mu'^{II}(\mathbf{r}_\alpha)$ and $\phi_\nu'^{II}(\mathbf{r}_\alpha)$ in equation (6-37) are the expanded wave functions of orbitals μ and ν for the atomic sphere α. The constant

potentials of orbitals μ and ν are used in the integrand of equation (6-37) for the integral of the expanded wave function, that is

$$
\begin{aligned}
&< \phi_\mu^{'I}(\mathbf{r}_\alpha)| \triangle V_{\mu\nu}^{SIC-\alpha}(r_\alpha)|\phi_\nu^{'I}(\mathbf{r}_\alpha) > \\
&\qquad = \int_0^{b_\alpha} \int_{\mathbf{\Omega}} \phi_\mu^I(\mathbf{r}_\alpha) \triangle V_{\mu\nu}^{SIC-\alpha}(r_\alpha)\phi_\nu^I(\mathbf{r}_\alpha) r_\alpha^2 dr_\alpha d\mathbf{\Omega}_\alpha \\
&\qquad + \int_{b_\alpha}^{b_{\alpha,new}} \int_{\mathbf{\Omega}} \phi_\mu^{exp}(\mathbf{r}_\alpha) \triangle \bar{V}_{\mu\nu}^{SIC} \phi_\nu^{exp}(\mathbf{r}_\alpha) r_\alpha^2 dr_\alpha d\mathbf{\Omega}_\alpha \qquad (6-38)
\end{aligned}
$$

where $b_{\alpha,new}$ is the new radius of the atomic sphere α including the electron charge contributed from the interatomic region.

Explicitly, the matrix element of $\Delta V_{\mu\nu}^{SIC}$ is

$$
\begin{aligned}
&< \phi_\mu |\Delta V_{\mu\nu}^{SIC}| \phi_\nu > \\
&\qquad = \sum_{i,j} M_{\mu i} M_{\nu j} \Bigg\{ \sum_\alpha \Bigg[\sum_L C_{iL}^\alpha \sum_{L'} C_{jL'}^\alpha \delta(l,l')\delta(m,m') \\
&\qquad \int_0^{b_\alpha} R_{il}^\alpha(r_\alpha) \triangle V_{\mu\nu}^{SIC-\alpha}(r_\alpha) R_{jl'}^\alpha(r_\alpha) r_\alpha^2 dr_\alpha \\
&\qquad + \Delta \bar{V}_{\mu\nu}^{SIC} \int_{b_0}^{b_{\alpha,new}} R_{il}^\alpha(r_\alpha) R_{jl'}^\alpha(r_\alpha) r_\alpha^2 dr_\alpha \Bigg] \\
&\qquad + \sum_L C_{iL}^0 \sum_{L'} C_{jL'}^0 \delta(l,l')\delta(m,m') \\
&\qquad \int_{b_0}^{\infty} R_{il}^0(r_0) \triangle V_{\mu\nu}^{SIC-0}(r_0) R_{il'}^0(r_0) r_0^2 dr_0 \Bigg\} \qquad (6-39)
\end{aligned}
$$

where $\delta(l,l')$ and $\delta(m,m')$ are Kroenecker delta functions. From equation (6-39), it is obvious that the angular part of the integration is already calculated analytically, because the potentials in the MS-Xα method are only dependent on the radial variables in the atomic and extramolecular regions and are a constant in the interatomic region.

CHAPTER VII

APPLICATION OF THE SIC-MS-Xα METHOD TO MOLECULES AND MOLECULAR ANIONS

VII-1. Introduction

It is clear that the off-diagonal Lagrange multipliers are not equal to zero in equations (6-16), (6-17), and (6-18), because the SIC potentials are orbital-dependent. It is much more difficult to solve the one-electron Schrödinger equation with non-zero off-diagonal Lagrange multipliers[29,30], because the wave functions in the interatomic region (equation (6-18)) might be no longer Bessel functions.

Pederson et al.[189] used a projection technique to cast the individual Hamiltonian into one unified Hamiltonian. The one-electron Schrödinger equation with only-diagonal Lagrange multipliers was solved easily for the occupied orbitals. In their later paper[189], they showed that the off-diagonal Lagrange multipliers were small. Other authors also showed that the difference of the one electron eigenvalues calculated using the non-orthogonal wave functions and the orthogonal wave functions in the orbital-dependent LDF theory is small[22,24,29,30] in the atomic calculation. When the off-diagonal Lagrange multipliers in equations (6-16), (6-17), and (6-18) in the SIC-MS-Xα method are ignored, the one-electron Schrödinger equations in the atomic, interatomic, and extramolecular regions reduce to

$$\left[-\nabla^2 + V^{\alpha}(r_{\alpha}) + V_i^{SIC-\alpha}(r_{\alpha}) \right] \psi_i^I(\mathbf{r}_{\alpha}) = \epsilon_{ii} \psi_i^I(\mathbf{r}_{\alpha}) \qquad (7-1)$$

$$\left[-\nabla^2 + V^{0}(r_0) + V_i^{SIC-0}(r_0) \right] \psi_i^{III}(\mathbf{r}_0) = \epsilon_{ii} \psi_i^{III}(\mathbf{r}_0) \qquad (7-2)$$

and

$$\left[-\nabla^2 + \kappa_i''^2 \right] \psi_i^{II}(\mathbf{r}) = 0 \qquad (7-3)$$

with

$$\kappa_i''^2 = \bar{V} + \bar{V}_i^{SIC} - \epsilon_{ii} \qquad (7-4)$$

Cook and Case's MS-Xα program[195] was modified to solve the equations (7-1), (7-2), and (7-3) with the orbital-dependent SIC potentials to obtain the wave functions in the SCF procedure. The coefficients in equations (6-3), (6-5), and (6-8) or (6-10) are determined as those in the MS-Xα method, that is, by matching the wave functions and the derivatives of the wave functions at all sphere boundaries.

The wave functions in the SIC-MS-Xα method are, then, used to calculate the matrix elements in equation (6-34) for each pair of orbitals and search the transformation coefficients $M_{\mu i}$ in equation (6-23), to give the minimum of the total SIC energy. Obviously, because the spherically averaged potentials in the atomic and extramolecular regions and the volume-averaged potential in the interatomic region were employed in the MS-Xα method, equation (6-30) is already satisfied for the pairs of orbitals which span two different symmetry representations. This implies that there is no mixture between any two different symmetry representations during the minimization of the total SIC energy in the SIC-MS-Xα method.

Once the transformation coefficients are found, the second SCF procedure is applied to yield self-consistent wave functions and one-electron eigenvalues using the SIC potentials which are generated by means of wave functions $\left\{\phi\right\}$. When the differences of the total potentials between the $(i+1)^{th}$ and the i^{th} iterations for all orbitals are less than 10^{-5}, the calculation is self-consistent.

VII-2. Molecules in the SIC-MS-Xα Method

To test the reliability of the self-interaction corrected multiple-scattering Xα method, it will first be applied to three small molecules, ethylene, formaldehyde, and ozone, two planar conjugated organic molecules, benzene and pyrazine, and two tetrahedral molecules, carbon tetrafluoride and carbon tetrachloride. The ionization potentials and statistical energies are calculated. The results of the SIC-MS-Xα calculation will be compared with those from the MS-Xα and transition state MS-Xα methods, and other theoretical calculations, like HF, CNDO/2 and etc.

The experimental equilibrium geometries for ethylene (C_2H_4), formaldehyde (H_2CO), ozone (O_3), carbon tetrafluoride (CF_4), and carbon tetrachloride (CCl_4) were from Ref. 196 and for molecules benzene (C_6H_6) and pyrazine ($C_4H_4N_2$) from Ref. 178. The exchange parameter values of α's were from Ref. 10, except for hydrogen, where the polarized value[197] is preferred for the individual atomic spheres. For the extramolecular and interatomic regions, the averaged values of α's were obtained by weighting the α for each atom by its number of valence electrons.

The radii of the atomic spheres and the outer sphere are from the Norman criterion[198] scaling by a factor of 0.8 for the molecules C_2H_4, H_2CO, O_3, CF_4, and CCl_4; the overlapping percentages of the atomic spheres for these molecules are between 10 and 35. The radii of the atomic and outer spheres for C_6H_6 and $C_4H_4N_2$ are from Ref. 178, that is, $b_H = 0.95\ a_0$, $b_C = b_N = 1.60\ a_0$ for both C_6H_6 and $C_4H_4N_2$ (a_0 is the Bohr radius), and $b_0 = 5.63\ a_0$ for C_6H_6 and $b_0 = 5.58\ a_0$ for $C_4H_4N_2$, in order to compare the present results with the previous ionization potentials for benzene and pyrazine in the transition state MS-Xα calculations.

Partial waves up to $l = 3$ for the outer sphere, $l = 1$ for the carbon and nitrogen atoms and $l = 0$ for the hydrogen atom were used in the C_6H_6 and $C_4H_4N_2$ calculation, and $l = 4$ for the outer sphere, $l = 2$ for the carbon, oxygen, fluoride,

and chloride atoms, l = 1 for hydrogen in the other molecular calculations. The ground states and the transition states were carried out self-consistently using the updated version of the MS-Xα program modified by Cook and Case[195].

Tables VII-1 to VII-7 show the negative of one-electron eigenvalues for ethylene, formaldehyde, ozone, carbon tetrafluoride, carbon tetrachloride, benzene, and pyrazine in the MS-Xα, the transition state MS-Xα, the SIC-MS-Xα, and the total SIC energy minimized SIC-MS-Xα methods (henceforth, called the MS-Xα, TS-MS-Xα, SIC-MS-Xα, and M-SIC-MS-Xα, respectively). The geometries of the molecules, parameters, radii of outer and atomic spheres are the same for the same molecule in all methods. The present one-electron eigenvalues are compared to those from the *ab-initio* HF, the LCAO-Xα, the Green function (GF), and other theoretical calculations, and with the experimental ionization potentials. Table VII-8 summarizes the statistical total energies from various methods.

VII-2.1 One-Electron Eigenvalue

In the Xα method, the one-electron eigenvalue is equal to the derivative of the statistical total energy with respect to the occupation number[199], that is,

$$\epsilon_k = \left(\frac{\partial E}{\partial N_k}\right)_Z \qquad (7-5)$$

The ionization potential in the Xα method under the frozen orbital approximation is equal to

$$\begin{aligned} I_k &= E(N_k - 1) - E(N_k) \\ &\approx -\epsilon_k + \frac{1}{2} < kk||kk > -\left(\frac{3}{8\pi}\right)^{1/3} \alpha \int \rho_k^2(\mathbf{r}) \Big[\rho(\mathbf{r})\Big]^{-2/3} d\mathbf{r} \end{aligned} \qquad (7-6)$$

where $< kk||kk >$ is the self-Coulomb interaction energy and the last term of equation (7-6) is the second derivative of the statistical exchange total energy with

respect to the occupation number of orbital k; the statistical total energy is considered correct in the Xα method. However, the ionization potential in the HF method is equal to the negative of one-electron eigenvalue of the corresponding orbital, i.e.

$$I_k = -\epsilon_k^{HF} \qquad (7-7)$$

under the frozen orbital approximation (Koopmans' theorem)[54,199]. When the SIC is introduced into the Xα method, equation (7-6) becomes

$$I_k = -\epsilon_k + \left(\frac{3}{8\pi}\right)^{1/3} \alpha \int \rho_k^2(\mathbf{r}) \left\{ \left[\rho_k(\mathbf{r})\right]^{-2/3} - \left[\rho(\mathbf{r})\right]^{-2/3} \right\} d\mathbf{r} \qquad (7-8)$$

The introduction of the SIC greatly reduces the deviation of ϵ_k from the ionization potential. The results listed in Tables VII-1 to VII-7 support this analysis.

TABLE VII-1

The negative of the one-electron eigenvalues of ethylene (C_2H_4) in the MS-Xα, TS-MS-Xα, SIC-MS-Xα, and M-SIC-MS-Xα methods, compared with other calculation and experimental ionization potentials (eV)

Orbital	Xα	TS-Xα	SIC-Xα	M-SIC-Xα	TS-Xα[a]	Expt[b]
$1b_{1u}$	6.34	9.89	9.90	10.06	12.12	10.51
$1b_{1g}$	9.48	13.28	12.15	12.23	11.72	12.38
$2a_g$	10.62	14.53	14.61	14.46	14.72	14.47
$1b_{3u}$	12.04	15.80	15.28	15.39	15.48	15.68
$1b_{2u}$	14.83	18.65	18.12	18.24	18.12	18.87
$1a_g$	19.08	22.96	23.10	24.10	23.95	≈ 23

a. Reference 173;
b. Reference 200.

C_2H_4: Table VII-1 and Fig. 7-1 show the negative of the one-electron eigenvalues for ethylene in the MS-Xα, TS-MS-Xα, SIC-MS-Xα, and M-SIC-MS-Xα methods

FIGURE 7-1

The one-electron eigenvalues (eV) for the valence orbitals of ethylene (C_2H_4), compared with the experimental ionization potentials

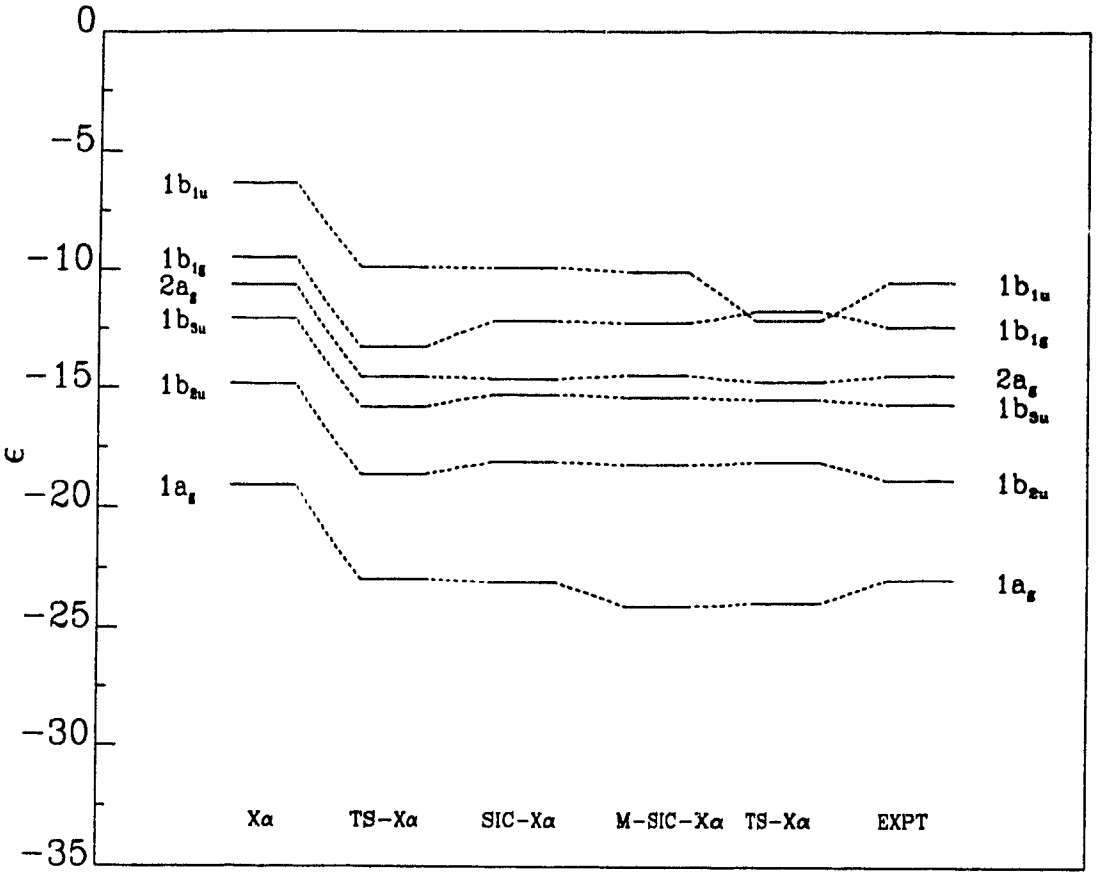

(columns II to V) compared to other theoretical calculations and exp riment. Rosch et al.[173] studied ethylene using the transition state MS-Xα calculation to test the overlapping sphere technique. The exchange parameters and the radii of the atomic and outer spheres in their work differs from those used in the present work. The experimental ionization potentials are from Ref. 200. The negative of one-electron eigenvalues in the MS-Xα method, as expected, are much smaller than the experimental ionization potentials. But the negative of one-electron eigenvalues in the SIC-MS-Xα method are excellent in the agreement with experiment, even better than those from the transition state calculation in which, as in the present work, the results are taken from the negative of one-electron eigenvalues obtained by removing half-electron from the highest occupied orbital, $1b_{1u}$. The present transition state calculation is much better than the early work[173], because of the choice of the atomic and outer sphere radii and the overlapping percentage between the atomic spheres; the volume and electron charge in the interatomic region are dependent on the percentage of the overlapping between the atomic spheres, therefore the one-electron eigenvalues and statistical total energies are sensitive to the potential in the interatomic region in the MS-Xα method. The one-electron eigenvalues in the M-SIC-MS-Xα method are higher than those in both the TS-MS-Xα and SIC-MS-Xα methods in absolute value, because minimizing the total SIC energy lowers the statistical total energy and makes the molecule more stable. The potential of the atomic spheres in the M-SIC-MS-Xα is lower than in the SIC-MS-Xα method, and consequently the binding energies of the electrons are higher than in SIC-MS-Xα, and therefore the ethylene ionization potentials from the negative of the one-electron eigenvalues in the M-SIC-MS-Xα are slightly better than those in the SIC-MS-Xα method for orbitals $1b_{1u}$, $1b_{1g}$, $2a_g$, $1b_{3u}$, and $1b_{2u}$. But, for orbital $1a_g$, the value is too high compared to experiment.

TABLE VII-2

The negative of the one-electron eigenvalues of formaldehyde (H_2CO) in the MS-Xα, TS-MS-Xα, SIC-MS-Xα, and M-SIC-MS-Xα methods, compared with other calculation and experimental ionization potentials (eV)

Orbital	Xα	TS-Xα	SIC-Xα	M-SIC-Xα	TS-Xα[a]	LCAO-Xα[a]	HF[b]	GF[c]	Expt[d]
$2b_2$	6.97	11.43	10.81	13.17	12.03	11.26	12.03	10.84	10.88
$1b_1$	9.88	14.41	15.09	13.85	15.55	15.41	14.60	14.29	14.38
$3a_1$	12.64	17.27	17.08	16.52	17.93	16.31	17.77	16.36	16.00
$1b_2$	12.21	16.61	15.88	16.58	17.55	17.72	18.82	17.13	16.78
$2a_1$	15.85	20.34	19.60	20.10			23.59		21.8
$1a_1$	27.40	32.28	33.51	31.22			38.28		

a. Reference 181;
b. Reference 201;
c. Reference 202;
d. Reference 204.

H_2CO: Formaldehyde has been widely investigated by the tangent sphere and overlapping sphere MS-Xα[181], the LCAO-Xα[181], the HF[201], the Green-function (GF)[202], and the ordinary third-order Rayleigh-Schrödinger perturbation[203] methods and experimently[204]. The present results are listed in Table VII-2 and compared to these calculations and experiments. The one-electron eigenvalues of the highest four occupied orbitals are plotted in Fig. 7-2. The results strongly support the ordering already obtained by the HF method[201]. The ordering of orbitals $3a_1$ and $1b_2$ was reversed in the MS-Xα, TS-MS-Xα, SIC-MS-Xα methods, although quantitatively, the one-electron eigenvalues in the TS-MS-Xα and SIC-MS-Xα methods are much better than those in the HF method, even better than the transition state LCAO-Xα calculation. The SIC-MS-Xα method is comparable to the TS-MS-Xα method. Furthermore, the ionization potentials from the negative of one-electron eigenvalues in both SIC-MS-Xα method and TS-MS-Xα method in which half-electron was removed from the highest orbital $2b_2$ to infinity are much better than

FIGURE 7-2

The one-electron eigenvalues (eV) for the valence orbitals of formaldehyde (H_2CO), compared with the experimental ionization potentials

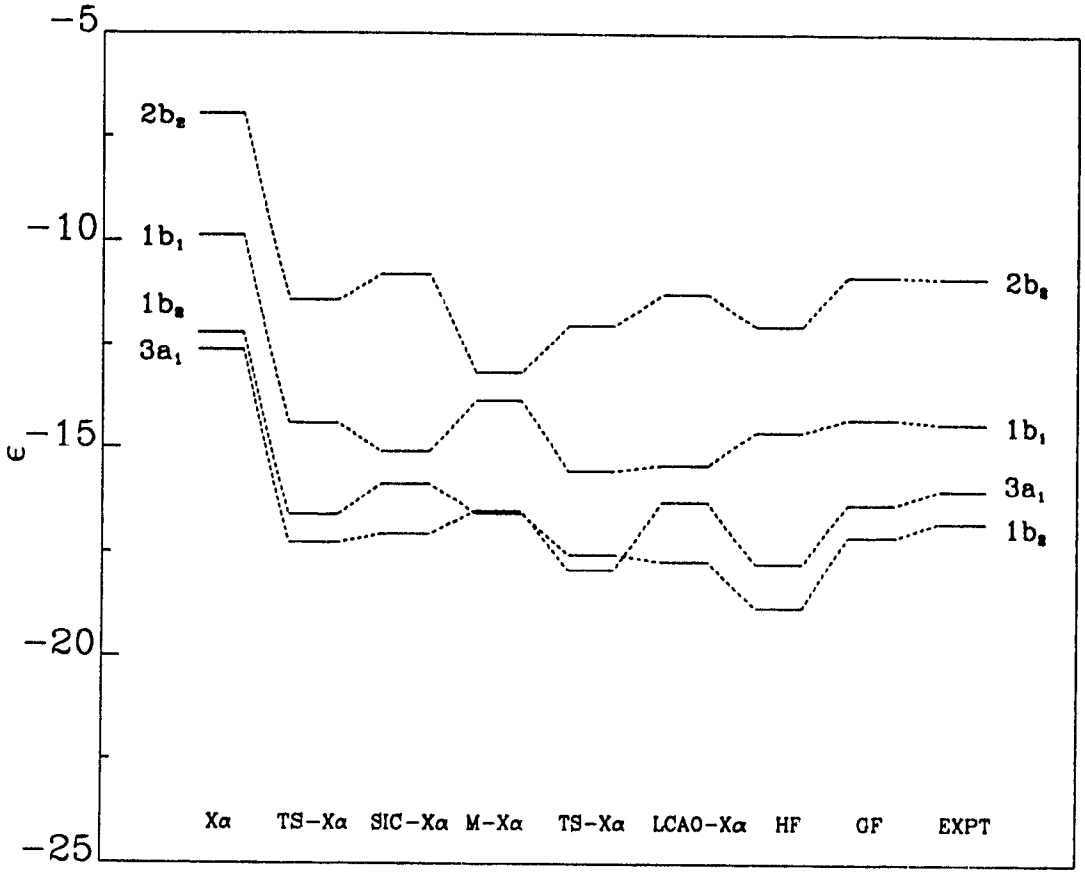

those in the early transition state MS-Xα calculation[181], the present number of partial waves and the radii of the atomic and outer spheres differ from those used previous work[181], in which the partial waves up to l = 2 for the outer sphere, l = 0 for the hydrogen atom and l = 1 for the carbon were employed. However, the partial waves up to l = 4 for the outer sphere, l = 1 for the hydrogen atom and l = 2 for the carbon were used in the present work and include the polarization function. It is interesting that the ordering of orbitals $3a_1$ and $1b_2$ is correct in the M-SIC-MS-Xα method and the M-SIC-MS-Xα results are better than the TS-MS-Xα and SIC-MS-Xα, except for orbital $2b_2$.

TABLE VII-3

The negative of the one-electron eigenvalues of ozone (O_3) in the MS-Xα, TS-MS-Xα, SIC-MS-Xα, and M-SIC-MS-Xα methods, compared with other calculation and experimental ionization potentials (eV)

Orbital	Xα	TS-Xα	SIC-Xα	M-SIC-Xα	TS-Xα[a]	LCAO-Xα[a]	HF[b]	PT[c]	Expt[d]
4 a_1	9.50	14.14	13.62	13.42	13.20	11.92	15.83	12.94	12.75
3 b_2	9.22	13.84	13.29	12.44	13.17	12.20	16.31	13.27	13.03
1 a_2	9.87	14.49	13.91	13.05	13.62	12.60	14.02	14.07	13.57
2 b_2	16.03	20.75	20.30	20.87	20.74	18.22	21.93	19.44	19.99
1 b_1	14.70	19.38	19.81	18.30	19.44	18.88	22.15		
3 a_1	15.17	19.87	20.04	18.83	19.94	18.36	23.26		
2 a_1	21.09	25.79	25.14	24.90	25.30	22.98			24.7
1 b_2	27.41	32.19	31.52	30.94	32.42	31.86			
1 a_1	33.68	38.51	38.68	37.31	39.38	39.00			

a. Reference 181;
b. Reference 205;
c. Reference 206;
d. Reference 207.

O_3: Ozone is a widely investigated molecule by means of the MS-Xα[181], the LCAO-

FIGURE 7-3

The one-electron eigenvalues (eV) for the valence orbitals of ozone (O_3), compared with the experimental ionization potentials

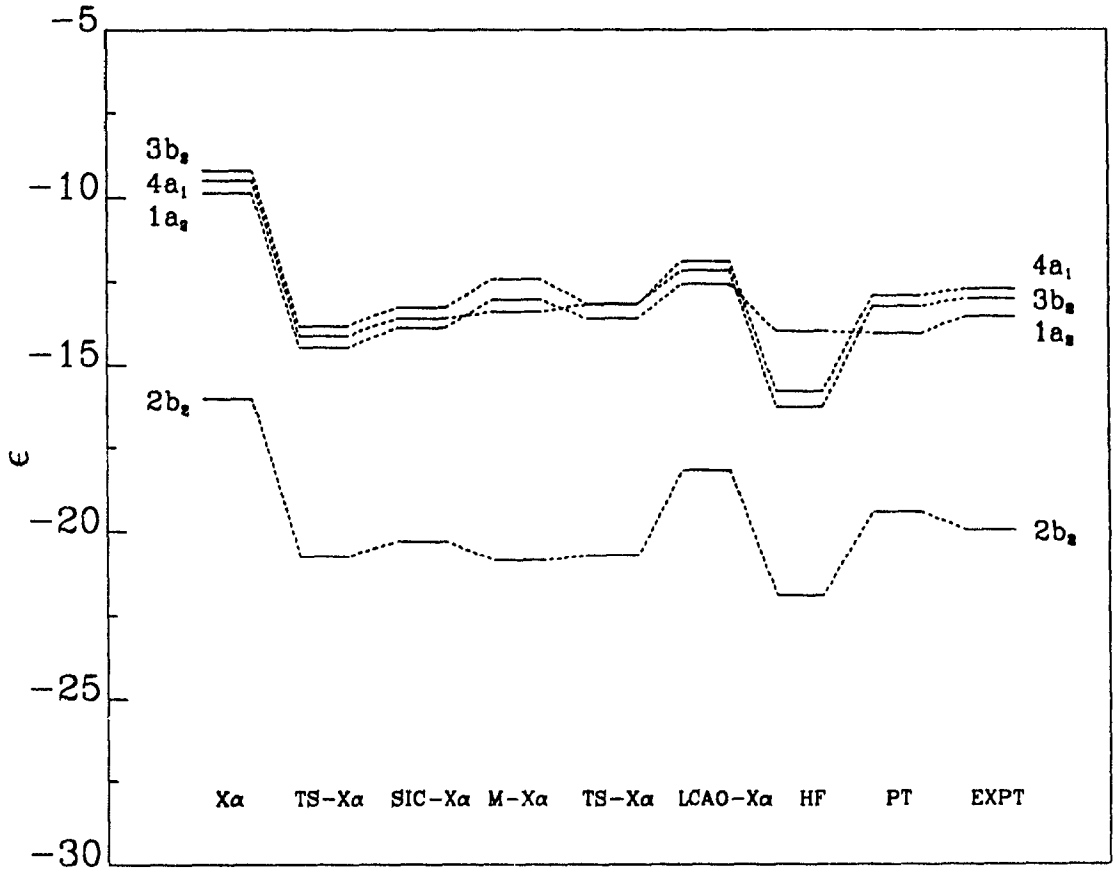

Xα[181], the HF[205], and the Rayleigh-Schrödinger perturbation (PT)[206] methods and experimently[207]. The present TS-MS-Xα calculation, which was carried out by removing half-electron from the highest orbital $4a_1$ to infinity, the SIC-MS-Xα, and M-SIC-MS-Xα calculations for ozone are presented in Table VII-3. The one-electron eigenvalues of the highest four occupied orbitals are compared, in Fig. 7-3, with those from the LCAO-Xα, the HF, the PT methods and from experiments. The present TS-MS-Xα calculation is slightly worse than the early calculation[181], in which the results were obtained orbital by orbital, that is, the ionization potential for each orbital was obtained by removing a half electron from the corresponding orbital, which is the preferred method[181], although occasionally it is possible to obtain identical results by removing a half electron from the highest symmetry occupied orbital. The ionization potentials taken from the negative of one-electron eigenvalues in the SIC-MS-Xα method are better than the present TS-MS-Xα calculation and comparable with the early work[181]. The results in the M-SIC-MS-Xα methods are no better than those in the SIC-MS-Xα method. Unfortunately, the ordering of orbitals $4a_1$ and $3b_2$, and $2b_2$, $1b_1$, and $3a_1$ are reversed by the TS-MS-Xα method, and in the SIC-MS-Xα method. The reversed ordering also happened in the HF method for orbitals $4a_1$, $3b_2$, and $1a_2$ and in the transition state LCAO-Xα method for $1b_1$ and $3a_1$. Hence the reversed order in the SIC-MS-Xα method is not caused by the 'muffin-tin' approximation.

C_6H_6: Benzene has been studied by the transition state MS-Xα[173,178], and the HF[208] methods, and experimentally[209–211]. The assignment of the experimental ionization potentials follows the many body calculation[212]. The present results are shown in Table VII-4 and Fig. 7-4 and compared with the others. The ionization potentials taken from the negative of one-electron eigenvalues in the SIC-MS-Xα method are better than the TS-MS-Xα calculation in which half-electron is removed

TABLE VII-4

The negative of the one-electron eigenvalues of benzene (C_6H_6) in the MS-Xα, TS-MS-Xα, SIC-MS-Xα, and M-SIC-MS-Xα methods, compared with other calculation and experimental ionization potentials (eV)

Orbital	Xα	TS-Xα	SIC-Xα	M-SIC-Xα	TS-Xα[a]	TS-Xα[b]	HF[c]	Expt[d]
$1e_{1g}$	7.51	10.35	10.03	10.25	10.08	10.45	10.15	9.3
$2e_{2g}$	10.17	13.03	12.18	12.21	11.48	13.21	14.26	11.48
$1a_{2u}$	10.25	13.08	12.77	12.98	12.85	13.16	14.56	12.29
$2e_{1u}$	11.97	14.82	14.00	14.07	13.56	14.97	16.92	13.94
$1b_{2u}$	13.82	16.82	16.53	16.82	13.53	17.18	18.01	14.80
$1b_{1u}$	12.59	15.40	14.24	14.39	16.09	15.52	17.80	15.46
$2a_{1g}$	14.31	17.13	16.37	16.50	16.07	17.25	20.08	16.86
$1e_{2g}$	17.10	20.03	19.64	20.27	18.90	20.27		19.0
$1e_{1u}$	20.67	23.62	23.19	23.66	22.82	23.87		22.7
$1a_{1g}$	23.34	26.30	25.88	26.22	26 12	26.56		25.9

a. Reference 173;
b. Reference 178;
c. Reference 208;
d. References 178,204.

from orbital $1b_{1u}$, except for the $1b_{1u}$, and are much better than the HF method. The ionization potentials in the M-SIC-MS-Xα method are higher than those in the SIC-MS-Xα method, but no better than those in the SIC-MS-Xα method. The early transition state MS-Xα calculations for benzene given by Rosch et al.[173] are mostly better than the present calculations, because they did the SCF procedure orbital by orbital. The present ionization potentials in the TS-MS-Xα method are slightly better than Case et al.[178] work, in which the spin-polarized MS-Xα method was used. Obviously, when the transition state concept is involved, the electron-configuration is no longer full occupied. The exchange effects for the spin-up and spin-down electrons are different. Hence the spin-polarized MS-Xα method is better in carrying out the transition state calculation.

FIGURE 7-4

The one-electron eigenvalues (eV) for the valence orbitals of benzene (C_6H_6), compared with the experimental ionization potentials

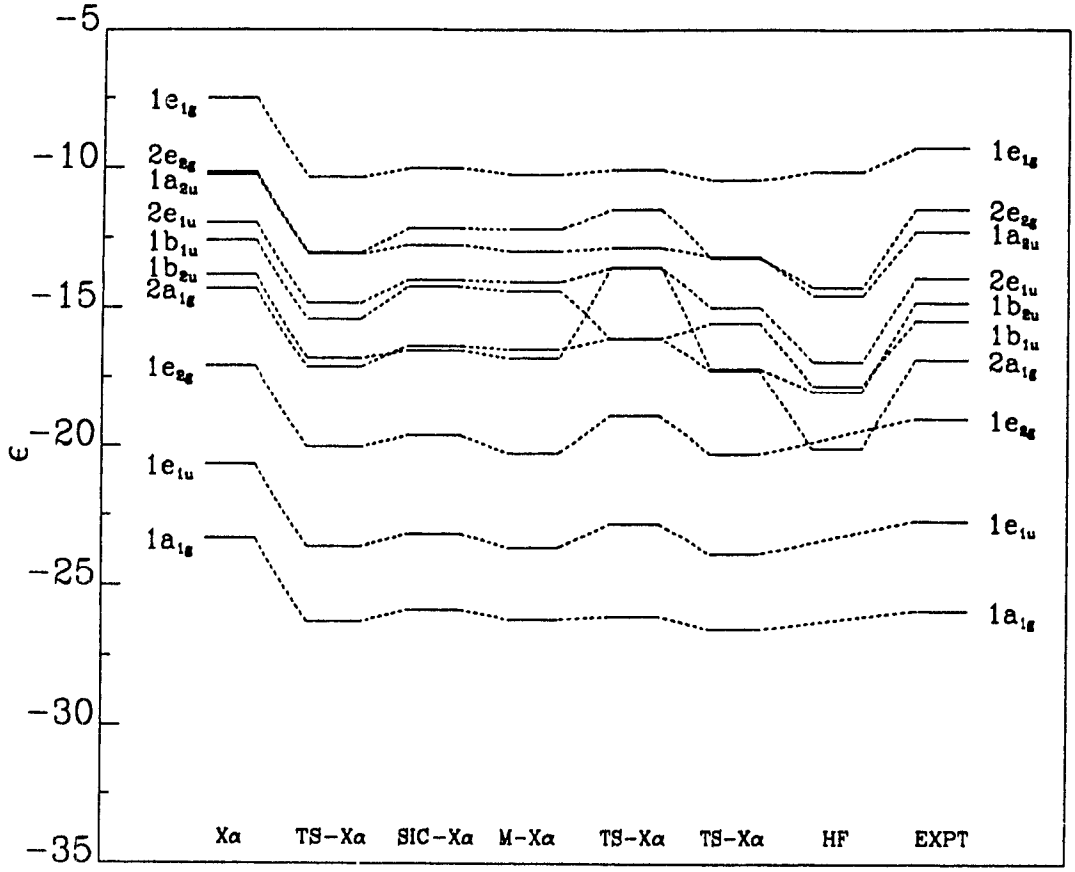

TABLE VII-5

The negative of the one-electron eigenvalues of pyrazine ($C_4H_4N_2$) in the MS-Xα, TS-MS-Xα, SIC-MS-Xα, and M-SIC-MS-Xα methods, compared with other calculation and experimental ionization potentials (eV)

Orbital	Xα	TS-Xα	SIC-Xα	M-SIC-Xα	TS-Xα[a]	Expt[b]
$4a_g$	8.04	11.17	10.95	9.96	11.28	9.4
$1b_{1g}$	7.86	10.85	10.24	8.90	10.94	10.2
$3b_{1u}$	9.52	12.68	12.52	11.27	12.90	11.4
$1b_{2g}$	9.15	12.24	12.00	10.49	12.33	11.7
$2b_{3g}$	11.22	14.23	13.23	12.26	14.34	13.3
$1b_{3u}$	11.36	14.39	14.19	12.75	14.39	14.0
$3b_{2u}$	12.44	15.42	14.35	12.89	15.59	15.0
$2b_{1u}$	13.21	16.16	15.01	13.67	16.56	16.2
$3a_g$	14.31	17.31	16.71	15.70	17.66	17.0
$2b_{2u}$	15.66	18.89	18.73	18.68	19.16	17.1
$2a_g$	18.62	21.77	21.46	20.86	21.97	20.6
$1b_{3g}$	18.65	21.83	21.56	20.47	22.00	21.0
$1b_{2u}$	21.58	24.71	24.27	23.42	24.93	24.0
$1b_{1u}$	24.45	27.70	27.46	26.10	27.80	
$1a_g$	26.28	29.49	29.23	29.52	29.63	

a. Reference 178;
b. Reference 213.

$C_4H_4N_2$: The photoelectron spectrum of this molecule has been analyzed by Almlof et al.[213] A theoretical study has been done by Case et al.[178] in the spin-restricted MS-Xα calculation. In order to test the efficiency of the present SIC-MS-Xα method, the calculation was duplicated using the same exchange parameters, α's, and the radii of the atomic and outer spheres in the spin-polarized TS-MS-Xα method, the SIC-MS-Xα and M-SIC-MS-Xα methods. From Table VII-5 and Fig. 7-5, it can be seen that the spin-polarized transition state calculation (column 3) are only slightly better than the spin-restricted transition state calculation[178] (column 6). The ionization potentials taken from the negative of one-electron eigenvalues in the SIC-MS-Xα method are slightly better than the results of both spin-restricted and spin-polarized transition state calculations and are in very good agreement

FIGURE 7-5

The one-electron eigenvalues (eV) for the valence orbitals of pyrazine ($C_4H_4N_2$), compared with the experimental ionization potentials

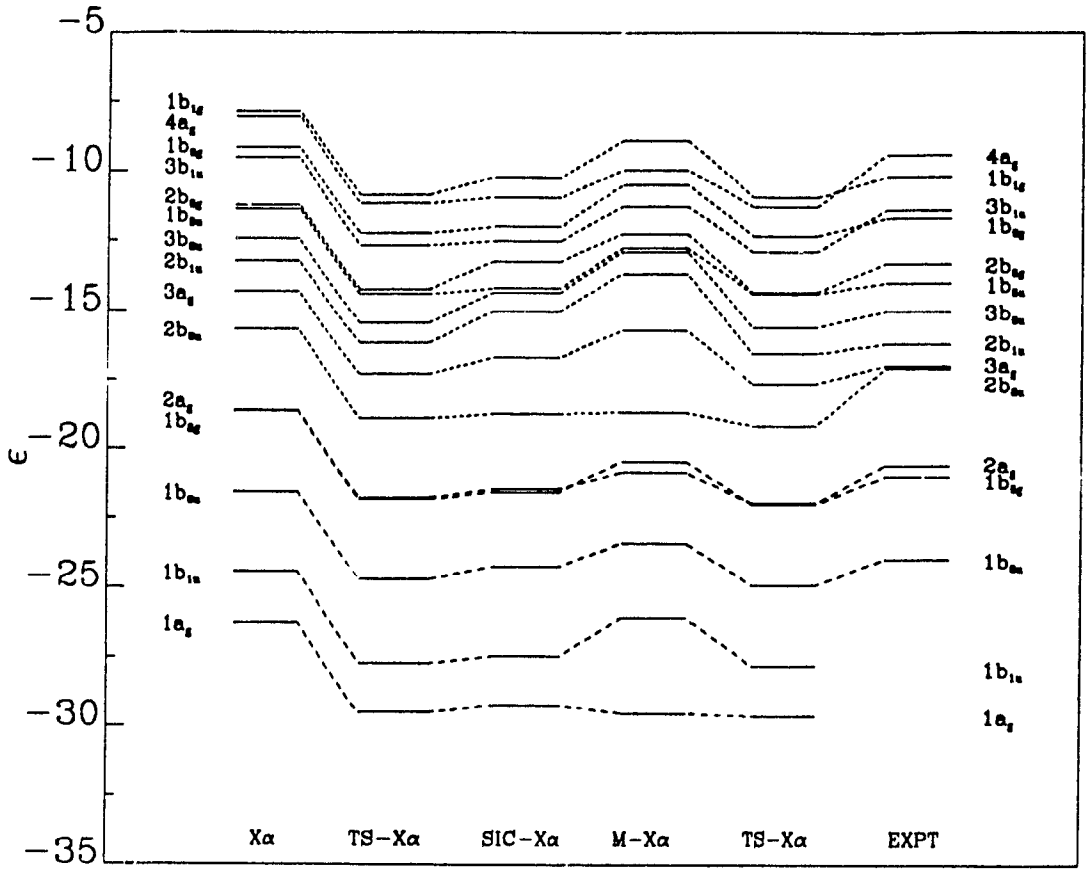

with the experimental results. The M-SIC-MS-Xα ionization potentials are no better than the SIC-MS-Xα results.

TABLE VII-6

The negative of the one-electron eigenvalues of tetrafluoride (CF_4) in the MS-Xα, TS-MS-Xα, SIC-MS-Xα, and M-SIC-MS-Xα methods, compared with other calculations and experimental ionization potentials (eV)

Orbital	Xα	TS-Xα	SIC-Xα	M-SIC-Xα	HF[a]	CNDO/2[a]	Expt[b]
1 t_1	12.27	16.45	15.66	15.66	19.40	22.24	16.20
3 t_2	13.14	17.29	16.67	16.63	19.65	20.20	17.40
1 e	13.81	17.94	17.31	17.29	21.34	23.30	18.50
2 t_2	17.16	21.36	21.14	21.23	24.89	28.18	22.12
2 a_1	19.99	24.22	23.83	24.30	28.15	29.48	25.12
1 t_2	32.54	36.75	35.88	35.84	46.65	48.22	
1 a_1	34.89	39.11	38.51	38.80	50.50	54.63	

a. Reference 214;
b. Reference 215.

CF_4: Carbon tetrafluoride has Td symmetry and is ideal for the MS-Xα calculation. This molecule was calculated by *ab-initio* HF method[214] and CNDO/2 empirical method[214] and measured experimently[215]. The present transition state calculation listed in Table VII-6 was performed by removing half-electron from the highest orbital $1t_1$. Fig. 7-6 plots the one-electron eigenvalues in the MS-Xα method and compares with those from the HF, the CNDO/2 methods and experiments. The ionization potentials in the transition state calculation are in excellent agreement with experiment and slightly better than those in the SIC-MS-Xα method in which the results are slightly smaller than those in the transition state procedure. Furthermore, the present results in both TS-MS-Xα and SIC-MS-Xα methods are much

FIGURE 7-6

The one-electron eigenvalues (eV) for the valence orbitals of tetrafluoride (CF_4), compared with the experimental ionization potentials

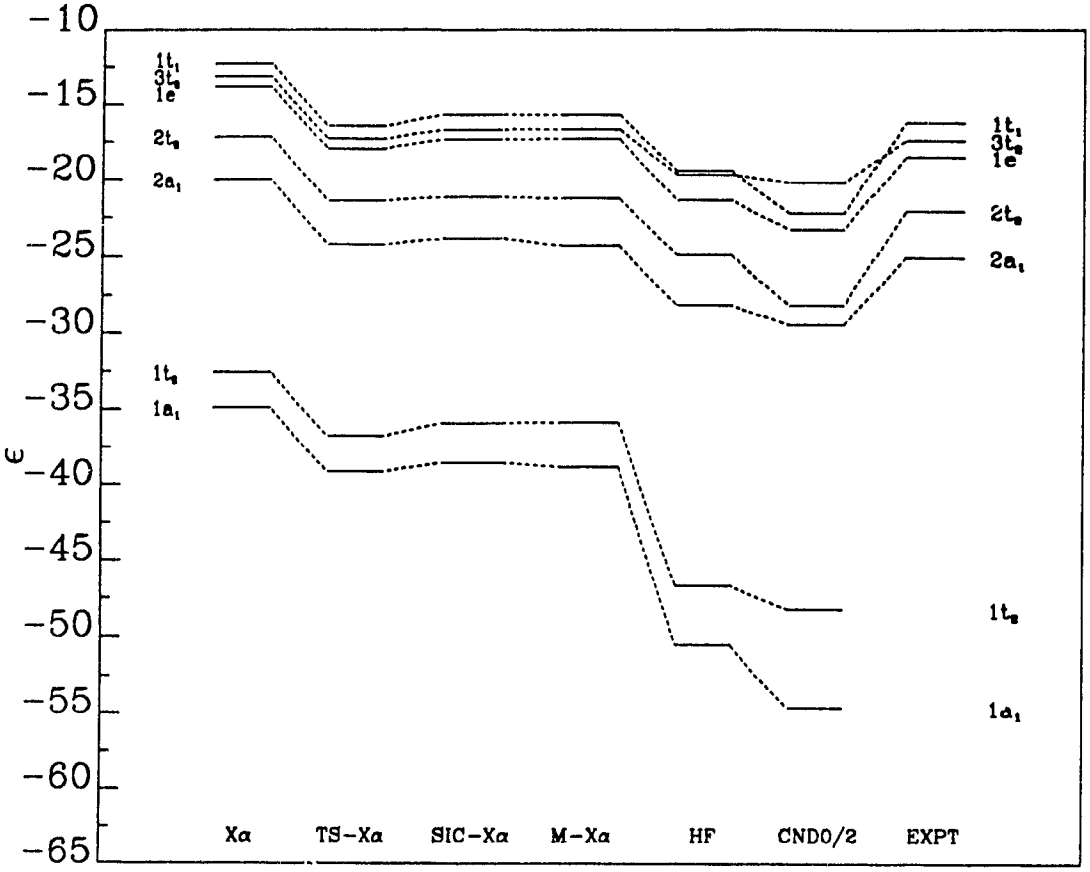

better than the values in the HF and CNDO/2 methods. The one-electron eigenvalues in the SIC-MS-Xα method are slightly changed by the minimization of the total SIC energy with respect to the orbital transformation.

TABLE VII-7

The negative of the one-electron eigenvalues of tetrachloride (CCl_4) in the MS-Xα, TS-MS-Xα, SIC-MS-Xα, and M-SIC-MS-Xα methods, compared with other calculation and experimental ionization potentials (eV)

Orbital	Xα	TS-Xα	SIC-Xα	M-SIC-Xα	CNDO/2[a]	Expt[b]
1 t_1	9.03	11.97	11.46	9.97	13.68	11.60
3 t_2	9.74	12.66	12.34	10.86	15.21	12.40
						12.60
						12.75
1 e	10.34	13.25	12.85	11.36	16.60	13.40
2 t_2	13.23	16.22	16.27	15.14	21.49	16.60
2 a_1	17.07	20.08	19.99	20.32		
1 t_2	22.31	25.32	24.87	23.41		
1 a_1	25.10	28.12	28.02	27.41		

a. Reference 216;
b. Reference 217.

CCl_4: Carbon tetrachloride has Td symmetry. Table VII-7 and Fig. 7-7 shows the present results and compares to the empirical CNDO/2 calculation[216] and the experimental ionization potentials[217]. The ionization potentials in the SIC-MS-Xα method are better than those in the TS-MS-Xα calculation, in which the results were obtained by removing half-electron from the highest occupied orbital $1t_1$, except for orbital 1e. Both the TS-MS-Xα and SIC-MS-Xα methods are much better than the CNDO/2 method in predicting the ionization potentials. Furthermore, M-SIC-MS-Xα method is no better than the SIC-MS-Xα method.

FIGURE 7-7

The one-electron eigenvalues (eV) for the valence orbitals of tetrachloride (CCl_4), compared with the experimental ionization potentials

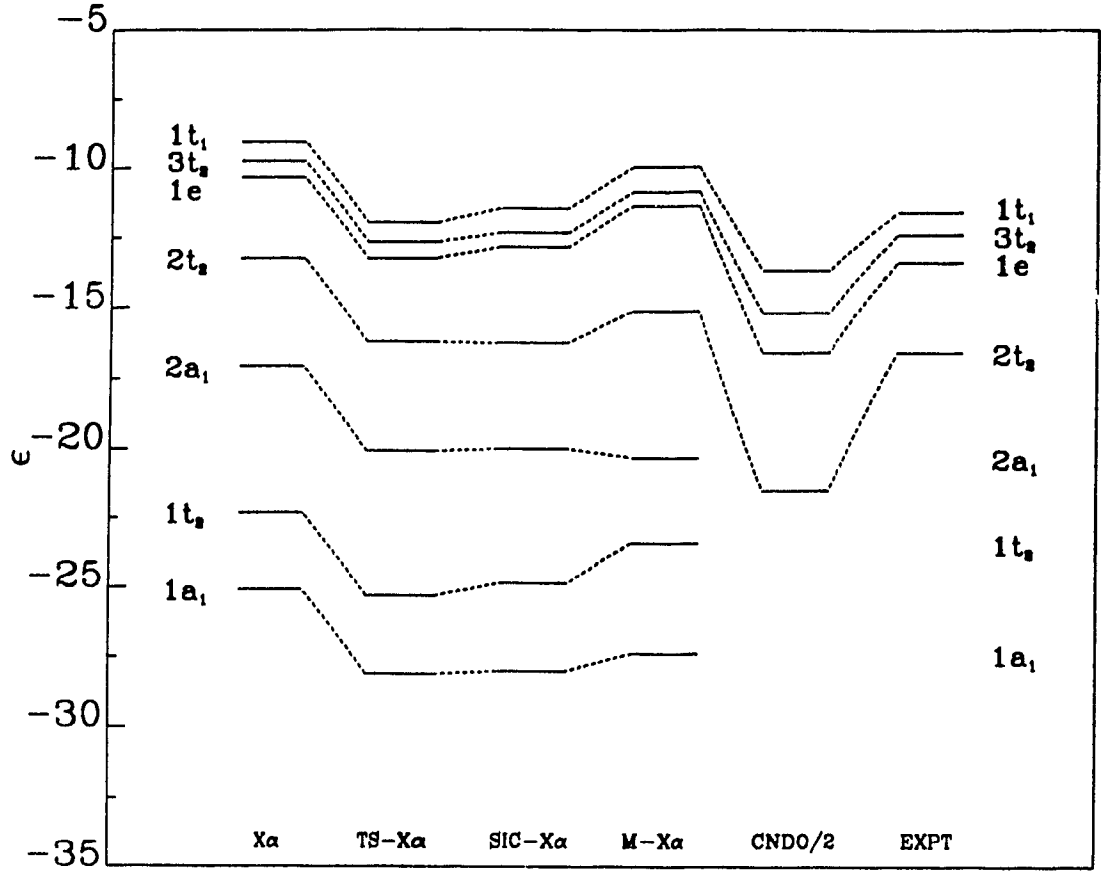

The ionization potential is not exactly equal to the negative of one-electron eigenvalue in the HF method, because the relaxation in the ionization process is important, it is much more important in a molecule than in an atom, for which ionization potentials taken from the negative of one-electron eigenvalue is in very good agreement with experiment. The ionization potential is also not equal to the negative of one-electron eigenvalue in the Xα method even using the frozen orbital approximation. It is clear from equation (7-8) that the ionization potentials should be bigger than the negative of one-electron eigenvalue, because the value of the integral in equation (7-8) is always positive, except for a system with only two paired electrons. The relaxation effect is to decrease the ionization potential, but the second term in equation (7-8) is to increase the ionization potential. They partly cancel. This is why the ionization potentials obtained from the negative of one-electron eigenvalues in the SIC-MS-Xα method to be much better than the HF method by using the Koopmans' theorem.

TABLE VII-8

The statistical total energies for several molecules (eV) in the MS-Xα, SIC-MS-Xα, and minimized SIC-MS-Xα methods

Molecule	MS-Xα	SIC-MS-Xα	M-SIC-MS-Xα
C_2H_4	−156.7532	−153.0174	−153.1182
H_2CO	−228.2903	−228.3149	−228.4970
O_3	−448.8199	−443.5352	−443.8501
C_6H_6	−459.4779	−445.2743	−445.4223
$C_4H_4N_2$	−524.2504	−509.8879	−510.5779
CF_4	−871.3409	−854.6787	−854.8670
CCl_4	−3750.786	−3703.434	−3703.806

VII-2.2 Statistical Total Energy

The statistical total energies are unreliable in the MS-Xα method. It is sensitive to the amount of overlap between atomic spheres, because of the 'muffin-tin' approximation. To compare the SIC energy contribution, Table VII-8 summarizes the statistical total energies for the several molecules in the MS-Xα, the SIC-MS-Xα, and the M-SIC-MS-Xα methods. In Table VII-8, the total SIC energy contributions to the statistical total energies are negative for H_2CO and positive for all other molecules, unlike atomic calculations in which the total SIC energy contributions to the statistical total energies are always positive[30].

Comparing the statistical total energies in the M-SIC-MS-Xα in column 4 with those in column 3 in the SIC-MS-Xα method shows that the minimization process lowers the statistical total energies for all molecules, but the differences between the unminimized and the minimized SIC-MS-Xα statistical total energies are very small. As mentioned before, there is no mixture of the orbitals which span two symmetric irreducible representations, because the spherically averaged

and volume-averaged potentials for the atomic, extramolecular, and interatomic regions in the MS-Xα method were used. The minimization is not necessary in the SIC-MS-Xα calculation.

In conclusion of this section, it can be seen that the SIC-MS-Xα method presents a significant improvement over the conventional MS-Xα for the following reasons:

(i) Theoretically, the SIC-MS-Xα method includes the SIC, which corrects the unphysical self-interaction from the Coulomb-integral and the exchange-integral. The self-interaction corrected theory should be accurate and closer to the real system than the uncorrected theory.

(ii) Numerically, the SIC-MS-Xα method gives very good ionization potentials in agreement with experiment and comparable with the transition state calculation in the MS-Xα method which arbitrarily removes the self-interaction by the $\frac{1}{2}$e trick. From the examples mentioned above, it is clear that if the ordering of orbitals is reversed in the TS-MS-Xα calculation, it also is reversed in the SIC-MS-Xα method, so that the reversion of the ordering of orbitals is not caused by SIC. A single SCF procedure can give both the ionization potentials and wave functions which can be used to calculate other properties for the system. Computational time is slightly increased by introducing the SIC, but much less than twice the computational time for two SCF procedures, one for the the ionization potentials in the transition state calculation, and the other for the wave function in the ground state or excited state calculation required by conventional MS-Xα calculations. The present method is therefore attractive, especially for a very large molecules usually chosen for calculation by the MS-Xα method. The wave functions from the SIC-MS-Xα method will be better than those from the MS-Xα method for calculating other properties of the molecule.

The minimization of the total SIC energy is time-consuming, because one has to search the transformation coefficients by calculating the matrix elements in equation (6-34) and unnecessary, at least, by using Edmiston and Ruedenberg's method.

The SIC-MS-Xα method can be used for the very large molecule and cluster calculations with acceptable accuracy and reasonable computation time.

VII-3. Stability of the Molecular Anions ClO_4^-, HCO^-, and O_3^-

Molecular anions are experimentally[218–222] and theoretically[135,137,223–229] interesting, because of the importance of their electronic structure and molecular electron affinity in physics and chemistry. Theoretical calculation of molecular anions tests the reliability of the theory.

The calculation of molecular anion electronic structure and molecular electron affinity is very difficult[223,224], because both are strongly dependent on the nature of the basis set employed in the *ab-initio* Hartree-Fock method. The choice of the basis set becomes the prime focus of the work. The major energy contribution to the electron affinity is electron correlation, and in molecules with very small electron affinities, the choice of electron configuration in the configuration-interaction Hartree-Fock (CI) calculation is difficult.

Most calculations on molecular anions[135,137,223–229] were *ab-initio* Hartree-Fock or CI calculations. A few were performed using the local-density functional (LDF) method, like, the LCAO-Xα method[181–183], the discrete variational Xα (DV-Xα) method[184–186], or the multiple-scattering Xα (MS-Xα) method[160,161], despite their usefulness in describing the electron structure of large molecules and

containing heavy atoms. The lack of calculations for the molecular anions using the LDF method might be due to the non-convergence problem in solving the one-electron Schrödinger equation numerically. The cause of the non-convergency is obvious if the details of the MS-Xα method[160-161] are considered.

As mentioned before, the MS-Xα method is based on the division of molecular space into non-overlapping atomic, interatomic, and extramolecular regions, with spherically averaged potentials for the atomic and extramolecular regions and a volume-averaged potential for the interatomic region, and the conventional Xα approximation to the exchange-correlation. The one-electron Schrödinger equation in the atomic and extramolecular regions are solved numerically In the Xα method, the ionization potential, I_k, for orbital k can be expressed as[82]

$$I_k \approx -\epsilon_k + \frac{1}{2} < kk||kk > \qquad (7-9)$$

under the frozen-orbital approximation, in which ϵ_k is the one-electron eigenvalue for the orbital k and $< kk||kk >$ is the self-Coulomb energy of the electron k, which is usually about 1eV. Normally, the ionization potential of the highest occupied orbital for most stable molecular anions is a very small positive value[127,141] and less than its self-Coulomb energy. Hence the one-electron eigenvalue of the highest occupied orbital for most molecular anions might be positive in the Xα method.

Following the numerical approach of Herman and Skillman[48], the wave function is obtained by outward numerical integration starting from r=0 and inward numerical integration starting from r=∞. The wave functions at the first several mesh points in both directions are calculated by solving the one-electron Schrödinger equation analytically with the asymptotic forms of the potential $V^{lim}(r)$ for the corresponding orbital, when r approaches zero and infinity. The radial wave function is of the form

$$P_{nl}(r) = c_0 e^{-[q_{nl}(r)]^{1/2} r} \qquad (7-10)$$

when r approaches infinity, where c_0 is the normalization constant and $q_{nl}(r)$ is written as

$$q_{nl}(r) = V^{\infty}(r) - \epsilon_{nl} \qquad (7-11)$$

and ϵ_{nl} is the one-electron eigenvalue. In the Xα method, the asymptotic potential, $V^{\infty}(r)$, when r approaches infinity, is

$$V^{\infty}(r) = -\frac{2(Z-N)}{r} \qquad (7-12)$$

in the Rydberg atomic units. In equation (7-12), Z is the total nuclear charge and N the total electron number in the system. It is clear that V^{∞} (r) = 0 for a neutral system. Equation (7-10) becomes

$$P_{nl}(r) = c_0 e^{-[-\epsilon_{nl}]^{1/2} r} \qquad (7-13)$$

when r approaches infinity. Consequently, P_{nl} (r) is not a bound wave function when $\epsilon_{nl} > 0$ for the highest occupied orbital of molecular anions in the MS-Xα method.

To solve the one-electron Schrödinger equation self-consistently, Norman[135] applied a Watson sphere with charge +1 and radius equal to the outer sphere to simulate the stabilizing influence of a crystal lattice in the ClO_4^- calculation. Obviously, the size of the Watson sphere is arbitrary, and the energy, potential, and, in turn, the one-electron eigenvalues of the system depend on the radius of the Watson sphere and the charge on the Watson sphere. Hence it may not be used to predict the electron structure of molecular anions.

As mentioned in section III-1, the same problem occurs in calculating the atomic structure of negative ions of atoms[71]. The stable negative ions, such as H^-, O^-, F^-, and Cl^-[53,70,71] were predicted unstable by the Xα method and other LDF methods. Sen[53] discussed the non-convergence problem in the Xα calculation

for the atomic negative ions and pointed out that the non-convergence problem is because the self-interaction is not canceled in the Coulomb integral by that in the exchange integral in the Xα method.

Previously (section VII-2)[190], it has been shown that the self-interaction correction in the MS-Xα method, the self-interaction corrected MS-Xα (SIC-MS-Xα) method, significantly improves the molecular results over the conventional MS-Xα results, especially for the one-electron eigenvalues, which are as good as those from the Slater transition-state calculation and in the agreement with the experimental ionization potentials. The SIC-MS-Xα method has the correct asymptotic behaviour of the potential,

$$V(r) = -\frac{2}{r}[Z - N + 1] \qquad (7-14)$$

when r approaches infinity in the extramolecular region in the SIC-MS-Xα method. Hence the wave function is expected to be better than that in the MS-Xα method.

In this work, the SIC-MS-Xα method is employed to calculate the molecular anions ClO_4^-, HCO^-, and O_3^-. The effect of the electron correlation energy functional by using the Vosko, Wilk, and Nusair[39,138] (VWN) correlation energy functional on the one-electron eigenvalues and the charge distribution among the individual region are discussed. The negative of the one-electron eigenvalues is compared with other theoretical calculations and experiment.

Details relevant to the present calculations are given below.

Experimental equilibrium geometries are taken from Ref. 230 for ClO_4^-, Ref. 220 for HCO^-, and Ref. 223 for O_3^-. Schwarz's values[10] for the exchange parameter, α, were employed for fluorine, oxygen, and carbon atoms, and the α value of 0.77725 from Ref. 197 was used for hydrogen atom. α values for the interatomic and extramolecular regions were made equal and taken as the valence-electron weighted average of all atomic α values.

TABLE VII-9

Geometries of molecules, radii of the atomic and outer spheres, and overlapping percentages between spheres (a.u.)

Molecule	Sphere	x	y	z	r_α	Overlap
ClO_4^a	*Out*	0.0	0.0	0.0	4.074	$14.8(Cl-O)$
	Cl	0.0	0.0	0.0	1.611	
	O	−1.5821	1.5821	1.5821	1.534	
		1.5821	−1.5821	1.5821	1.534	
		1.5821	1.5821	−1.5821	1.534	
		−1.5821	−1.5821	−1.5821	1.534	
HCO^b	*Out*	1.1772	0.0	0.0	3.770	$47.1(C-O)$
	C	1.1772	0.0	0.0	1.680	$29.5(C-H)$
	O	−1.0905	0.2939	0.0	1.683	
	H	1.6605	−2.3508	0.0	1.428	
O_3^c	*Out*	0.0	0.0	0.0	3.564	$32.1(Oc-Ot)$
	Oc	0.0	0.0	0.8436	1.525	
	Ot	0.0	−2.0570	−0.4218	1.665	
	Ot	0.0	2.0570	−0.4218	1.665	

a. Reference 230;
b. Reference 220;
c. Reference 223.

The initial molecular potential was generated from the superposition of SCF-Xα charge densities for the fluorine, oxygen, and carbon atoms. Partial waves up to l=4 for the outer sphere, l=2 for fluorine, oxygen, and carbon, and l=1 for hydrogen.

The sphere radii were determined by the Norman criterion[198]. Overlapping sphere radii were chosen nonempirically by using a scaling factor of 0.80 for ClO_4^- and 0.88 for HCO^- and O_3^- over the atomic number sphere radii, since ClO_4^- possesses tetrahedral symmetry (Td), which is much more suitable to the MS-Xα calculation than planar molecular symmetry, such as HCO^- and O_3^-; the percentage of the atomic region in the molecular space is much higher in tetrahedral symmetry than a planar system in the tangent sphere MS-Xα calculation. The coordinates

for the atoms and the center of the outer sphere, the radii of the atomic and outer spheres, and the overlapping percentages of the atomic spheres are listed in Table VII-9.

The initial calculations are based on the original version of Cook and Case's MS-Xα program[195] in order to perform the SCF calculations for the ground state and Slater transition state for ClO_4^-, HCO^-, and O_3^-. The modified MS-Xα program including the self-interaction correction is employed to carry out the ground state calculation for the molecular anions ClO_4^-, HCO^-, and O_3^- including and excluding the VWN[39] correlation energy functional[138].

Since the Coulomb and exchange potentials in the SIC-MS-Xα method are orbital dependent, the wave function is not invariant under orbital transformations. Previously (section VII-2)[190], it has been shown that the dependence of wave functions on orbital transformations is not very important for the spherically averaged potentials for the atomic and extramolecular regions and the volume-averaged potential for the interatomic and the overlapping spheres in the SIC-MS-Xα method. Hence orbital transformation is ignored in the present calculation.

The SCF calculations for the ground state of ClO_4^- in the MS-Xα and SIC-MS-Xα methods and the transition-state in the MS-Xα method performed very well, because it is a well-bound system with the ionization potential of 6.2eV for its highest occupied orbital. Unfortunately, the SCF was only possible for the ground state in the SIC-MS-Xα method and the transition-state in the MS-Xα method for HCO^- and O_3^-, and failed for the ground states in the MS-Xα method, giving positive eigenvalues for the highest occupied orbitals. The negative of the one-electron eigenvalues for all valence occupied orbitals of ClO_4^-, HCO^-, and O_3^- are listed in Tables VII-10, VII-12, and VII-13, respectively, and compared with other calculations and experiment. The electron charge distribution among the atomic,

interatomic, and extramolecular regions and the charge partition to the partial waves are summarized in Table VII-11 for the ground state of ClO_4^- in the MS-Xα and SIC-MS-Xα methods and the transition state in the MS-Xα method.

TABLE VII-10

The negative of the one-electron eigenvalues (eV) in the MS-Xα, TS-MS-Xα, SIC-MS-Xα, and SIC-MS-Xα-VWN methods for the negative ion of ClO_4, compared with the electron affinity in the Watson sphere applied TS-MS-Xa calculation and experiment

Orbital	Xα	TS-Xα	SIC-Xα	SIC-Xα-VWN	WS-TS-Xα[a]	HF[b]	Expt[c]
1 t_1	3.71	7.07	6.23	7.61	11.65	7.66	6.2
3 t_2	5.56	8.87	8.40	9.76	13.88	9.65	8.8
1 e	5.90	9.23	8.75	10.10	13.88	10.01	8.8
2 t_2	10.34	13.68	13.47	14.86	18.75	15.47	13.4
2 a_1	13.95	17.30	16.73	18.13	21.97	19.38	16.4
1 t_2	21.79	25.21	24.65	26.06	30.89	33.07	27.0
1 a_1	27.95	31.37	31.63	33.04	37.31	40.59	34.4

a. Ref. 135, transition state calculation in the MS-Xα method with a Watson sphere;
b. Ref. 231, from *ab-initio* HF calculation with the basis set (Cl/10,6,1) (O/7,3);
c. Ref. 218, from the X-ray photoelectron spectra of $LiClO_4$.

ClO_4^-: To vertify the asymptotic form of the potential numerically in the extramolecular region, Fig. 7-8 shows the potential behaviour in the extramolecular region for the highest occupied orbital, $1t_1$, of ClO_4^- in the MS-Xα and SIC-MS-Xα methods. The behaviour of the potentials for all other occupied valence orbitals is approximately the same as for $1t_1$. The potential multiplied by r approaches +2 in the MS-Xα method and zero in the SIC-MS-Xα method when r approaches infinity. The ionization potentials of ClO_4^- have been measured by Prins[231] from the X-ray photoelectron spectra of $LiClO_4$; and studied theoretically with the *ab-initio* HF method[231] and the MS-Xα method[135] using a Watson sphere of charge +1 around

FIGURE 7-8

Potential behaviour in the extramolecular region for the highest occupied orbital, $1t_1$, of ClO_4^- in the MS-Xα and SIC-MS-Xα methods vs the radial r

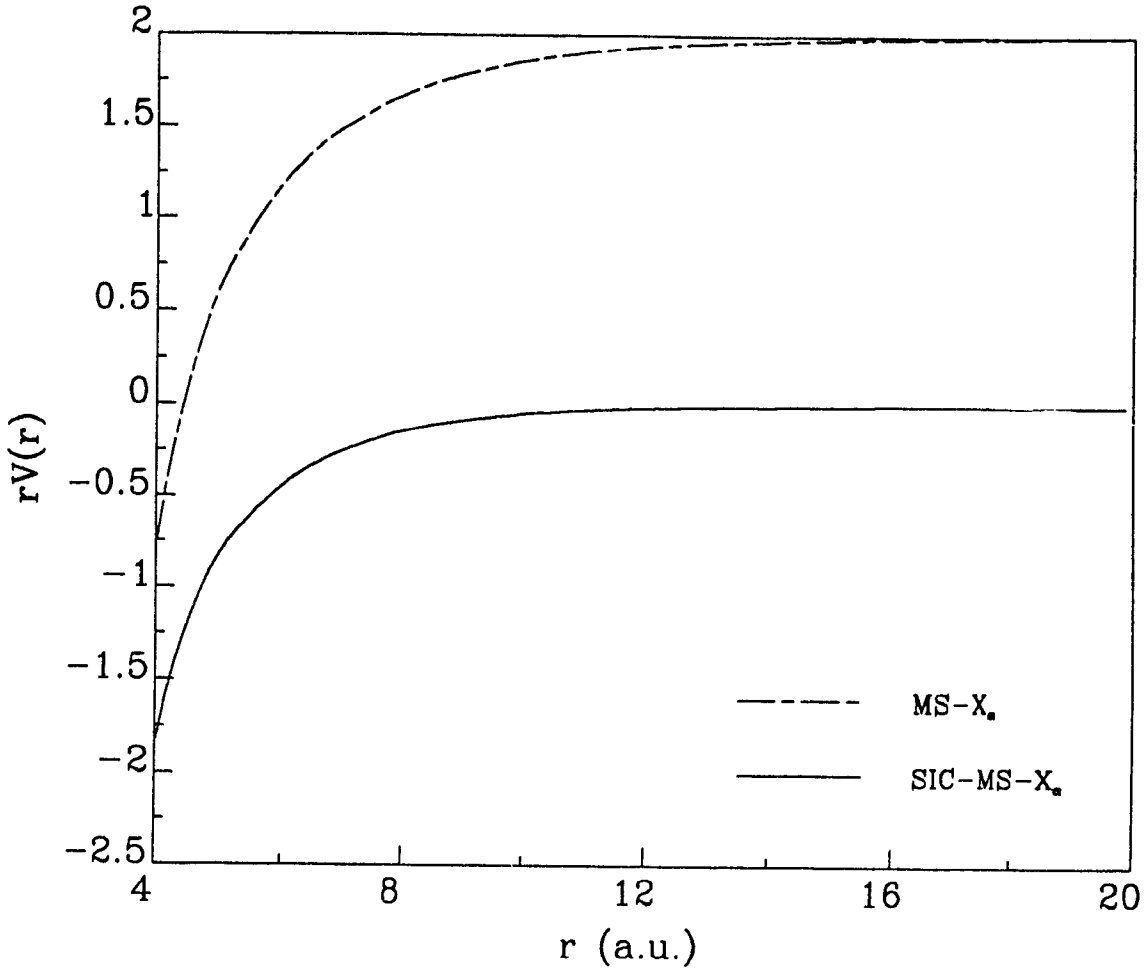

the atomic and interatomic regions. The present SCF calculations was carried out without any Watson sphere. The negative of the one-electron eigenvalues are listed in Table VII-10 and compared in Fig. 7-9. Table VII-10 gives the negative of the one-electron eigenvalues in the MS-Xα method, column 2, the ground state; column 3, the transition state when half electron is removed from the highest occupied orbital, $1t_1$, to infinity; column 4, the SIC-MS-Xα method; and, column 5, the VWN correlation energy functional included SIC-MS-Xα method (henceforth, called the MS-Xα, TS-MS-Xα, SIC-MS-Xα, and SIC-MS-Xα-VWN, respectively). The present results are compared to other theoretical calculations[135,231] and experiment[218]. The ionization potentials listed in column 6 were obtained previously by Norman[135] using the MS-Xα method with Watson sphere stabilization.

The negative of the one-electron eigenvalues in the MS-Xα method, as expected, are much smaller than the experimental ionization potentials, and those in the TS-MS-Xα method are significantly improved using the Slater transition-state concept and are in reasonable agreement with experiment. The negative of the one-electron eigenvalues in the SIC-MS-Xα method gives the ionization potentials in excellent agreement with experiment except for the two lowest occupied valence orbitals. The SIC remarkably increases the size of one-electron eigenvalues. The SIC-MS-Xα method gives the best ionization potentials of the anion ClO_4^- among all these methods. The electron-correlation correction increases the binding energies of the orbitals and makes the one-electron eigenvalues closer to those in the *ab-initio* HF method.

The charge distribution in the molecular space and the percentage composition for the individual orbitals of the molecular anion ClO_4^- in the MS-Xα, TS-MS-Xα, SIC-MS-Xα, and SIC-MS-Xα-VWN methods are in Table VII-11. Comparing the charge distribution of the atomic, interatomic, and extramolecular regions in

FIGURE 7-9

The one-electron eigenvalues (eV) for the valence orbitals of the negative ion ClO_4^-, compared with experiment

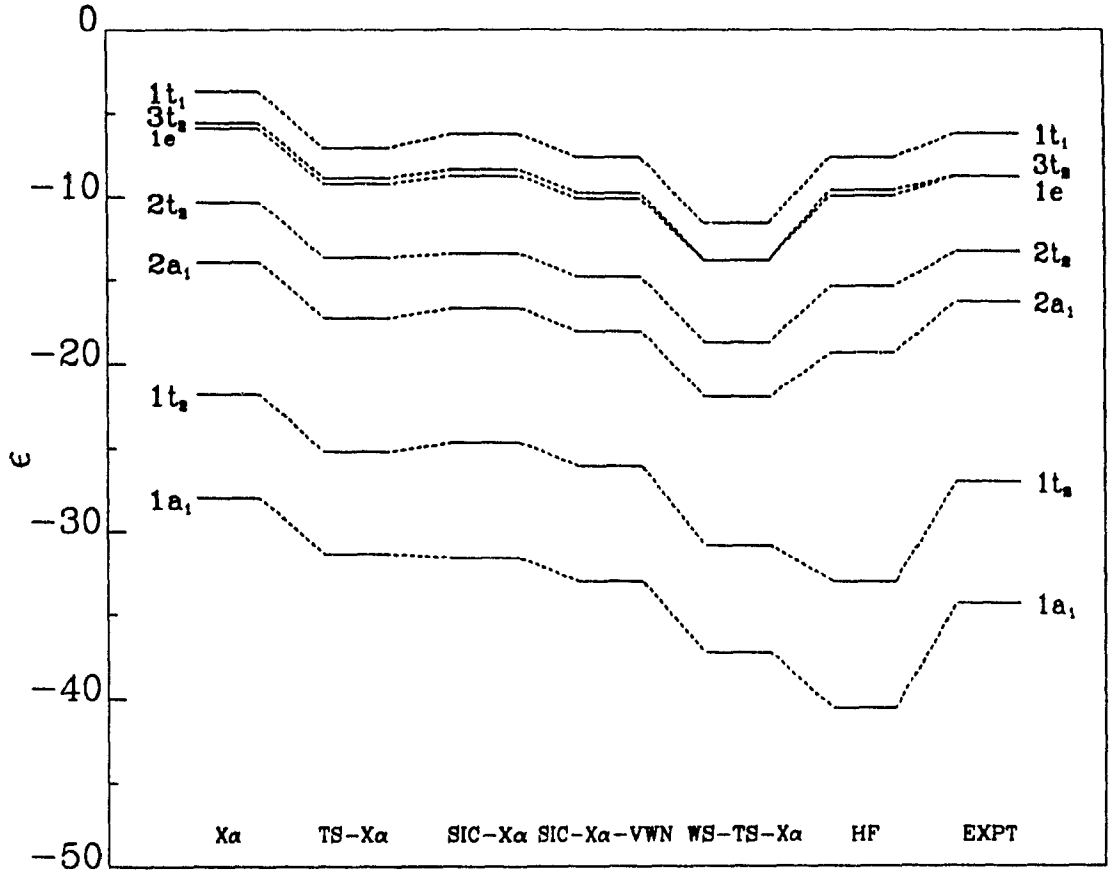

the MS-Xα and TS-MS-Xα methods, it can be seen that the effect of removing half electron from the highest occupied valence orbital, $1t_1$, is to slightly move the electron charge into the atomic region and reduce the electron charge in the interatomic and extramolecular regions. The partition of the electron charge between the partial waves in the atomic and extramolecular regions did not alter. However, the SIC pushes the electron charge of the atomic and interatomic regions into the extramolecular region, compared to the MS-Xα method. This is reasonable, because the asymptotic form of the potential, when r approaches infinity, is repulsive in the MS-Xα method, but neutral in the SIC-MS-Xα method for the molecular anion. The electron-correlation moves the electron charge from the interatomic and extramolecular regions to the atomic region. The contribution of electron-correlation energy functional to the potential is usually negative and approximately proportional to the electron density. Obviously, the electron densities in the interatomic and extramolecular regions are much smaller than the electron densities in the atomic region. Hence, the effect of the correlation-energy functional to the potentials in the atomic region is much bigger than that in the interatomic and extramolecular regions. Consequently, the VWN correlation attracts the electron charge from the interatomic and extramolecular regions to the atomic region.

HCO^-: The anion HCO^- was studied by Wasada and Hirao[224] using the CI method theoretically and experimentally observed in the negative ion mass spectra of small alcohols by Murray et al.[220] and Chandrasekhar et al.[221]. The ionization potential of 0.470 eV for the highest occupied valence orbital of HCO^- in the CI calculation, in which the valence basis set is double-zeta plus one polarization function and three diffuse functions (DZP+3), is very close to the very recent (1986) experimental value[220], 0.313$\pm$0.005 eV, which differs from the early (1981) experimental measured ionization potential[221], 0.174$\pm$0.174 eV. In this work, the

TABLE VII-11

Charge analysis for the ground state of ClO_4^- in the MS-Xα(MS), TS-MS-Xα(TS), SIC-MS-Xα(SIC), and SIC-MS-Xα-VWN(VWN) methods

State	(Cl)	*s*	*p*	*d*	(O)	*s*	*p*	*d*	Q(3)	*s*	*p*	*d*	*f*	*g*	Q(2)
						MS									
1 t_1	0	0	0	0	77.1	0	100	0	5.6	0	0	0	82	18	17.3
1 e	3.7	0	0	100	65.4	0	99	1	5.2	0	0	94	0	6	25.7
1 a_1	44.1	100	0	0	41.9	78	19	3	0.5	73	0	0	23	4	13.5
2 a_1	17.4	100	0	0	65.4	68	30	2	8.7	52	0	0	39	9	8.5
1 t_2	15.6	0	87	13	71.4	94	5	1	2.2	0	51	33	8	7	10.9
2 t_2	23.4	0	99	1	56.8	22	76	2	7.3	0	19	58	17	6	12.6
3 t_2	5.4	0	3	97	66.5	0	99	1	7.6	0	78	2	0	20	20.5
						TS									
1 t_1	0	0	0	0	78.2	0	100	0	4.7	0	0	0	81	19	17.1
1 e	3.7	0	0	100	66.6	0	99	1	4.4	0	0	93	0	7	25.3
1 a_1	44.2	100	0	0	42.0	78	19	3	0.5	73	0	0	22	4	13.4
2 a_1	17.5	100	0	0	66.1	69	30	1	8.0	51	0	0	40	9	8.4
1 t_2	15.7	0	87	12	71.6	94	5	1	2.0	0	51	33	8	7	10.7
2 t_2	23.5	0	99	1	57.4	22	76	2	6.6	0	19	57	17	7	12.5
3 t_2	5.5	0	2	98	68.1	0	99	1	6.3	0	75	2	0	23	20.1
						SIC									
1 t_1	0	0	0	0	75.5	0	100	0	6.0	0	0	0	82	18	18.5
1 e	4.4	0	0	100	63.2	0	99	1	5.4	0	0	94	0	6	27.1
1 a_1	43.0	100	0	0	42.3	78	19	3	0.5	75	0	0	22	4	14.2
2 a_1	16.7	100	0	0	65.3	69	30	1	9.0	54	0	0	37	9	9.2
1 t_2	16.5	0	88	12	69.4	93	6	1	2.2	0	54	32	7	7	11.8
2 t_2	22.8	0	99	1	56.1	23	75	2	7.1	0	17	60	17	6	14.0
3 t_2	6.0	0	3	97	64.6	0	99	1	7.7	0	78	2	0	20	21.6
						VWN									
1 t_1	0	0	0	0	76.0	0	100	0	5.7	0	0	0	82	18	18.3
1 e	4.4	0	0	100	63.7	0	99	1	5.1	0	0	93	0	7	26.9
1 a_1	43.0	100	0	0	42.4	78	19	3	0.5	74	0	0	22	4	14.1
2 a_1	16.6	100	0	0	65.5	69	30	1	8.7	53	0	0	38	9	9.1
1 t_2	16.6	0	88	12	70.0	93	6	1	2.2	0	54	32	7	7	11.7
2 t_2	22.9	0	99	1	56.3	23	75	2	6.9	0	17	60	17	6	13.8
3 t_2	6.2	0	3	97	65.1	0	99	1	7.3	0	77	2	0	21	21.4

SCF calculations for HCO^- were performed in the TS-MS-Xα method by removing half-electron from the highest occupied valence orbital 5a′ to infinity and in the SIC-MS-Xα method. But the SCF process failed for the ground state of HCO^- in the MS-Xα method, in which the one-electron eigenvalue of the highest occupied valence orbital for HCO^- is positive. The negative of the calculated one-electron eigenvalues for HCO^- in the TS-MS-Xα, SIC-MS-Xα, and SIC-MS-Xα-VWN methods is presented in Table VII-12 and compared in Fig. 7-10.

The negative of the highest occupied valence orbital one-electron eigenvalues, 0.32eV, is in excellent agreement with the recent experimental ionization potential, 0.313eV; and the agreement is much better than in the TS-MS-Xα, SIC-MS-Xα-VWN methods, and much better than the DZP+3 CI calculation. Except for the highest and lowest occupied valence orbitals, the SIC-MS-Xα one-electron eigenvalues are intermediate between the TS-MS-Xα and SIC-MS-Xα-VWN results. Unfortunately, the experimental ionization potentials for other occupied valence orbitals are not available for comparison, and the present results are predictive.

O_3^-: The ionization potential of O_3^- is a quantity of considerable significance in atmospheric phenomena. It has been investigated experimentally by Beaty[223] using photodetachment measurements and Chupka et al.[219] from the reaction $I^- + O_3 \rightarrow O_3^- + I$; it has been calculated theoretically by Heaton et al.[223] using the CI method with large Gaussian basis sets and symmetry adapted complex functions, 272 spin-space configurations for O_3^-, and 30 spin-space configurations for O_3. The calculated value of the ionization potential for the highest occupied valence orbital of O_3^- in the CI method is 2.27409eV and very close to the experimental value, 2.1-2.2eV. The calculations were done in the present work by using the TS-MS-Xα, SIC-MS-Xα, and SIC-MS-Xα-VWN methods. The negative of the one-electron eigenvalues is listed in Table VII-13 and plotted in Fig. 7-11. The calculation in

TABLE VII-12

The negative of the one-electron eigenvalues (eV) in the TS-MS-Xα, SIC-MS-Xα, and SIC-MS-Xα-VWN method for the negative ion HCO^{-}*

Orbital	TS-Xα	SIC-Xα	SIC-Xα-VWN
5 a′	1.06	0.32	1.31
4 a′	6.59	6.89	7.77
1 a″	7.15	8.13	9.07
3 a′	8.69	8.71	9.57
2 a′	12.48	13.34	14.30
1 a′	28.46	27.26	28.23

* The Calculated ionization potential for the highest occupied orbital, 5′, is 0.470eV in the CI method (Ref. 224) and experimental result is 0.313eV (Ref. 220).

the MS-Xα method for O_3^- failed to give a self-consistent value.

The present results show that the negative of the one-electron eigenvalues for the highest occupied valence orbital of O_3^- in the TS-MS-Xα and SIC-MS-Xα methods, 2.14 eV and 2.06eV respectively, are in excellent agreement with the experimental ionization potential (2.1-2.2eV) and much better than that in the SIC-MS-Xα-VWN method, and comparable with the CI calculation. For other occupied valence orbitals, the negative of the one-electron eigenvalues in the TS-MS-Xα and SIC-MS-Xα method are very close to each other and smaller than those in the SIC-MS-Xα-VWN method.

The ionization potentials of the occupied orbitals in the *ab-initio* HF method using the Koopmans′ theorem are usually much higher than experiment, because of the relaxation which occurs during ionization. The ionization changes the equilibrium geometries and the electron distribution, and reduces the total energies of

FIGURE 7-10

The one-electron eigenvalues (eV) for the valence orbitals of the negative ion HCO^-

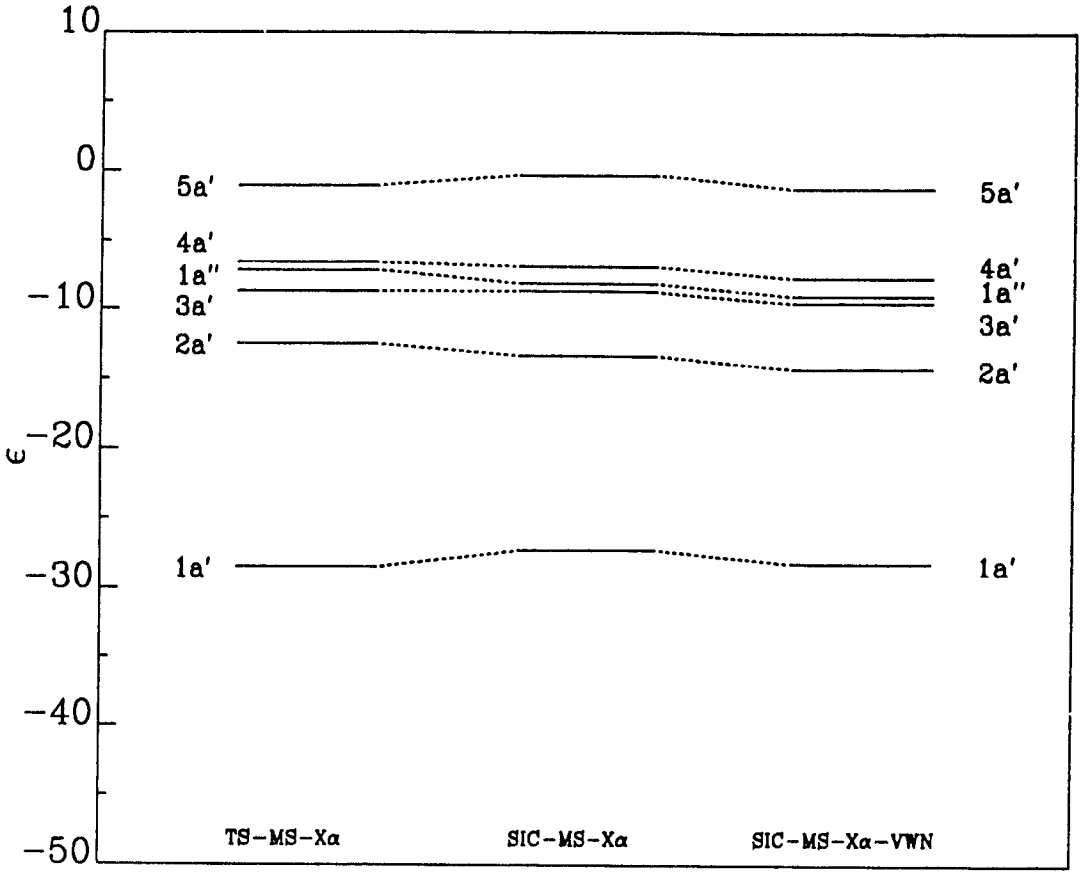

TABLE VII-13

The negative of the one-electron eigenvalues (eV) of the negative ion O_3^- in the TS-MS-Xα, SIC-MS-Xα, and SIC-MS-Xa methods *

Orbital	TS-Xα	SIC-Xα	SIC-Xα-VWN
2 b_1	2.14	2.06	3.26
3 b_2	4.11	3.86	5.11
4 a_1	4.29	4.11	5.36
1 a_2	4.69	4.45	5.69
1 b_1	9.48	10.11	11.37
3 a_1	10.14	10.73	11.99
2 b_2	11.32	11.18	12.44
2 a_1	15.68	15.46	16.72
1 b_2	22.98	22.54	23.83
1 a_1	29.38	29.65	30.95

* The Calculated ionization potential for the highest occupied orbital, 2 b_1, is 2.27 in the CI method (Ref. 223) and experimental result is 2.1-2.2eV (Ref. 223).

molecular anions. Hence, the ionization potentials in the relaxed theoretical method are smaller than those in the unrelaxed calculations. As discussed previously[190], the negative of the one-electron eigenvalues in the SIC-MS-Xα method is not equal to the ionization potential, even under the frozen orbital approximation, equation (7-8). The effect of the relaxation on the ionization potential, which lowers the magnitude, is partly canceled by the value of the integral in the equation (7-8), which is always non-negative. Furthermore, the electron-correlation energy functional normally increases the one-electron eigenvalue in magnitude, because of the negative contribution of the correlation energy functional to the potential. Therefore, the second term in the right hand side of equation (7-8) is also partly balanced by the correlation correction. This is the reason why the ionization potentials obtained from the negative of one-electron eigenvalues in the SIC-MS-Xα method are much better than those from the SIC-MS-Xα-VWN method and from the *ab-initio* HF

FIGURE 7-11

The one-electron eigenvalues (eV) for the valence orbitals of the negative ion O_3^-

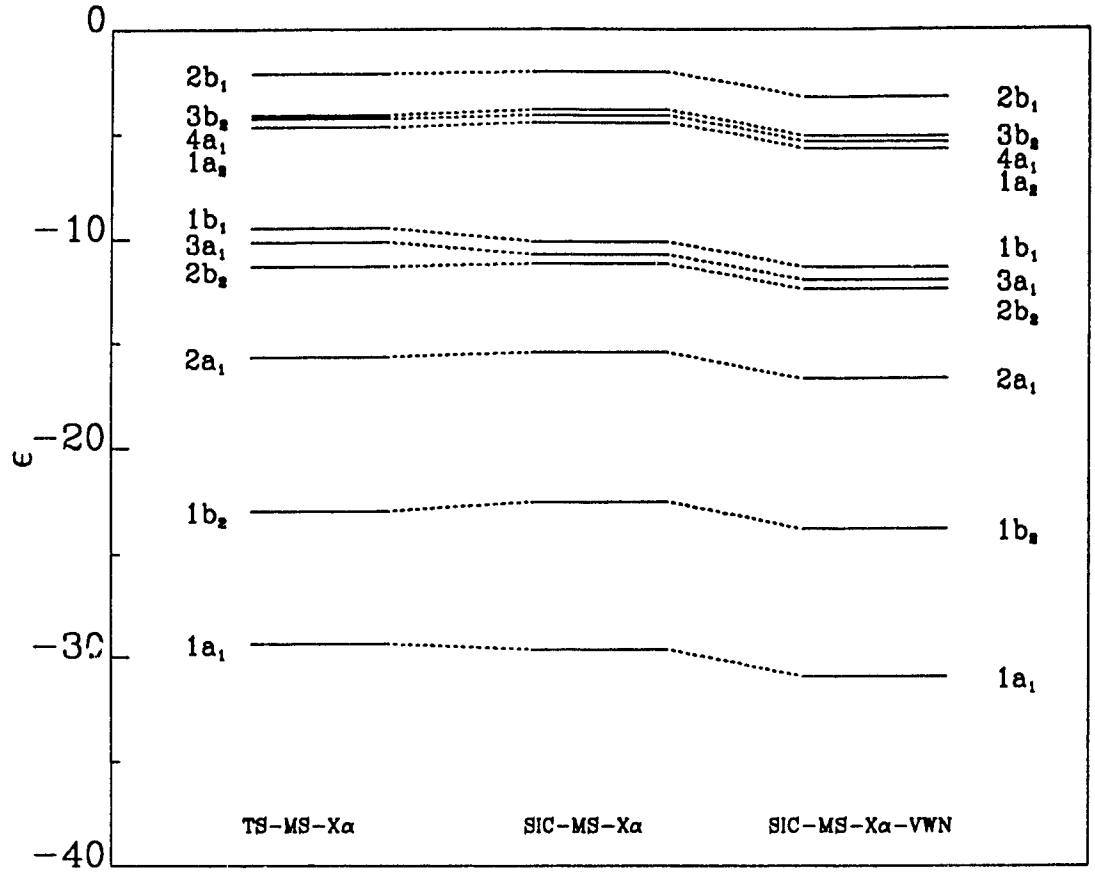

method, when the Koopmans' theorem is used.

The ionization potentials of molecular anions from the negative of the one-electron eigenvalues in the SIC-MS-Xα method agree with experiment and are better than those in the *ab-initio* HF calculation and comparable to the CI results, when the correct sphere sizes are chosen in the SIC-MS-Xα method. The SIC-MS-Xα method gives convergent wave function for the stable molecular anions. The wave functions in the SIC-MS-Xα method are expected to be better than in the conventional MS-Xα method and can be used to calculating other one-electron properties for the stable molecular anions. Furthermore, a single SCF procedure in the SIC-MS-Xα method produces both a reasonable good ionization potential and the correct wave function for the molecular anion; the transition-state theory cannot be used to predict the one-electron properties in the MS-Xα method. This is a remarkable improvement over the MS-Xα method, especially for the application of the MS-Xα method to large and heavy molecules.

The method being part of a completely tested theory has great validity for predicting such ions.

CHAPTER VIII

CONCLUSIONS, CLAIMS TO ORIGINAL RESEARCH, AND SUGGESTIONS TO FUTURE WORK

VIII-1. Conclusion

The present work is summarized below.

VIII-1.1 The G-LSD and GX-LSD Theories

The G-LSD theory[24] gives a master equation for the single-electron exchange energy density, and other theories, such as, the GX-LSD theory[22], the Ξa theory[17], the $X\alpha$ theory[9], the GKS theory[7,8], and the HFS theory[6] can be obtained by using additional approximations, by choosing a certain Fermi-hole shape or using the high electron-density approximation. Therefore, the GX-LSD theory is a restriction of the G-LSD theory. Furthermore, there is no approximation used to derive the G-LSD theory except the local-density approximation; the boundary conditions and sum rule of the Fermi-correlation factor are generated from the HF limit in the HF theory. Hence, theoretically the G-LSD theory is more rigorous than the GX-LSD theory, the Ξa theory, the $X\alpha$ theory, the GKS theory, and the HFS theory.

The exchange potential in the G-LSD theory is orbital dependent and more correct than the $X\alpha$, GKS, and HFS exchange potentials which depend on the total electron density. In fact, the electrons in different orbitals are certainly surrounded by different environment created by the other electrons in a system. The HF theory has this feature[3].

An another interesting feature in the G-LSD theory is that the Fermi-hole

parameters are fixed for all atoms and ions, when the Fermi-hole shape has been chosen (e.g. the GWB[27] or the Wigner[26] or the Homogeneous[9] Fermi-hole shape) or the Fermi-hole parameters can be determined by the asymptotic form of the exchange potential as the electron density approaches infinty, i.e., the FEL Fermi-hole parameters[22]. Consequently, the G-LSD theory can avoid the time-consuming step in searching the optimal exchange parameter α for each atom or ion.

VIII-1.2 The Self-Interaction Correction

The self-interaction correction is very important, it is essential in calculating the electronic structures of negative ions of atoms by the LDF theory in the SCF procedure. The non-convergency in the self-consistent calculation for most experimentally stable negative ions of atoms was caused by the incomplete cancellation of the self-interaction in the Coulomb and exchange integrals. As discussed in section VII-3, the self-interaction uncorrected LDF theory does not give any bound solutions for molecular anions.

When the SIC is carried out by removing the exact self-Coulomb from the Coulomb-interaction term and the approximate exchange from the local-exchange term[29,30], the SIC-LDF theory gives much better one-electron eigenvalues and statistical total energies for atoms than the self-interaction uncorrected LDF theory, in comparison with HF results and experiment. The SIC-LDF theory has the correct asymptotic form of the potential with 1/r for the neutral atoms. Numerically, once the SIC is invoked, the self-consistent procedure works properly for most experimentally stable negative ions of atoms[15,73,74].

The self-interaction correction is very interesting in the molecular calculations. As shown in section VII-2, the ionization potentials given in terms of the negative of the one-electron eigenvalues are in excellent agreement with experiment

and as good as those given by the Slater transition state calculation in the MS-Xα method, when the SIC was introduced. One can certainly expect that the SIC-MS-Xα method should give more accurate wave functions for molecules in calculating other one-electron properties, because the potential is closer to the real system than that in the self-interaction uncorrected MS-Xα method. Furthermore, the SIC-MS-Xα method can give both the ionization potentials and the correct wave functions with a single SCF calculation, whereas to get both a reasonably good ionization potential and the correct wave function for a molecule, the SCF procedure has to be carried out twice in the self-interaction uncorrected MS-Xα method, one for the transition state in which a half electron is removed from a occupied valence orbital (usually the highest occupied valence orbital), and another for the ground state or the excited state. This is inefficient and expensive for large molecules containing heavy atoms.

The SIC-MS-Xα method works very well in the SCF calculation for the experimentally stable molecular anions. The electron affinities obtained from the negative of the one-electron eigenvalue of the highest occupied valence orbital are in reasonable good agreement with experiment. The wave function can be produced by the SIC-LDF theory, whereas it is impossible to solve the one-electron Schrödinger equation and obtain the wave function for most molecular anions with very small positive electron affinities in the self-interaction uncorrected LDF theory, because of the non-convergency problem.

The present work has shown that a remarkable improvement of the one-electron eigenvalues and the wave functions can be obtained for molecules and molecular anions by introducing the SIC. It is certainly expected that the SIC is very important in improving the agreement of calculated results and experiment for other one-electron properties and total energy more efficient than other more

rigorous theories, such as, the LCAO-Xα method, the DV-Xα method, and the full numerical LDA method which have rarely been applied to such systems.

VIII-1.3 The Electron-Correlation Correction

Electron-correlation is a very important concept in evaluating the electron structures of negative ions of atoms. It is essential in obtaining a converged solution for the one-electron Schrödinger equation for the alkaline-earth elements, most actinide elements, and rare gasses, although the electron-correlation functional to the total potential is very small[92,101]. The electron-correlation energy correction to electron affinities is larger than the kinetic, Coulomb, and exchange energy contribution for most atoms. Hence, the existence of stable negative ions for most atoms might be attributed to electron correlation, and not to the Coulomb attractive potential between the nucleus and electrons, because each electron partially screens the nucleus from all other electrons. The accurate expression of the electron correlation is required to give trustworthy electron affinities for atoms. Comparing the results obtained by using the VWN correlation expression[39] and the SPP expression[38] shows that the VWN correlation expression is more accurate than the SPP correlation. This agrees with Perdew and Zunger's conclusion.

The electron correlation energy correction plays a role in calculating the ionization potentials for atoms and multiply charged ions of atoms. The results obtained from the LDF theory are comparable with those in the HF theory. To get accurate ionization potentials of atoms, electron-correlation is necessary.

VIII-1.4 Relaxation

The relaxation effect in the ionization process is another important concept[81]. Normally, the relaxation effect reduces the total energy of a system and therefore, reduces the ionization potential and increases the electron affinity for a atom as shown in Fig. 3-1. The ionization potential and electron affinity for an atom are different in the relaxed method and non-relaxed method. Whereas the electron-correlation increases the ionization potential and electron affinity. Therefore, the ionization potential obtained from both the electron-correlation and relaxation uncorrected LDF theory are in very good agreement with experiment. This means that in order to get a correct ionization potential, one can either use both the electron-correlation corrected and relaxation corrected LDF theory or use the electron-correlation ignored and relaxation ignored LDF theory. Certainly, both the electron-correlation and relaxation corrected LDF theory is more accurate theoretically and numerically than both the electron-correlation and relaxation ignored LDF theory.

This work showed that the relaxation is more important than the electron-correlation in the ionization potential calculation, whereas, the electron-correlation is more important than the relaxation in the electron affinity calculation for an atom. The relaxation is very important in the calculation of molecular ionization potentials. The ionization potentials given by Koopmans' theorem in the LCAO-HF method are much larger than experiment. Whereas, the ionization potentials given by the negative of the one-electron eigenvalues in the SIC-MS-Xα method are in very good agreement with experiment, because the higher terms of the derivatives of the exchange and self-exchange energies with respect to the occupation number in equation (7-8) are partly cancelled by the relaxation correction[190].

VIII-1.5 The SIC-G-LSD and SIC-GX-LSD theories

The SIC-G-LSD theory gives the statistical total energies for atoms in excellent agreement with HF, and much better than the XO-LSD theory, when the GWB Fermi-hole parameters are used. The one-electron eigenvalues in the SIC-G-LSD theory with the GWB Fermi-hole parameters are in reasonable good comparing with the HF orbital energies.

Comparing the results of atoms in the SIC-G-LSD theory and in the SIC-GX-LSD theory shows that the total energies of atoms in the SIC-G-LSD theory are only slightly better than those in the SIC-GX-LSD theory, when the FEL Fermi-hole parameters are used. This implies the physical restriction of the Fermi-correlation factor used in the GX-LSD theory is not severe numerically. Consequently, the SIC-GX-LSD theory is still valid and useful.

The electron-correlation corrected SIC-G-LSD theory with the GWB Fermi-hole parameters can be used to estimate the electron affinities for any atoms and predict the ionization potentials of atoms and multiply charged positive ions with acceptable computational time, when the experimental ionization potentials and the electron affinities are unknown. Furthermore, the atomic wave function in the SIC-G-LSD theory with the GWB Fermi-hole parameters is expected to give good other atomic properties, such as, the oscillation strength, photoionization cross section, etc.

VIII-1.6 Convergence Technique

The convergence techniques in the SCF calculation for negative ions of atoms introduced in the present work, that is, the adiabatic convergence technique and the Watson sphere aided technique, worked so successfully that it can be employed in

the HF calculation for the loose bound negative ions of atoms to study the stability of the singly charged negative ions of rare gasses and actinides and the second charged negative ions of the rest elements in the periodic table.

VIII-2. Claims to Original Research

1. Section I-2.

   The boundary conditions and sum rule of the Fermi-correlation factor were generated systematically by the HF limit.

2. Section I-3.

   The pair-electron distribution function, $\rho_{ss}(\mathbf{r}_1, \mathbf{r}_2)$, was written into equation (1-50) to reflect the difference of the correlation factors for different orbitals. This is a very important step in obtaining the G-LSD theory.

   The derivation and analysis of the G-LSD theory.

3. Section I-4.

   The GX-LSD theory, the Ξa theory, and the XO-LSD theory, and the Xα theory were obtained from the G-LSD theory.

4. Section I-5.

   The derivation of the self-interaction correction in the density functional theory and the introduction of the SIC-G-LSD theory.

5. Section I-6.

   The orbital-dependent exchange potential in the SIC-G-LSD theory.

6. Section II-1.2

   The analysis of the self-interaction correction in the SIC-G-LSD theory, the SIC-XO-LSD theory, and the HFS theory.

7. Section II-1.5

   The analysis and comparison of the one-electron eigenvalues of atoms in the SIC-G-LSD theory and in the HF theory.

8. Section II-1.7

   Numerical proof of the validity of the SIC-GX-LSD theory.

9. Section II-2

   Successful calculations of the single-charged negative ions for some atoms in the SIC-GX-LSD theory.

10. Section III-2

    The first through fourth derivations with respect to the occupation number were given in the GX-LSD theory; and numerically, the ionization potentials of atoms can be generated approximately by the first two derivations of the statistical total energies with respect to the occupation number in the GX-LSD theory, because of the partly cancellation of the higher order terms in equation (3-16) with the Coulomb correlation correction.

11. Section III-2.2

    The Coulomb-correlation correction is very important in calculating the electron affinities of atoms.

12. Section III-2.3

    The hardnesses of the acids and bases in the GX-LSD theory by the definitions in equations (3-22) and (3-24) agree very well with those calculated by the experimental ionization potentials and electron affinities.

13. Section III-3

    The experimental ionization potentials of the low-Z atoms were duplicated very well by the differences of the total energies in the electron-correlation

energy corrected SIC-GX-LSD theory with the GWB Fermi-hole parameters. The comparison of the ionization potentials shows that the VWN expression for the electron correlation is better than the SPP parametrization.

The electron affinities of the low-Z atoms in the electron correlation corrected SIC-GX-LSD theory with the GWB Fermi-hole parameters are reasonable good in comparison with experiment. The contribution of the electron correlation to the electron affinities is larger than that from the kinetic, Coulomb, and exchange energies for some atoms.

14. Section III-4.

The relativistic correction to the removal energy of the outermost s orbital of the alkaline-earth elements and the outermost p orbital of the elements in group IIIB can be estimated by the QR-SIC-GX-LSD theory, in which the spin-orbital coupling term was neglected, with the GWB Fermi-hole parameters. The ionization potentials for the high-Z atoms evaluated by the electron-correlation corrected SIC-GX-LSD theory with the GWB Fermi-hole parameters agree well with experiment and the agreement is better than those in the DF theory with the SPP correlation and relaxation correction.

The electron affinities for the high-Z atoms in the electron-correlation corrected QR-SIC-GX-LSD theory are in reasonable good agreement with experment.

15. Section III-5.

The ionization potentials of the multiply charged ions for atoms are in excellent agreement in the electron-correlation corrected SIC-GX-LSD theory with experiment. The electron-correlation correction plays a role in the ionization potentials of the multiply charged ions.

14. Section IV-1.

The analysis on the non-convergence of the doubly-charged negative ions in the LDF theory.

15. Section IV-2.

    Successful calculation of the negative ions for the alkaline-earth elements in the LDF theory; and the calculations of the electron affinities for them in the electron correlation corrected SIC-GX-LSD and QR-SIC-GX-LSD theories with the GWB Fermi-hole parameters support the prediction of existence of stable negative ions for the alkaline-earth elements, except for Mg^-. Successful SCF results in the QR-SIC-GX-LSD theory for the actinides were obtained and predicted the stability of the negative ions for actinides.

16. Section IV-3.1

    Adiabatic convergence technique was given in the LDF theory.

17. Section IV-3.2

    Successfully converged for the negative ions of rare gasses in the electron-correlation corrected SIC-GX-LSD theory with the GWB Fermi-hole parameters were given and predicted the existence of stable negative ions for the rare gasses with several milli-rydbergs electron affinities.

18. Section IV-4.1

    Watson sphere simulation for the doubly charged negative ions of atoms in crystals was proposed.

19. Section IV-4.2

    The second electron affinities of atoms in crystals were estimated in the electron-correlation corrected SIC-GX-LSD theory with the GWB Fermi-hole parameters. The electron affinities are reported to be negative for them in the first time.

20. Section IV-5.

Asymptotic approximation for the second electron affinities of atoms in gas phase was given, when the Watson sphere radius approaches infinity.

The approximate second electron affinities for the first category elements in the second and third periods were estimated in the electron-correlation corrected SIC-GX-LSD theory with the GWB Fermi-hole parameters.

21. Section V-2.

The ionization potentials of the fractional charged atoms were given in the LDF theory in the first time. The comparison of the present results with the Lackner and Zweig interpolation shows that the agreement of the calculated and interpolated ionization potentials is excellent for the fractional charged atoms with $Z = N \pm \frac{1}{3}$ and $Z = N + \frac{2}{3}$; and corrects the inaccurate interpolated results for those with $Z = N - \frac{2}{3}$, because of the loose bound electron in the outermost orbital.

22. Section V-3.

Successful calculation for the electron affinities for the fractional charged negative ions with $Z = N - \frac{1}{3}$ and $Z = N - \frac{2}{3}$.

23. Section V-4.

The hardnesses for the fractional charged atoms are of the same trend as the ordinary atoms.

24. Section VI-3.

The self-interaction corrected MS-Xα theory was given.

25. Section VI-4.

The procedure of the minimization of the total self-interaction correction energy in the SIC-MS-Xα theory was outlined.

26. Section VII-2.

    The SIC was tested for some small and middle size molecules in the first time by means of the MS-Xα method. The efficiency of the SIC in the molecular calculation was established: a single SCF calculation for the ground state of a molecule gives both the ionization potentials and the wave function, instead of two SCF calculations in the conventional MS-Xα method to get both the ionization potentials and the wave function. The minimization of the SIC energy is not important in the MS-Xα method, because of the employment of the spherically-averaged and the volume-averaged potentials.

27. Section VII-2.1

    The reason why the ionization potentials given by the negative of the one-electron eigenvalues in the SIC-MS-Xα method are much better than those in the *ab-initio* HF method is discussed.

28. Section VII-3.

    The reasons why the non-convergence in SCF calculation of the MS-Xα method for the experimentally stable molecular anions with small positive electron affinities are discussed. The molecular anions, ClO_4^-, HCO^-, and O_3^- are successfully converged in the SIC-MS-Xα method. The electron affinities given by the SIC-MS-Xα method are in excellent agreement with experiment.

VIII-3. Suggestions to the Future Work

The basic suggestions to the future work are theoretical improvement on the SIC and electron-correlation correction in the G-LSD theory and the application of the SIC-G-LSD theory and the SIC-MS-Xα method to molecules, clusters, and

solid state.

VIII-3.1 Theoretical Modification

Theoretically, the SIC-G-LSD theory with the FEL Fermi-hole parameters should give more reliable results than the SIC-G-LSD theory with other Fermi-hole parameters, because the FEL Fermi-hole parameters were derived from the free electron-density limit, when the electron density approaches infinity, and do not rely on any assumptions of the Fermi-hole shape. But, numerically, the SIC-G-LSD theory with the GWB Fermi-hole parameters gives the best statistical total energies of atoms among all the Fermi-hole parameters in comparison with the HF total energy. The statistical total energy of an atom is underestimated in magnitude by the SIC-G-LSD theory with the FEL Fermi-hole parameters. As discussed before, this deviation is mainly caused by the overestimation of the self-exchange correction in the SIC-G-LSD theory with the FEL Fermi-hole parameters. In the SIC-G-LSD theory, the radius of self-exchange Fermi-hole for the orbital i, equation (1-83), is only dependent on its own electron density. It is clear that the environment of the self-exchange Fermi-hole disturbs it. As in equation (1-59), the radius of the exchange Fermi-hole, r_F, decreases as the number of total electrons in the system increases. This implies the Fermi-hole is squeezed by increasing the electrons in the system. Therefore, the effect of changing the environment should be considered in correcting the self-exchange interaction in the SIC-G-LSD theory.

The correlation of electrons with different spins were treated, so far, by parametrization[38,39] based on some accurate calculations or by assuming the Coulomb hole factor obeying some certain functions[33,232]. It would be very interesting to calculate the Coulomb-correlation without any assumptions and parametrizations. It appears possible to derive the Coulomb-correlation expression in the same manner

as in deriving the single-electron exchange energy expression in the present work.

VIII-3.2 Application of the SIC-G-LSD Theory to Molecules

The SIC-G-LSD theory with the GWB Fermi-hole parameters gives such good statistical total energies for atoms, compared to HF, that it is certainly expected the SIC-G-LSD theory should give very good statistical total energies for molecules, if the SIC-G-LSD theory with the GWB Fermi-hole parameters is combined with the LCAO method[181-183] or the discrete-variational(DV) method[184-186] using good enough Gaussian basis sets and fit functions. The statistical total energy, in turn, can be used to calculate the dissociation energy, energy surface, etc. The reasonable good wave function can be employed to evaluate other one-electron properties of the molecule, such as, the dipole moments, quadrupole moments, diamagnetic susceptibilities, nuclear quadrupole coupling constants, and etc. The potentials in the SIC-G-LSD theory is orbital dependent and the statistical total energy including the SIC total energy is not invariant under the molecular orbital transformation. Consequently, a test of the effect of the orbital transformation on the statistical total energy is necessary, when the SIC-G-LSD theory is applied in molecular calculations.

VIII-3.3 Application of the SIC-MS-Xα Method to Large Molecules and Clusters

Because of the division of a molecular space and the use of the "muffin-tin" approximation, the MS-Xα is much easier to use and to wield for large molecular calculations. But electron structures and statistical total energies of molecules are sensitive to a percentage of the constant region in the molecular space in the MS-Xα

method. Fortunately, it has been shown[171,177,179–181] that the most reliable results, the electron structures, the ionization potentials, and the wave functions, can be obtained by using the Norman criterion of the atomic spheres and scaling by a factor between 0.8 - 0.88 The present work shows that the ionization potentials and the correct wave functions can be obtained by a single SCF calculation for a molecule. It saves a lot of computational time by introducing the SIC into the MS-Xα method. Hence, the MS-Xα method can be applied to large molecules containing heavy atoms, clusters, and solid state with very reasonable and acceptable computation time and excellent numerical results.

Transition-metal complexes are very interesting to the chemists. To date, a considerable effort has been made to explore and understand the chemistry of transition-metal hydrides complexes Most of these investigations have focused on their structure and reactivity[233–238], only a few theoretical studies on the electron structure have been undertaken Indeed, there is still a lack of rigorous quantum mechanical description of the metal-hydrogen interaction essential to the interpretation of the observed chemistry Publications[180] have appeared in the literature dealt with the transition-metal complexes by the MS-Xα method, but it is expected that the SIC-MS-Xα method gives more reliable results than the MS-Xα method.

The MS-Xα method is not convergent for most experimental stable molecular anions, one has to use a Watson sphere in the MS-Xα method to stablize the calculation[135]. The electron structures of anions are certainly disturbed by the Watson sphere. However, it is possible for most experimental stable molecular anions to get the converged electron structures in the MS-Xα method by introducing the SIC into it. The present work showed that the reasonable good electron affinities of molecules can be obtained by the SIC-MS-Xα method.

Small metal clusters are currently the subject of both experimental[239,240]

and theoretical[241-247] investigations. In theoretical studies of chemisorption small clusters are often used to model the metal substrate[244]. The study of the small clusters (of order of 8 - 13 atoms) by the MS-Xα method has emerged in the literature[248,249]. The important difference between the MS-Xα method and LCAO-HF method or the extended Hückel calculations has appeared in the small copper cluster electron structure calculations.

One of the interesting properties in calculating clusters is the local-density-of-states (LDOS), which is defined by[245]

$$\rho_\mu(E) = \sum_k P_k(\mu) \frac{\sigma/\pi}{(E-\epsilon_k)^2 + \sigma^2} \qquad (8-1)$$

where $P_k(\mu)$ is the Mulliken gross orbital population of an orbital μ in the cluster state k; ϵ_k is the orbital energy of the cluster state k; and σ is a Lorentzian width parameter. It is clear that the meaning of the one-electron eigenvalues in the LCAO-HF method and in the MS-Xα method are different. Hence, it is understandable that the LDOS's are different in the LCAO-HF and MS-Xα methods

The SIC remarkably reduces the difference of the one-electron eigenvalues in the LCAO-HF method and in the MS-Xα method. Therefore, the SIC-MS-Xα method is expected to give reliable LDOS for the cluster calculation, comparing with the LCAO-HF method.

BIBLIOGRAPHY

1. D.A.McQuarrie, *Quantum Chemistry* (Mill Valley, California, 1983).
2. P.W.Atkins, *Molecular Quantum Mechanics*, 2nd ed. (Oxford, New York, 1983).
3. C.F.Fischer, *The Hartree-Fock Method for Atoms* (Wiley, New York, 1977).
4. A.D Becke and M.R.Roussel, *Phys. Rev. A* **39**,3761(1989).
5. P.A.M.Dirac, *Proc. Cambridge Philos. Soc.* **26**, 376(1930).
6. J.C.Slater, *Phys. Rev.* **81**, 385(195_).
7. R.Gáspár, *Acta Phys. Acad. Sci. Hung.* **3**, 263(1954).
8. W.Kohn and L.J.Sham, *Phys. Rev.* **140**, A1133(1965).
9. J.C.Slater, *Quantum Theory of Molecules and Solids*, Vol. 4 (McGraw-Hill, New-York, 1974)
10. K.Schwarz, *Phys. Rev B* **5**, 2466(1972).
11. K.Schwarz *Theor Chim. Acta* **34**, 225(1974).
12. Z.Zhang and Y.Zhao, *The Xα Wave Functions of Atoms* (Atomic Energy Press, Beijing, 1983)
13. J.C Slater, *Phys. Rev* **165**, 658(1968).
14. F.Herman, J P.Van Dyke, and I.B.Ortenburger, *Phys. Rev. Lett.* **22**, 807(1969).
15. F.Herman, I B.Ortenburger, and J.P.Van Dyke, *Int. J. Quantum Chem.* **3S**, 827(1970).
16. A.M Boring, *Phys Rev. B* **2**, 1506(1970).
17. M.S.Gopinathan, *Phys. Rev. A* **15**, 2135(1977).
18. T.J Tseng and M.A Whitehead, *Phys Rev. A* **24**, 16(1981).
19. T.J.Tseng and M.A.Whitehead, *Phys. Rev. A* **24**, 21(1981).
20. B.Rooney, T.J.Tseng, and M.A.Whitehead, *Phys. Rev. A* **22**, 1375(1980).
21. W.Kutzelnigg, G. Del Re, and G.Berthier, *Phys. Rev.* **172**, 49(1968).
22. S.Manoli and M A Whitehead, *Phys Rev. A* **34**, 4629(1986).
23. S Manoli, Ph.D. Thesis (McGill University, Montreal, Canada).

24. Y.Guo and M.A.Whitehead, *Phys. Rev. A* (in press).

25. R.McWeeny, *Rev. Mod. Phys.* **32**, 335(1960).

26. J.L.Gázquez and J.Keller, *Phys. Rev. A* **16**, 1358(1977).

27. M.S.Gopinathan, M.A.Whitehead, and R.Bogdanovic, *Phys. Rev. A* **14**, 1(1976).

28. E.Wigner, *Phys. Rev.* **46**, 1002(1934).

29. I.Lindgren, *Int. J. Quantum Chem.* **5**, 411(1971).

30. J.P.Perdew and A.Zunger, *Phys. Rev. B* **23**, 5048(1981).

31. J.P.Perdew, *Chem. Phys. Lett.* **64**, 127(1979).

32. S.Manoli and M.A.Whitehead, *Phys. Rev. A* **38**, 630(1988).

33. J.Keller and J L.Gázquez *Phys. Rev. A* **20**, 1289(1979).

34. H.Stoll, E.Golka, and H Preuss, *Theor. Chim. Acta* **55**, 29(1980).

35. A.Savin, P.Schwerdtfeger, H Preuss, H Silberbach, and H Stoll, *Chem. Phys. Lett.* **98**, 226(1983).

36. D.M.Ceperley, *Phys. Rev. B* **18**, 3126(1978).

37. U.von Barth and L.Hedin, *J. Phys. C* **5**, 1629(1972).

38. H.Stoll, C.M.E.Pavlidou, and H.Preuss, *Theor. Chim. Acta* **49**, 143(1978).

39. S.H.Vosko, L.Wilk, and M.Nusair, *Can. J. Phys.* **58**, 1200(1980).

40. D.M.Ceperley and B.J.Alder, *Phys. Rev. Lett.* **45**, 566(1980).

41. I.P.Grant, in *Relativistic Effects in Atoms, Molecules, and Solids*, edited by G.L.Malli (plenum, New York, 1983).

42. R.D.Cowan and D C Griffin, *J Opt Soc. Am* **66**, 1010(1976).

43. J.H.Wood and A M.Boring, *Phys. Rev B* **18**, 2701(1978).

44. V.Selvaraj and M S.Gopinathan, *Phys. Rev. A* **29**, 3007(1984).

45. Y.Guo and M.A.Whitehead, *Phys. Rev. A* **38**, 3166(1988).

46. L.I.Shiff, *Quantum Mechanics*, 3rd ed (McGraw-Hill, New York, 1968).

47. I.P Grant, *Proc. R. Soc. London, Ser. A* **262**, 555(1961).

48. F.Herman and S.Skillman, *Atomic Structure Calculations* (Prentice-Hall, Englewood Cliffs, NJ, 1963).

49. J.G.Harrison, *J. Chem. Phys.* **86**, 2849(1987).

50. J.C.Slater and J.H.Wood, *Int. J. Quantum Chem.* **4**, 3(1971).

51. E.Clementi and C.Roetti, *At. Data Nucl. Data Tables* **14**, 177(1974).

52. E.H.Lieb, *Phys. Rev. A* **29**, 3018(1984).

53. K.D.Sen, *Chem. Phys. Lett.* **74**, 201(1980).

54. T.A.Koopmans, *Physica* **1**, 104(1933).

55. J.L.Gázquez and E.Ortiz, *J. Chem. Phys.* **81**, 2741(1984).

56. R.G.Parr and L.J.Bartolotti, *J. Am. Chem. Soc.* **104**, 3801(1982).

57. K.Raghavachari, *J. Chem. Phys.* **82**, 4142(1985).

58. H.Hotop and W.C.Lineberger, *J. Phys. Chem. Ref. Data* **14**, 731(1985).

59. O.Gunnarsson, J.Harris, and R.O.Jones, *J. Chem. Phys.* **67**, 3970(1979).

60. B.I.Dunlap, J.W.Connolly, and J.R.Sabin, *J. Chem. Phys.* **71**, 4993(1979).

61. V.L.Moruzzi, J.F.Janak, and A.R.Williams, *Calculated Electronic Properties of Metals* (Pergamon, New York, 1978).

62. O.Gunnarsson, *J Phys. F* **6**, 587(1976).

63. S.H.Vosko, J.P.Perdew, and A.H.MacDonald, *Phys. Rev. Lett.* **35**, 1725(1975).

64. A.Zunger and A.J.Freeman, *Phys. Rev. B* **15**, 47(1977); **17**, 2030(1978).

65. N.D.Lang, *Solid State Phys.* **28**, 225(1973).

66. R.Monnier and J.P.Perdew, *Phys. Rev. B* **17**, 2595(1978).

67. J.A.Appelbaum and D.R.Hamann, *Rev. Mod. Phys.* **48**, 3(1976).

68. G.P.Kerker, K.M.Ho, and M.L.Cohen, *Phys. Rev. Lett.* **40**, 1593(1978).

69. A.Zunger, *Phys. Rev. B* **22**, 959(1980).

70. H.B.Shore, J.H.Rose, and Ξ.Zaremba, *Phys. Rev. B* **15**, 2858(1977).

71. K.Schwarz, *Chem. Phys. Lett.* **57**, 605(1978).

72. H.Hotop and W.C.Lineberger, *J. Phys. Chem. Ref. Data* **4**, 539(1975).

73. Y.Guo and M.A.Whitehead, *Phys. Rev. A* **39**, 28(1989).

74. Y.Guo, S.Manoli, and M.A.Whitehead, *Phys. Rev. A* **38**, 1120(1988).

75. S.H.Vosko and L.Wilk, *J. Phys. B· At. Mol. Phys.* **16**, 3687(1983).

76. L.J.Bartolotti, S.R.Gadre, and R.G.Parr, *J. Am. Chem. Soc.* **102**, 2945(1980).

77. R.G.Parr and R.G.Pearson, *J. Am. Chem. Soc.* **105**, 7512(1983).

78. A.R.Orsky and M.A.Whitehead, *Can. J. Chem.* **65**, 1970(1987).

79. M.C.Böhm and P.C.Schmidt, *Ber. Bunsenges. Phys. Chem.*(Germany) **90**, 913(1986).

80. K.Ohwada, *Polyhedron*(GB) **3**, 853(1984).

81. Y.Guo and M.A.Whitehead, *Phys. Rev. A* **39**, 2317(1989).

82. M.S.Gopinathan, *J. Phys. B: At. Mol. Phys.* **12**, 521(1979).

83. C.E.Moore, *Atomic Energy Levels*, Natl. Bur. Stand. (U.S.), Circ. No. 467(U.S.GPO, Washington, D.C., 1949), Vol. I; 1952, Vol. II; 1955, Vol. III.

84. S. Manoli and M.A.Whitehaed, *J. Chem Phys.* **81**, 841(1984).

85. S. Manoli and M.A.Whitehaed, *Phys. Rev. A* **23**, 2150(1981).

86. K.K.Sunil and K.D.Jordan, *J. Chem. Phys.* **82**, 873(1985).

87. K.Jankowski and M.Polasik, *J. Phys. B: At. Mol. Phys.* **18**, 2133(1985).

88. F.Sasaki and M.Yoshimine, *Phys. Rev. A* **9**, 17, 26(1974).

89. B.H.Botch and T.H.Dunning,Jr., *J. Chem. Phys* **76**, 6046(1982).

90. J.Kalcher and R.Janoscher, *Chem. Phys.* **104**, 251(1986).

91. R.N.Barnett, P.J.Reynolds, and W.A.Lester,Jr., *J. Chem. Phys.* **84** 4992(1986).

92. Y.Guo, M.C.Wrinn, and M.A.Whitehead, *Phys. Rev. A* **40**, 6685(1989).

93. S.Fraga, J.Karwowski, and K.M.S.Saxena, *Handbook of Atomic Data* (Elsevier, Amsterdam, 1976).

94. S.H.Vosko, J.B.Lagowski, and I.L.Mayer, *Phys. Rev A* **39**, 446(1989).

95. J.P.Desclaux, *Comput. Phys. Commun.* **9**, 31(1975).

96. T.A.Carlson, C.W.Nestor, N.Wasserman,Jr., and J.D.McDowell, *At. Data* **2**, 63(1970).

97. R.Gáspár and Á. Nagy, *J. Phys. B: At. Mol. Phys.* **20**, 3631(1987).

98. J.Binder, H.R.Kaslowski, B.A.Huber, and K.Wiesemann, *10th International Conference on Atomic Physics*, Ed. by H.Narumi and I Shimamura, Tokyo, 1986.

99. M.A.Chaudhry, A.J.Duncan, R.Hippler, and H.Kleinpoppen, *10th International Conference on Atomic Physics*, Ed. by H.Narumi and I.Shimamura, Tokyo, 1986.

100. E.Clementi, S.J.Chakravorty, G.Coronigiu, and V.Carravetta, *Modern Techniques in Computational Chemistry* (to be published)

101. Y.Guo and M.A.Whitehead, *Phys. Rev. A* **40**, 28(1989).

102. E.Clementi, IBM *J. Res Dev.* **9**, 2(1965).

103. S.Bashkin and J.O.Stoner,Jr., *Atomic Energy Levels and Grotrian Diagrams* (Amsterdam, North-Holland, 1975).

104. K.Mori and T.Kato, *At. Data Nucl. Data Tables* **23**, 196(1979).

105. Y.Guo and M.A.Whitehead, *Can. J. Chem.* **xx**, xxxx(1990).

106. C.F.Fischer, J.B Lagowski, and S H.Vosko, *Phys. Rev. Lett.* **59**, 2263(1987).

107. D.J.Pegg, J.S.Thompson, R.N.Compton, and G.D.Alton, *Phys. Rev. Lett.* **59**, 2267(1987).

108. C.F.Fischer, *Phys. Rev. A* **39**, 963(1989).

109. P.Fuentealba, A.Savin, H.Stoll, and H.Preuss, *Phys. Rev. A* **40**, 2163(1989).

110. C.E.Kuyatt, J.A.Simpson, and S.R.Mielczarek, *Phys. Rev.* **138**, A385(1965).

111. R.J.Zollweg, *J. Chem. Phys.* **50**, 4251(1969).

112. A.V.Bunge and C.F.Bunge, *Phys. Rev. A* **19**, 452(1979).

113. K.T.Chung, *Phys. Rev A* **22**, 1341(1980).

114. C.A.Nicolaides, Y.Komninos, and D.R.Beck, *Phys. Rev. A* **24**, 1103(1981).

115. C.F.Bunge, M.Galán, R.Jáuregui, and A.V.Bunge, *Nucl. Instrum. Methods* **202**, 299(1982).

116. S.G.Bratsch and J.J.Lagowski, *Chem. Phys. Lett.* **107**, 136(1984).

117. K.D.Sen and P.Politzer (Private communication).

118. L.A.Cole and J.P.Perdew, *Phys. Rev. A* **25**, 1265(1982).

119. W.K.Stuckey and R.W.Kiser, *Nature* (London) **211**, 963(1966).

120. J.H.Fremlin, *Nature* (London) **212**, 1453(1966).

121. J.E.Ahnell and W.S.Koski, *Nature* (London) *Phys. Sci.* **245**, 30(1973).

122. H.Baumann, E.Heinicke, H.J.Kaiser, and K.Bethge, *Nucl. Instrum. Methods* **95**, 389(1971).

123. B.Peart and K.Dolder, *J. Phys. B* **6**, 1497(1973).

124. R.Schmtzer and M.Anbar, *J. Chem Phys.* **64**, 2466(1976).

125. B.Hird and S.P.Ali, *Can J. Phys.* **56**, 867(1979); *J. Chem. Phys.* **74**, 3620 (1981).

126. B.Hird and H.C.Suk, *Phys. Rev. A* **14**, 928(1976).

127. H.S.W.Massey, *Negative Ions*, 3rd ed. (Cambridge, London, 1976).

128. E.C.Baughan, *Trans. Faraday Soc.* **55**, 736(1959); 2025(1959); **57**, 1863(1961).

129. R.Gáspár and P.Csavinszky, *Acta Phys. Acad. Sci. Hung.* **4**, 125(1956).

130. R.E.Watson, *Phys. Rev.* **111**, 1108(1958).

131. E.Clementi and A.D.McLean, *Phys. Rev.* **133**, A419(1964).

132. R.Ahlrichs, *Chem. Phys. Lett.* **34**, 570(1975).

133. M.A.Robb and I.G.Csizmadia, *Int. J. Quantum Chem.* **5**, 605(1971).

134. J.Kalcher, *Chem. Phys.* **115**, 33(1987).

135. J.G.Norman,Jr., *Mol. Phys.* **31**, 1191(1976).

136. K.H.Johnson, *Ann Rev. Phys. Chem.* **26**, 39(1975); *J. Phys. Paris* **3**, 195(1972).

137. J.S.-Y. Chao and K D.Jordan, *J. Phys. Chem.* **91**, 5578(1978).

138. G.S.Painter, *Phys. Rev. B* **24**, 4264(1981).

139. Y.Guo and M A.Whitehead, *Can. J. Chem.* **xx**, xxxx(1990).

140. A.G.Ginsberg and J.M Miller, *J. Inorg. Nucl. Chem.* **7**, 351(1958).

141. J.E.Huheey, *Inorganic Chemistry*, 3rd ed. (Harper and Row, New York, 1983).

142. Y.Guo and M A.Whitehead (Submitted).

143. L. Pauling, *The Nature of the Chemical Bond*, 3rd ed. (Cornell University Press, New York, 1960).

144. K.D.Sen, P C Schmidt, and M.C.Bohm, *Struct Bonding* **66**, 99(1987).

145. P.Politzer, *J Chem. Phys.* **86**, 1072(1987).

146. P.Politzer and H.Weinstein, *J. Chem Phys.* **71**, 4218(1979).

147. R.G.Parr, R.A.Donnelly, M Levy, and W.E.Palke, *J. Chem. Phys.* **68**, 3801 (1978).

148. R.G.Pearson, *Inorg. Chem.* **27**, 734(1988).

149. S.C.Vinayagam and K D.Sen, *Chem. Phys Lett* **144**, 178(1988).

150. Z.Zhou and R.G Parr, *J Am Chem. Soc.* **111**, 7371(1989).

151. C.Goycoolea, M.Barrera, and F.Zuloaga, *Int. J. Quantum Chem.* **36**, 455(1989).

152. J.Todd and M A.Whitehead, *Theo. Chem* **202**, 99(1989).

153. K.S.Lackner and G.Zweig, *Phys. Rev. D* **28**, 1671(1983).

154. A.P.Ginsberg and J.M.Miller, *J. Inorg. Nucl. Chem.* **7**, 351(1958).

155. R.S Mulliken, *J. Chem. Phys.* **2**, 782(1934).

156. J.P.Perdew, R.G.Parr, M.Levy, and J.L.Balduz,Jr., *Phys. Rev. Lett.* **49**, 1691(1982).

157. K.S.Lackner and G.Zweig, *Phys Rev. D* **36**, 1562(1987).

158. K.D.Sen, J.M.Seminario, and P Politzer, *Phys. Rev. A* **40**, 2260(1989).

159. Y.Guo and M A Whitehead, *Int J. Quantum Chem* (in press).

160. J.C Slater, *J Chem Phys.* **43**, S228(1965).

161. K.H Johnson, *J. Chem. Phys.* **45**, 3085(1966); *Int. J. Quantum Chem.* **S1**, 361(1967); **S2**, 233(1968), *Adv. Quantum Chem.* **7**, 143(1973).

162. F.C.Smith,Jr. and K H Johnson, *Phys. Rev. Lett.* **22**, 1168(1969).

163. K.H.Johnson, J G Norman,Jr., and J.W.D.Connolly, *Computational Methods for Large Molecules and Localized States in Solids*, ed. F.Herman, A.D.Maclean, and R.D Nesbet (Plenum Press, New York, 1973).

164. J.W D.Connolly and J.R Sabin, *J. Chem. Phys.* **56**, 5529(1972).

165. U.Wahlgren and K.H Johnson, *J Chem. Phys* **56**, 3715(1972).

166. F Herman, A R.Williams, and K H.Johnson, *J. Chem. Phys.* **61**, 3508 (1974).

167. J.W D Connolly, H Siegbahn, U.Gelius, and C.Nordling, *J Chem. Phys.* **58**, 4265(1973)

168. J.G.Norman,Jr., *Mol. Phys.* **31**, 1191(1976).

169. A E Foti, V.H.Smith,Jr., and M.A.Whitehead, *Mol. Phys.* **45**, 385(1982).

170. E Broclawik, J.Mrozek, and V.H.Smith,Jr., *Chem. Phys.* **66**, 417(1982).

171. E.M.Berhsoy and M.A.Whitehead, *J. Chem. Soc. Faraday Trans* **84**, 1707 (1988), *Tetrahedron* **44**, 7517(1988).

172. J S.Tse, Z F.Liu, J D Bozek, and G.M Bancroft, *Phys. Rev. A* **39**, 1791(1989).

173. N Rosch, W.G Klemperer, and K.H.Johnson, *Chem. Phys. Lett.* **23**, 149(1973).

174. J.C.Slater, *Computational Methods in Band Theory*, ed. P.M.Marcus, J.F.Janak, and A R Williams (Plenum Press, New York, 1971).

175. J F.Janak, *Phys. Rev B* **18**, 7105(1978).

176. D.A.Case and M.Karplus, *Chem. Phys. Lett.* **39**, 33(1976).

177. M.Cook and M.Karplus, *J. Chem. Phys.* **72**, 7(1980).

178. D.A.Case, M.Cook, and M.Karplus, *J. Chem. Phys.* **73**, 3294(1980).

179. M.C.Wrinn and M.A.Whitehead, *J. Chem. Soc. Faraday Trans.* **86**, 890(1990)

180. C.J.Eyermann and A.Chung-Phillips, *J Chem. Phys* **81**, 1517(1984); *J. Am. Chem. Soc.* **106**, 7437(1984); *Inorg. Chem.* **23**, 2025(1984).

181. G.De Alti, P Decleva, and A.Lisini, *Chem. Phys.* **66**, 425(1982).

182. H.Sambe and R.H.Felton, *J Chem. Phys.* **62**, 1122(1975).

183. B.I.Dunlap, J.W.D Connolly, and J.R.Sabin, *J. Chem Phys.* **71**, 3396(1979).

184. E.J Baerends, D E.Ellis, and P.Ros, *Chem. Phys.* **2**, 41(1973).

185. E.J.Baerends and P.Ros, *Chem. Phys.* **2**, 52(1973).

186. F.W Averill and D.E.Ellis, *J. Chem. Phys.* **59**, 6412(1973).

187. A.D.Becke, *J Chem. Phys.* **76**, 6037(1982); **78**, 4787(1983); **84**, 4524(1986); **88**, 2547(1988).

188 R.A.Heaton, J G Harrison, and C.C.Lin, *Solid State Commun.* **41**, 827(1982), *Phys. Rev B* **28**, 5992(1983); **31**, 1077(1985).

189. M.R.Pederson, R.A Heaton, and C.C.Lin, *J. Chem Phys.* **80**, 1972(1984); **82**, 2688(1985).

190. Y.Guo and M.A.Whitehead, *Theo. Chem.* (in press).

191. C.Edmiston and K.Ruedenberg, *Rev. Mod. Phys.* **35**, 457(1963); *J. Chem. Phys.* **43**, S97(1965).

192. M.R.Pederson and C.C.Lin, *J. Chem. Phys* **88**, 1807(1988).

193. K.H.Johnson, F Herman, and R.Kjellander, *Electronic Structure of Polymers and Molecular Crystals*, ed. J.M.Andre and J Ladik (Plenum Press, New York, 1975).

194. P.Weinberger and K.Schwarz, *Physical Chemistry*, Vol. I, ed. A.D.Buckingham and C.A Coulson (Butterworths, London and Boston, 1975).

195. M Cook and D A Case, *Program XASW*, NRCC Catalog 1980 Vol 1; Quantum Chem. Program Exchange Bulletin, **1**, 98(1981).

196. A.L.Andrews, R.J Bishop, B.Cleaver, A E Dennard, D E.Henn, B.E.Loader, A.L.Mackay, H.Mendel, D.J.Morgan, P.G.Owston, and D C.Phillips, *Tables of In-*

teratomic Distances and Configuration in Molecules and Ions, ed. L.E.Sutton(The Chemistry Society, London, 1965).

197. J.C.Slater, *Int J. Quantum Chem.* **S7**, 533(1973).

198. J.G.Norman Jr., *J. Chem. Phys* **61**, 4630(1974).

199. J C Slater and K H Johnson, *Phys Rev. B* **5**, 844(1972).

200. A J Meier and R S Mulliken, *Chem. Rev.* **69**, 639(1969).

201. B.J.Garrison, H F.Schaefer III, and W.A.Lester,Jr., *J. Chem. Phys.* **61**, 3039(1974)

202. L S.Cederbaum and W.Domcke, *Adv. Chem. Phys.* **36**, 205(1977).

203. D.P Chong, F.G Herring, and D.WcWilliams, *J. Chem. Phys.* **61**, 78(1974).

204. D W.Turner, C.Baker, A.D Baker, and C.R.Brundle, *Molecular Photoelectron Spectroscopy* (Wiley-Interscience, New York, 1970).

205. T. H. Lee, R. J. Colton, M. G. White, and J W. Rabalais, *J. Am. Chem. Soc.* **97**, 4845(1975)

206. D.P.Chong, F.G.Herring, and D.McWilliams, *J. Electron Spectry.* **7**, 445(1975).

207. J.M.Dyke, L Golob, N.Jonathan, A.Morris, and M.Okuda, *J. Chem. Soc. Faraday Trans* **2**, 1828(1974)

208. J.M.Schulman and J W Moskowitz, *J. Chem. Phys.* **47**, 3491(1967).

209. B.Jonsson and E.Lindholm, *Ark. Fys.* **39**, 65(1968).

210. J.A.Sell and A Kuppermann, *Chem. Phys.* **33**, 367(1978).

211. U.Gelius, C.J.Allan, G.Johansson, H.Siegbahn, D.A.Allison, and K.Siegbahn, *Phys Scr.* **3**, 237(1971).

212. W.Von Niessen, L.S.Cederbaum, and W.P.Kraemer, *J. Chem. Phys.* **65**, 1378(1976).

213. J.Almlof, B.Roos, U.Wahlgren, and H.Johansen, *J. Electron Spectrosc. Relat. Phenom* **2**, 51(1973).

214. M.S.Banna, B.E.Mills, D.W.Davis, D.A.Shirley, *J Chem. Phys.* **61**, 4780(1974).

215. C.R.Brundle and M B.Robin, *J. Chem Phys.* **53**, 2196(1970).

216. S.Katsumata and K Kimura, *Bulletin Chem. Soc. Japan* **46**, 1342(1973).

217. J.C.Green, M.L.H.Green, P.J.Joachim, A.F.Orchard, and D.W.Turner, *Phil. Trans. Roy. Soc.*(London) **A268**, 111(1970).

218. R.Prins, *J. Chem. Phys.* **61**, 2580(1974).

219. W.A.Chupka, J.Berkowitz, and D.Gutman, *J Chem. Phys.* **55**, 2733(1971).

220. K.K.Murray, T M.Miller, D.G.Leopold, and W.C.Lineberger, *J. Chem. Phys.* **84**, 2520(1986).

221. J.Chandrasekhar, J.G.Andrade, and P von R.Schleyer, *J. Am. Chem Soc.* **103**, 5612(1981).

222. T.M.Miller, D.G.Leopold, K.K.Murray, and W.C.Lineberger, *J. Chem. Phys* **85**, 2368(1986).

223. M.M.Heaton, A.Pipano, and J.J.Kaufman, *Int. J. Quantum Chem.* **6**, 181 (1972).

224. H.Wasada and K.Hirao, *Chem. Phys. Lett.* **139**, 155(1987).

225. N.Heirich, W.Koch, and G.Frenking, *Chem. Phys Lett.* **124**, 20(1986).

226. Y.Sakai and E Miyoshi, *J. Chem Phys* **87**, 2885(1987).

227. P.Stampfli and K H.Bennemann, *Phys. Rev Lett* **58**, 2635(1987).

228. C.W.Bauschlicher,Jr , S.R.Langhoff, and P.R Taylor, *J. Chem. Phys* **88**, 1041(1988).

229. E.Miyoshi, Y.Sakai, and S.Miyoshi, *J. Chem. Phys.* **88**, 1470(1988).

230. M.R.Truter, D.W.J.Cruickshunk, and G.A.Jeffrey, *Acta Crystallogr.* **13**, 855(1960).

231. H.Johansen, *Theor. Chim. Acta* **32**, 273(1974).

232. M.Vijayakumar, N.Vaidehi, and M.S.Gopinathan, *Phys. Rev. A* **40**, 6834(1989).

233. L.L.Lohr,Jr. and W N.Lipscomb, *Inorg Chem.* **3**,22(1964).

234. R.F.Fenske and R L.DeKock, *Inorg. Chem.* **9**,1053(1970).

235. M.F.Guest, M B.Hall, and I H.Hillier, *Mol Phys.* **25**, 629(1973).

236. J.Grima, F.Chaplin, and G.Kaufmann, *J. Organomet. Chem.* **129**, 221(1977).

237. N.Fonnesbech, J Hjortkjaer, and H.Johansen, *Int J. Quantum Chem.* **11S**, 95(1977).

238. D.M.Hood, R.M.Pitzer, H.F Schaefer III, *J. Chem. Phys.* **71**, 705(1979).

239. G.A.Ozin, *Catal. Rev. Sci. Eng.* **16**, 191(1977).

240. M.Moskowitz, *Accounts Chem. Res.* **12**, 229(1979).

241. C.Bachman, J.Demuynck, and A.Veillard, *Faraday Symp.* **14**, 71(1980).

242. J.Demuynck, M.Rohmer, A.Strich, and A.Veillard, *J. Chem. Phys.* **75**, 3443(1981).

243 H.Basch, M.D.Newton, and J.W.Moskowitz, *J. Chem. Phys.* **73**, 4492(1980).

244. R P Messmer, in: *The nature of the surface chemical bond*, eds. T.N.Rhodin and G Erti (North-Holland, Amsterdam, 1979).

245. E.J.Baerends and P.Ros, *Int. J. Quantum Chem.* **12S**, 169(1978).

246. D.Post and E.J.Baerends, *Chem Phys. Lett.* **86**, 176(1982).

247. I.Kojima, A.K.Srivastava, E.Miyazaki, and H.Adachi, *J. Chem. Phys. 84*, 4455(1986).

248. R.P.Messmer, S.K.Knudson, K.H.Johnson, J.B.Diamond, and C.Y.Yang, *Phys. Rev. B* **13**, 1396(1976).

249. R.P.Messmer, C.W.Tucker, and K.H.Johnson, *Chem. Phys. Lett.* **36**, 423(1975).